REACHING AND GRASPING THE MULTISENSORY SIDE OF DEXTEROUS MANIPULATION

EDITED BY: Ivan Camponogara, Luigi F. Cuturi, Simone Toma and
Marco Santello

PUBLISHED IN: Frontiers in Psychology and Frontiers in Neuroscience

frontiers Research Topics

Frontiers eBook Copyright Statement

ISSN 1664-8714
ISBN 978-2-88974-377-3
DOI 10.3389/978-2-88974-377-3

About Frontiers

Frontiers is more than just an open-access publisher of scholarly articles: it is a pioneering approach to the world of academia, radically improving the way scholarly research is managed. The grand vision of Frontiers is a world where all people have an equal opportunity to seek, share and generate knowledge. Frontiers provides immediate and permanent online open access to all its publications, but this alone is not enough to realize our grand goals.

Frontiers Journal Series

The Frontiers Journal Series is a multi-tier and interdisciplinary set of open-access, online journals, promising a paradigm shift from the current review, selection and dissemination processes in academic publishing. All Frontiers journals are driven by researchers for researchers; therefore, they constitute a service to the scholarly community. At the same time, the Frontiers Journal Series operates on a revolutionary invention, the tiered publishing system, initially addressing specific communities of scholars, and gradually climbing up to broader public understanding, thus serving the interests of the lay society, too.

Dedication to Quality

Each Frontiers article is a landmark of the highest quality, thanks to genuinely collaborative interactions between authors and review editors, who include some of the world's best academicians. Research must be certified by peers before entering a stream of knowledge that may eventually reach the public - and shape society; therefore, Frontiers only applies the most rigorous and unbiased reviews.
Frontiers revolutionizes research publishing by freely delivering the most outstanding research, evaluated with no bias from both the academic and social point of view.
By applying the most advanced information technologies, Frontiers is catapulting scholarly publishing into a new generation.

What are Frontiers Research Topics?

Frontiers Research Topics are very popular trademarks of the Frontiers Journals Series: they are collections of at least ten articles, all centered on a particular subject. With their unique mix of varied contributions from Original Research to Review Articles, Frontiers Research Topics unify the most influential researchers, the latest key findings and historical advances in a hot research area! Find out more on how to host your own Frontiers Research Topic or contribute to one as an author by contacting the Frontiers Editorial Office: frontiersin.org/about/contact

REACHING AND GRASPING THE MULTISENSORY SIDE OF DEXTEROUS MANIPULATION

Topic Editors:
Ivan Camponogara, New York University Abu Dhabi, United Arab Emirates
Luigi F. Cuturi, Italian Institute of Technology (IIT), Italy
Simone Toma, Arizona State University, United States
Marco Santello, Arizona State University, United States

Citation: Camponogara, I., Cuturi, L. F., Toma, S., Santello, M., eds. (2022). Reaching and Grasping the Multisensory Side of Dexterous Manipulation. Lausanne: Frontiers Media SA. doi: 10.3389/978-2-88974-377-3

Table of Contents

04 Editorial: Reaching and Grasping the Multisensory Side of Dexterous Manipulation
Simone Toma, Luigi F. Cuturi, Marco Santello and Ivan Camponogara

06 Grasping Weber's Law in a Virtual Environment: The Effect of Haptic Feedback
Aviad Ozana, Sigal Berman and Tzvi Ganel

21 Effects of Tool Novelty and Action Demands on Gaze Searching During Tool Observation
Yoshinori Tamaki, Satoshi Nobusako, Yusaku Takamura, Yu Miyawaki, Moe Terada and Shu Morioka

31 The Role of Haptic Expectations in Reaching to Grasp: From Pantomime to Natural Grasps and Back Again
Robert L. Whitwell, Nathan J. Katz, Melvyn A. Goodale and James T. Enns

47 Humans Can Visually Judge Grasp Quality and Refine Their Judgments Through Visual and Haptic Feedback
Guido Maiello, Marcel Schepko, Lina K. Klein, Vivian C. Paulun and Roland W. Fleming

58 Convergent and Distinct Effects of Multisensory Combination on Statistical Learning Using a Computer Glove
Christopher R. Madan and Anthony Singhal

65 Reach-to-Grasp: A Multisensory Experience
Sonia Betti, Umberto Castiello and Chiara Begliomini

71 Role of Tactile Noise in the Control of Digit Normal Force
Abdeldjallil Naceri, Yasemin B. Gultekin, Alessandro Moscatelli and Marc O. Ernst

84 Motor Imagery Training of Reaching-to-Grasp Movement Supplemented by a Virtual Environment in an Individual With Congenital Bilateral Transverse Upper-Limb Deficiency
Joanna Mencel, Anna Jaskólska, Jarosław Marusiak, Łukasz Kamiński, Marek Kurzyński, Andrzej Wołczowski, Artur Jaskólski and Katarzyna Kisiel-Sajewicz

97 Multisensory Integration in Stroke Patients: A Theoretical Approach to Reinterpret Upper-Limb Proprioceptive Deficits and Visual Compensation
Jules Bernard-Espina, Mathieu Beraneck, Marc A. Maier and Michele Tagliabue

118 Grasping of Real-World Objects Is Not Biased by Ensemble Perception
Annabel Wing-Yan Fan, Lin Lawrence Guo, Adam Frost, Robert L. Whitwell, Matthias Niemeier and Jonathan S. Cant

138 Visually and Tactually Guided Grasps Lead to Different Neuronal Activity in Non-human Primates
Daniela Buchwald and Hansjörg Scherberger

frontiers
in Psychology

EDITORIAL
published: 17 March 2022
doi: 10.3389/fpsyg.2022.866608

Editorial: Reaching and Grasping the Multisensory Side of Dexterous Manipulation

*Simone Toma[1], Luigi F. Cuturi[2,3], Marco Santello[1] and Ivan Camponogara[4]**

[1] School of Biological and Health Systems Engineering (SBHSE), Arizona State University, Tempe, AZ, United States, [2] Unit for Visually Impaired People (U-VIP), Italian Institute of Technology (IIT), Genova, Italy, [3] Dipartimento di Filosofia e Comunicazione, Alma Mater Studiorum, Università di Bologna, Bologna, Italy, [4] Division of Science, New York University Abu Dhabi, Abu Dhabi, United Arab Emirates

Keywords: multisensory integration, reaching, grasping, dexterous manipulation, vision-binocular and stereopsis, haptic (tactile) perception

OPEN ACCESS

Edited and reviewed by:
Bernhard Hommel,
University Hospital Carl Gustav
Carus, Germany

****Correspondence:***
Ivan Camponogara
ic39@nyu.edu

Specialty section:
This article was submitted to
Cognition,
a section of the journal
Frontiers in Psychology

Received: *31 January 2022*
Accepted: *08 February 2022*
Published: *17 March 2022*

Citation:
Toma S, Cuturi LF, Santello M and Camponogara I (2022) Editorial: Reaching and Grasping the Multisensory Side of Dexterous Manipulation.
Front. Psychol. 13:866608.
doi: 10.3389/fpsyg.2022.866608

Editorial on the Research Topic

Reaching and Grasping the Multisensory Side of Dexterous Manipulation

The wide range of reaching and grasping actions we perform every day stems from the use and integration of multiple sources of sensory inputs within the motor commands. Both sensory and motor signals associated with these goal-directed behaviors provide separate and redundant information necessary to successfully complete object reaching, grasp and manipulation. In this Research Topic we collected a series of original studies investigating such multisensory-motor integration processes. As outlined by the review article by Betti et al., reach-to-grasp movements are affected by the myriad of information we gather through the visual, proprioceptive, auditory, taste, and olfactory senses. Several contributions reported in this review paper revealed how modulating each of the above-mentioned sensory signals affects grasping performance and manipulation performance. Thus, the present Research Topic enriches and expands the existing literature on multisensory-motor integration for reaching, grasping and manipulation by presenting a collection of original research papers addressing five main research areas: (1) the role of haptic and tactile feedback in grasping and manipulation; (2) the effect of visual exploration on grasping and tool use; (3) the relationship between the sensory deficit and multisensory integration; (4) multisensory motor learning; and (5) the neural correlates of visuo-haptic integration in primates.

The role of the haptic feedback in grasping and manipulation has been investigated by Whitwell et al., who showed that advanced knowledge of haptic feedback modulated action performance. Specifically, they used a mirror apparatus where subjects were able to see a "virtual" object reflected in the mirror, spatially coincident with the real one. Subjects had to reach and grasp the object behind the mirror, which could be either physically present or not, with or without concurrent verbal cues signaling the presence (or not) of the physical object. They showed that cueing haptic feedback before performing the action led to a smaller peak of grip aperture than when haptic feedback was uncued and unexpected. This work extended their previous works on visual cueing, showing a flexible use of natural and pantomimed grasping according to the haptic expectation. Concurrently, through the use of a virtual reality setup, Ozana et al. found that withdrawing the haptic feedback at the end of a bimanual grasping task (i.e., not presenting a physical object with matching dimensions of the object presented in virtual reality) increased the hand's aperture variability compared to when haptic feedback was provided. These findings demonstrated that grasping adheres to Weber law only when haptic feedback is absent (pantomimed grasping). Maiello et al. found that haptic feedback is crucial to judge grasp quality.

Specifically, grasp quality is better inferred following an active grasp, where subjects had previously experienced the haptic feedback through enclosing the digits on the physical object, than passively viewing the grasping point on the object or watching a video of someone else's grasp on the same object. The role of tactile feedback in object manipulation was investigated by Naceri et al., who found that tactile feedback is fundamental to modulate the forces applied on a lifted object. By reducing the tactile sensitivity through a rubber thimble, they showed an increased grasping force relative to baseline on the covered fingers, demonstrating an independent control of the digits' force when lifting an object.

The effect of visual exploration on grasping and tool use was addressed by Fan et al., who investigated whether surrounding a to-be-grasped object with distractors affected the grasping performance. They found that distractors do not affect object grasping performance, and the latter does not influence object representation. Tamaki et al. investigated two aspects of pre-grasp tool-use behavior. First, these authors asked whether familiarity with an object influences pre-grasp visual exploration, and second, if the intention to use the object as a tool leads participants to shift their gaze on object functional parts (i.e., technical reasoning). Tamaki et al.'s main finding was that technical reasoning increases when the object is only visually explored (without manipulation) and when it is used as a tool, relative to when the object is just lifted. The authors interpreted their findings proposing two different types of technical reasoning associated with tool-use, which they defined as automatic and intentional.

The relationship between the sensory deficit and multisensory integration was thoroughly explored by Bernard-Espina et al., who provided a new theoretical approach to multisensory integration in post-stroke proprioceptive deficits. By merging optimal sensory integration framework with reference frames models (Tagliabue and McIntyre, 2021) they suggested that post-stroke proprioceptive deficits stem from the inability to encode proprioceptive information in a non-joint space. Mencel et al. found that the brain-related activity during a motor imagery training of a patient with bilateral upper limb deficiency in a virtual environment is enhanced compared to healthy individuals and was modulated according to the familiarity with the task. The change of brain activity following motor imagery training was interpreted as training-induced plasticity in patients.

Multisensory-motor learning was addressed by Madan and Singhal, who investigated whether providing tactile and auditory feedback during a visually-guided tapping task improves implicit and explicit learning. They found that while explicit learning benefits from separate unisensory feedback, implicit learning was best when all the sensory modalities were involved. Lastly, by investigating the neural correlates of visuo-haptic integration in non-humans primates Buchwald and Scherberger found that different sensory neural streams subserve grasping performance, even though movement kinematics remained unchanged.

The present Research Topic complements and advances existing literature investigating the variety of contexts where the integration of motor commands with multisensory inputs plays a central role in reaching and grasping. On the one hand, a portion of contributions collected here complements existing literature on behavioral Betti et al. and neurophysiological Buchwald and Scherberger aspects of multisensory integration for object manipulation and motor performance in healthy and motor impaired patients. On the other hand, a second portion of evidence presented here advances the literature of this topic by exploring new research avenues linking grasping behaviors and multisensory integration to grasp quality judgement Maiello et al., grip force modulation Naceri et al., sensory compensation/substitution Bernard-Espina et al., contextual statistics Fan et al., expectations Whitwell et al., motor imagery Mencel et al., tool use Tamaki et al., and motor performance in VR Ozana et al. Due to the wide spectrum of approaches and evidence presented, we believe the present research collection can be of interest for a multidisciplinary audience such as cognitive neuroscientists to engineers.

AUTHOR CONTRIBUTIONS

IC and ST wrote the manuscript. IC, ST, LC, and MS revised the manuscript. All authors contributed to the article and approved the submitted version.

FUNDING

This material is based upon work supported by the National Science Foundation under Grant No. BCS-1827752.

REFERENCES

Tagliabue, M., and McIntyre, J. (2021). A modular theory of multisensory integration for motor control. *Front. Comput. Neurosci.* 8, 1. doi: 10.3389/fncom.2014.00001

Conflict of Interest: The authors declare that the research was conducted in the absence of any commercial or financial relationships that could be construed as a potential conflict of interest.

frontiers in Psychology

ORIGINAL RESEARCH
published: 19 November 2020
doi: 10.3389/fpsyg.2020.573352

Grasping Weber's Law in a Virtual Environment: The Effect of Haptic Feedback

Aviad Ozana[1,2], Sigal Berman[2,3] and Tzvi Ganel[1,2]*

[1] Department of Psychology, Ben-Gurion University of the Negev, Beer-Sheva, Israel, [2] Zlotowski Center, Ben-Gurion University of the Negev, Beer-Sheva, Israel, [3] Department of Industrial Engineering and Management, Ben-Gurion University of the Negev, Beer-Sheva, Israel

Recent findings suggest that the functional separation between vision-for-action and vision-for-perception does not generalize to situations in which virtual objects are used as targets. For instance, unlike actions toward real objects that violate Weber's law, a basic law of visual perception, actions toward virtual objects presented on flat-screens, or in remote virtual environments, obey to Weber's law. These results suggest that actions in virtual environments are performed in an inefficient manner and are subjected to perceptual effects. It is unclear, however, whether this inefficiency reflects extensive variation in the way in which visual information is processed in virtual environments or more local aspects related to the settings of the virtual environment. In the current study, we focused on grasping performance in a state-of-the-art virtual reality system that provides an accurate representation of the 3D space. Within this environment, we tested the effect of haptic feedback on grasping trajectories. Participants were asked to perform bimanual grasping movements toward the edges of virtual targets. In the haptic feedback condition, physical stimuli of matching dimensions were embedded in the virtual environment. Haptic feedback was not provided in the no-feedback condition. The results showed that grasping trajectories in the feedback, but not in the no-feedback condition, could be performed more efficiently, and evade the influence of Weber's law. These findings are discussed in relevance to previous literature on 2D and 3D grasping.

Keywords: perception and action, grasping, Weber's law, 2D objects, virtual environment, object perception

OPEN ACCESS

Edited by:
Ivan Camponogara,
New York University Abu Dhabi,
United Arab Emirates

Reviewed by:
Zhongting Chen,
East China Normal University, China
Dimitris Voudouris,
University of Giessen, Germany
Robert Leslie Whitwell,
Western University, Canada

***Correspondence:**
Tzvi Ganel
tganel@bgu.ac.il

Specialty section:
This article was submitted to
Educational Psychology,
a section of the journal
Frontiers in Psychology

Received: *17 June 2020*
Accepted: *05 October 2020*
Published: *19 November 2020*

Citation:
Ozana A, Berman S and Ganel T (2020) Grasping Weber's Law in a Virtual Environment: The Effect of Haptic Feedback. Front. Psychol. 11:573352. doi: 10.3389/fpsyg.2020.573352

INTRODUCTION

People interact with physical objects in their surroundings by reach-to-grasp movements. Current advances in immersive technology aim to simulate a similar sense of control when interacting with virtual objects within virtual environments. Recent studies, however, suggest that virtual interactions are (still) performed differently from interactions with 3D objects in the physical environment (Holmes and Heath, 2013; Freud and Ganel, 2015; Ozana and Ganel, 2018, 2019a). For instance, grasping gestures toward physical 3D objects are typically performed analytically. In particular, the shaping of the grip aperture is unaffected by tasks-irrelevant, perceptually driven information about objects and their surroundings (Aglioti et al., 1995; Ganel and Goodale, 2003; Ganel et al., 2008; Chen et al., 2015; Namdar et al., 2018 but see Franz and Gegenfurtner, 2008; Kopiske et al., 2016). These findings have been attributed to the proposed functional separation between visual perception and visual control of action (Goodale and Milner, 1992; Milner and Goodale, 2008; but see Glover and Dixon, 2001; Smeets and Brenner, 2008; Rossit et al., 2018 for different views). These findings have been recently extended to two-hand, bimanual motor control (Ganel et al., 2017; Ozana and Ganel, 2020). Yet, unlike grasping movements toward physical objects, previous evidence shows that when 2D objects are used as targets, actions toward these objects become less efficient and are performed in a relative rather than analytic manner. Such actions are susceptible to perceptual heuristics (Holmes and Heath, 2013; Freud and Ganel, 2015; Ozana and Ganel, 2018, 2019a; Ganel et al., 2019). This evidence suggests that efficient visuomotor control is compromised when 2D objects are used as targets.

Compelling evidence for the difference between visuomotor interactions with 2D and 3D objects comes from experiments that looked at the adherence of grasping movements to Weber's law. According to Weber's law, the smallest detectable change along the size of an object is proportional to its initial size. The Just noticeable differences (JNDs), therefore, linearly increases with size, an indication of the relative nature of human perceptual resolution. Previous studies have shown that for grasping movements performed toward physical objects, JNDs (measured at the point in which the maximum grip aperture, MGA, is achieved) do not increase with the target's size, in violation of Weber's law (Ganel et al., 2008, 2014; Heath et al., 2011; Ganel, 2015). However, when grasping movements are directed to 2D targets, grasping apertures show an abnormal pattern of adherence to Weber's law (Holmes and Heath, 2013; Hosang et al., 2016; Ozana and Ganel, 2019a; Ozana et al., 2020). These findings, again, suggest that visuomotor interactions with virtual objects are subjected to perceptual and relative heuristics.

Physical objects provide rich visual cues about surface, depth, and perspective, and provide haptic feedback upon touch. Such objects may afford a sense of agency upon the interaction, a sense of agency that may be compromised in virtual interactions (Freud et al., 2018; Ozana and Ganel, 2019a). It is unclear, however, which of the visual and non-visual characteristics that lack in virtual interactions contribute to the observed difference between grasping trajectories toward 3D and 2D objects. For example, 2D grasping does not provide object-specific haptic information upon touch. This feedback may be used to calibrate and to refine visuomotor interactions in repeated trials (Davarpanah Jazi and Heath, 2016; Hosang et al., 2016; also see, Bingham et al., 2007; Johansson and Flanagan, 2009; Whitwell et al., 2016; Cesanek and Domini, 2017; Kopiske et al., 2017). The results of a recent study from our lab, however, showed that the provision of haptic feedback did not change the nature of the grasping trajectories in virtual settings (Ozana et al., 2018). In this study, participants were asked to "grasp" virtual objects within a remote virtual environment, with the use of a haptic telerobotic system that provided digitized representation of the location of the fingers, as well as object-specific haptic feedback upon virtual interception of the object. Although the system we used could potentially emulate visuomotor interactions with objects within the computerized space, the results showed that grasping trajectories within this system were atypical; Just as in the case of interactions with 2D images of objects, grip apertures obeyed to Weber's law. Furthermore, the pattern of adherence to Weber's law in the haptic feedback condition was similar to that obtained in a matched no-feedback condition. These findings converge with previous results (Afgin et al., 2017), to suggest that visuomotor control in virtual environments relies on less efficient, relative computations of size. Such inefficiency might be accounted for by an inadequate level of authenticity of the virtual system in terms of the quality of the visual and tactile feedback it provides (Ozana et al., 2018). It is possible that unreliable haptic feedback may not evoke the dedicated set of computations that support normal visuomotor control during interactions with physical objects. In the current study, we used an advanced VR system to simulate a more reliable sense of control of virtual objects. We tested whether such interactions could be supported by efficient visuomotor control that evades the influence of Weber's law. To achieve this purpose, we tested the potential contribution of informative haptic feedback upon touch.

VR systems are considered as hallmarks of immersive technology. Modern devices are capable of providing rich 3D binocular and monocular cues, as well as motion parallax cues, which correspond to the observer's position with respect to virtual objects in the digitized space. Compared to older virtual settings, modern virtual environments are designed to simulate a reliable sense of control in interactions with virtual objects and to allow natural and efficient visuomotor control within the virtual settings. Nevertheless, state-of-the-art VR systems still suffer from technical drawbacks in precision and temporal synchronization between their various components. For example, current technology does not provide complete transparency between the operator's movement and its digitized representation (Furmanek et al., 2019). As noted above, these technical disadvantages might compromise the sense of agency or potential interaction with the target. Hence, it is still unclear whether virtual interactions using current VR technology could operate in an efficient manner.

We note, that inefficient visuomotor control in virtual interactions could also be attributed to lack of familiarity with the task within the virtual settings. In the context of visual illusions, for example, it has been demonstrated that unpracticed, awkward grasping movements are more likely to be prone to illusory effects, compared to highly practiced precision grasps, In addition, the lack of efficiency during awkward grasping can be attenuated after extensive training (Gonzalez et al., 2008). In the current study, besides from studying the effect of haptic feedback on motor control in the VR, we were also able to look at the effect of practice, by comparing performance during sequential experimental blocks (bins) throughout the task.

Therefore, the present investigation was aimed at examining whether the typical pattern of grasping trajectories that characterizes 3D grasping would extend to actions toward virtual targets in a virtual space. To this end, participants performed bimanual grasping movements within a state-of-the-art VR environment that permits interactions with large objects using two-handed grasping. We note that while most of the cited work here focused on unimanual, precision grasps, two recent studies from our lab demonstrated action-perception dissociations during bimanual grasping (Ganel et al., 2017; Ozana and Ganel, 2020). Relevant to the current study, a dissociable pattern of adherence to Weber's law was recently found between bimanual grasping and perceptual adjustments (with the former type of response violating Weber's law) (Ganel et al., 2017). As in previous studies, the current study utilizes the adherence to the psychophysical principle of Weber's law as a tool to probe the nature of the underlying processes (Ganel, 2015; Ganel et al., 2017). To test the potential contribution of haptic feedback to the effect, we manipulated the availability of haptic information at the end of the grasp. In Experiment 1, different-sized virtual targets were presented for grasp while haptic feedback was not provided upon touch. In Experiment 2, we used the same experimental settings, but now haptic feedback was provided upon touch from a matching set of physical objects (see Hosang et al., 2016). Could grasping in a 3D VR environment escape the influence of Weber's law? What contribution does haptic feedback have to grasping performance within VR?

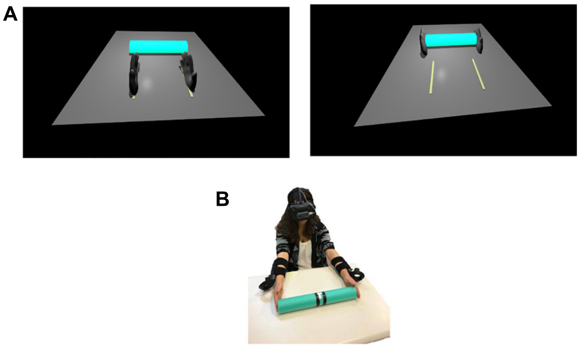

FIGURE 1 | Stimuli and experimental design. Participants performed bimanual grasping movements toward virtual objects presented in the virtual environment. Illustration of the participant view of the virtual environment **(A)**. Illustration of the experimental procedure in Experiment 2 (feedback condition) **(B)**.

EXPERIMENT 1

Materials and Methods

Participants

Fourteen healthy undergraduate students (six males, average age= 25.6, *SD* =1.3) participated in the experiment for the equivalent of 15$. All of the participants provided informed consent, which was approved by the BGU ethics committee.

Apparatus and Stimuli

Participants sat on a height-adjustable chair. An HTC Vive system that includes a head-mounted display (AMOLED, 1,080 × 1,200 pixels per eye, 90 Hz) and two motion trackers (SteamVR tracking Inc.) was used to display the virtual environment, and to capture movement within the environment. The apparatus tracked the 3D position of two controllers attached separately to the participant's left and right forearms (90 Hz sampling rate). A TouchDesigner software (version 2018.27300, Derivative, Toronto, ON) was used to control trial sequence and stimulus presentation.

Four tube-shaped virtual objects of different sizes (programmed to appear as 15, 25, 35, and 45 cm in length, 4 cm in height, and 5 cm in depth) were used as targets. In each trial, one target object was presented in the center of the 3D virtual environment that was constructed based on the physical environment of the lab. Two virtual hands represented the location of the motion trackers, which were attached to the participant's forearms, within the virtual environment (**Figure 1**).

In a recent study, we found that actions toward virtual targets are prone to speed-precision tradeoff effects (Ozana and Ganel, 2019b), an increase in the aperture velocities with target size that can lead to a pattern of scalar variability (a linear increase of the within-subject SDs of the response, as predicted by Weber's law) during grasping (Foster and Franz, 2013; Ganel et al., 2014, 2017; Ozana and Ganel, 2019b). To avoid the potential confounding effect of aperture velocities on the pattern of adherence to Weber's law, the initial distance between the participant's hands was dynamically adjusted to each target size. This procedure has been shown effective in previous research to attenuate the relation between velocity and size, accounting for the possibility of speed-precision tradeoff effects (Ganel et al., 2014, 2017; Ozana and Ganel, 2019b). Notably, adjusting the initial distance between the hands can also reduce the inherent relation between movement time and target size, which can lead to spurious grip scaling in normalized movement procedures (such as the one used here) (Whitwell and Goodale, 2013). Two virtual strips in four different distances were used as starting positions. The distance between the lines was always 5 cm smaller than the target object's length (10, 20, 30, 40 cm). Velcro strips (4 cm in length) were used to provide haptic feedback for each starting point. The distance between the starting position and the target object was 25 cm (measured from the center of the Velcro strip to the target edges). The participant's viewing distance from the target object was about 35 cm.

Procedure

Prior to each trial, the participants placed their right and left hands on the virtual strips (starting position). The participants were asked to "grasp" the edges of the target upon hearing a "go" signal, and to keep their hands on the stimulus edges until a second tone was presented. No haptic feedback was provided in Experiment 1. Once the second tone was presented, participants returned their hands to the starting position and waited for the beginning of the next trial. The go signal was presented 1 sec after the visual presentation of the target, and the second tone was presented 4 sec after the first one.

After a short equipment calibration, during which the participants were acquainted with the virtual environment, each participant underwent three sequential experimental blocks, in which each stimulus was presented 15 times in a pseudo-randomized order (180 trails in total).

Data Analysis

The 3D trajectories of the hands were recorded for each trial and were analyzed offline using MATLAB software (Version 9.0, The Mathworks, Natick, MA). The grip aperture was computed as the Euclidean distance between the two trackers (after the positions of both markers were transformed into a common coordinate system using homogeneous transformations). The aperture data were filtered offline using a standard 2-way (zero lag), low-pass, third-order Butterworth filter with a 6 Hz cutoff. The cutoff frequency was verified visually with the data. Grip aperture tangential velocity was computed by differentiating the vector of the grip aperture. Movement onset was set at the point in time after the presentation of the go command, in which the grip aperture's tangential velocity exceeded 10% of its maximal velocity for a consecutive duration of 100 ms, and then tracing back the point in time in which the difference between velocity samples was positive (positive acceleration). Movement offset was set at the point in time after the maximal grip aperture velocity and before the point in time of the presentation of the second tone, in which the grip aperture's tangential velocity was lower than 10% of its maximal velocity for a consecutive duration of 100 ms, and then by tracing forward the time in which the difference between velocity samples was negative (negative acceleration). The determination of the aperture and the points of onset and offset was visually supervised. Each aperture trace was animated using a stick diagram, and the onset and offset markers were presented with respect to the grip aperture velocity and could be manually adjusted by the operator.

To analyze grip apertures, each movement was divided into 10 equal intervals (10–100%). The average grip aperture and JNDs were calculated for each interval and for each object size separately. As in previous studies, JNDs were measured by the within-subject standard deviation of the aperture (Ganel et al., 2008). The adherence to Weber's law was measured with a within-subject planned comparison test of the linear component of object size during each percentile of the movement, with emphasis on the more crucial, second part of the normalized movement (60–100%). JNDs were also computed at the point in time in which MGA was achieved. The analysis of the JND data at different time points within the movement was conducted to account for potential issues related to time-dependent scaling of the MGA during virtual grasping. Specifically, while the MGA is considered a reliable measure of the sensitivity of aperture to physical objects size in 3D grasping, accumulating evidence suggests that the MGA is a less reliable measure of performance during 2D grasping (Afgin et al., 2017; Ozana et al., 2018; Ozana and Ganel, 2018, 2019b). Additional kinematic aspects of the movement were also calculated: Reaction time (RT), which reflects the time between the go signal and between movement initiation, the absolute time to MGA (tMGA), and the total movement time (MT). The possible effect of practice was tested by comparing JNDs and grip apertures across the three sequential experimental blocks. The main independent variables were therefore, block (block 1, block 2, block 3), normalized movement time (10 levels), and object size (15, 25, 35, 45 cm).

We applied a correction for outliers on each participant's aperture data. Trials in which the grip apertures at the point of movement completion were 2.5 standard deviations higher or lower than the participant's mean aperture for the same object were removed from the analysis. The correction resulted in the exclusion of less than 2% of the trials.

Results

Movement Profile

Average grip apertures (for each interval) toward the virtual targets are presented in **Figure 2**. As can be seen in the figure, grip apertures reflected the size differences between the objects. First, a repeated-measures ANOVA with block (3 levels), normalized movement time (10 levels), and object size (15, 25, 35, 45 cm) as within-subject independent variables was conducted on the *grip aperture data*. A Greenhouse-Geisser correction was applied for cases in which sphericity assumption was violated (based on Mauchly's Test of Sphericity). The main effect of block was not significant [$F_{(1.1,17.3)} = 1.3$, $p = 0.28$], indicating that grip apertures were stable across blocks. Significant main effects of normalized movement time [$F_{(1,7,22.7)} = 160.5$, $p < 0.001$, $\eta_p{}^2 = 0.92$] and object size [$F_{(1.6,21.2)} = 4{,}719$, $p < 0.001$, $\eta_p{}^2 = 0.99$] showed that grip apertures changed throughout the movement and corresponded to the target size. The interaction between block and movement was not significant [$F_{(18,234)} = 1.3$, $p = 0.18$]. Yet, a significant interaction between block and size [$F_{(6,78)} = 2.4$, $p = 0.03$, $\eta_p{}^2 = 0.15$], indicated that grip apertures differently corresponded to size at different blocks of the experiment. There was a significant interaction between movement and size [$F_{(27,351)} = 11.4$, $p < 0.001$, $\eta_p{}^2 = 0.47$], indicating that sensitivity to size developed throughout the movement. A significant three-way interaction [$F_{(54,702)} = 1.6$, $p < 0.01$, $\eta_p{}^2 = 0.11$], showed that the time-dependent scaling of the aperture differed across blocks. MGAs also showed sensitivity to the target's size [$F_{(1.3,17.1)} = 4{,}536$, $p < 0.001$, $\eta_p{}^2 = 0.99$] (26, 37, 47, 57 cm from the smallest to the largest object, respectively).

The response time data for the three blocks is presented in **Table 1**. A repeated-measures ANOVA test with block and size as the independent variables was conducted on RT data. The main effect of block was not significant [$F_{(1.1,15.4)} = 1.8$, $p = 0.17$]. A significant effect of object size [$F_{(3,39)} = 9.8$, $p < 0.001$, $\eta_p{}^2 = 0.43$], indicated that time to initiate the movement differed between the different target sizes (461, 444, 460, 436 ms). There was a significant interaction, however, between block and size, that showed that the relation between RT and size differed across the three blocks [$F_{(679)} = 3.8$, $p < 0.01$, $\eta_p{}^2 = 0.22$]. Unlike the RT data, a repeated-measures ANOVA on tMGAs showed a significant effect of block [$F_{(1.4,18.5)} = 5.3$, $p = 0.01$, $\eta_p{}^2 = 0.30$] (908, 859, 836 ms, for the first, second, and third block, respectively), which indicates that time to reach maximum grip aperture differed in different blocks. The main effect of size was not significant [$F_{(1.3,17)} = 2.2$, $p = 0.99$]. Yet, a significant interaction between block and size [$F_{(3,39.8)} = 4.9$, $p < 0.001$, $\eta_p{}^2 = 0.27$] showed that the relation between the tMGA and size was different across blocks. Finally, a similar analysis of the MT data showed a significant main effect of block [$F_{(1.2,15.6)} = 12$, $p < 0.001$, $\eta_p{}^2 = 0.48$]. *Post hoc* test with Bonferroni correction showed that mean

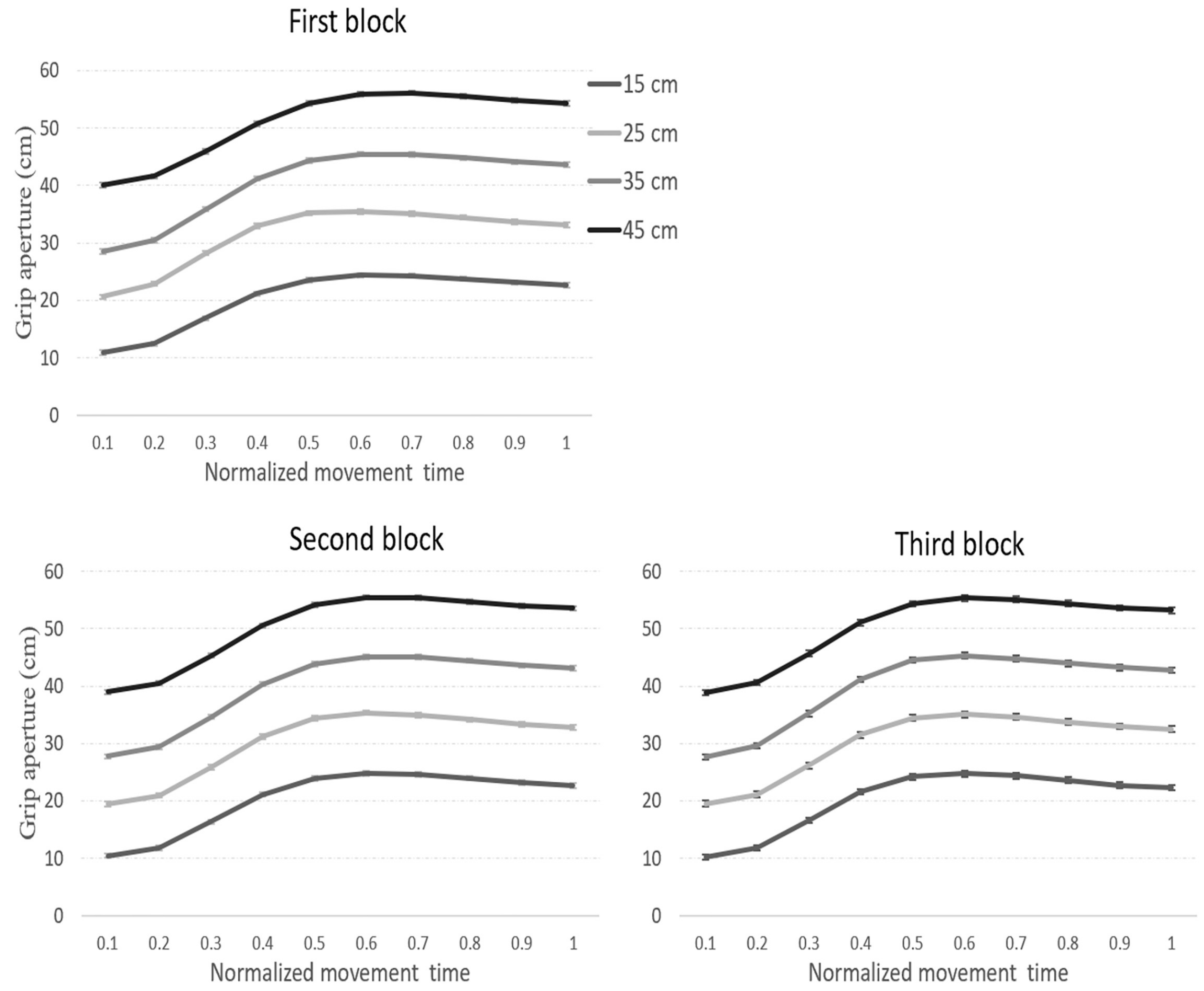

FIGURE 2 | Average grip apertures across the three sequential experimental blocks in Experiment 1. Throughout the three blocks, apertures reflected the size differences between the objects. Error bars represent confidence intervals in repeated measures ANOVAs (Jarmasz and Hollands, 2009).

TABLE 1 | Mean RTs, tMGAs, and MTs in ms (± 1 SD) for each of the objects in Experiment 1.

		15 cm	**25 cm**	**35 cm**	**45 cm**
Block 1	RT	468 ± 72	468 ± 84	494 ± 109	449 ± 84
	tMGA	957 ± 101	840 ± 98	905 ± 104	957 ± 101
	MT	1,777 ± 224	1,797 ± 260	1,759 ± 165	1,803 ± 194
Block 2	RT	456 ± 73	437 ± 76	431 ± 65	415 ± 62
	tMGA	839 ± 95	842 ± 72	883 ± 83	869 ± 110
	MT	1,589 ± 116	1,662 ± 114	1,651 ± 126	1,658 ± 193
Block 3	RT	460 ± 106	426 ± 77	456 ± 115	445 ± 122
	tMGA	841 ± 144	828 ± 107	822 ± 118	853 ± 131
	MT	1,584 ± 115	1,620 ± 82	1,600 ± 130	1,611 ± 114

difference between the first block (1,784 ms) and the second block (1,640 ms) [$t_{(11)} = 4.8$, $p < 0.001$], and between the first block and the third block (1,604 ms) [$t_{(11)} = 3.4$, $p = 0.01$] were both significant. These results indicate that the time to complete the movement was relatively slower in the first block. A test of the within-subject contrasts showed a significant linear trend, indicating that the time to complete the movement decreased with practice [$F_{(1,13)} = 11$, $p <$

0.001, $\eta_p^2 = 0.47$] (1,784, 1,640, 1,601 ms, respectively). The main effect of size did not reach statistical significance [$F_{(3,39)} = 2.6$, $p = 0.06$]. The interaction between block and size was also not significant [$F_{(2.8,37.2)} = 0.90$, $p = 0.48$]. We also note that times to complete the movement (MTs) were considerably longer and that maximum grip apertures arrived at a relatively early stage in the normalized movement (52%) compared to previous 3D grasping (Jakobson and Goodale, 1991; Smeets and Brenner, 1999; see Ozana et al., 2018, for similar findings).

Thus, while the movement showed some characteristics that were similar to normal 3D grasping control and while apertures were sensitive to the target's size, other kinematics of the movement were somewhat atypical. There were also differences among several kinematic aspects across different blocks of the movement, which suggest that practice with the task had an effect on grasping performance. The effect of practice on JNDs will be further explored in the next section.

JNDs

JNDs across the movement are presented in **Figure 3**. JNDs during the second part of the movement increased with the target size, in line with Weber's law.

As we mentioned earlier, the main analysis of the JNDs data was conducted on the second part of the normalized movement time. A repeated-measures ANOVA with block, normalized movement time (5 levels, 60–100%), and object size as independent variables was conducted on the data. The main effect of block [$F_{(1.4,18.5)} = 0.3$, $p = 0.97$] was not significant, which indicates that practice did not affect the overall size of the JND. There were significant main effects of normalized movement time [$F_{(1,14.2)} = 56$, $p < 0.001$, $\eta_p^2 = 0.81$] and object size [$F_{(3,39)} = 11.1$, $p < 0.001$, $\eta_p^2 = 0.46$], which indicate that JNDs differed across the normalized movement, and for different object sizes. The interaction between block and size [$F_{(3.5,45.9)} = 2.2$, $p = 0.08$], however, was not significant. The interaction between block and movement [$F_{(2.7,35.8)} = 0.1$, $p = 0.99$], between

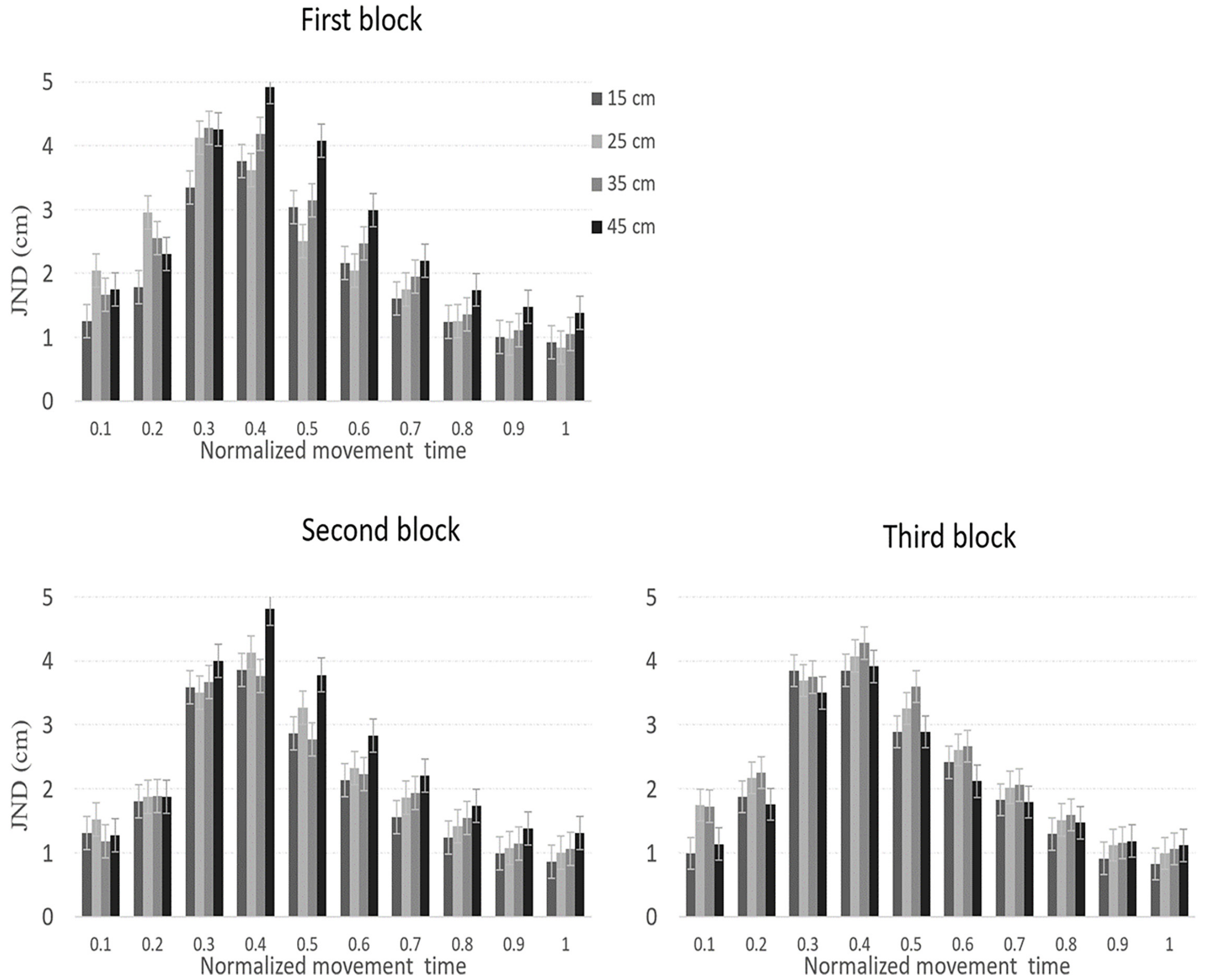

FIGURE 3 | JNDs across the three sequential experimental blocks in Experiment 1. In all blocks, JNDs increased with size throughout most of the movement, in line with Weber's law. Error bars represent confidence intervals in repeated measures ANOVAs (Jarmasz and Hollands, 2009).

movement and size [$F_{(3.7,48.5)} = 0.5$, $p = 0.85$] and the three-way interaction were also non-significant [$F_{(24,312)} = 0.4$, $p = 0.98$]. Lastly, the main effect of object size at the point in which MGAs were achieved was not significant [$F_{(3,39)} = 1.1$, $p = 0.34$].

To test for adherence to Weber's law, we performed a within-subject planned comparison test of the linear component of object size during the second part of the movement. The test showed that JNDs linearly increased with size [$F_{(1,13)} = 33$, $p < 0.001$, $\eta_p^2 = 0.72$] (1.4, 1.5, 1.6, 1.8 cm) in line with Weber's law. As discussed earlier, the (linear) pattern of the JNDs could be confounded by the velocity of the grip aperture (Ganel et al., 2014; Ozana and Ganel, 2019b). Therefore, a similar repeated-measures ANOVA test with block, normalized movement time, and size as independent variables was conducted on the aperture velocities during the second part of the normalized movement. Importantly, the main effect of block was not significant [$F_{(1.1,14.9)} = 2.2$, $p = 0.12$]. The main effects of size [$F(3, 39) = 2.7$, $p = 0.058$] and the interaction between block and size [$F_{(2.7,35.6)} = 2.2$, $p = 0.09$] approached significance. The reader should note that these trends toward significance might have resulted from performance during the first block (see **Table 2**). Indeed, as can be seen in the table, in the first block (but not the second or third blocks), aperture velocity linearly increased with size in each percentile of the second part of the movement. Also note that the linear pattern of JNDs is still maintained when excluding the first block from the analysis [$F_{(1,13)} = 11$, $p = 0.01$, $\eta_p^2 = 0.46$]. A potential speed-precision tradeoff effect between aperture velocities and JNDs could therefore be ruled out from the final two blocks but could have affected performance in the first block (**Table 2**). Finally, to provide a thorough investigation of the pattern of adherence to Weber's law across different stages of the normalized movement, planned comparisons of the linear component of size were conducted separately on the JNDs and aperture velocities data for each movement percentile and in each block. The results are also shown in **Table 2**. Note, that JNDs increased with the target size at the final stages of the movement.

The results of Experiment 1 show that when tactile feedback is not available at the end of the movement, actions in VR are subjected to perceptual regularities of object size, and obey to Weber's law. This pattern of results indicates that grasping movements relied on less effective, relative computations of the target, compared to normal 3D grasping. The results also show several variations in kinematic aspects of the movement between blocks. Yet, we note that these differences between the blocks along the pattern of adherence to Weber's law did not reach statistical significance. Experiment 2 was designed to examine the role of haptic feedback in the adherence to Weber's law. The experimental design was similar to the one used in Experiment 1, but now object-specific haptic information was provided upon touch.

EXPERIMENT 2

Materials and Methods

Participants

Fourteen additional participants (six males, average age = 25.2, *SD* = 1.3) participated in the experiment for the same monetary compensation as in Experiment 1. The result of one participant was excluded from the analysis because she failed to follow the experimental instructions.

Procedure and Design

The procedure was similar to the one used in Experiment 1, except that now a matching size set of 3D objects (15, 25, 35, 45 cm) made out of polyester, were embedded in the virtual environment in a location that matched that of the virtual target. In each trial, one 3D object was placed by the experimenter prior to movement initiation and provided object-specific haptic information upon touching the virtual target. Less than 2% of the

TABLE 2 | Planned comparisons of the linear component of size for the JNDs and aperture velocity data in each of the normalized movement percentiles in Experiment 1.

	Experiment 1 (No haptic feedback)											
	Block 1				Block 2				Block 3			
	JND		Aperture velocity		JND		Aperture velocity		JND		Aperture velocity	
	F	η_p^2	*F*	η_p^2	*F*	η_p^2	F	η_p^2	*F*	η_p^2	*F*	η_p^2
10%	0.8	0.06	6.3*	0.32	0.3	0.02	0.3	0.02	1.1	0.11	0.8	0.06
20%	1.7	0.11	0.8	0.007	0.4	0.03	1.3	0.09	0.6	0.005	0.5	0.04
30%	6.2**	0.32	5.8*	0.31	3.4	0.20	1.3	0.09	0.4	0.03	1.5	0.10
40%	9.8**	0.43	7.8*	0.37	5.1*	0.28	3.3	0.20	0.6	0.04	2.9	0.18
50%	7.4**	0.36	6.4*	0.33	5.1*	0.28	7.5*	0.36	0.4	0.03	2.6	0.17
60%	8.6**	0.40	7.3*	0.36	3.7	0.22	1.9	0.12	0.5	0.004	0.3	0.003
70%	16.9**	0.56	5.7*	0.30	21.1**	0.62	1.2	0.08	0.1	0.009	0.3	0.003
80%	12.5**	0.49	4.2	0.24	28.6**	0.68	0.7	0.05	2.2	0.15	0.05	0.000
90%	15.3**	0.54	5.6*	0.30	27.2**	0.67	0.4	0.03	5.2*	0.28	0.2	0.02
100%	13.2**	0.50	13.1**	0.50	23.9**	0.64	0.8	0.06	7.9**	0.38	0.8	0.06

*$p < 0.05$, **$P < 0.01$.

trials were considered as outliers based on the same criterion used in Experiment 1.

Results

Movement Profile

Average grip apertures in Experiment 2 are presented in **Figure 4**. As in Experiment 1, grip apertures reflected the size differences between the objects. A repeated-measures ANOVA with size, block, and normalized movement time (10 levels) was conducted on the grip aperture data. The main effect for block was not significant [$F_{(1.3,17.3)} = 1.3$, $p = 0.28$]. There were significant main effects of normalized movement time [$F_{(1.7,22.7)} = 160.5$, $p < 0.001$, $\eta_p^2 = 0.92$], and of object size [$F_{(1.6,21.2)} = 4719$, $p < 0.001$, $\eta_p^2 = 0.99$]. The interaction between block and movement was not significant [$F_{(18,234)} = 1.3$, $p = 0.18$]. Yet, as in Experiment 1, there was a significant interaction between block and size [$F_{(6,78)} = 2.4$, $p = 0.03$, $\eta_p^2 = 0.15$], which indicates that grip apertures were shaped differently to different target sizes at different blocks of the movement. The interaction between movement and size was significant [$F_{(27,351)} = 11.9$, $p < 0.001$, $\eta_p^2 = 0.47$]. There was also a significant three-way interaction [$F_{(54,702)} = 1.6$, $p < 0.01$, $\eta_p^2 = 0.11$], which indicates that the relation between the movement and grip aperture with respect to size differed across the blocks. An analysis of the MGA data showed a significant main effect for size [$F_{(1.4,17.3)} = 2469$, $p < 0.001$, $\eta_p^2 = 0.99$] (25, 35, 44, 54 cm, from the smallest to the largest target, respectively).

Response times for each block in Experiment 2 are presented in **Table 3**. A repeated-measures ANOVA of the RT data revealed a significant main effect of block [$F_{(2,24)} = 6.6$, $p < 0.01$, $\eta_p^2 = 0.35$]. *Post hoc* tests with Bonferroni correction showed that mean difference between the first block (450 ms) and the second block (424 ms) did not reach statistical significance [$t_{(10)} = 2$, $p = 0.18$]. However, the mean difference between the first and third block (409 ms) was significant [$t_{(10)} = 3.1$, $p = 0.02$]. There was also a

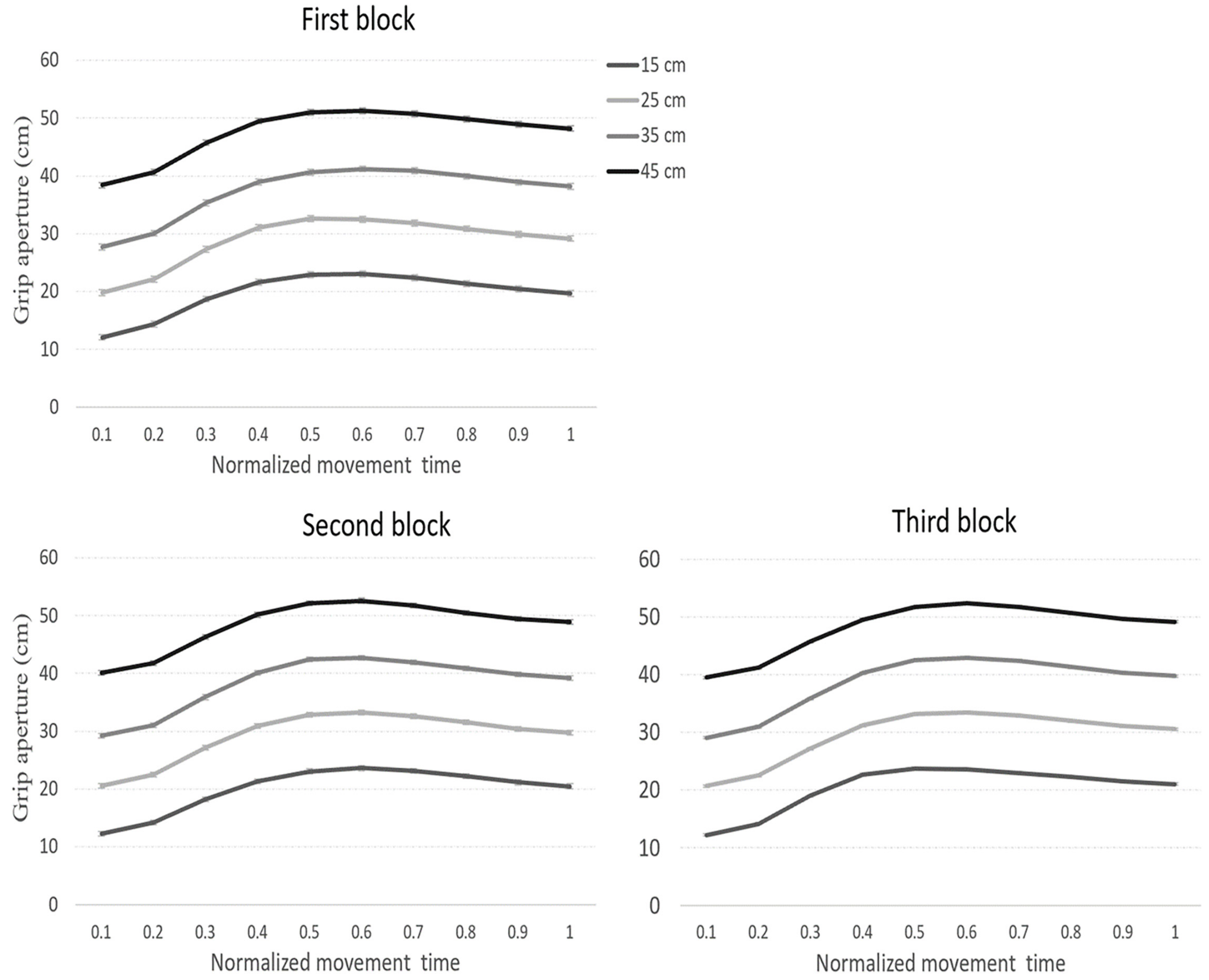

FIGURE 4 | Average grip apertures across the three sequential experimental blocks Experiment 2. Grip apertures reflected the size differences between the objects. Error bars represent confidence intervals in repeated measures ANOVAs (Jarmasz and Hollands, 2009).

TABLE 3 | Mean RTs, tMGAs, and MTs (±1 SD) in ms for each of the objects in Experiment 2.

		15 cm	25 cm	35 cm	45 cm
Block 1	RT	483 ± 76	435 ± 52	436 ± 50	446 ± 32
	tMGA	741 ± 92	781 ± 144	842 ± 132	753 ± 87
	MT	1, 575 ± 380	1, 624 ± 307	1, 654 ± 277	1, 591 ± 332
Block 2	RT	433 ± 60	415 ± 38	421 ± 22	431 ± 59
	tMGA	742 ± 72	703 ± 55	748 ± 108	714 ± 79
	MT	1, 594 ± 299	1, 496 ± 219	1, 543 ± 279	1, 491 ± 223
Block 3	RT	428 ± 39	404 ± 31	406 ± 30	399 ± 31
	tMGA	680 ± 83‘	685 ± 67	699 ± 73	725 ± 92
	MT	1, 505 ± 253	1, 461 ± 199	1, 470 ± 214	1, 507 ± 227

significant main effect of size [$F_{(2,24)} = 6.8, p < 0.01, \eta_p{}^2 = 0.36$]. The *post hoc* tests with Bonferroni correction did not show a significant difference between the mean score of the 15 cm target (smallest target, 448 ms) and the 25 cm target (418 ms) [$t_{(10)} = 2.8, p = 0.08$], or between the smallest target and the 45 cm target (425 ms) [$t_{(10)} = 2.5, p = 0.15$]. However, there was a significant difference between the mean score of the smallest target and that of the 35 cm target (421 ms) [$t_{(10)} = 3.2, p = 0.04$]. The interaction between block and size [$F_{(2,24)} = 1.2, p = 0.27$] was not significant. Analysis of the tMGA data also showed significant main effects of block [$F_{(2.24)} = 13.4, p < 0.001, \eta_p{}^2 = 0.52$] (779, 729, 697 ms, respectively) and of size [$F_{(3,36)} = 5.1, p < 0.01, \eta_p{}^2 = 0.30$] (721, 723, 763, 731 ms, respectively), which indicate that the time in which the MGA was achieved was different in the different blocks and for the different sizes. The interaction between block and size was also significant [$F_{(2,24.6)} = 4.5, p = 0.02, \eta_p{}^2 = 0.27$], indicating that the relation between tMGA and size differed between the blocks. Unlike RTs and tMGAs, an analysis of the MT data did not show a significant main effect of block [$F_{(2,24)} = 2.7, p = 0.08$] or of size [$F_{(2.1,25.8)} = 1, p = 0.36$]. A significant interaction [$F_{(2.27)} = 3.9, p = 0.02, \eta_p{}^2 = 0.24$], however, indicated that time to complete the movement in relation to target size differed between the blocks.

The overall differences along the response time pattern in experiments 1 and 2 did not reach statistical significance. A mixed-model ANOVA of MTs with block and size as independent factors did not reveal a significant main effect of experiment [$F_{(1,25)} = 3.4, p = 0.07$]. Similarly, tests conducted on the relative time of the MGA in the normalized movement [$F_{(1,25)} = 3.4, p = 0.07$], and on RTs [$F_{(1,25)} = 2.9, p = 0.09$], did not show a significant effect of experiment. We note that as in Experiment 1, the time to complete the movement toward the virtual target was relatively longer than in typical 3D grasping tasks, and that MGAs arrived at a relatively early part of the movement (48%) (Jakobson and Goodale, 1991; Smeets and Brenner, 1999).

JNDs

JNDs across the normalized movement trajectory are presented in **Figure 5**. As can be seen in the figure, and unlike the pattern of results in Experiment 1, JNDs did not increase with size at the final stages of the movement, in violation of Weber's law.

A repeated-measures ANOVA with block, normalized movement time during the second part of the movement (5 levels), and object size as independent variables was conducted on the JND data. There was a significant main effect for block [$F_{(1.3,13.1)} = 5.5, p = 0.03, \eta_p{}^2 = 0.31$]. Simple within-subject contrasts revealed that JNDs in the first block were significantly larger than the second block [$F_{(1,12)} = 6.9, p = 0.02, \eta_p{}^2 = 0.36$] and the third block [$F_{(1,12)} = 4.7, p = 0.05, \eta_p{}^2 = 0.28$] (2.5, 1.8, 1.9 cm, for the first, second, and third block, respectively), indicating that practice decreased the overall size of JNDs (and therefore, increased precision in the task). There was a main effect of movement [$F_{(1.1,13.2)} = 21.6, p < 0.001, \eta_p{}^2 = 0.64$], which indicates that JNDs values were different at different stages of the movement. Yet, the main effect of size was not significant [$F_{(3,36)} = 1.2, p = 0.31$]. Importantly, the interactions between block and movement [$F_{(2.2,27.1)} = 0.94, p = 0.48$], block and size [$F_{(6,72)} = 0.64, p = 0.69$], and between movement and size [$F_{(3.3,40.6)} = 1.7, p = 0.16$], were not significant. A significant three-way interaction [$F_{(24,288)} = 1.6, p = 0.03, \eta_p{}^2 = 0.11$], indicated that the relation between movement and size was different at different blocks. The main effect of size at the point of MGA was not significant [$F_{(3,36)} = 1, p = 0.38$] (2.2, 2.4, 2.3, 2.2 cm, from the smallest to the largest object).

Unlike the results of Experiment 1, a within-subject planned comparison test of the linear component of size did not show a linear increase in JNDs with size [$F_{(1,12)} = 1.1, p = 0.30$], in violation of Weber's law. To test if the JND pattern in the current experiment was significantly different from that obtained in Experiment 1 (when no feedback was allowed), a mixed ANOVA with experiment as a between-subjects factor, and block, normalized movement time, and size as a within-subject factors was conducted on the JND data. Notably, significant interaction between experiment and size [$F_{(2.8,71.4)} = 3.4, p = 0.02, \eta_p{}^2 = 0.12$] indicated that the JND pattern was different between the two experiments (see **Figure 6**). Planned comparisons of the linear component of size for each percentile of the movement are presented in **Table 4**. Note that as in Experiment 1, the pattern of scalar variability of JNDs with size that was obtained in block 1 was confounded by the velocity of the grip aperture. Therefore, it is unclear whether the linear increase of the JNDs in the first block reflects genuine adherence to Weber's law. We also note that there was a peculiar pattern of an increase of JNDs with size at 10% of the

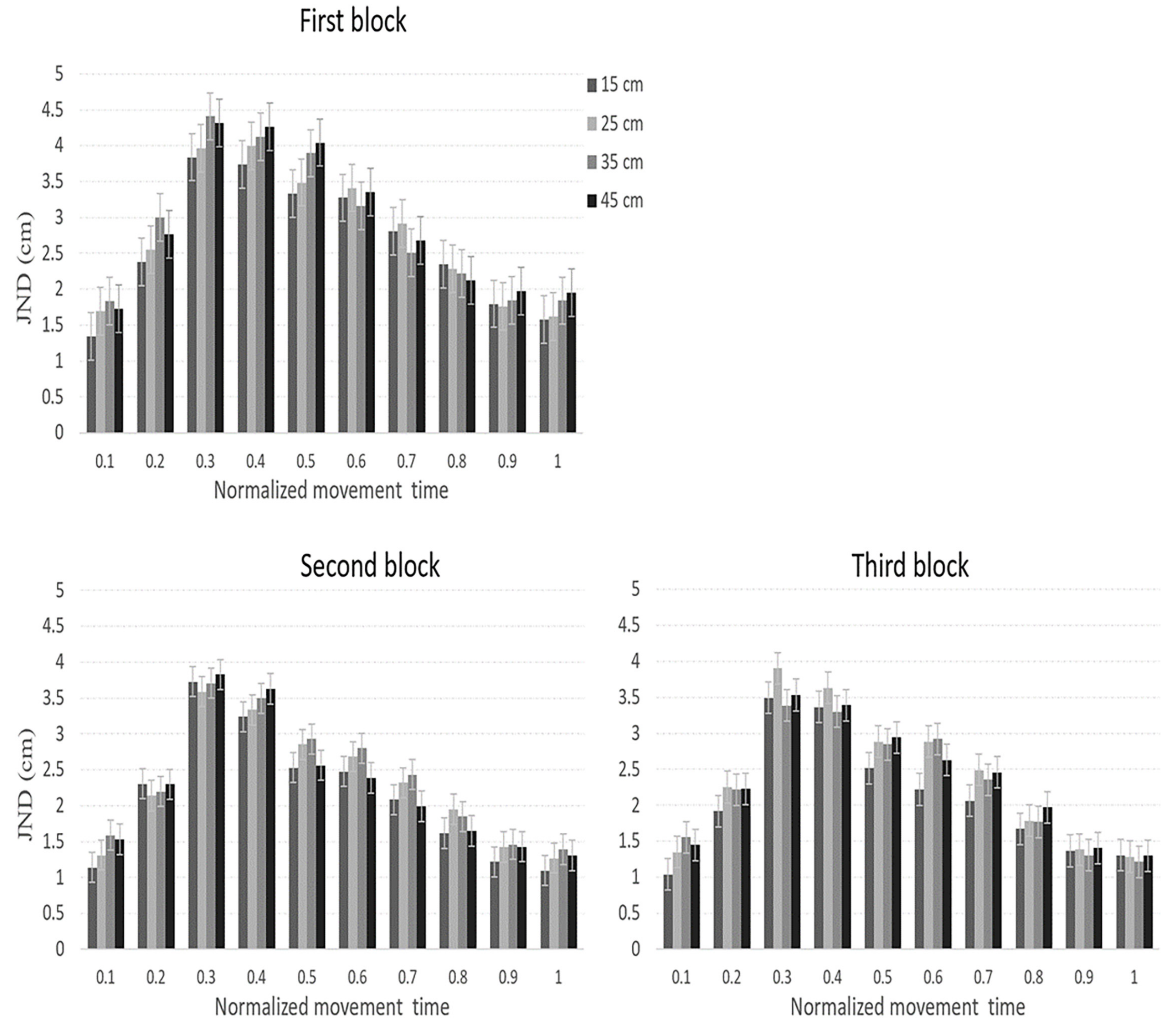

FIGURE 5 | JNDs across the three sequential experimental blocks in Experiment 2. In all blocks, and unlike the results of Experiment 1, JNDs generally did not increase with size, in violation of Weber's law. Error bars represent confidence intervals in repeated measures ANOVAs (Jarmasz and Hollands, 2009).

movement. However, this unexpected pattern probably does not represent genuine adherence to Weber's law because JNDs did not show stable increase with size throughout the entire size range (see **Figures 5**, **6**).

The results of Experiment 2 suggest that the availability of accurate haptic information upon touch contributes to efficient performance in VR in terms of resistance to perceptual regularities. Unlike Experiment 1 (and similarly to 3D grasping), interactions that entail obtaining accurate haptic feedback from the target were refractory to Weber's law, which could indicate more analytic computation of size.

The results also suggest that practice affected participants' performance in the task. JNDs in the first block were significantly larger than the JNDs in the remaining blocks, which is an indication of poorer visual resolution to size (but could also indicate more stochastic noise). It is unclear, to which extent did training contributed to the overall pattern of resistance to Weber's law. Indeed, while during the first block (but not for the remaining blocks) JNDs at the point of movement completion adhered to Weber's law, a similar pattern of aperture velocity also emerged at this point in time. As we mentioned earlier, such co-occurrence could serve as an alternative account to a pattern of scalar variability; it may simply reflect a speed-precision tradeoff effect (Foster and Franz, 2013; Ganel et al., 2014; Ozana and Ganel, 2019b). The possible effect of training on the adherence to Weber's law in VR haptic systems should be further explored in future studies.

Finally, it should be noted that while actions in the feedback condition showed a typical pattern of resistance

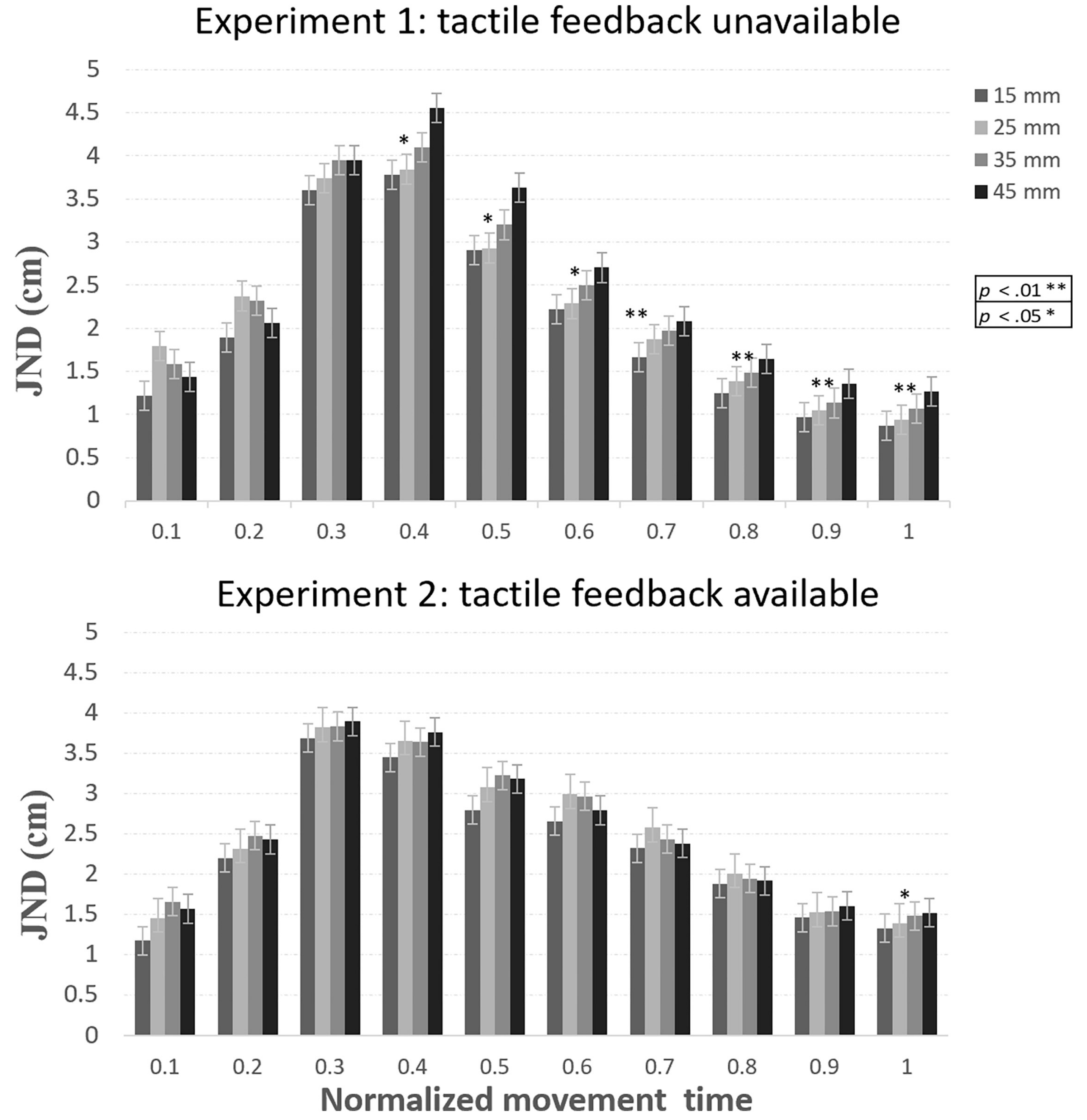

FIGURE 6 | Average JNDs across the three blocks in Experiments 1 and 2. In Experiment 1, JNDs adhered to Weber's law throughout most stages of the movement. Conversely, in Experiment 2, Weber's law was violated in most stages of the movement. Error bars represent confidence intervals in repeated measures ANOVAs (Jarmasz and Hollands, 2009). $^*p < 0.05$; $^{**}p < 0.01$.

to Weber's law, they were still some divergences along several kinematic aspects of the movement. For instance, just as in Experiment 1, movements were relatively slow compared to actions directed to 3D objects. These differences might be attributed to participants' unfamiliarity with the computerized environment, which could be further attenuated via extensive training.

GENERAL DISCUSSION

In the current study, we examined the nature of visuomotor interactions with digitized objects in a virtual environment. The results suggest that haptic information affects the way visual information is processed within virtual settings. When haptic information was not available, grip apertures showed

TABLE 4 | Planned comparisons of the linear component of size for the JNDs and aperture velocity data in each of the normalized movement percentiles in Experiment 2.

	Experiment 2 (haptic feedback)											
	Block 1				Block 2				Block 3			
	JND		Aperture velocity		JND		Aperture velocity		JND		Aperture velocity	
	F	η_p^2	*F*	η_p^2	*F*	η_p^2	*F*	η_p^2	*F*	η_p^2	*F*	η_p^2
10%	2.3	0.16	0.2	0.09	7.9**	0.40	0.00	0.02	6.5*	0.35	1.0	0.07
20%	2.4	0.16	3.2	0.21	0.01	0.00	0.1	0.01	0.6	0.005	0.04	0.004
30%	1.6	0.12	6.9*	0.36	0.1	0.01	4.6	0.27	1.0	0.08	2.3	0.16
40%	1.3	0.10	2.2	0.16	0.9	0.07	1.1	0.08	0.5	0.004	6.1*	0.33
50%	2.9	0.20	0.01	0.002	0.02	0.002	1.0	0.08	1.4	0.10	2.2	0.15
60%	0.0	0.00	2.9	0.19	0.7	0.006	1.9	0.12	1.4	0.10	3.3	0.21
70%	0.5	0.04	0.1	0.01	0.9	0.007	4.9*	0.29	1.5	0.11	7.9*	0.39
80%	0.6	0.05	2.2	0.15	0.0	0.00	2.8	0.19	3.0	0.20	4.6	0.28
90%	0.8	0.06	3.5	0.22	1.2	0.09	3.0	0.20	0.1	0.001	5.8*	0.32
100%	5.6*	0.32	8.5*	0.41	1.7	0.12	0.9	0.07	0.7	0.006	3.4	0.22

*$P < 0.05$, **$P < 0.01$.

an abnormal pattern and were subjected to a perceptual heuristic of relative size, obeying Weber's law. However, when grasping movements were accompanied with accurate haptic feedback upon touch, Weber's law was violated throughout most stages of the movement, a pattern that also characterizes normal 3D grasping.

The idea that the visual system is divided into two functionally distinct pathways has gained ample support from neurological and behavioral studies (for a review, see Milner and Goodale, 2008). For example, previous studies showed that Weber's law does not fully apply to bimanual and precision grasping movements, suggesting that the visual control of action relies on analytical coding of object size (Ganel et al., 2008, 2017; but see Smeets and Brenner, 2008 for an alternative account). However, recent studies have shown that when 2D objects are used as targets, actions are no longer immune to Weber's law (Holmes and Heath, 2013; Ozana and Ganel, 2019a,b), as well as to other perceptual regularities (Chen et al., 2015; Freud and Ganel, 2015; Ozana and Ganel, 2018). These results suggest that the dissociation between action and perception does not extend to visuomotor interactions with virtual, 2D objects. The current results, however, show that virtual interactions in state-of-the-art virtual settings could still evade Weber's law, provided that accurate haptic feedback is available upon touch. These findings indicate that crucial aspects of normal visuomotor control could generalize to interactions with virtual objects, given that such interactions provide a reliable sense of control. In consideration of previous studies, this suggests that the efficiency of the action toward virtual targets in terms of resistance to task-irrelevant information depends on the degree of authenticity provided by the virtual system (Afgin et al., 2017; Ozana et al., 2018). Indeed, it could be argued that interactions within a 3D environment that entails immediate haptic feedback from a virtual object can be considered as more reliable than other types of interactions with virtual objects, interactions that are performed on touch screens or in remote virtual settings and do not provide authentic haptic feedback. This idea is also in line with the suggestion that visuomotor computations are influenced by the potential outcome of the interaction (Hosang et al., 2016; Freud et al., 2018; Ozana and Ganel, 2019a).

It should be noted, however, that while the results of the current study suggest that actions toward virtual targets could be performed in an analytical and efficient manner, the extent to which this could apply to present immersive technologies remains unclear. For example, in an attempt to maximize the potential effect of tactile feedback from the virtual target on visuomotor control, haptic information in our feedback condition was provided from physical objects of matched sizes, which were embedded in the virtual environment. Furthermore, we used experimental instructions that encouraged participants to grasp the virtual targets the same way they grasp real 3D objects. It is unclear whether current tactile virtual technology (e.g., feedback from tactile gloves) can evoke a similar sense of interaction. Such virtual feedback devices, for example, may still lack in terms of precision and timing delays, which could compromise the sense of agency, leading to inefficient performance (Rohde and Ernst, 2016), and the usage of relative metrics (Afgin et al., 2017). Virtual interactions may also entail different gestures other than grasping, which could rely on different computations of size (Ozana et al., 2020). Hence, further research should explore the mechanisms that permit normal performances within VR.

Previous studies highlighted the role of tactile feedback in 2D and 3D grasping (Bingham et al., 2007; Johansson and Flanagan, 2009; Whitwell et al., 2014, 2016; Davarpanah Jazi et al., 2015; Hosang et al., 2016; Cesanek and Domini, 2017; Kopiske et al., 2017). For instance, it was argued that the provision of terminal haptic feedback could support analytic visuomotor control via visuo-haptic calibration on subsequent trials (Davarpanah Jazi et al., 2015; Hosang et al., 2016). In 2D grasping, initial support for this idea was obtained in a study that utilized a delayed haptic-feedback design, in which a 3D object of matching size was placed between the participant's index and thumb following movement completion. In line with the current results, the findings showed that actions in this delayed feedback condition violated Weber's law (Hosang et al., 2016). However, the ecological validity of Hosang et al. (2016) results could be limited by the fact that haptic feedback was provided only after movements were completed. It could be argued that such atypical settings might encourage participants to treat the task of 2D grasping and 3D grasping as separate events. Indeed, as discussed in the introduction, these findings were inconsistent with the results of a more recent study from our lab in which immediate haptic feedback was provided during 2D grasping by haptic feedback simulator. In this study, actions obeyed Weber's law throughout the entire movement trajectory, regardless of the availability of haptic information (Ozana et al., 2018). In a complementary manner, in a different study from our lab, participants performed grasping gestures toward different-sized 3D objects placed beyond a transparent glass. While the tactile feedback provided in this task was partial (similar to the feedback typically available in interactions with 2D objects), the results showed that grasping violated Weber's law (Ozana and Ganel, 2019a). Thus, it seems that while tactile information can have an important role in grasping performance, efficient, analytic visuomotor control is not contingent only upon this source of information. Therefore, analytic visuomotor control probably depends on the availability of cross-modal, converging sources of information that are available in 3D grasping. Such visual and tactile cues may evoke a dedicated set of computations that support efficient motor control.

The potential effect of tactile feedback on grasping was also illustrated in recent studies conducted on DF, a patient who suffers from visual form agnosia due to bilateral damages to her ventral stream. Remarkably, although DF is unable to discriminate between different-sized objects she can accurately scale her fingers to grasp them, arguably relaying on her intact dorsal stream (see Whitwell et al., 2014). Importantly, however and in line with the results of Experiment 2, recent work suggests that DF's (normal) performance in grasping tasks depends on her ability to obtain tactile information when grasping the target's edges (Schenk, 2012). For example, when DF is asked to perform pantomime movements toward objects her fingers do not longer scale to the size of the target. This finding is in line with the current results, further supporting the idea that tactile feedback has a role in action-perception dissociations. We note, however, that DF's visual processing might still differ substantially from that of healthy controls. For example, while the actions of healthy subjects are compromised when 2D objects (that only provide general tactile feedback from touching the flat surface) are used as targets, DFs show sensitivity to 2D and 3D targets during grasp (Whitwell et al., 2014).

An alternative explanation of the findings of the current study could be that bimanual grasping in rich VR environments relies on a double pointing (Smeets and Brenner, 2008). According to this account, grasping depends on independently pointing each digit to a different location, rather than encoding the object size. Indeed, this model could potentially explain why perceptual regularities about object size and context typically do not affect visuomotor control (Smeets et al., 2019). We note, however, that while the current results are consistent with this simple, double-pointing account, this proposal is not in line with previous evidence about 2D grasping, a task, which arguably should also involve directing the digits at two discrete locations. However, simple interactions with 2D objects (as well as with 3D virtual objects in Experiment 1) typically obey perceptual regularities (Holmes and Heath, 2013; Freud and Ganel, 2015; Ozana and Ganel, 2018, 2019a), which goes against a simple double pointing strategy account (but see, Smeets et al., 2019).

As in recent studies that involve virtual interactions with 2D objects, MGA data from our no-feedback condition did not reflect the pattern of adherence to Weber's law obtained in the second part of the movement trajectory (Afgin et al., 2017; Ozana et al., 2018; Ozana and Ganel, 2019b). A possible reason for the inconsistency between the pattern of JNDs during MGAs and between the pattern of JNDs at the rest of the movement in 2D (but not in 3D) interactions, may be related to task requirements. In particular, in 3D grasping, MGAs are considered as basic and stable kinematic signature of grip apertures that reflects the safety margin required to firmly grasp the target object prior to lifting it up. Yet, actions that do not entail the grasping of physical objects do not require such safety margins. As a result, these interactions usually have a different movement profile, which lacks a reliable point in which MGAs are achieved (Ozana et al., 2018). To account for this issue, JNDs in the current study were measured at different intervals of the movement trajectory. The results showed that MGAs did not represent the pattern of JNDs in other stages of the movements, including the critical stage in which the fingers approached the target object. Therefore, together with previous findings, the current results suggest that when grasping is less typical, MGA may not provide a reliable measure of performance (Afgin et al., 2017; Ozana et al., 2018).

Another potential pitfall is related to the possible effect of the aperture velocity on the pattern of adherence to Weber's law during virtual grasping. In a typical grasping task, participants are required to pinch their fingers together prior to movement initiation, a design that might encourage them to open their fingers faster to big compared to small objects. This relation between aperture velocity and size can lead to speed-precision tradeoff effects. Such effects may also lead to a decrease in precision (larger SDs) for bigger objects (Foster and Franz, 2013; Ganel et al., 2014; but see, Heath et al., 2012). In 3D grasping, this potential confound has been shown to affect early stages of the movement. However, in a recent study, we found that actions directed to 2D targets could be subjected to speed-precision tradeoff effects throughout the entire movement. Hence, in atypical grasping tasks, adherence to Weber's law could reflect the relation between the aperture's velocity and SD rather than the visual resolution of the response (Ozana and Ganel, 2019b).

To summarize, actions toward 3D and 2D targets typically show distinctive patterns of adherence to psychophysical principles. Actions toward 2D objects are typically subjected to perceptual regularities, the same regularities that do not affect normal 3D grasping. Here, we showed that this dissociation between action and perception extends to advanced immersive surroundings in which accurate haptic feedback is available upon touch. These results suggest that the inefficient control of action, found in various types of 2D visuomotor interactions, could be attributed to a reduced sense of interaction with the target, which might lead to atypical behavior. The presence of visual and haptic cues from the environment could facilitate an elevated sense of interaction, and enable more accurate and natural grasping performance in a virtual environment.

DATA AVAILABILITY STATEMENT

The raw data supporting the conclusions of this article will be made available by the authors, without undue reservation.

ETHICS STATEMENT

The studies involving human participants were reviewed and approved by Institutional Ethics Committee, Ben-Gurion University of the Negev. The patients/participants provided their written informed consent to participate in this study.

AUTHOR CONTRIBUTIONS

TG, AO, and SB planned the experiments, analyzed the data, reviewed the manuscript, and contributed to edits and updates of the manuscript. AO ran the experiments, performed initial data analyses, and wrote the initial draft of the manuscript. All authors contributed to the article and approved the submitted version.

FUNDING

The study was supported by an Israel Science Foundation (ISF) grant 274/15 to TG and to Daniel Algom and by the Helmsley Charitable Trust through the Agricultural, Biological and Cognitive (ABC) Robotics Center of Ben-Gurion University of the Negev.

ACKNOWLEDGMENTS

We thank Tal Pal for her contribution to the segmentation software and Shaked Elkiss, Itay Ridel, and Shahar Agami for their assistance in the experiments and software development.

REFERENCES

Afgin, O., Sagi, N., Nisky, I., Ganel, T., and Berman, S. (2017). Visuomotor resolution in telerobotic grasping with transmission delays. *Front. Robot. AI* 4:54. doi: 10.3389/frobt.2017.00054

Aglioti, S., DeSouza, J. F. X., and Goodale, M. A. (1995). Size-contrast illusions deceive the eye but not the hand. *Curr. Biol.* 5, 679–685. doi: 10.1016/S0960-9822(95)00133-3

Bingham, G., Coats, R., and Mon-Williams, M. (2007). Natural prehension in trials without haptic feedback but only when calibration is allowed. *Neuropsychologia* 45, 288–294. doi: 10.1016/j.neuropsychologia.2006.07.011

Cesanek, E., and Domini, F. (2017). Error correction and spatial generalization in human grasp control. *Neuropsychologia* 106, 112–122. doi: 10.1016/j.neuropsychologia.2017.09.026

Chen, J., Sperandio, I., and Goodale, M. A. (2015). Differences in the effects of crowding on size perception and grip scaling in densely cluttered 3-D scenes. *Psychol. Sci.* 26, 58–69. doi: 10.1177/0956797614556776

Davarpanah Jazi, S., and Heath, M. (2016). Pantomime-grasping: advance knowledge of haptic feedback availability supports an absolute visuo-haptic calibration. *Front. Hum. Neurosci.* 10:197. doi: 10.3389/fnhum.2016.00197

Davarpanah Jazi, S., Hosang, S., and Heath, M. (2015). Memory delay and haptic feedback influence the dissociation of tactile cues for perception and action. *Neuropsychologia* 71, 91–100. doi: 10.1016/j.neuropsychologia.2015.03.018

Foster, R. M., and Franz, V. H. (2013). Inferences about time course of Weber's Law violate statistical principles. *Vis. Res.* 78, 56–60. doi: 10.1016/j.visres.2012.11.012

Franz, V. H., and Gegenfurtner, K. R. (2008). Grasping visual illusions: consistent data and no dissociation. *Cogn. Neuropsychol.* 25, 920–950. doi: 10.1080/02643290701862449

Freud, E., and Ganel, T. (2015). Visual control of action directed toward two-dimensional objects relies on holistic processing of object shape. *Psychon. Bull. Rev.* 22, 1377–1382. doi: 10.3758/s13423-015-0803-x

Freud, E., Macdonald, S. N., Chen, J., Quinlan, D. J., Goodale, M. A., and Culham, J. C. (2018). Getting a grip on reality: grasping movements directed to real objects and images rely on dissociable neural representations. *Cortex* 98, 34–48. doi: 10.1016/j.cortex.2017.02.020

Furmanek, M. P., Schettino, L. F., Yarossi, M., Kirkman, S., Adamovich, S. V., and Tunik, E. (2019). Coordination of reach-to-grasp in physical and haptic-free virtual environments. *J. Neuroeng. Rehabil.* 16:78. doi: 10.1186/s12984-019-0525-9

Ganel, T. (2015). Weber's law in grasping. *J. Vis.* 15, 18–18. doi: 10.1167/15.8.18

Ganel, T., Chajut, E., and Algom, D. (2008). Visual coding for action violates fundamental psychophysical principles. *Curr. Biol.* 18, 599–601. doi: 10.1016/j.cub.2008.04.052

Ganel, T., Freud, E., and Meiran, N. (2014). Action is immune to the effects of Weber's law throughout the entire grasping trajectory. *J. Vis.* 14, 11–11. doi: 10.1167/14.7.11

Ganel, T., and Goodale, M. A. (2003). Visual control of action but not perception requires analytical processing of object shape. *Nature* 426, 664–667. doi: 10.1038/nature02156

Ganel, T., Namdar, G., and Mirsky, A. (2017). Bimanual grasping does not adhere to Weber's law. *Sci. Rep.* 7, 1–7. doi: 10.1038/s41598-017-06799-4

Ganel, T., Ozana, A., and Goodale, M. A. (2019). When perception intrudes on 2D grasping: evidence from Garner interference. *Psychol. Res.* 84, 2138–2143. doi: 10.1007/s00426-019-01216-z

Glover, S. R., and Dixon, P. (2001). Dynamic illusion effects in a reaching task: evidence for separate visual representations in the planning and control of reaching. *J. Exp. Psychol.* 27, 560–572. doi: 10.1037/0096-1523.27.3.560

Gonzalez, C. L. R., Ganel, T., Whitwell, R. L., Morrissey, B., and Goodale, M. A. (2008). Practice makes perfect, but only with the right hand: sensitivity to perceptual illusions with awkward grasps decreases with practice in the right but not the left hand. *Neuropsychologia* 46, 624–631. doi: 10.1016/j.neuropsychologia.2007.09.006

Goodale, M. A., and Milner, A. D. (1992). Separate visual pathways for perception and action. *Trends Neurosci.* 15, 20–25. doi: 10.1016/0166-2236(92)90344-8

Heath, M., Holmes, S. A., Mulla, A., and Binsted, G. (2012). Grasping time does not influence the early adherence of aperture shaping to Weber's law. *Front. Hum. Neurosci.* 6:332. doi: 10.3389/fnhum.2012.00332

Heath, M., Mulla, A., Holmes, S. A., and Smuskowitz, L. R. (2011). The visual coding of grip aperture shows an early but not late adherence to Weber's law. *Neurosci. Lett.* 490, 200–204. doi: 10.1016/j.neulet.2010.12.051

Holmes, S. A., and Heath, M. (2013). Goal-directed grasping: the dimensional properties of an object influence the nature of the visual information mediating aperture shaping. *Brain Cogn.* 82, 18–24. doi: 10.1016/j.bandc.2013.02.005

Hosang, S., Chan, J., Davarpanah Jazi, S., and Heath, M. (2016). Grasping a 2D object: terminal haptic feedback supports an absolute visuo-haptic calibration. *Exp. Brain Res.* 234, 945–954. doi: 10.1007/s00221-015-4521-4

Jakobson, L. S., and Goodale, M. A. (1991). Factors affecting higher-order movement planning: a kinematic analysis of human prehension. *Exp. Brain Res.* 86, 199–208. doi: 10.1007/BF00231054

Jarmasz, J., and Hollands, J. G. (2009). Confidence intervals in repeated-measures designs: the number of observations principle. *Can. J. Exp. Psychol.* 63, 124–138. doi: 10.1037/a0014164

Johansson, R. S., and Flanagan, J. R. (2009). Coding and use of tactile signals from the fingertips in object manipulation tasks. *Nat. Rev. Neurosci.* 10, 345–359. doi: 10.1038/nrn2621

Kopiske, K. K., Bruno, N., Hesse, C., Schenk, T., and Franz, V. H. (2016). The functional subdivision of the visual brain: is there a real illusion effect on action? A multi-lab replication study. *Cortex* 79, 130–152. doi: 10.1016/j.cortex.2016.03.020

Kopiske, K. K., Cesanek, E., Campagnoli, C., and Domini, F. (2017). Adaptation effects in grasping the Müller-Lyer illusion. *Vis. Res.* 136, 21–31. doi: 10.1016/j.visres.2017.05.004

Milner, A. D., and Goodale, M. A. (2008). Two visual systems re-viewed. *Neuropsychologia* 46, 774–785. doi: 10.1016/j.neuropsychologia.2007.10.005

Namdar, G., Algom, D., and Ganel, T. (2018). Dissociable effects of stimulus range on perception and action. *Cortex* 98, 28–33. doi: 10.1016/j.cortex.2016.12.017

Ozana, A., Berman, S., and Ganel, T. (2018). Grasping trajectories in a virtual environment adhere to Weber's law. *Exp. Brain Res.* 236, 1775–1787. doi: 10.1007/s00221-018-5265-8

Ozana, A., and Ganel, T. (2018). Dissociable effects of irrelevant context on 2D and 3D grasping. *Attent. Percept. Psychophys.* 80, 564–575. doi: 10.3758/s13414-017-1443-1

Ozana, A., and Ganel, T. (2019a). Weber's law in 2D and 3D grasping. *Psychol. Res.* 83, 977–988. doi: 10.1007/s00426-017-0913-3

Ozana, A., and Ganel, T. (2019b). Obeying the law: speed–precision tradeoffs and the adherence to Weber's law in 2D grasping. *Exp. Brain Res.* 237, 2011–2021. doi: 10.1007/s00221-019-05572-5

Ozana, A., and Ganel, T. (2020). A double dissociation between action and perception in bimanual grasping: evidence from the Ponzo and the Wundt–Jastrow illusions. *Sci. Rep.* 10:14665. doi: 10.1038/s41598-020-71734-z

Ozana, A., Namdar, G., and Ganel, T. (2020). Active visuomotor interactions with virtual objects on touchscreens adhere to Weber's law. *Psychol. Res.* 84, 2144–2156. doi: 10.1007/s00426-019-01210-5

Rohde, M., and Ernst, M. O. (2016). Time, agency, and sensory feedback delays during action. *Curr. Opin. Behav. Sci.* 8, 193–199. doi: 10.1016/j.cobeha.2016.02.029

Rossit, S., Harvey, M., Butler, S. H., Szymanek, L., Morand, S., Monaco, S., et al. (2018). Impaired peripheral reaching and on-line corrections in patient DF: optic ataxia with visual form agnosia. *Cortex* 98, 84–101. doi: 10.1016/j.cortex.2017.04.004

Schenk, T. (2012). No dissociation between perception and action in patient DF when haptic feedback is withdrawn. *J. Neurosci.* 32, 2013–2017. doi: 10.1523/JNEUROSCI.3413-11.2012

Smeets, J. B. J., and Brenner, E. (1999). A new view on grasping. *Motor Control* 3, 237–271. doi: 10.1123/mcj.3.3.237

Smeets, J. B. J., and Brenner, E. (2008). Grasping Weber's law. *Curr. Biol.* 18, R1089–R1090. doi: 10.1016/j.cub.2008.10.008

Smeets, J. B. J., van der Kooij, K., and Brenner, E. (2019). A review of grasping as the movements of digits in space. *J. Neurophysiol.* 122, 1578–1597. doi: 10.1152/jn.00123.2019

Whitwell, R. L., Buckingham, G., Enns, J. T., Chouinard, P. A., and Goodale, M. A. (2016). Rapid decrement in the effects of the Ponzo display dissociates action and perception. *Psychon. Bull. Rev.* 23, 1157–1163. doi: 10.3758/s13423-015-0975-4

Whitwell, R. L., David Milner, A., Cavina-Pratesi, C., Byrne, C. M., and Goodale, M. A. (2014). DF's visual brain in action: the role of tactile cues. *Neuropsychologia* 55, 41–50. doi: 10.1016/j.neuropsychologia.2013.11.019

Whitwell, R. L., and Goodale, M. A. (2013). Grasping without vision: time normalizing grip aperture profiles yields spurious grip scaling to target size. *Neuropsychologia* 51, 1878–1887. doi: 10.1016/j.neuropsychologia.2013.06.015

Whitwell, R. L., Milner, A. D., and Goodale, M. A. (2014). The two visual systems hypothesis: new challenges and insights from visual form agnosic patient DF. *Front. Neurol.* 5:255. doi: 10.3389/fneur.2014.00255

Conflict of Interest: The authors declare that the research was conducted in the absence of any commercial or financial relationships that could be construed as a potential conflict of interest.

frontiers in Psychology

ORIGINAL RESEARCH
published: 23 November 2020
doi: 10.3389/fpsyg.2020.587270

Effects of Tool Novelty and Action Demands on Gaze Searching During Tool Observation

Yoshinori Tamaki[1]*, Satoshi Nobusako[2,3], Yusaku Takamura[2,4], Yu Miyawaki[2,5,6], Moe Terada[7] and Shu Morioka[2,3]

[1] Department of Rehabilitation, Kohnan Hospital, Shiga, Japan, [2] Graduate School of Health Sciences, Kio University, Nara, Japan, [3] Neurorehabilitation Research Center, Kio University, Nara, Japan, [4] Department of Rehabilitation for the Movement Functions, Research Institute, National Rehabilitation Center for Persons With Disabilities, Saitama, Japan, [5] Research Fellow of Japan Society for the Promotion of Science, Tokyo, Japan, [6] Department of Rehabilitation Medicine, Keio University School of Medicine, Tokyo, Japan, [7] Department of Rehabilitation, Murata Hospital, Osaka, Japan

Technical reasoning refers to making inferences about how to use tools. The degree of technical reasoning is indicated by the bias of the gaze (fixation) on the functional part of the tool when in use. Few studies have examined whether technical reasoning differs between familiar and unfamiliar novel tools. In addition, what effect the intention to use the tool has on technical reasoning has not been determined. This study examined gaze shifts in relation to familiar or unfamiliar tools, under three conditions (free viewing, lift, and use), among 14 healthy adults (mean age ± standard deviation, 29.4 ± 3.9 years). The cumulative fixation time on the functional part of the tool served as a quantitative indicator of the degree of technical reasoning. The two-way analysis of variance for tools (familiar and unfamiliar) and conditions (free viewing, lift, and use) revealed that the cumulative fixation time significantly increased under free viewing and use conditions, compared to lift conditions. Relative to the free viewing condition, cumulative fixation time for unfamiliar tools significantly decreased in the lift condition and significantly increased in the use condition. Importantly, the results showed that technical reasoning was performed in both the use and the free viewing conditions. However, technical reasoning in the free viewing condition was not as strong as in the use condition. The difference between technical reasoning in free viewing and use conditions may indicate the difference between automatic and intentional technical reasoning.

Keywords: technical reasoning, tool use, tool novelty, action demands, gaze

Edited by:
Simone Toma,
Arizona State University, United States

Reviewed by:
Lotje Van Der Linden,
Aix-Marseille Université, France
François Osiurak,
Lumière University Lyon 2, France

***Correspondence:**
Yoshinori Tamaki
ot44tama@gmail.com

Specialty section:
This article was submitted to
Perception Science,
a section of the journal
Frontiers in Psychology

Received: *27 July 2020*
Accepted: *15 October 2020*
Published: *23 November 2020*

Citation:
Tamaki Y, Nobusako S, Takamura Y, Miyawaki Y, Terada M and Morioka S (2020) Effects of Tool Novelty and Action Demands on Gaze Searching During Tool Observation. Front. Psychol. 11:587270. doi: 10.3389/fpsyg.2020.587270

INTRODUCTION

Humans live in environments surrounded by a variety of tools. In both daily (e.g., eating, cooking, and grooming) and occupational activities, tools are selected according to the intended use or the activity to be performed. Two reasoning systems are required when using such tools; the first system is semantic reasoning, which concerns itself with what to do, based on the functional knowledge of the tool (Osiurak, 2014); the second is technical reasoning, which is the ability to solve physical problems, especially regarding tool use, based on abstract physical principles (i.e., mechanical knowledge) acquired through experience (Osiurak, 2014; Osiurak et al., 2020). For example, semantic reasoning is performed when recalling the act of combing one's hair while looking at a comb or searching for a comb – with the intention to use it. Technical reasoning is used when one alters their grip and movements to accommodate the size and shape of different combs. Technical reasoning ability is important when dealing with a novel tool, which has an unknown function or when employing a tool for something beyond its standard use (e.g., stirring coffee with a butter knife) (Osiurak et al., 2009; Osiurak, 2014).

Apraxia is a neurological condition that develops after a left hemisphere stroke, making it difficult to use tools. Apraxia symptoms vary widely and include gestures and pantomime disorders (Signoret and North, 1984). Notably, tool use challenges are often a problem during rehabilitation in living situations. Patients with tool use disorders have been found to struggle to guess the function of unfamiliar novel tools (Goldenberg and Hagmann, 1998) as well as the applied use of familiar daily tools (Osiurak et al., 2009, 2013). Moreover, technical reasoning involves the left inferior parietal lobe (IPL), an area that is often damaged in patients with apraxia (Osiurak et al., 2020). Thus, technical reasoning is an important ability for tool use.

Neuroimaging research shows that when a tool is observed by someone with no intention to use it, activity is seen in the brain areas responsible for tool recognition and in motor-related areas, like the premotor cortex (Lewis, 2006). This is physiological evidence that the visual representation of the tool automatically initiates the process that prepares for its potential use. Moreover, when observing with no intention to use, the observer's spatial attention was attracted to the functional part: an act known as or the characteristic gaze (Roberts and Humphreys, 2011; Myachykov et al., 2013; Van Der Linden et al., 2015). This is considered the effect of affordances, which owes to characteristics like having functional knowledge of tools (Van Der Linden et al., 2015). Affordance refers to the potential behaviors afforded to a subject by the environment (Gibson, 1985). A study on gaze response showed that, in familiar daily tools with a functional and grasping part separated along the long axis, the first fixation was biased toward the center and the next was biased toward the functional part; this fixation bias on the functional part was deemed a higher-order affordance effect, based on functional knowledge of tools (Van Der Linden et al., 2015). Other reports on the free observation of the combination of familiar tools and objects showed that, when the combination was consistent, participants gazed more the grasping part of the tool, whereas when the combination was inconsistent, participants gazed more its functional part (Federico and Brandimonte, 2019, 2020). However, the characteristics of spatial attention or gaze response when observing an unfamiliar novel tool without the intention to use it remain unclear.

In an action situation, gaze data, especially fixation time, are used to quantify the degree of preparation for an object, like a tool, to be manipulated. This is because gaze control serves to collect information concerning actions when one uses objects and tools in everyday situations (Hayhoe et al., 2003; Land and Tatler, 2009). In a study that determined which part of the operation target one gazes at, the first fixation was the object's center of gravity, and the second was the point where the object is gripped so the action may take place (Brouwer et al., 2009; Belardinelli et al., 2015). Notably, there are studies that presented familiar daily tools and unfamiliar novel tools with a functional and grasping part (separated along the long axis) that required a mime to lift and use the tool; in these cases, the gaze was biased toward the functional part of the tool when the use was requested. This effect has also been shown to be stronger with unfamiliar novel tools than with familiar daily tools (Belardinelli et al., 2016). The subject's biased fixation on the functional part of the novel tool when requesting use indicates that they are actively trying to process the mechanical properties to guess how to use the tool. In other words, when we intend to use familiar everyday tools, we can easily understand what to do by looking at the functional parts. With unfamiliar novel tools, however, it is often necessary to observe functional parts and guess how to use them based on their shapes. This suggests that the degree of technical reasoning can be expressed through the duration of fixation on the functional part of the tool. However, they compared the intention to lift, in which technical reasoning was not required, and the intention to use, in which technical reasoning was required (Belardinelli et al., 2016). Yet, one may still be preparing for potential use when one observes tools without that explicit intention. Indeed, during this time, we may be opting to use the tool through automatic reasoning. Consequently, it is hypothesized that, with or without familiarity, gaze bias toward the functional part of the tool will take place. This is expected to be the case during free observation as well as during intention to use, more so than during intention to lift.

The study aims to determine the impact that the presence or absence of action intention has on technical reasoning in healthy subjects. To this end, we compared the cumulative fixation time to the functional part of the tool. This was achieved by observing familiar daily tools and unfamiliar novel tools under three conditions: free observation, demand for use, and demand for lift. The cumulative fixation time on the functional part of the tool served as a quantitative indicator of the degree of technical reasoning. Notably, previous studies have used cumulative fixation time as the result, and changes in gaze shift over time were not clear. To examine these differences in more detail, we confirmed the temporal gaze shift in addition to the cumulative fixation time. It is important to examine the impact of tool novelty and action demands on technical reasoning to understand the pathogenesis of apraxia and develop rehabilitation techniques.

MATERIALS AND METHODS

Participants

The experiment involved 14 healthy adults (age: 29.4 ± 3.9 years old; 10 females and 4 males). Participants were right-handed and had normal vision with normal or corrective eyeglasses. This study was conducted with the approval of the Research Ethics Committee of Kio University. Based on the Declaration of Helsinki, we gave due consideration to subjects' safety, fully explained the research methods and potential risks, and conducted the study with consent.

Setting

In the experimental room, each subject took a seated position approximately 60 cm from the monitor presenting the stimulus image. To record eye movements, an eye tracker with a sampling frequency of 60 Hz (Tobii Pro X2-60: Toby Technology Co., Ltd., Tokyo) was installed at the bottom of the monitor. The monitor used a 17.3-inch laptop PC (HP ProBook 470 G2/CT Notebook PC: HP Japan, Tokyo) with a resolution of 1,920 × 1,080 pixels.

Stimulus

Stimuli comprised 12 tool images: six general, everyday life tools (familiar tools) and six novel tools (unfamiliar tools). Each tool was lengthy, held horizontally, could be used with one hand, and had its functional and grip parts clearly separated along its axis. Each image was created using the image editing software Photoshop CC (Adobe Systems Inc., Tokyo), so they all had the same length. The center of the tool was set at a viewing angle of 5.15° above the center of the screen, displayed horizontally at 13.69°, and the grip was always on the left.

Conditions

The tool images were viewed under three conditions. The free viewing conditions came first and only required participants to gaze at the screen. The lift conditions came second and required a pantomime of lifting the tool with the left hand. Finally came the third condition, which required a pantomime of using the tool with one's left hand. Under both mime conditions, the examiner instructed the subject to perform the mime according to instructions, after the latter reached out to the monitor, assuming there was a tool in front of it. Under the use condition, the examiner requested that the subject use their imagination if they did not know how to use the tool.

Procedures

The experiment started with a nine-point calibration for each subject. **Figure 1A** shows the experimental procedure. In each set, the instruction associated with the condition ("Just keep your eyes on the screen"/"Lift it"/"Use it") was displayed at the center of the screen for 3 s. Then, a cross point was displayed at the center of the screen for 1 or 2 s (random). After that, the tool image was presented for 5 s (see **Figure 1A**). The experiment was blocked for each condition. Furthermore, each condition had 12 tools displayed once in random order. Each condition was performed once, in succession, with a 1-min break after free viewing, lift, and use. Subjects underwent 36 trials each: three conditions using 12 tool images. Eye movements during the tool display were recorded, and results were recorded for each condition and tool type (familiarity). Each subject practiced each condition with another three tool images before performing this experiment. Tobii Studio (Tobii Technology Co., Ltd., Tokyo, Japan) was used to create the task and to measure eye movements. **Figure 1B** shows the actual experimental scene.

Post-experiment Evaluation

(1) After the experiment, subjects drew rectangles of the range of the functional and of the grasping part of each tool. This amounted to a total of 12 for each of the tool images (Belardinelli et al., 2016). The image editing software Paint was used for the drawing.

(2) Subjects were asked to indicate their degree of familiarity with each tool on a scale of 1 to 5. Echoing previous studies (Belardinelli et al., 2016), each scale was set as follows, 5: I see it every week or every day, 4: I have seen it in the last month to a year, 3: I have seen it once or twice before, 2: I know it exists, and 1: I have never used it, seen it, or heard about it.

Data Analysis

Visualization of Fixations

The minimum analysis time for eye movements was 1/60 of second; the target time was 5,000 ms, from the beginning to the end of each tool image presentation. Using the analysis software, Tobii Studio, heat maps were created, based on the fixation points of each tool. Using the Tobii Studio Clear View fixation filter, we set the minimum time required for a fixation at 100 ms. The velocity threshold selected was 100 pixels/16.6 ms, corresponding to a viewing angle of approximately 2° (Tobii Studio User's Manual Version 3.4.5, 2020).

Region of Interest Settings and Cumulative Fixation Time on Functional Parts

Following a previous study (Belardinelli et al., 2016), the region of interest (ROI) for each tool's functional and grasp parts was defined, based on the average of the range drawn by all subjects. Also, the midpoint of the centers of both ROIs was defined as the center of each tool (**Figure 2A**). The cumulative fixation time on the ROI for functional parts for each subject was extracted for each condition and familiarity. This was achieved using the analysis software, Tobii Studio. Finally, the cumulative fixation time on the functional part of the tool served as a quantitative indicator of the degree of technical reasoning.

Visualization of Time-Series Gaze Movement and Cumulative Fixation Position

For the eye movement data, we standardized the horizontal axis coordinates using the specified center of each tool as the origin (**Figure 2A**). This standardized the distance from the center to the outer edge of the functional ROI as + 100. The distance to the outer edge of the grasping ROI was standardized as −100. Data outside of both ROIs were treated as missing values.

The average gaze position of each subject was calculated for each condition and familiarity level. This took place every 250 ms from the standardized eye movement data. The average gaze position of all subjects was calculated and coordinated to visualize the movement of gaze points over time. Moreover, histograms (number of bins: 10) were created for each condition and familiarity level. This was based on the number of measurements of gaze data at standardized horizontal axis coordinates for all subjects. Finally, MATLAB R2017b was used to process these data.

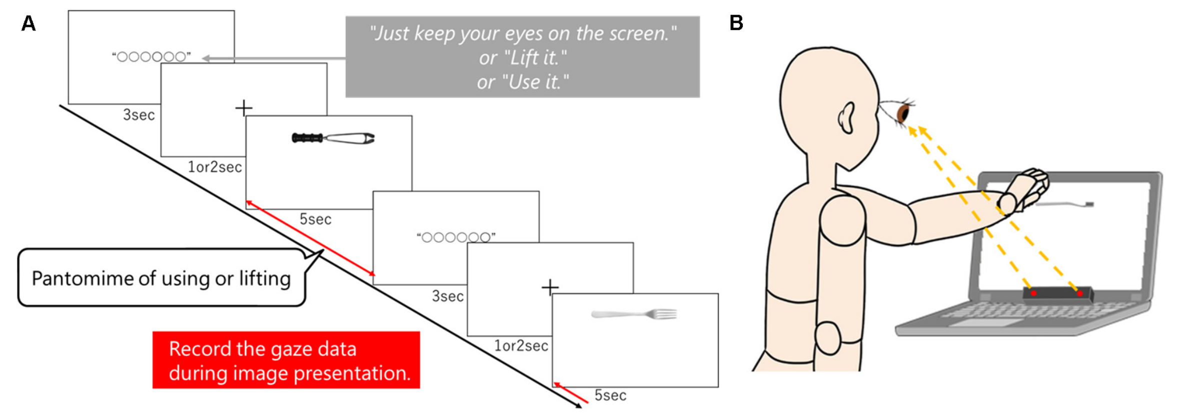

FIGURE 1 | (A) Experimental protocol. The instructions for each condition were displayed for 3 s during each trial. Following this, a cross gaze point was randomly displayed in the center of the screen for 1 or 2 s, and then the tool image was displayed for 5 s. The tool images were displayed in the upper center of the screen, with the grasping part on the left and the functional part on the right. During each condition, 12 tool images were randomly displayed one time each. Under the use and lift conditions, subjects were instructed to perform an appropriate pantomime in front of the tool image display. We recorded participants' eye movement recorded during the exercise. **(B)** Experimental scene. Participants took a seated position. In the lift and use conditions, participants reached for the screen and pantomimed the action of grasping the tool.

Statistical Analysis

A Mann–Whitney's U-test was performed to test the degree of familiarity of the six familiar and the six unfamiliar tools.

The ROI areas for the functional part of familiar and unfamiliar tools were compared using the t-test (first, the F-test and then the Welch's test).

A two-way analysis of variance for tools (familiar and unfamiliar) and conditions (free to see, lift, and use) was conducted on the cumulative fixation time of the ROI for the functional part. A multiple comparison test was also undertaken, using the Shaffer method.

The statistical software, R version 3.4.1, was used for these statistical processes. The significance level was set at 5%.

RESULTS

Degree of Familiarity

Familiar tools had a higher degree of familiarity than unfamiliar tools ($P < 0.01$). The median value of the familiar tools was 5 or 4, the maximum was all 5, and the minimum was 4 or 5. The median value of all unfamiliar tools was 1, the maximum value was either 1 or 3, and the minimum value was all 1.

Region of Interest for the Functional Part and Region of Interest for the Grasping Part

Figure 2B shows the ROI for the functional part, the ROI for the grasping part, and the center of the tool calculated from the average of the range drawn by the subjects.

Region of Interest Area of the Functional Part

There was no significant difference in the ROI area of the functional part between familiar and unfamiliar tools ($P = 0.3575$).

Heat Map of All Fixations and Cumulative Fixation Position

Figure 3A shows the heat maps for each condition, based on all fixations for the two familiar and unfamiliar tools. Compared to the lift conditions, the fixations in the use and free viewing conditions were biased toward the functional parts.

Figure 3B is a histogram of the cumulative gaze position average, based on gaze data with standardized horizontal axis coordinates. The bias of the gaze in the direction of the functional part was observed under the use and free viewing conditions, though not the lift condition. Moreover, under the use conditions, the gaze was deflected to the functional part for the unfamiliar tools more so than the familiar ones.

Cumulative Fixation Time on Functional Parts

The two-way analysis of variance showed a main effect on conditions ($F(2,26) = 28.2112$, $P < 0.01$). The cumulative fixation times under free viewing and use conditions significantly increased, compared with those under lift conditions ($P < 0.01$). There was no main effect on familiarity ($F = (1,13) = 0.0903$, $P = 0.7686$). There was an interaction between condition and familiarity ($F(2,26) = 9.3635$, $P < 0.01$). The cumulative fixation time increased for the unfamiliar tool under the use conditions ($P < 0.01$), while the cumulative fixation time increased for the familiar tool under the lift conditions ($P < 0.05$). The cumulative fixation time for the familiar tool had a significantly greater increase during the free viewing ($P < 0.01$) and use conditions ($P < 0.05$) than it did during the lift conditions. Furthermore, relative to the free viewing condition, the cumulative fixation time for unfamiliar tools significantly decreased during the lift conditions ($P < 0.01$) and significantly increased during the use conditions ($P < 0.05$) (**Figure 4**).

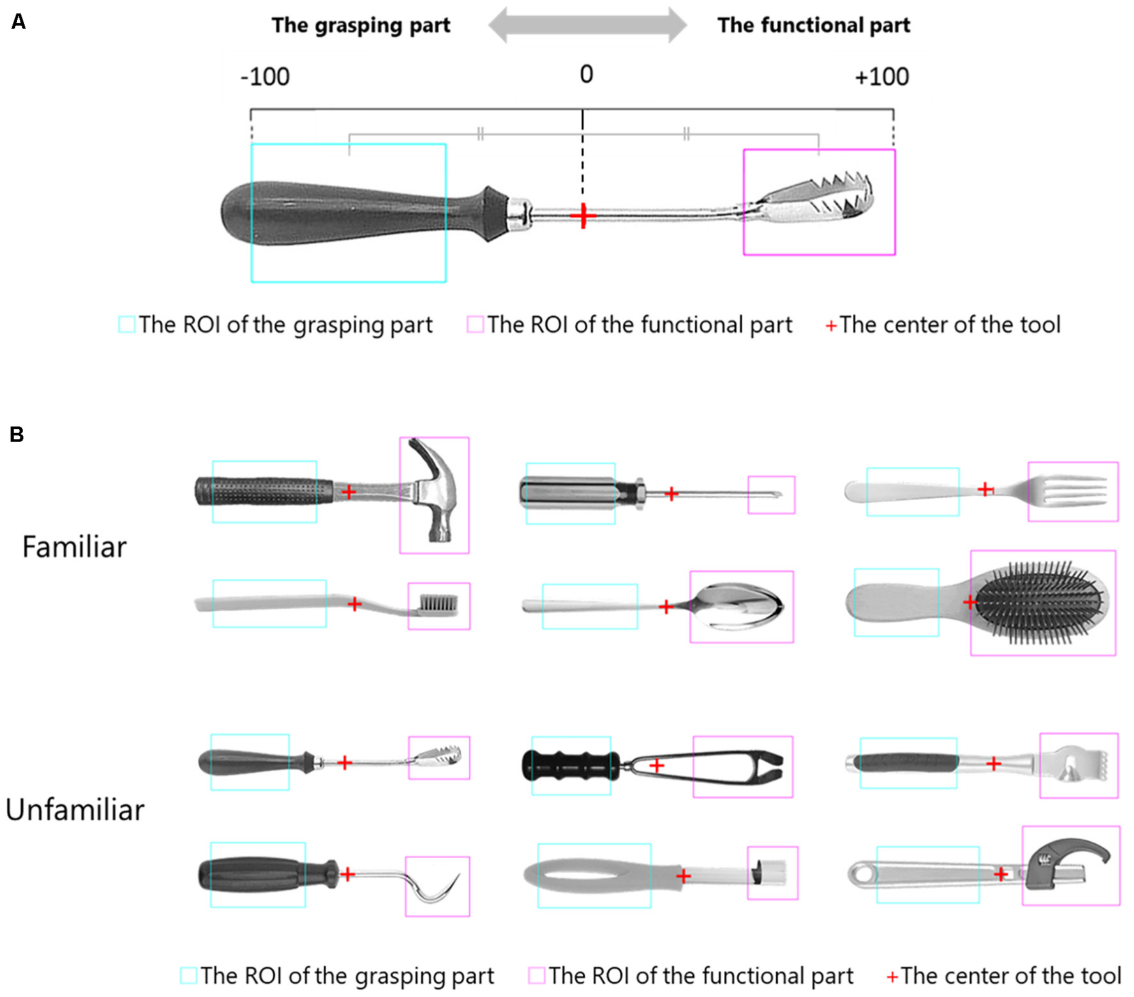

FIGURE 2 | (A) An example of the region of interest (ROI) for the functional part, the ROI of the grasping part, and the standardization of horizontal coordinates from the tool center. The center of the tool was set at the midpoint (red +) of the center of the ROI for the functional part (the range surrounded by magenta lines) and the ROI for the grasping part (the range surrounded by blue lines), defined by the average of each subject. The horizontal coordinates of each line of sight were standardized from the center to the outer edge of each ROI, with the functional part as + 100 and the grasping part as −100. **(B)** All tool images, with the ROI for the grasping part, the ROI for the functional part, and the center of the visible tool. Top two rows: familiar tools; bottom two rows: unfamiliar tools. The ROI for the grasping part is indicated by the blue line, and the ROI of the functional part is indicated by the magenta line. The center of the tool is indicated by the red cross.

Visualization of Time Series Gaze Movement

Figure 5 shows a graph of the average gaze position movement every 250 ms and a histogram using the cumulative gaze position average, based on gaze data with standardized horizontal axis coordinates. The bias of the gaze in the direction of the functional part was visualized more under the use and free viewing conditions, compared with the lift condition. Under the use conditions, the mean fixation position moved across the center and toward the grasp (only with the familiar tools) at 750–1,000 ms and 1,000–1,250 ms.

DISCUSSION

There was no significant difference between familiar and unfamiliar tools in ROI area – which was extracted from the mean of the functional part drawn by all subjects. This suggests that the difference in the area between tools did not affect the difference in cumulative fixation time for the ROI of the functional part. The degree of familiarity was significantly higher for familiar tools than for unfamiliar tools. This suggests that our selection of tools was reasonably familiar. In cumulative fixation time, there was a main effect on the condition, but no main effect on the familiarity of tools. A multiple comparison test showed that the use and free viewing conditions resulted in a greater increase in cumulative fixation time on the functional parts, compared with the lift conditions. This result is consistent with a previous study (Belardinelli et al., 2016), which showed that the gaze was biased toward the functional part of the tool only when the subject was asked to use it. In our results, this was not found to be the case when the subject was asked to lift the tool, regardless of familiarity, namely, this result indicates

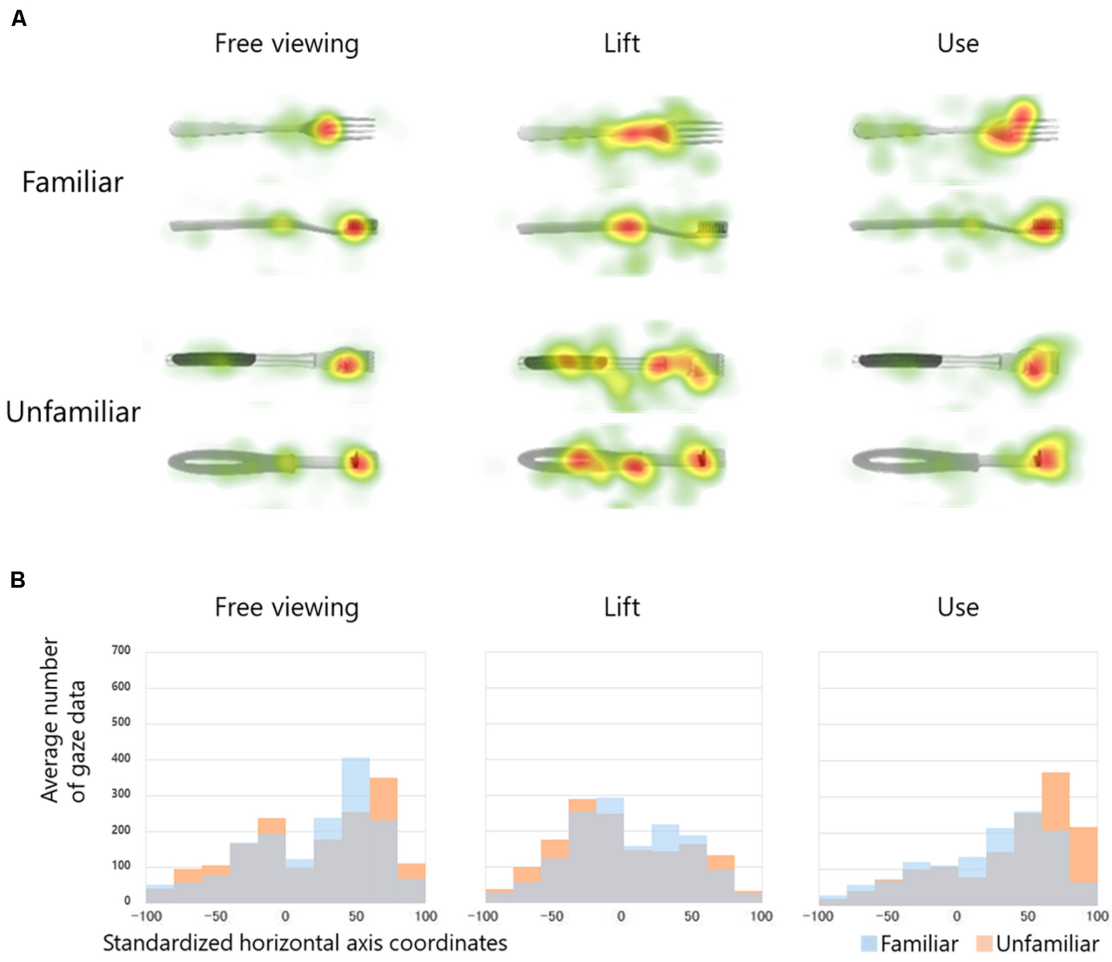

FIGURE 3 | (A) Heat map of all fixations. Top two rows: two excerpts from familiar tools; bottom two rows: two excerpts from unfamiliar tools. Left: free viewing conditions; center: lift conditions; right: use conditions. Heat maps for each condition created based on all fixations (two familiar tools and two unfamiliar tools). Areas with a long fixation time are indicated in red. **(B)** Histogram of cumulative fixation position. Vertical axis shows the average number of gaze data in each bin, and the horizontal axis indicates the standardized horizontal coordinates.

that, similar to what happened in a prior study (Myachykov et al., 2013), the intention to lift caused participants to prioritize looking at the grasping part – an action meant to infer the lifting of the tool – over its functional part – an action meant to infer tool use. Furthermore, the amount of time spent looking at functional parts increased during free viewing (without the intention to use) more so than it did during the intention to lift. This suggests that participants' reasoning work was similar during free viewing and viewing with the intention to use the tool. However, it might be possible that participants only inspected the functional part first, namely, the search for the characteristic functional part of the tool occurred in the free viewing condition, but not in the lift condition. However, in the use condition (i.e., the last one), we observed the greater gaze bias toward the functional part of the unfamiliar tool compared with other conditions; this suggests that the necessity of technical reasoning increases with the intention to use the tool. To make it clearer that technical reasoning is automatically activated in the free viewing condition owing to an automatic inference toward use, future researchers could present two conditions (i.e., the lift and free viewing conditions) at random. Future studies should endeavor to explore if technical reasoning is indeed activated in the free viewing condition owing to an automatic inference toward tool use, researchers could present the lift and the free viewing conditions at random.

We also found an interaction between condition and familiarity. Under the use conditions, participants spent more time looking at the functional parts of unfamiliar tools than those of familiar tools. This suggests that, depending on the intention of use, participants are more deliberate about observing the mechanical structure of the functional part and analogizing its use (i.e., technical reasoning). Furthermore, this increased deliberation is more pronounced for unfamiliar tools than familiar ones. On the other hand, under the lift conditions, participants spent more time looking at the functional parts of familiar tools than unfamiliar ones, namely, although the intention to lift led subjects to prioritize looking at the grasping part of the tool (an action meant to infer the lifting of the

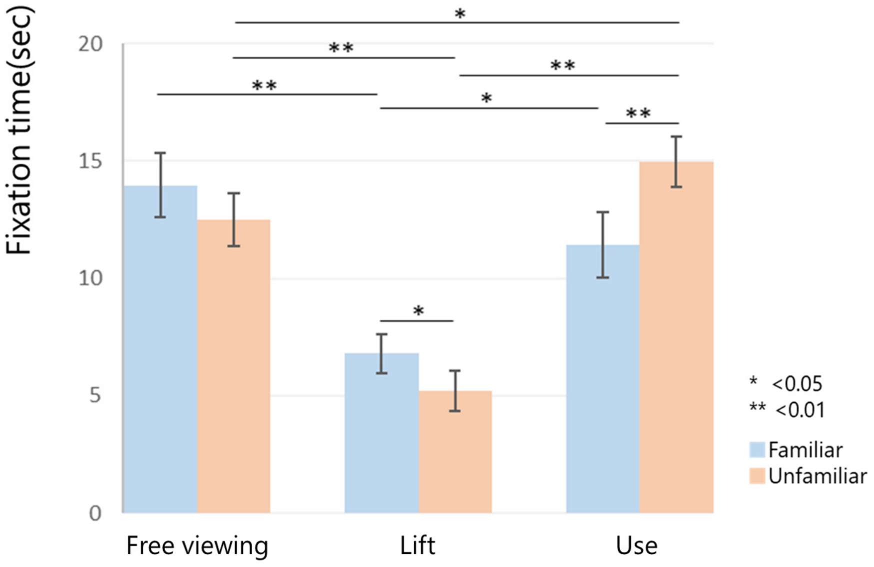

FIGURE 4 | The cumulative fixation time on the functional part. The cumulative fixation time on the functional ROI for each condition and familiarity is shown. We found a main effect for conditions (*F*(2,26) = 28.2112, *P* < 0.01) and no main effect for the familiarity (*F* = (1,13) = 0.0903, *P* = 0.7686). The cumulative fixation times under the free viewing and use conditions significantly increased, compared to those under lift conditions (*P* < 0.01). Furthermore, there was an interaction between condition and familiarity (*F*(2,26) = 9.3635, *P* < 0.01). Relative to the free viewing conditions, the cumulative fixation time for unfamiliar tools significantly decreased during the lift conditions (*P* < 0.01) and significantly increased during the use conditions (*P* < 0.05). *P < 0.05; **P < 0.01.

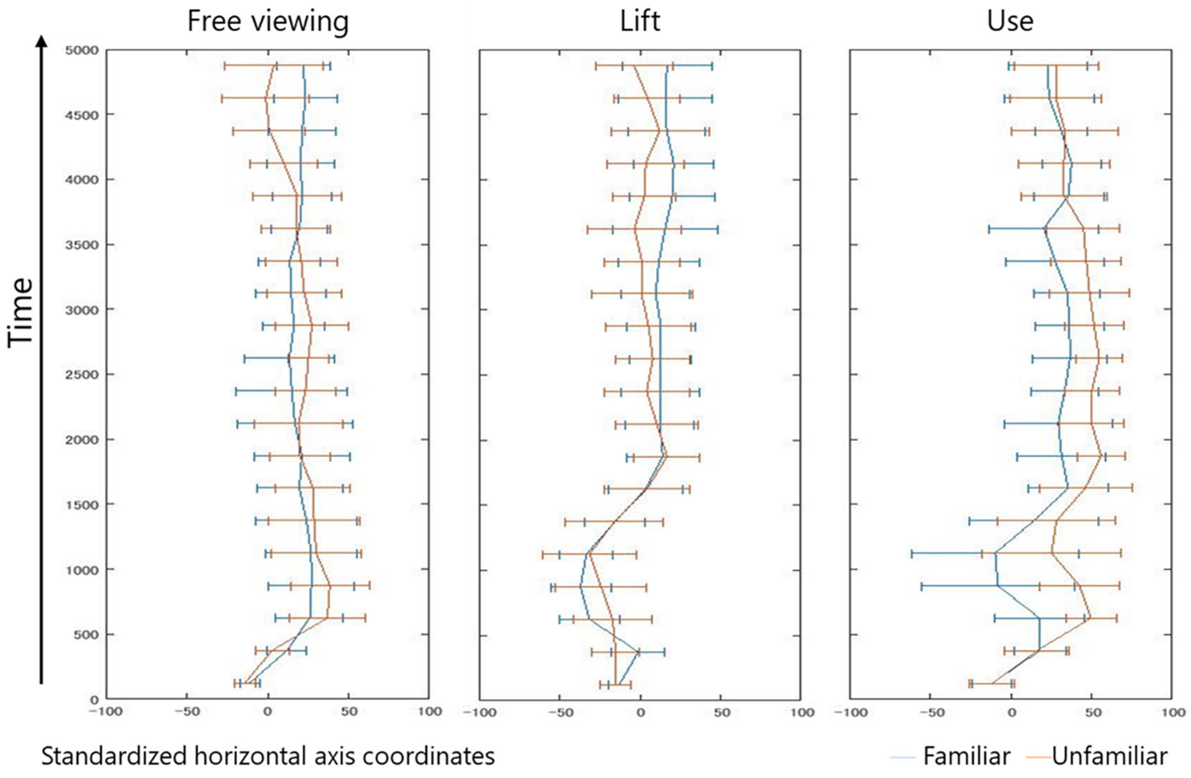

FIGURE 5 | Time series change in mean gaze position. The vertical axis indicates time, and the horizontal axis indicates the standardized horizontal coordinates. The figure shows the average gaze position every 250 ms. Error bars indicate the standard deviation.

tool) over its functional part (an action meant to infer tool use), we observed that, under the lift conditions for familiar tools, participants had greater gaze bias toward the functional part; still, we highlight that this may owe to a higher-order affordance effect based on functional knowledge, as was remarked in a past study (Van Der Linden et al., 2015). This is corroborated by the fact that, even with familiar tools, the time spent looking at the functional parts was longer during the use and free viewing conditions than the lift conditions. Thus, there may have indeed been less gaze bias toward the functional parts upon intention to lift, that is, participants prioritized looking at the grasping part of the tool – an action meant to infer the lifting of the tool – over its functional part – an action meant to infer tool use. This may also be supported by the finding that, for unfamiliar tools, the time spent looking at the functional parts was longer during the use and free viewing conditions than the lift conditions.

Importantly, there was an apparent gaze bias toward the functional parts even during free viewing, and it is likely that participants were automatically doing reasoning work for use – even if they did not intend to act on it. The gaze bias toward the functional part during free viewing may reflect a process of preparation for potential use that is automatically initiated during the observation of the tool (Lewis, 2006). For familiar daily tools, this is an automatic semantic reasoning based on functional knowledge (evoked from the shape of the functional part), as shown in a past study (Van Der Linden et al., 2015); for unfamiliar tools, this is an automatic technical reasoning afforded from the mechanical characteristics of the shape of the functional part – a reasoning meant to analogize the usage method.

There was no difference between the free viewing and use conditions for the familiar tools; nonetheless, the fixation time on the functional part was longer during the use conditions than the free viewing conditions for the unfamiliar tools. These results on familiar tools may indicate that knowledge on tool function leads to automatic preparation for use during free observation – in which people are not required to use the tool. Despite this lack of intent for use, the preparation is almost equal to that observed in the condition where people had the intent to use the tool. However, in the time-series gaze position shift, there was a gaze shift in the direction of the grasping part that took place approximately 1,000 ms after the presentation. This gaze shift may reflect the subjects' confirmation of the actual part that they will need to grasp to use the tool. This may support findings that the gaze shifts occur first toward the actual grasping point, in accordance with the action intention (Brouwer et al., 2009; Belardinelli et al., 2015). Along with that, the results may indicate that free observation of the familiar tool involves automatic reasoning work, but does not evoke an image of the actual movement.

Interestingly, these results above seem to contradict prior studies; two research found that participants gazed more at the grasping part when they could freely observe a familiar tool and an object with a consistent combination (Federico and Brandimonte, 2019, 2020). However, in one of these studies, when the combination was consistent and presented at a spatially distant location, participants gazed more at the functional part of the tool (Federico and Brandimonte, 2019), namely, if the tool and the combined object are not in a spatial position where they can be manipulated, people may not automatically imagine the action of using the tool. Thus, these specific results seem consistent with our results. Furthermore, in our study, we did not present another object in combination with the tool; instead, we presented only the tool. This experimental condition corresponds methodologically to the free viewing condition of Federico and Brandimonte (2020), in which the object and the tool are inconsistently combined. Moreover, the short-term recognition task of tools (or objects) present in Federico and Brandimonte (2020)'s study corresponds methodologically to the use condition in the current study, since it involves the process of recalling how to use the tools (or objects). The results of these conditions in Federico and Brandimonte (2020)'s study are consistent with the results of the free viewing and use conditions in our study – an increase in gaze on the functional parts of the tools. Therefore, our results are consistent with those of Federico and Brandimonte (2020)'s study.

The results for unfamiliar tools reveal that, although technical reasoning is still present in free observation, it is present to a lesser degree than when the subject intends to use the tools. When we are asked to use a tool, there is a need to actively extract its mechanical properties to guess how it will be used. Such a need does not arise during free observation. This difference may represent the difference between intentional and automatic technical reasoning. Thus, in a tool observation task with different degrees of familiarity, discerning the degree of technical reasoning may depend on the distinction between viewing with intention to use and free viewing.

In the future, it is important to compare the characteristics of gaze search for familiar and unfamiliar tools in patients with tool use disorder; specifically, we suggest research exploring the pathological mechanisms of tool use disorder. Methodologically, this can be done by conducting comparisons at the time of request for use and during free viewing; if the gaze bias toward the functional area does not change between the use and free viewing conditions, the lack of technical reasoning may be one of the causes of tool use disorder. On the other hand, if the gaze bias is increased, it may be inferred that the patient is trying to make technical reasoning, although with some struggle. Moreover, patients with tool use disorder often show left hemisphere brain damage, so there is a tendency to motor paralysis of the right hand (i.e., usually the dominant hand) in this population; this leads to a propensity to perform tool use with the left hand (i.e., non-dominant hand). In our experiment, to reduce differences in motor effort, tool orientation was standardized so that right-handed participants performed tool use with the left hand; it was likely that participants had greater experience with using their right hands to manipulate familiar tools, which would evoke lesser motor effort compared with using the left hand. Thus, we believe that our present results – found based on methods that ensured participants would perform tool use with the non-dominant hand – may be useful for future comparisons with studies that conduct similar experimentations in patients with tool use disorder.

In this study, however, the actual use of tools was not the ultimate intention. Indeed, the aim was for participants to pantomime as if they were using the tools. Previous studies show that there were differences in fixation point characteristics between actual tool use and pantomime (Kobayakawa et al., 2007), and patient studies revealed a symptom of dissociation between actual tool use and pantomime (Motomura and Yamadori, 1994; Fukutake, 2003). Therefore, it should be noted that the results obtained by the application of this task require careful consideration. Additionally, to explore the possibility of bias toward gazing at the functional part of the tool first and overall attentional bias toward the right side of the screen, future studies are warranted to randomize and examine condition order and tool orientation.

CONCLUSION

The cumulative fixation time on the functional part of the tool during free viewing and intention to use was significantly higher than that during intention to lift. Thus, during intention to lift, participants prioritized looking at the grasping part of the tool – an action meant to infer the lifting of the tool – over its functional part – an action that denotes reasoning work to use the tool; during free viewing, the reasoning work for using the tool was automatically performed. Cumulative fixation time for unfamiliar tools showed a significantly greater increase during free viewing compared with during intention to lift; this increase was also significantly greater during intention to use compared with during free viewing. Thus, the technical reasoning taking place during free viewing is not as intense as that during intent to use. It was suggested that the difference in technical reasoning between free viewing and intention to use may be reflective of the difference between automatic and intentional technical reasoning.

DATA AVAILABILITY STATEMENT

The raw data supporting the conclusions of this article will be made available by the authors, without undue reservation.

ETHICS STATEMENT

The studies involving human participants were reviewed and approved by the Research Ethics Committee of Kio University. The patients/participants provided their written informed consent to participate in this study.

AUTHOR CONTRIBUTIONS

YTam designed the study, collected and analyzed the data, and wrote the manuscript. YTak, YM, MT, and SM provided experimental equipment and helped with data analyses. SN and SM supervised the study. All authors read and approved the manuscript.

FUNDING

This work was supported by JSPS KAKENHI, Grant-in-Aid for Scientific Research B (20H04057).

ACKNOWLEDGMENTS

The authors wish to acknowledge and thank the subjects who participated in this study.

REFERENCES

Belardinelli, A., Barabas, M., Himmelbach, M., and Butz, M. V. (2016). Anticipatory eye fixations reveal tool knowledge for tool interaction. *Exp. Brain Res.* 234, 2415–2431. doi: 10.1007/s00221-016-4646-4640

Belardinelli, A., Herbort, O., and Butz, M. V. (2015). Goal-oriented gaze strategies afforded by object interaction. *Vis. Res.* 106, 47–57. doi: 10.1016/j.visres.2014.11.003

Brouwer, A. M., Franz, V. H., and Gegenfurtner, K. R. (2009). Differences in fixations between grasping and viewing objects. *J. Vis.* 9, 18.1–18.24. doi: 10.1167/9.1.18

Federico, G., and Brandimonte, M. A. (2019). Tool and object affordances: an ecological eye-tracking study. *Brain Cogn.* 135:103582. doi: 10.1016/j.bandc.2019.103582

Federico, G., and Brandimonte, M. A. (2020). Looking to recognise: the pre-eminence of semantic over sensorimotor processing in human tool use. *Sci. Rep.* 10:6157. doi: 10.1038/s41598-020-63045-63040

Fukutake, T. (2003). Apraxia of tool use: an autopsy case of biparietal infarction. *Eur. Neurol.* 49, 45–52. doi: 10.1159/000067027

Gibson, J. J. (1985). *The Ecological Approach to Visual Perception*. Tokyo: Saiensu-Sha, (Trans. T. Kozaki, A. Kozaki, K. Tsuji, and A. Murase).

Goldenberg, G., and Hagmann, S. (1998). Tool use and mechanical problem solving in apraxia. *Neuropsychologia* 36, 581–589. doi: 10.1016/s0028-3932(97)00165-166

Hayhoe, M. M., Shrivastava, A., Mruczek, R., and Pelz, J. B. (2003). Visual memory and motor planning in a natural task. *J. Vis.* 3, 49–63. doi: 10.1167/3.1.6

Kobayakawa, M., Odagiri, M., and Ohigashi, Y. (2007). Difference between pantomiming and actual object use: eye movement analysis during action preparation. *Higher Brain Funct. Res.* 27, 290–297. doi: 10.2496/hbfr.27.290

Land, M., and Tatler, B. (2009). *Looking and Acting Vision and Eye Movements in Natural Behavior*. Oxford: Oxford University Press.

Lewis, J. W. (2006). Cortical networks related to human use of tools. *Neuroscientist* 12, 211–231. doi: 10.1177/1073858406288327

Motomura, N., and Yamadori, A. (1994). A case of ideational apraxia with impairment of object use and preservation of object pantomime. *Cortex* 30, 167–170. doi: 10.1016/s0010-9452(13)80332-80332

Myachykov, A., Ellis, R., Cangelosi, A., and Fischer, M. H. (2013). Visual and linguistic cues to graspable objects. *Exp. Brain Res.* 229, 545–559. doi: 10.1007/s00221-013-3616-z

Osiurak, F. (2014). What neuropsychology tells us about human tool use? The four constraints theory (4CT): mechanics, space, time, and effort. *Neuropsychol. Rev.* 24, 88–115. doi: 10.1007/s11065-014-9260-y

Osiurak, F., Jarry, C., Allain, P., Aubin, G., Etcharry-Bouyx, F., Richard, I., et al. (2009). Unusual use of objects after unilateral brain damage: the technical reasoning model. *Cortex* 45, 769–783. doi: 10.1016/j.cortex.2008.06.013

Osiurak, F., Jarry, C., Lesourd, M., Baumard, J., and Le Gall, D. (2013). Mechanical problem-solving strategies in left-brain damaged patients and apraxia of tool use. *Neuropsychologia* 51, 1964–1972. doi: 10.1016/j.neuropsychologia.2013.06.017

Osiurak, F., Lesourd, M., Navarro, J., and Reynaud, E. (2020). Technition: when tools come out of the closet. *Perspect. Psychol. Sci.* 15, 880–897. doi: 10.1177/1745691620902145

Roberts, K. L., and Humphreys, G. W. (2011). Action-related objects influence the distribution of visuospatial attention. *Q. J. Exp. Psychol.* 64, 669–688. doi: 10.1080/17470218.2010.520086

Signoret, J. L., and North, P. (1984). *Les Apraxies Gestuelles*. Tokyo: Igaku-Shoin, (Trans. T. Watanabe and M. Terada).

Tobii Studio User's Manual Version 3.4.5 (2020). *Tobii Studio User's Manual Version 3.4.5*. Available online at: https://www.tobiipro.com/siteassets/tobii-pro/user-manuals/tobii-pro-studio-user-manual.pdf/ (accessed May 31, 2020).

Van Der Linden, L., Mathôt, S., and Vitu, F. (2015). The role of object affordances and center of gravity in eye movements toward isolated daily-life objects. *J. Vis.* 15:8. doi: 10.1167/15.5.8

Conflict of Interest: The authors declare that the research was conducted in the absence of any commercial or financial relationships that could be construed as a potential conflict of interest.

frontiers
in Psychology

ORIGINAL RESEARCH
published: 17 December 2020
doi: 10.3389/fpsyg.2020.588428

The Role of Haptic Expectations in Reaching to Grasp: From Pantomime to Natural Grasps and Back Again

Robert L. Whitwell[1]*, *Nathan J. Katz*[2], *Melvyn A. Goodale*[2] *and James T. Enns*[1]

[1] Department of Psychology, The University of British Columbia, Vancouver, BC, Canada, [2] Department of Psychology, Brain and Mind Institute, The University of Western Ontario, London, ON, Canada

When we reach to pick up an object, our actions are effortlessly informed by the object's spatial information, the position of our limbs, stored knowledge of the object's material properties, and what we want to do with the object. A substantial body of evidence suggests that grasps are under the control of "automatic, unconscious" sensorimotor modules housed in the "dorsal stream" of the posterior parietal cortex. Visual online feedback has a strong effect on the hand's in-flight grasp aperture. Previous work of ours exploited this effect to show that grasps are refractory to cued expectations for visual feedback. Nonetheless, when we reach out to pretend to grasp an object (pantomime grasp), our actions are performed with greater cognitive effort and they engage structures outside of the dorsal stream, including the ventral stream. Here we ask whether our previous finding would extend to cued expectations for haptic feedback. Our method involved a mirror apparatus that allowed participants to see a "virtual" target cylinder as a reflection in the mirror at the start of all trials. On "haptic feedback" trials, participants reached behind the mirror to grasp a size-matched cylinder, spatially coincident with the virtual one. On "no-haptic feedback" trials, participants reached behind the mirror and grasped into "thin air" because no cylinder was present. To manipulate haptic expectation, we organized the haptic conditions into blocked, alternating, and randomized schedules with and without verbal cues about the availability of haptic feedback. Replicating earlier work, we found the strongest haptic effects with the blocked schedules and the weakest effects in the randomized uncued schedule. Crucially, the haptic effects in the cued randomized schedule was intermediate. An analysis of the influence of the upcoming and immediately preceding haptic feedback condition in the cued and uncued random schedules showed that cuing the upcoming haptic condition shifted the haptic influence on grip aperture from the immediately preceding trial to the upcoming trial. These findings indicate that, unlike cues to the availability of visual feedback, participants take advantage of cues to the availability of haptic feedback, flexibly engaging pantomime, and natural modes of grasping to optimize the movement.

Keywords: grasping, pantomime, haptic feedback, expectations, cognitive supervision

Edited by:
Ivan Camponogara,
New York University Abu Dhabi,
United Arab Emirates

Reviewed by:
Gregory Króliczak,
Adam Mickiewicz University, Poland
Geoffrey P. Bingham,
Indiana University, United States
Luisa Sartori,
University of Padua, Italy

****Correspondence:***
Robert L. Whitwell
rwhitwel@gmail.com

Specialty section:
This article was submitted to
Cognition,
a section of the journal
Frontiers in Psychology

Received: *28 July 2020*
Accepted: *17 November 2020*
Published: *17 December 2020*

Citation:
Whitwell RL, Katz NJ, Goodale MA and Enns JT (2020) The Role of Haptic Expectations in Reaching to Grasp: From Pantomime to Natural Grasps and Back Again.
Front. Psychol. 11:588428.
doi: 10.3389/fpsyg.2020.588428

INTRODUCTION

Goal-directed grasping is multisensory and integrative in nature. The muscle extensions and contractions that are engaged when we reach out to pick a goal object are specified by motor cortex and rely on computations performed on real-time visual and somatosensory information, stored information about the object's function, and the agent's intention (Creem and Proffitt, 2001; Rosenbaum et al., 2001; Frey, 2008; Camponogara and Volcic, 2019; Isa, 2019; Parikh et al., 2020). Studies of the way in which the hand configures while in-flight before the fingers make contact with the object show the hand's aperture and the orientation of the wrist are smoothly tailored to suit the desired contact posture of the hand (grasp kinematics). Two counter-intuitive findings from studies of grasp kinematics in humans are (1) that the visual routes into and through the posterior parietal cortex (PPC) play a causal role in the planning and execution of visually guided actions (e.g., Tunik et al., 2005; Rice et al., 2007), and (2) grasps can be reliably performed without visual awareness of crucial spatial features of the target such as its location, shape, and size (for review, see Rizzolatti and Matelli, 2003; Jeannerod and Jacobb, 2005; Milner and Goodale, 2006; Frey, 2007; Kravitz et al., 2011).

The Visual Control of Natural Reaching and Grasping Is Largely Encapsulated From Visual Awareness

Some of the most compelling evidence for this claim comes from individuals with deficits in visual shape perception (e.g., visual form agnosic patients DF, Goodale et al., 1991, 1994b; Karnath et al., 2009) and individuals with cortically blind areas of their visual field due to damage to V1 (e.g., hemianopic patients PGJ, Perenin and Rossetti, 1996; Whitwell et al., 2011) or with damage encompassing the occipital cortex (Striemer et al., 2019; Whitwell et al., 2020). As their clinically defined deficits would predict, these patients perform at chance when reporting object shape, orientation, and/or size. Yet paradoxically, when they reach out to pick up the objects, the way the hand configures while it moves toward the target reliably expresses the target's spatial properties well-before the hand makes contact with the target (for a comprehensive review of "action blindsight," see Danckert and Rossetti, 2005). Equally as compelling are findings from cases in which bilateral damage to dorsal stream structures in the PPC leads to deficits in reaching and grasping, despite retention of the ability to make discriminative judgments about the target's location, size and shape (e.g., Jakobson et al., 1991; Goodale et al., 1994b; Jeannerod et al., 1994).

In normally sighted individuals, grasping resists a number of effects that influence perceptual judgments: grasp aperture resists the target size-distorting influence of illusory backgrounds (e.g, Whitwell et al., 2016, 2018; Carther-Krone et al., 2020; Navon and Ganel, 2020; Smeets et al., 2020; but see Kopiske et al., 2016); it resists Weber's Law, failing to show a positive relationship between precision and stimulus size (e.g., Ganel et al., 2008; Holmes et al., 2011; Heath et al., 2012; Ozana and Ganel, 2018b; but see Foster and Franz, 2013); and grasp preparation time is not prolonged in the filtering condition of the Garner interference paradigm, in which choice-response times increase when both the relevant and irrelevant dimensions of the target are varied (e.g., Ganel and Goodale, 2003, 2014; Eloka et al., 2015; Freud and Ganel, 2015; Ozana and Ganel, 2018a; but see Löhr-Limpens et al., 2020).

The Dorsal Stream Is Insufficient for Planning Grasps "for Use"

Much of the early neuropsychological work employed basic, canonical objects such as rectangular blocks, cylinders, and smooth pebble-like shapes. The objects possess few associated semantic features and there was often no additional manual manipulation required. Grasping objects with multiple components, such as tools, poses additional problems, because one must also choose where to direct the hand and how to configure it in a way suitable for the tool's intended use (Frey, 2007). Thus, the appropriate selection of which subcomponent of the goal object to grasp incorporates semantic and functional information. Functional MRI studies of grasping and using real 3D tools in normally sighted individuals show activity across a wide range of regions that overlap with the praxis representation network, which includes lateral occipital cortex (LOC), the posterior middle temporal gyrus, and supramarginal gyrus of the inferior parietal cortex, in addition to traditional dorsal stream structures in and around the intraparietal sulcus, and premotor cortex (Hermsdörfer et al., 2007; Brandi et al., 2014; Przybylski and Kroliczak, 2017; Styrkowiec et al., 2019). For technical reasons, functional MRI studies of passively observing tools and/or imagining using them are more common, but they often reveal a similar suite of cortical areas in the ventral and dorsal stream, inferior parietal cortex, and frontal and prefrontal areas (MacDonald and Culham, 2015; Chen et al., 2017).

Interestingly, neuropsychological work with DF, who has visual form agnosia following bilateral damage to the object-sensitive LOC in the ventral stream, but a functionally intact dorsal stream (James et al., 2003), has shown that when she reaches out to pick up and demonstrate the use of tools she cannot recognize, her initial grip posture is often inappropriate for using the object, particularly when the functional-end of the tool is oriented toward her. Only after a brief period of haptic exploration does she adjust her grip to better suit her subsequent demonstration of the tool's use (Carey et al., 1996). DF is similarly impaired when grasping a 3D cross, selecting grasp points across the cross's intersection rather than opposing ends of one (or the other) of the cross's composite bars, regardless of the orientation of the cross (Carey et al., 1996). Integrative visual agnosic patient HJA, whose lesions spared early visual cortex but are restricted to the ventral occipito-temporal cortex and extending about halfway into medial temporal cortex, selects inappropriate parts of tools in order to demonstrate their use, much like DF (Humphreys and Riddoch, 2013). Activity in LOC and other ventral stream structures is not only associated with functional or semantic object information, as these structures are also associated with signaling object weight in neurotypical individuals planning grasp-to-lift movements (Gallivan et al., 2014). Taken together, these studies support a role for the ventral stream and other visual areas outside the dorsal stream to assist with the extraction of hidden properties, such as weight, semantic properties and postural schemas associated with a goal-object's use. They also help to highlight the integrative, multimodal nature of grasping and manipulating objects.

Is the Dorsal Stream Insufficient for Making Natural-Looking Pantomimed Grasps?

In an early effort to define the limits of the automatic visuomotor modules of the PPC, Goodale et al. (1994a) compared the kinematics of natural and pantomimed grasping in both normally sighted controls and in DF. In controls, pantomime grasps led to longer movement planning times, slower reaches, a narrowing of the grasp aperture, inflation of the aperture's tendency to increase with target size, and a susceptibility to the effects of target magnitude on the precision of peak grip aperture (PGA) (e.g., Bingham et al., 2007; Fukui and Inui, 2013; Whitwell et al., 2015a). As for DF, Goodale et al. (1994a) reasoned that if pantomime grasps depend on visual awareness of a target object's 3D properties, then her pantomimed grasp aperture should not scale with the size of the target. In accordance with this prediction, when DF based her pantomime grasps on a short-term memory of a visual preview of the object, her in-flight grip aperture did not covary with the size of the remembered targets (Goodale et al., 1994a; Whitwell et al., 2015a). Nevertheless, when DF was instructed to direct her pantomimed grasps beside a nearby visible target, her grasp aperture covaried reliably with the target's size (Goodale et al., 1994a; Whitwell et al., 2015a). One account for this unexpected result was that when DF's grasps were displaced next to the visible target, her fingertips inadvertently also landed on the surface of the table. This tactile influence may have been enough to recruit her functioning dorsal stream to engage in visually guided automatic grasping.

Support for this tactile feedback hypothesis came from two studies: one showing that DF retained her grip scaling to object size when she reached out to pick up 2D printed rectangular shapes as if they were 3D objects (Westwood et al., 2002); and another showing that she loses her grip scaling when she reaches out to grasp a visible virtual object that is not physically there (Schenk, 2012). This latter result also suggests that visual target information in and of itself (e.g., Castiello, 1996) is not enough to drive DF's grip scaling. Indeed, under similar virtual circumstances, DF retains her grip scaling provided the size of the grasped object is held constant while the size of the visible target varies from trial to trial (Whitwell et al., 2014, 2015b). In fact, DF's grip aperture partially adapts to the size of the felt target, just as normally sighted controls do, despite being unaware of the mismatch in size (Säfström and Edin, 2004; Whitwell et al., 2014, 2015b). Taken together, these studies of DF suggest that tactile contact is a critical ingredient for normal dorsal-stream grasping and that, in the absence of any end-point whatsoever, structures outside the dorsal stream (including the ventral stream) become crucially engaged, even for geometrically simple rectilinear and cylindrical shapes. It is noteworthy to point out that a similar distinction within the apraxic literature exists between pantomimed tool-use while holding the tool and pantomimed tool-use made with gestures in thin air (e.g., Buxbaum et al., 2000; Goldenberg et al., 2004; Hermsdorfer et al., 2012).

Pantomimed Grasps as Natural Grasps Without Haptic Calibration

Perhaps the simplest account of pantomimed grasping is that it is the outcome of the natural haptics-dependent grasp system when it has been left uncalibrated by consistent absence of haptic feedback across iterative grasps. This line of reasoning is supported by the fact that many kinematic differences between grasps and pantomimed grasps vanish when haptic and non-haptic feedback trials are randomly intermixed (Bingham et al., 2007). Nevertheless, we suspect there is more to it than that, for at least three reasons. First, the haptic calibration account does not accommodate the possibility that cognitive supervision (e.g., Norman and Shallice, 1986; Shallice and Burgess, 1993) directly influences crucial parameters of pantomimed (uncalibrated) grasps such as hand aperture. Bingham et al. (2007) left open the possibility that cues to the availability of haptic feedback could shift control between pantomime and natural modes of grasping, because the expectation for haptic feedback was never manipulated independently of the trial schedule of haptic conditions. Without intermixing the two haptic conditions and manipulating expectations for haptic feedback, one cannot disentangle the influence of sensorimotor calibration from that of cognitive supervision. Second, the haptic calibration account cannot explain why pantomime grasps would be more susceptible than natural grasps to pictorial illusions (e.g., Westwood et al., 2000; Rinsma et al., 2017), particularly when the illusion is correlated with activity in the ventral stream structures, including LOC, that is early enough (< 300 ms) to putatively influence the grasp (Weidner et al., 2010). Third, haptic calibration cannot explain why the pantomime grasps performed by magicians more closely resemble "calibrated" natural grasps (Cavina-Pratesi et al., 2011; Rinsma et al., 2017), despite the absence of haptic feedback. Moreover, a magician's expertise in pantomime grasping does not confer immunity from the illusory effects of the Muller-Lyer illusion on displaced pantomime grasps made to simulate picking up 3D objects subjected to the illusion (Rinsma et al., 2017).

We take the "pantomime" grasps of naive participants as an example of performance under direct cognitive control or cognitive supervision. For "automatic" grasps, the selection and specification of parameters like wrist orientation, reach velocity and grasp aperture size (or the paths the fingers take) occurs with minimal awareness and minimal cognitive control, as is clearly the case for DF and in cases of action blindsight, in which the person cannot reliably perceive the geometry and spatial disposition of the goal object. Cognitive supervision under these more natural circumstances maintains focus on the overarching goal of the movement (which is typically to *do something* with the object) rather than on the details of the unfolding movement in real-time. Conversely, for grasps in which parameter specification is under direct cognitive control, cognitive supervision is focused on the unfolding movement in real-time, rather than on the overarching goal. Pantomime grasps and grasps made iteratively without haptic feedback exhibit signs of cognitive control: Relative to natural grasps, they take longer to initiate, the movement is slower, the hand's in-flight aperture is typically smaller, and the aperture's scaling to the size of the target is more variable, i.e., some participants use their hand aperture to grossly exaggerate the differences among target sizes, whereas others hardly bother to differentiate the target sizes at all (e.g., Bingham et al., 2007; Fukui and Inui, 2013; Whitwell et al., 2015a).

Study Overview

Here we tested the possibility that pantomime grasps performed by adults naïve to the task and directed at virtual objects are influenced by expectations about the availability of haptic feedback at the end of the reach. Note that this possibility does not negate the role of grip calibration from recent haptic end-point feedback (e.g., Bingham et al., 2007; Volcic and Domini, 2018). We fully expected that grip calibration would carry over from one trial to the next, based on the large body of work showing that, for example, grip aperture adjusts to mismatches between the haptic and visual size of the goal object, even in the absence of awareness of the mismatch (e.g., Säfström and Edin, 2004, 2008; Weigelt and Bock, 2007; Coats et al., 2008; Karok and Newport, 2010). Rather, we were asking here whether participant's explicit haptic expectations about the grasp they are about to perform can make unique contributions to grasp parameters over and above that of the calibration. Put another way, we tested the cognitive penetribility of grasps, in so far as this cognitive effort can exploit reliable cues to the availability of haptic feedback.

Our experimental design borrows from previous work that varied expectations for the availability of *visual* feedback in order to test the cognitive penetrability of grasps (Whitwell et al., 2008). The authors did this by using verbal cues to manipulate the participant's expectation for receiving online *visual* feedback on an upcoming reach and observing how these expectations influenced, if at all, a well-established effect of visual feedback on grasp aperture: grasps executed without online visual feedback exhibit wider in-flight grip aperture, compared to grasps executed *with* online visual feedback (e.g., Hesse and Franz, 2010; for review, see Smeets and Brenner, 1999; for the effects of partial removal of visual feedback, see Bozzacchi et al., 2018). Whitwell et al. (2008) organized the two visual feedback conditions into four different sets of trials: two sets, one for each visual condition (blocked); a third set in which the visual conditions predictably alternated from one trial to the next (alternating); and a fourth set in which they were randomly intermixed and unpredictable (randomized). Participants were verbally cued before the beginning of each trial set about the nature of the order of the visual condition. If expectations about the visual condition were cognitively exploitable, then performance in the alternating (predictable) trial set would look like performance when the visual conditions were blocked separately but would differ from performance in the randomized schedule, in which the visual condition was not predictable. If, in contrast, the parameterization of the grasp was influenced by previous grasps, rather than predictive information about the upcoming visual condition, then performance on the visual conditions would homogenize in both the alternating and randomized schedules, because the visual conditions are intermixed, but would dissociate in the blocked schedules in which stable visual conditions would afford optimal calibration. Whitwell et al. (2008) observed the latter outcome. In a follow-up experiment, a trial-by-trial analysis of the different visual conditions showed the performance diverges with successive trials of one visual condition compared to the other, in-line with a sensorimotor-calibration based account (Whitwell and Goodale, 2009).

We based our current experiment primarily on the design of Whitwell et al. (2008), but rather than varying the expectations for *visual* feedback, we vary the expectations for *haptic* feedback. We did this by comparing grasps made with and without haptic feedback into five different sets of trials: in two sets of trials, the two haptic conditions were blocked separately (*blocked*); in a third set of trials the haptic conditions alternated predictably from one trial to the next (*alternating*); and in a fourth and fifth set of trials, the haptic conditions were randomly intermixed with identical trial orders (*randomized*). Crucially, in one of these two randomized schedules, the availability of haptic feedback was made known to the participant in advance (*random cued* vs. *random uncued*). The two randomized schedules possess the same sequence of haptic conditions and are, therefore, controlled for trial-to-trial haptic-calibration based influences.

This design affords two approaches to data analysis: First, we performed targeted tests for the influence of the cues on block-level performance. This analysis addresses the hypothesis that reliable expectations regarding haptic feedback can promote pantomime-like grasps on upcoming trials *without* haptic feedback and more natural-like grasps on upcoming trials *with* haptic feedback. Thus, support for the role of cues and cognitive control should be reflected in a larger effect of removing haptic feedback in the randomized trial set with cues than in the one without cues. Second, we tested the unique influences of (1) the pending haptic condition on the current trial (t) on grip aperture and (2) the haptic condition on the immediately preceding trial ($t - 1$). If cues about the availability of haptic feedback can flexibly switch the response-mode between natural and pantomime grasps, as cognitive control (cognitive penetrability) would predict, then we should observe an influence of the pending, cued haptic condition on grip aperture and little or no influence of the immediately preceding haptic condition. Furthermore, in the absence of cues, we should observe a greater influence of the immediately preceding haptic condition on grip aperture and no influence of the pending and unknown (to the participant) haptic condition on grip aperture.

MATERIALS AND METHODS

Participants

Thirty right-handed participants with normal or corrected-to-normal vision were recruited at the University of Western Ontario (20 females, aged 18–57 years (M = 22.4, SD = 7.99). Participants provided written and informed consent prior to participating in the study. Ethical procedures were approved by the local ethics committee. Participants were compensated $10 for their time, and they were naïve to the purpose of the study.

Apparatus and Experimental Setup

Figure 1 shows the experimental setup, which employed a mirror-apparatus allowing the experimenter to manipulate the presence or absence of haptic feedback (e.g., Whitwell et al., 2015a). In brief, the mirror-apparatus comprised an upright mirror with reflective side perpendicular to the horizontal plane and oriented 45° clockwise from the edge of the table nearest the participant. When seated, the participants faced the reflective side of the mirror at the 45° clockwise orientation.

The participant's starting location was a microswitch that was fixed to the table surface 10 cm away from the table edge along the participant's sagittal plane. Between trials, and before the start of each reach, the participant used their index finger and thumb, pinched together, to depress the microswitch. The microswitch was used to help control the state of the lenses of a pair of PLATO goggles (Translucent Technologies, Toronto, ON, Canada). The lenses of the goggles can switch between the two states (translucent and transparent) in < 6 ms. The lenses of the goggles assumed a default translucent state that blocks the wearer's view. The lenses remained translucent between trials but were cleared at the start of each trial to reveal the workspace, which included the virtual target cylinder. When participants released the microswitch at movement initiation, the lenses switched back to their default translucent state. Thus, participants did not receive visual input about the target or their hand throughout their reach; actions performed under these circumstances are referred to as being performed in visual "open loop."

The principal reason for using open loop stemmed from the fact that the mirror obstructs the view of the participant's hand throughout most of the reach. Using an open loop procedure in this context means that the participant does not have the experience of seeing their hand disappear behind the mirror and, for the subset of movements in which their hand makes contact with an object, the experience of lifting an object behind the mirror while it remains visibly static in the mirror. In other words, the visual open loop condition was believed to minimize a reduction in immersion.

The set of target objects were three pairs of wooden cylinders painted matte black. Each pair differed only in diameter (3.5, 4.8, and 6 cm). On any given trial, any one of the three different objects was positioned in front of the mirror, so that the participant would see its reflection in the mirror (the virtual object), while its partner (an identical cylinder) could be positioned behind the mirror such that this hidden cylinder was spatially coincident with the virtual cylinder. Thus, the cylinders behind the mirror were located mirror-opposite of the cylinders in front. The cylinders in front of the mirror could be located at any one of two possible locations and the distance between them was 10 cm. To ensure a consistent and accurate placement, the cylinders each had holes drilled into the bottom, so that each cylinder could be placed onto the peg of small square wooden plates, painted matte white, that were fixed to the table surface. This was done for the cylinder locations behind the mirror as well. The distance between the start position and the closest cylinder location was ∼17 cm. The start position was allowed to vary by small amounts to suit each participant's preference for comfortability provided it did not block the participants ability to see their hand, because (1) target distance was not a variable of theoretical interest and (2) the manipulations of theoretical interest were within-subjects.

The positions of three infrared emitting diodes (IREDs) affixed to the inner nails of the index finger and thumb, and the wrist of the right hand, was recorded with submillimeter precision at sampling rate of 200 Hz by an active optoelectronic motion capturing system, OPTOTRAK^{TM} 3020 (Northern Digital, Waterloo, ON, Canada) with a positional measurement error of $< \pm 21$ mm.

Procedure

The subject was seated comfortably at the table in front of the mirror and oriented so that (1) the occluding board blocked a direct view of the cylinder at each one of the two locations, but (2) did not block a binocular view of the virtual cylinder

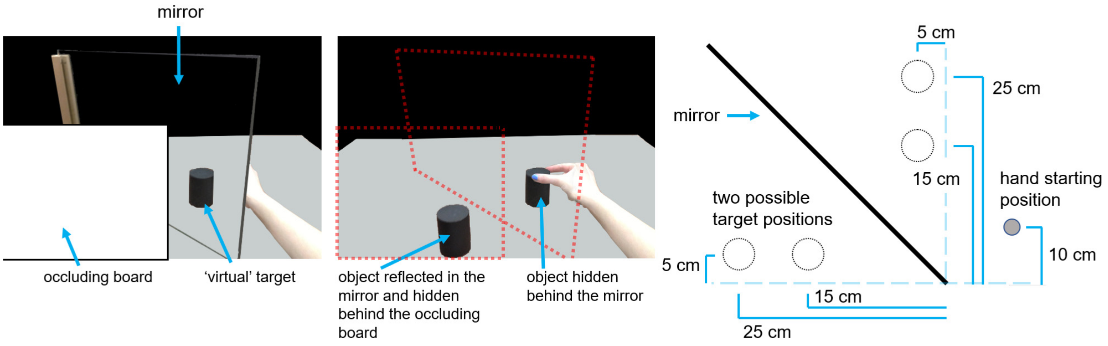

FIGURE 1 | Mirror apparatus and setup. Illustration of the participant's view of the virtual target (leftmost panel), the occluding board and mirror removed to reveal the object reflected in the mirror, and the identically sized object hidden behind the mirror and positioned to as to match the apparent position of the virtual object (middle panel), and a schematic bird's-eye view of the setup, including the mirror, the hand's approximate starting position, and the two possible object locations, which are indicated with circles with dotted outlines (rightmost panel).

at each location. The experimenter explained the task, using demonstrations, after which the three IREDs were attached with medical tape to the participant's right hand: one at the corner of the proximal base of the thumb nail, one at the corner of the proximal base of the index finger nail, and one at the proximal end of the index finger on the dorsal face. The medical tape was used to secure the IREDs and to ensure that the pads of the index finger and thumb were uncovered and would receive typical tactile feedback from touching objects. Note that the distance between the IREDs was non-zero and, therefore, the computed distance between the IREDs will include this additional amount.

Participants started each trial with the tips of their index finger pinched together and depressing the microswitch. They were instructed to use visibility of the workspace as the imperative to locate the virtual cylinder and then reach out behind the mirror to grasp it. Furthermore, the participants were asked to reach out naturally, neither speeded nor labored. On trials in which a cylinder was positioned behind the mirror (haptic feedback trials), participants were to grasp the cylinder, lift it, and move it to the right side of the table, and then return to the starting position (the microswitch). The participants were also asked to simulate grasping, lifting, and moving the virtual cylinder on trials in which no cylinder was positioned behind the mirror (no-haptic feedback trials), before returning to the starting position. The participants were asked to simulate holding the object so that the fingers would not go through it (e.g., Whitwell et al., 2015a).

Trials were organized into separate sets that differed with respect to their schedule of haptic and no-haptic feedback conditions (see section "Experimental Design"). On all trials, the experimenter positioned an object first in front of the mirror and then behind the mirror. If that trial called for no-haptic feedback, after positioning the object behind the mirror, the experimenter removed it as they withdrew their hand. This was done so that the same sequence of experimenter events and timing occurred for both the haptic and no-haptic feedback trials. Before the trial was initiated and depending on the trial set, the experimenter verbally cued the participant about whether an object was behind the mirror or not.

Between each set, the participant was invited to remove the goggles and to rest for up to 5 min. During this time, the experimenter familiarized the participant with the nature of the haptic- and no-haptic trial expectancies for the next set of trials.

Experimental Design

Each participant was tested across five sets trial schedules. The five trial sets were dubbed *blocked* (no-haptic feedback and haptic feedback trials administered in separate blocks of trials); *alternating* haptic and no-haptic feedback; randomized haptic- and no-haptic feedback without reliable cues (*randomized uncued*); and randomized haptic- and no-haptic feedback with cues (*randomized cued*).

In a given set of trials, each cylinder was presented three times at each of the two locations in pseudorandom order for a total of 18 trials for each of the haptic and no-haptic feedback conditions (if present). Target position was manipulated to reduce the contribution of memory to the responses and to keep the task more engaging for the participants. Thus, the blocked haptic and no-haptic trial sets each consisted of 18 trials, and the alternating and randomized haptic- and no-haptic feedback trial-sets each consisted of 36 trials (18 for the haptic feedback condition and 18 for the no-haptic feedback condition). In total, each participant was administered 144 trials. The order in which the five trial sets were administered was pseudo-randomized from one participant to the next and counterbalanced across all participants. Notably, the presence or absence of an object hidden behind the mirror was always discovered by the participant at the end of their reach, regardless of presence or absence of the verbal cue (or what the participant believed would be the case).

Data Processing

Positional data was Butterworth lowpass filtered at 20 Hz after which the 3D derivatives corresponding to speed and acceleration were computed for each sample frame for each IRED. Grip aperture was computed at each sample frame as the 3D distance between the IREDs positioned on the index-finger and thumb and the first derivative of this variable was computed (grip aperture velocity). Our principal dependent measure was PGA, which was isolated on each trial by operationally defining the forward reach component of the response. The first sample frame in which the velocity of the forward reach exceeded 5 cm/s for 100 ms was defined as the point at which the forward reach was initiated, and the time from trial start to the initiation of the forward reach was operationally defined as the movement preparation time (MPT). The forward reach was operationally terminated on the first sample frame in which the velocity of the wrist IRED fell below 10 cm/s. The length, in ms, of this time window comprised the movement time (MT). PGA was the largest grip aperture observed throughout the forward reach. Peak hand velocity (PHV) was the fastest velocity achieved by the wrist IRED throughout the forward reach time. In order to define the final grip aperture (FGA) for grasps made with haptic feedback and the pantomimed ones made without haptic feedback, we used the grip aperture velocity and defined FGA as the first sample frame in which the grip aperture velocity remained within a range ±1 cm/s following the sample frame in which PGA was achieved. We performed linear regression analysis to derive the slope relating target size to PGA and to FGA. Finally, the time it took from movement start to achieve PGA (tPGA) was also computed. Each trial was visually inspected to ensure the algorithm selected sensible sample frames.

Statistical Analysis

For a given participant, the dependent measures from each trial were grouped by their corresponding unique conditions, which were the unique combinations of target size, target distance, haptic feedback, and haptic trial schedule. The means of these groupings served as the basic unit of analysis for each participant for repeated measures ANOVA (rmANOVA). The factors of interest for the rmANOVA were *haptic feedback* (available or not available) and the *schedule* in which these two conditions were administered (four variants: blocked, alternating, randomized cued, and randomized uncued). An expanded ANOVA that included target size as an additional factor was of no theoretical interest for the dependent measures other than PGA and FGA. Furthermore, for those measures the slopes relating target size to PGA and to FGA, by definition, capture the linear influence of target size on PGA. Type I error rate (alpha) was defined as 0.05 for each rmANOVA effect. Violations of sphericity were addressed using Greenhouse-Geisser adjustments to the degrees of freedom. Note that, as mentioned in section "Apparatus and Experimental Setup," target distance was of no theoretical interest, and so the means for target size, target distance, haptic feedback, and haptic trial schedule were weighted accordingly.

Significant main effects of haptic trial schedule (or the superseding haptic feedback × schedule interaction) were analyzed using sets of orthogonal paired-samples *t*-tests. Relative to pair-wise alternatives, orthogonal tests reduce the number of comparisons made, which reduces the correction for multiple comparisons and increase statistical power, and they analyze unique, rather than redundant, variance. For the interactions, the first orthogonal contrast involved the haptic trial schedules that were most similar: the alternating trials and the randomly interleaved ones with reliable haptic cues. These condition pairs were tested, and, if non-significant, were averaged together and contrasted against either the blocked or randomized haptic condition schedule without reliable haptic cues. A non-significant difference at this stage led us to average together the three tested conditions into one to test the remaining haptic trial schedule. The alpha error rate was defined per family of tests, and the Holms step-down variant of the Bonferonni correction was used to control it at 0.05 (Holm, 1979).

Given our interest in PGA and the influence that preceding haptic availability exerts on it, we (1) performed a single paired-samples *t*-test to contrast mean PGA on and the mean slopes from the two randomly interleaved variants for a targeted check on the influence of reliable haptic cues on PGA and the slopes; and (2) we applied multiple linear regression to predict the average PGA on a given trial as a function of the haptic feedback condition of that trial and of the immediately preceding trial. We included the size and distance of the target on the given trial as covariates. For each participant, this regression was run separately for each of the two randomly interleaved haptic schedules. Four means were computed using the regression coefficients relating the availability of haptic feedback on the current trial to PGA and the availability of haptic feedback on the immediately preceding trial to PGA for the two randomly interleaved schedules. If inducing reliable expectations about the availability of haptic feedback can flexibly switch the response mode between natural and pantomime variants, then we should observe an influence of the haptic condition on the current trial and little influence of the haptic condition on the previous trial. Furthermore, in the absence of reliable haptic expectations, we should observe a larger influence of haptic feedback on the previous trial and no influence of haptic feedback on the current trial.

RESULTS

General Remarks

The results of the rmANOVAs for each measure are presented in **Table 1**. **Table 2** reflects the conditions means for several relevant dependent measures as a function of distance and haptic feedback.

TABLE 1 | The effects tested with repeated measures ANOVA across the dependent measures.

Dependent measures		Effects								
		Schedule			Haptic feedback			Interaction		
		F	p	η_p^2	F	p	η_p^2	F	p	η_p^2
Grip	PGA	15.71	< 0.001	0.35	6.54	< 0.02	0.18	3.85	< 0.03	0.12
	Slope (PGA)	9.78	< 0.001	0.25	26.49	< 0.001	0.48	19.31	< 0.001	0.4
	FGA	5.18	< 0.008	0.15	40.87	< 0.001	0.59	5.55	< 0.006	0.16
	Slope (FGA)	7.62	< 0.001	0.21	4.95	< 0.04	0.15	5.05	< 0.004	0.15
Transport and temporal	MPT	3.99	< 0.02	0.12	44.28	< 0.001	0.6	21.99	< 0.001	0.43
	PHV	1.47	> 0.23	N/A	76.2	< 0.001	0.72	28.14	< 0.001	0.49
	tPGA	4.14	< 0.01	0.13	29.74	< 0.001	0.51	28.97	< 0.001	0.5
	MT	2.09	> 0.1		26.03	< 0.001	0.47	12.9	< 0.001	0.31

TABLE 2 | Dependent measures as a function of target distance ('near' and 'far') and haptic condition.

Dependent measures		Haptic feedback		No haptic feedback	
		Near	Far	Near	Far
Grasp	*PGA (mm)*	88.5 (8)	91.3 (8.8)	86.2 (10.3)	88.4 (10.9)
	FGA (mm)	62.1 (2.5)	62.1 (2.7)	55.8 (6.5)	54.8 (6.6)
Transport and temporal	*PHV (mm/s)*	477 (90)	600 (108)	444 (92)	565 (102)
	RT (mm)	655 (175)	676 (184)	714 (185)	722 (187)
	tPGA (ms)	298 (59)	332 (75)	314 (56)	344 (69)
	MT (ms)	740 (91)	872 (107)	785 (102)	909 (113)

All measures showed a main effect of removing haptic feedback, which can be viewed in the leftmost panels of **Figures 2–4**. All measures except PHV and MT showed a main effect of haptic schedule. All measures showed an interaction of haptic feedback and schedule, which is illustrated in the middlemost and rightmost panels of **Figures 2–4**. The middle panels reflect the effect of removing haptic feedback on each schedule. The rightmost panels show the condition means. In **Figures 2–4**, the red bars reflect the blocked schedules in which the haptic conditions were unmixed; the blue bars reflect the mixed uncued schedule; while the purple bars reflect the mixed cued schedules.

The pattern of results shown here for haptic feedback are, at first blush, strikingly similar to the results for visual feedback (c.f., Whitwell et al., 2008). For example, the largest influence of haptic feedback, like that of visual feedback in the earlier studies, occurred under the blocked schedules and the smallest differences for the mixed ones. Nevertheless, a crucial difference emerged in that there were clear differences between the cued mixed schedules, on one side, and the randomized uncued schedule on the other. These differences are expanded on below.

For each measure, we found a null difference between the alternating haptic schedule and the randomly interleaved haptic schedule with reliable cues. The only difference between these two schedules was the opportunity, in the randomly interleaved schedule, to encounter small runs of trials with or without haptic feedback. Note too that in both of these haptic trial schedules, participants were given cues concerning haptic feedback.

Transport and Temporal Component Measures

The left panels of **Figure 2** show the results for temporal measures. Removing haptic feedback increased MPT, slowed the PHV, increased the time taken tPGA and increased the MT. The middle panels of **Figure 2** show that these effects were most prominent in the blocked schedules. In the mixed schedules these haptic effects were significantly reduced but not abolished entirely provided reliable haptic expectations were available. When haptic expectations were unreliable, as they were in the uncued randomized schedule, the haptic effect was null for all measures except for the MT, which was 12 ms longer without haptic feedback than with it. This likely reflects the brief continued movement of the hand when there is no object for the fingers to make contact with and the participant has no expectation for haptic feedback. The right panels of **Figure 2** show that an absence of reliable expectation is similar to the effect of removing haptic feedback in terms of the direction of its effect on each measure. More generally, the right panels show that the measures on no-haptic feedback trials were generally less affected by schedules than they were on haptic feedback trials.

In-Flight Grip Component Measures

Figure 3 shows the results for the in-flight grip component measures, PGA and the slope relating target size to PGA (b_{PGA}).

The leftmost panels of **Figure 3** show that removing haptic feedback reduced PGA and exaggerated the b_{PGA}. The middle panels show that these haptic effects were strongest in the blocked schedule, intermediate in the cued mixed schedules, and, in the uncued randomized schedule, negligible for the PGA but, interestingly, reversed for the b_{PGA}. For PGA, the haptic effect was greater in the blocked schedule than in the randomized uncued schedule [$t(29) = 2.41, p < 0.03$], and significantly greater in the randomized cued schedule than in the randomized uncued schedule [$t(19) = 2.06, p < 0.05$]. For PGA, the right panel shows that the mixed schedules increase PGA in both haptic conditions, but more so in the no haptic feedback condition. Furthermore, the PGA was greatest in the uncued randomized schedule. For b_{PGA}, the right panel shows that, relative to the blocked schedules, the mixed cued schedules reduced b_{PGA} on no-haptic feedback trials but increased b_{PGA} on haptic feedback trials. This pattern was the most extreme in the uncued randomized schedule in which haptic effect reversed.

"Final" Grip Component Measures

Figure 4 shows the results for the "final" grip component measures, FGA and the slope relating target size to FGA (b_{FGA}).

The leftmost panels of **Figure 4** show that removing haptic feedback reduced the mean FGA and exaggerated the mean b_{FGA}. The middle panels show that, for the FGA, the haptic effect was equivalent across the schedules in which cues were available. The haptic effect on FGA was greatest in the uncued random schedule. As the rightmost FGA panel shows, this was primarily driven by the much smaller mean FGAs observed when haptic feedback was not available in this schedule. The middle panels also show that, for b_{FGA}, the haptic effect was weakest in the cued schedules, and greatest in the uncued randomized schedule. The rightmost panel for the b_{FGA} show that mean b_{FGA} approached unitary in all of the haptic feedback conditions, regardless of schedule, which would be expected given that participants were most likely to be holding the target at that point. The haptic effect on b_{FGA} was greatest in the uncued randomized schedule. This was driven by the no-haptic feedback condition in which participants exhibited a much smaller mean slope.

Peak Grip Aperture as a Function of Pending and Immediately Preceding Haptic Feedback

As described in section "Materials and Methods," we used multiple regression to predict, for each participant, PGA as a function of the current haptic feedback condition and the immediately preceding one for the cued and uncued versions of the randomized schedules. If cues to haptic feedback are used predictively, then the main haptic contribution to PGA should stem from reliable expectation for haptic feedback on the current trial, rather than on the availability of haptic feedback on the immediately preceding trial. In the absence of reliable cues, the biggest haptic contribution to PGA should stem from the availability of haptic feedback on the immediately preceding trial.

Figure 5 shows that this pattern is exactly what we found. On a trial-to-trial basis, participants took advantage of reliable cues regarding haptic feedback to switch between two modes of responding: larger PGA in accurate anticipation of grasping an

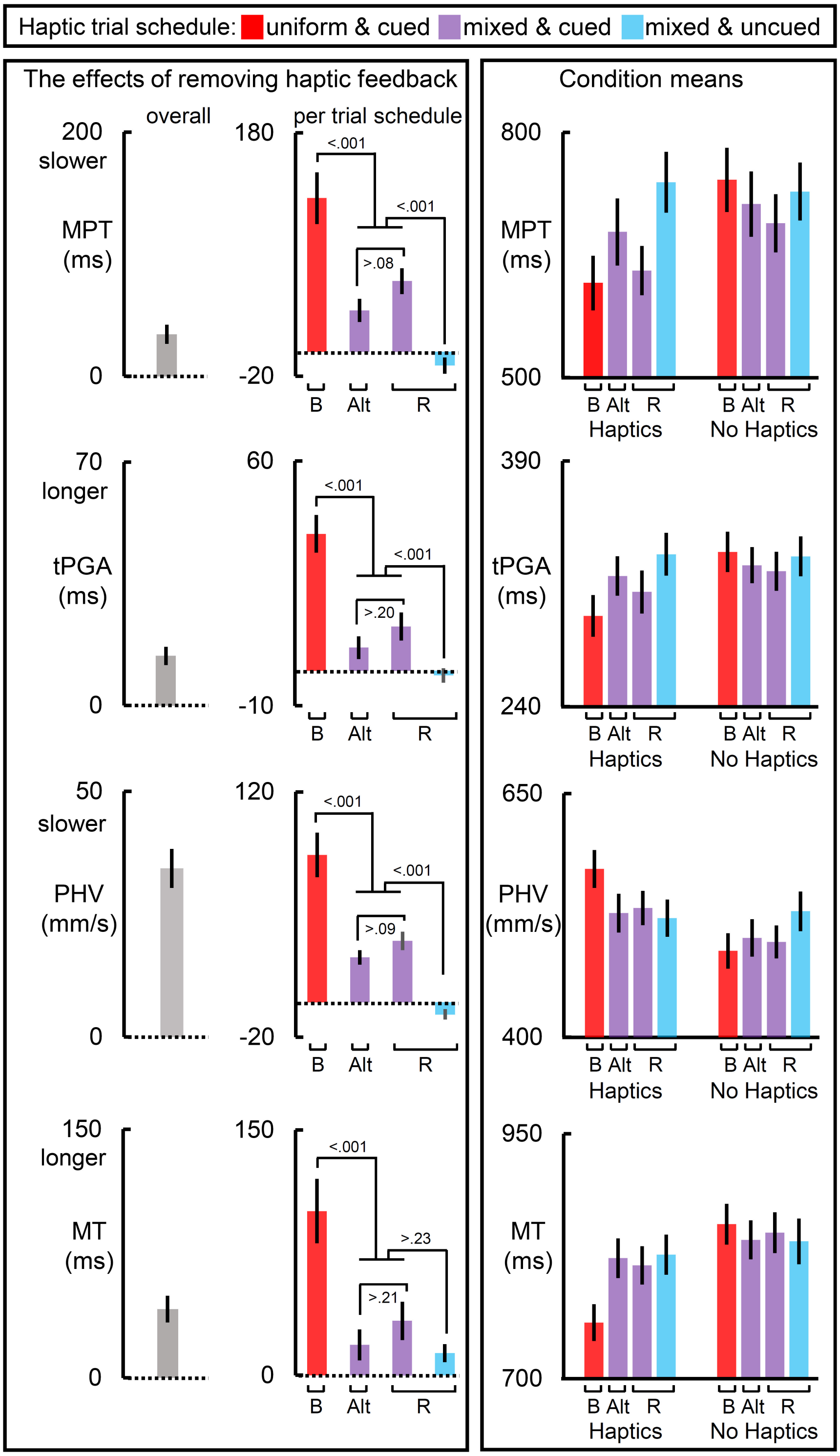

FIGURE 2 | The effects of removing haptic feedback on temporal and transport measures. The leftmost and middle columns of panels reflect the effect of removing haptic feedback on movement preparation time (MPT), time to achieve peak grip aperture (tPGA), peak hand velocity (PHV), and the movement time (MT). Removing haptic feedback slowed MPT, PHV, and MT, and prolonged tPGA. Most notably, the schedule of haptic feedback modulated these effects (middle column of panels). On each of these measures, the blocked scheduled (red bars) yielded the largest effect, the cued mixed schedules yielded an intermediate one, and the uncued randomized schedule yielded the weakest effect (with the exception of MT). The raw condition means for each measure are depicted in the rightmost column of panels. Bar label "B" refers to the blocked trial order; "Alt." alternating block of trials; and "R" randomized ones. Dotted lines reflect null of removing haptic feedback. All error bars reflect SEMs, and the dotted lines reflect the null hypothesis for tests against zero.

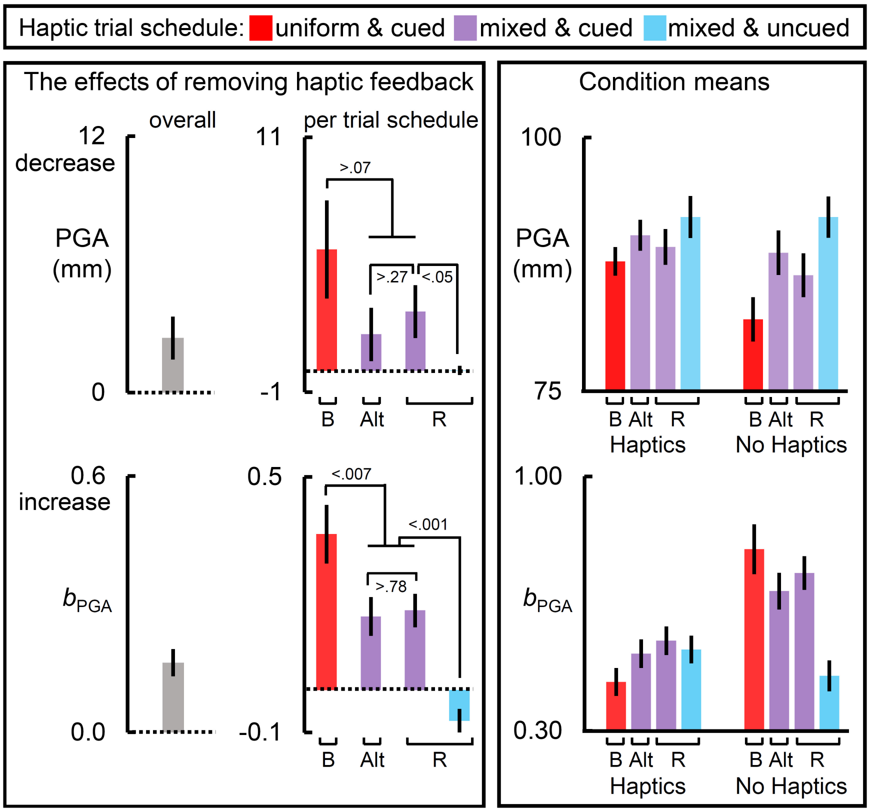

FIGURE 3 | The effects of removing haptic feedback on the in-flight grip component measures. The leftmost and middle columns of panels reflect the effects of removing haptic feedback on peak grip aperture (PGA) and the slope relating target size to PGA (b_{PGA}). Removing haptic feedback reduced PGA and increased b_{PGA}. Most notably, the schedule of haptic feedback modulated these effects (middle column of panels). On each measure, the blocked schedule yielded the largest effect, the cued mixed schedules yielded an intermediate one, and the randomly interleaved uncued schedule yielded the weakest effect. The raw condition means for each measure are depicted in the rightmost panels. Bar label "B" refers to the blocked trial order; "Alt." alternating block of trials; and "R" randomized ones. Dotted lines reflect a null effect of removing haptic feedback. All error bars reflect SEMs, and the dotted lines reflect the null hypothesis for tests against zero.

object and smaller PGA in accurate anticipation of grasping thin-air. Furthermore, in the absence of reliable cues, we find that the haptic feedback condition on the immediately preceding trial but not the pending one, influenced PGA. Specifically, PGA was larger following a trial in which no object was grasped (and vice versa following a trial in which an object was grasped).

DISCUSSION

This study examined the influences of both trial-to-trial calibration and of expectations about the availability of haptic feedback on reaching to grasp virtual objects. From the outset, we expected that the sensorimotor system responsible for natural goal-directed grasps would exploit the haptic experience on previous grasps to reduce error on subsequent grasps (e.g., Säfström and Edin, 2008). We also expected iterative grasps performed without haptic feedback to take on the stereotypical characteristics of pantomimed grasps, including slower reach velocities, longer movement planning times, smaller PGA, and an exaggerated scaling of in-flight grip aperture to target size (grip scaling). Our primary question was whether grasps under these conditions are influenced only by the trial history of haptic feedback, chiefly from the immediately preceding trial, or whether they are also influenced by cued expectations about the availability of the target for grasping. We asked this question to help us understand whether the specification of parameters for real-time grasps are cognitively accessible (and subject to cognitive supervision) or if they are refractory to them, as is thought to typically occur for natural grasps.

We implemented a task in which participants reached behind a mirror to pick up visible "virtual" objects, which were sometimes available for the hand to make contact with (haptic feedback), and at other times were not (no haptic feedback). In all haptic trial schedules except one, we provided verbal cues to the availability of haptic feedback. We reasoned that cognitively accessible operations should be capable of predictively exploiting cues about the availability of haptic feedback at the end of the reach, particularly in otherwise randomized haptic-feedback schedules. Our results demonstrate that cognitive supervisory processes can exploit verbal cues about the availability of haptic feedback to plan grip aperture for future events.

We manipulated expectations about the availability of haptic feedback by varying the availability of verbal cues to the participant before the start of the trial. In the blocked trial schedule in which an object was always available for the hand to

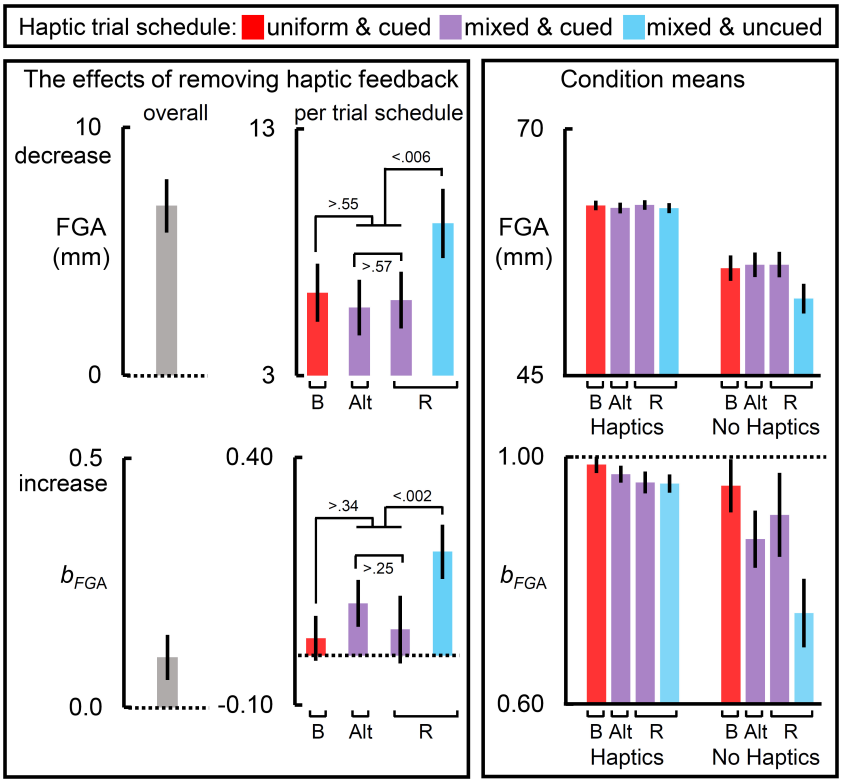

FIGURE 4 | The effects of removing haptic feedback on the "final" grip component measures. The leftmost and middle columns of panels reflect the effects of removing haptic feedback on the final grip aperture (FGA) and the slope relating target size to FGA (b_{FGA}). Removing haptic feedback decreased FGA and increased b_{FGA} (leftmost panels). Most notably, the schedule of haptic feedback modulated these effects (middle column of panels). On each measure, the blocked scheduled yielded the largest effect, the cued mixed schedules yielded an intermediate one, and the randomly interleaved schedule yielded the weakest effect. The raw condition means for each measure are depicted in the rightmost panels. Bar label "B" refers to the blocked trial order; "Alt." alternating block of trials; and "R" randomized ones. Dotted lines reflect a null effect of removing haptic feedback. All error bars reflect SEMs, and the dotted lines reflect the null hypothesis for tests against zero (left panels and middle bottom panel) or one (bottom right panel).

make contact with at the end of the reach, participants' grasps were free to be influenced both by the recent history of haptic-experience (calibration) and the expectation that the hand would make contact with the object at the end of the reach. In the blocked trial schedule in which an object was not present behind the mirror and so the hand grasped "thin-air," the expectation for no haptic feedback was available but no haptic information was available to calibrate subsequent grasps. The blocked schedules led to the greatest differences in haptic effect across all measures tested, in line with previous work drawing similar comparisons (e.g., Bingham et al., 2007; Whitwell et al., 2015a).

In three additional haptic condition schedules, the object was available on some trials and not on others, permitting intermittent opportunities for haptic calibration to occur. One set consisted of a strict schedule of alternation between haptic feedback and no feedback, allowing participant expectations about feedback to potentially be based on the regular pattern and/or their awareness of the alternating schedule. The two remaining sets consisted of randomized haptic schedules. Crucially, a verbal cue about the availability of haptic feedback on the upcoming trial was provided in only one of them. If grasps are dominated by dorsal stream operations that are inaccessible to cognitive supervisory processes, then the grasps should not dissociate as a function of the reliability of haptic expectations (as indexed by the reliability of the cues). Alternatively, if an absence of haptic feedback induces a switch to a pantomime mode of responding, recruiting structures outside the dorsal stream that are accessible to cognitive supervisory processing, then reliable haptic expectations in the cued randomized schedule should dissociate grasps made with and without haptic feedback, such that the former should look more like natural grasps while the latter should look more like pantomimed ones. Our findings support the alternative proposal. The haptic effects in the mixed schedules were reduced, relative to the effects observed in the blocked schedules, in-line with the influence of intermittent haptic calibration. Crucially, however, for all measures except for MT, reliable haptic expectations led to larger haptic effects relative to when haptic expectations were unreliable, indicating that cognitive supervisory processing can flexibly intervene to assume limited control over the response.

The analysis of PGA as a function of haptic feedback on the upcoming and immediately preceding trials in the cued and uncued randomized schedule further support the alternative viewpoint. First, with reliable haptic expectations

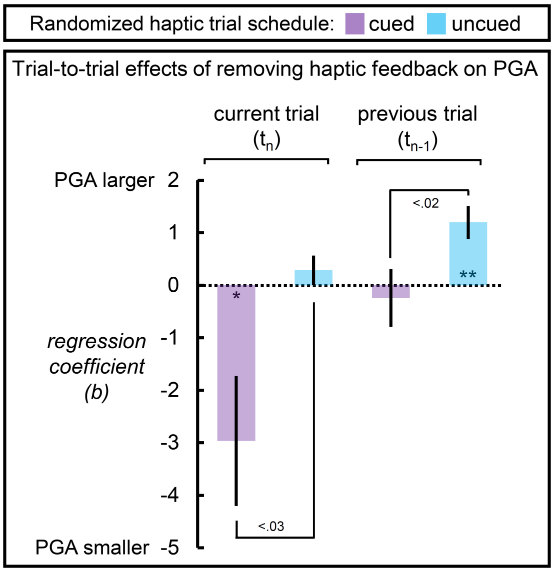

FIGURE 5 | Peak grip aperture as a function of the unique effects of removing haptic feedback on the current (upcoming) and immediately preceding trial for the randomized haptic trial schedules. When participants were reliably cued that haptic feedback would not be available on the current trial, PGA decreased; but when cues were unreliable, the availability of haptic feedback on the current trial was not predictive of PGA on the current trial. The reverse pattern was observed with respect to the availability of haptic feedback on the previous trial. When cues were reliable, the availability of haptic feedback on the previous trial was not predictive of PGA; but when cues were unreliable, an absence of haptic feedback on the previous trial led to an increase in PGA. Dotted line reflects a null effect of the haptic feedback removing haptic feedback. Error bars reflect SEMs. *$p < 0.05$; **$p < 0.01$.

on the upcoming trial, PGA was larger if haptic feedback was available on the upcoming trial and smaller when it was not, in-line with what one would predict if cognitive supervisory processing was flexibly engaged. Furthermore, the haptic feedback condition on the immediately preceding trial was discounted, making no contribution to PGA. In other words, reliable cues rendered grip aperture predictive with respect to the upcoming haptic condition. Second, in the absence of reliable haptic expectations, PGA was influenced by the haptic feedback condition on the immediately preceding trial *but not* the upcoming haptic condition. Specifically, PGA was smaller if haptic feedback was experienced on the immediately preceding trial than if it was not. There are two explanations for this second result. One interpretation is that without reliable cues, participants attempt to predict whether or not their hand would encounter an object on the upcoming trial, anticipating the opposite of their experience on the previous trial. Notably, this strategy would necessarily fail to differentiate the response to haptic and no-haptic feedback conditions across the trial set, because the haptic conditions are randomized. Furthermore, this explanation does not seem plausible, because participants were aware of the random nature of the haptic condition. A competing interpretation uses these considerations to suggest that participants simply adopt a wider "fail safe" margin in their PGA, resulting in the largest PGAs in this schedule (see top right panel of **Figure 3**); Experiencing haptic feedback on the previous trial, however, presents an opportunity to calibrate grip aperture toward the relatively smaller values more typical of natural grasps, relative to the increased PGA adopted by participants in this schedule; Whereas an absence of haptic feedback on the previous trial disrupts this process, leading to an increased safety margin on the subsequent grasp. Calibration, under the randomized uncued circumstance, competes between natural and a fail-safe modes of grasping.

The importance of both factors—calibration and cognitive control—in distinguishing pantomimed from natural grasping was also apparent in the analysis of the slopes relating target size to PGA (grip scaling). Grip scaling has been shown to be exaggerated more for pantomime grasps than for natural ones (e.g., Whitwell et al., 2015a). Our findings both reinforce and refine this observation. When cues for haptic feedback were reliable, grip scaling was greater on trials without haptic feedback than trials with it. The absence of reliable cues for haptic feedback, however, reversed this trend. In other words, when the availability of haptic feedback was unknown, grip scaling was greater on upcoming trials with haptic feedback than without it. Our explanation for this tendency is that under cognitive supervision, participants respond categorically or ordinally, rather than metrically (e.g., Dijkerman et al., 1998). This exaggerates the difference between the largest and smallest target sizes, particularly when there is no physical consequence for under or oversizing the grip aperture on no haptic feedback trials.

Our findings are consistent with those from a previous investigation that tested memory-guided pantomime grasps directed at the remembered location of a previewed object with and without haptic feedback (Davarpanah Jazi and Heath, 2016). In the haptic-feedback condition, after the participants completed their pantomime grasp, the previewed target was placed between their thumb and index finger. The haptic and no-haptic conditions were blocked separately or randomly interleaved and left uncued. The authors found that grip aperture violated Weber's law, which has been adopted as index of absolute vs. relative coding of target size (e.g., Ganel et al., 2008; Holmes et al., 2013; Manzone et al., 2017; Ozana and Ganel, 2018b; but see Foster and Franz, 2013; Löwenkamp et al., 2015), for the haptic conditions only when blocked separately (Davarpanah Jazi and Heath, 2016). It is unknown, however, whether their findings are due to a cued expectation for haptic feedback or to visuo-haptic calibration, because the authors did not test a cued variant of their randomized haptic schedule.

Our findings are also consistent with previous work using a similar virtual setup to test the effects of visual-haptic mismatches in target size on grasping (Gentilucci et al., 1995). In one of their experiments, the authors alerted the participants to the fact that the visual and haptic sizes of the targets would not match. The authors observed a wider grip aperture that peaked earlier in the reach (Gentilucci et al., 1995). These effects are observed when participants adopt a more cautious strategy, and so it is possible that the prospect of visual haptic mismatches encouraged a cautious strategy. Nevertheless, the findings make it clear that some aspects of natural grasps made in virtual environments are amenable to coarse cognitive control.

It will be important for future studies to examine more closely the ability of the dorsal stream to use calibration and to form expectations when it is dissociated from the ventral stream. A recent study has shown that an individual, MC, with large bilateral lesions to occipital cortex cannot only point to visual targets but is also susceptible to the effects of lateral shifts in the visual field that can be introduced with prism goggles (Striemer et al., 2019). Over the course of many trials, MC's reaches compensate for the error introduced by the prisms, indicating that the dorsal stream is capable of supporting a remarkable degree of calibration in the absence of normal phenomenological vision. Furthermore, MC also demonstrated a typical prism induced after-effect, such that, after the prisms were removed, her compensatory reaches persisted for several trials before returning back to their baseline accuracy levels (Striemer et al., 2019).

As we reviewed in the introduction, patient DF's ventral stream is compromised and yet, when instructed to direct her pantomimed grasps beside a nearby visible target, her grasp aperture covaried reliably with target size. How is the dorsal stream using tactile feedback in DF's case to automatically scale her grip aperture to the size of the target? The present results point to a range of possibilities. At the simplest extreme, the dorsal stream may only be able to benefit from calibration based on the most recent experience of tactile feedback. At an intermediate level, it may be able to harness memory for simple scheduling patterns such as an alternating sequence. At the most sophisticated level, it may be able to take full advantage of learned associations between reliable cues and their predictive relations to haptic feedback. We speculate, based on the literature we have reviewed, and of the role played by expectations in the present study, that the dorsal stream is only capable of calibration. But this question deserves a closer look in patients without functioning ventral streams and/or in studies using transcranial magnetic stimulation to temporarily disrupt the ventral stream contribution to a grasping task.

These findings also have important practical implications. One ready application is in virtual reality environments, where the aim is to enhance the user's immersive experience by simulating manual interactions with virtual objects as realistically as possible. Our findings reinforce a broad observation that participants tend to adopt pantomime styled grasps in these settings that consist of stereotypically different kinematic characteristics than do natural grasps. When combined with the virtual environment, motion tracking equipment sensitive enough to resolve fine movements of the fingers that occur during reach to grasp actions may benefit from algorithms that interpret the resultant kinematic data in a way that matches the agent's actual movements to virtual ones that more closely resemble natural grasps. Recent work has shown that although naïve individuals are poor at discriminating videos of pantomimed and natural grasps, magicians perform at above-chance levels, suggesting that expertise in sleight of hand and pantomime enhances discrimination of fine-grained differences between pantomimed and natural grasps (Quarona et al., 2020). Although it is clear from our experience that many individuals find grasping thin-air unusual, it is not clear whether naïve participants can use kinesthetic feedback to discriminate pantomimed and natural grasps. Mapping pantomime grasps to stereotypical, natural-looking grasps in visual virtual space may be a valid approach if users are unlikely to detect differences between their kinesthetic and visual experience; by that same token, a spatiotemporal mapping that closely approximates a point-to-point relationship of pantomimes to virtual movements may be necessary if users are likely to detect the discrepancy and experience a concomitant reduction in immersion[1].

Future work should examine the computational basis for inferring an agent's intended goal when they perform pantomime reaching and grasping in more realistic virtual environments with cluttered spaces and multiple possible goal objects within reach. Existing research has shown that an individual's intentions for a given grasp (e.g., to pour vs. to drink from a glass) are available in the visible kinematics (Koul et al., 2019). Studies that combine these techniques with measurements of the agent's level of immersion could track the effect that a closer mapping between intention, action, and environmental consequence has on immersion.

DATA AVAILABILITY STATEMENT

The raw data supporting the conclusions of this article will be made available by the authors, without undue reservation, to any qualified researcher.

ETHICS STATEMENT

The studies involving human participants were reviewed and approved by the Behavioural Research Ethics Board Western University. The patients/participants provided their written informed consent to participate in this study.

AUTHOR CONTRIBUTIONS

RW designed the experiment. NK administered the experiment. RW and NK analyzed the data. All authors contributed to writing of the manuscript.

FUNDING

This research was funded through a Natural Sciences and Engineering Research Council of Canada Discovery Grants (RGPIN-2018-03741) awarded to JE and (RGPIN-2017-04088) awarded to MG, and an NSERC Postdoctoral Fellowship (487969) awarded to RW.

---

[1] Here, "immersion," refers to the extent to which the VR experience feels real. McMahan's (2003) notion of "realism," for example, can be extended to action execution. An agent immersed in their VR experience would seem to forget, temporarily, that they were in a VR environment. This term can apply to the entire experience or just aspects of it, like reaching out to pick up a virtual object. The agent's knowledge that they are in a VR environment should not necessarily track the feeling that when they reach out to pick up a virtual environment, they are doing so naturally, automatically, with little cognitive effort. The agent is immersed with respect to their action.

REFERENCES

Bingham, G., Coats, R., and Mon-Williams, M. (2007). Natural prehension in trials without haptic feedback but only when calibration is allowed. *Neuropsychologia* 45, 288–294. doi: 10.1016/j.neuropsychologia.2006.07.011

Bozzacchi, C., Brenner, E., Smeets, J. B., Volcic, R., and Domini, F. (2018). How removing visual information affects grasping movements. *Exp. Brain Res.* 236, 985–995. doi: 10.1007/s00221-018-5186-6

Brandi, M.-L., Wohlschlager, A., Sorg, C., and Hermsdorfer, J. (2014). The neural correlates of planning and executing actual tool use. *J. Neurosci.* 34, 13183–13194. doi: 10.1523/jneurosci.0597-14.2014

Buxbaum, L. J., Giovannetti, T., and Libon, D. (2000). The role of the dynamic body schema in praxis: evidence from primary progressive apraxia. *Brain Cogn.* 44, 166–191. doi: 10.1006/brcg.2000.1227

Camponogara, I., and Volcic, R. (2019). Grasping movements toward seen and handheld objects. *Sci. Rep.* 9:3665. doi: 10.1038/s41598-018-38277-w

Carey, D. P., Harvey, M., and Milner, A. D. (1996). Visuomotor sensitivity for shape and orientation in a patient with visual form agnosia. *Neuropsvchologia* 34, 329–337. doi: 10.1016/0028-3932(95)00169-7

Carther-Krone, T. A., Senenayake, S. A., and Marotta, J. J. (2020). The influence of the Sander parallelogram illusion and early, middle and late vision on goal-directed reaching and grasping. *Exp. Brain Res.* 238, 2993–3003. doi: 10.1007/s00221-020-05960-2

Castiello, U. (1996). Grasping a fruit: selection for action. *J. Exp. Psychol.* 22, 582–603. doi: 10.1037/0096-1523.22.3.582

Cavina-Pratesi, C., Kuhn, G., Ietswaart, M., and Milner, A. D. (2011). The magic grasp: motor expertise in deception. *PLoS One* 6, 1–5. doi: 10.1371/journal.pone.0016568

Chen, J., Snow, J. C., Culham, J. C., and Goodale, M. A. (2017). What role does "Elongation" play in "Tool-Specific" activation and connectivity in the dorsal and ventral visual streams? *Cereb. Cortex* 28, 1117–1131. doi: 10.1093/cercor/bhx017

Coats, R., Bingham, G. P., and Mon-Williams, M. (2008). Calibrating grasp size and reach distance: interactions reveal integral organization of reaching-to-grasp movements. *Exp. Brain Res.* 189, 211–220. doi: 10.1007/s00221-008-1418-5

Creem, S. H., and Proffitt, D. R. (2001). Grasping objects by their handles: a necessary interaction between cognition and action. *J. Exp. Psychol.* 27, 218–228. doi: 10.1037/0096-1523.27.1.218

Danckert, J., and Rossetti, Y. (2005). Blindsight in action: what can the different sub-types of Blindsight tell us about the control of visually guided actions? *Neurosci. BioBehave. Rev.* 29, 1035–1046. doi: 10.1016/j.neubiorev.2005.02.001

Davarpanah Jazi, S., and Heath, M. (2016). Pantomime-grasping: advance knowledge of haptic feedback availability supports an absolute visuo-haptic calibration. *Front. Hum. Neurosci.* 10:197. doi: 10.3389/fnhum.2016.00197

Dijkerman, H. C., and Milner, A. D. (1998). The perception and prehension of objects oriented in the depth plane II. Dissociated orientation functions in normal subjects. *Exp. Brain Res.* 118, 408–414. doi: 10.1007/s002210050294

Eloka, O., Feuerhake, F., Janczyk, M., and Franz, V. H. (2015). Garner-interference in left-handed awkward grasping. *Psychol. Res. Psychol. Forsch.* 79, 579–589. doi: 10.1007/s00426-014-0585-1

Foster, R. M., and Franz, V. H. (2013). Inferences about time course of Weber's Law violate statistical principles. *Vis. Res.* 78, 56–60. doi: 10.1016/j.visres.2012.11.012

Freud, E., and Ganel, T. (2015). Visual control of action directed toward two-dimensional objects relies on holistic processing of object shape. *Psychon, Bull. Rev.* 22, 1377–1382. doi: 10.3758/s13423-015-0803-x

Frey, S. H. (2007). What puts the how in where? Tool use and the divided visual streams hypothesis. *Cortex* 43, 368–375. doi: 10.1016/s0010-9452(08)70462-3

Frey, S. H. (2008). Tool use, communicative gesture and cerebral asymmetries in the modern human brain. *Philos. Trans. R. Soc. Lond. B Biol. Sci.* 363, 1951–1957. doi: 10.1098/rstb.2008.0008

Fukui, T., and Inui, T. (2013). How vision affects kinematic properties of pantomimed prehension movements. *Front. Psychol.* 4:44. doi: 10.3389/fpsyg.2013.00044

Gallivan, J. P., Cant, J. S., Goodale, M. A., and Flanagan, J. R. (2014). Representation of object weight in human ventral visual cortex. *Curr. Biol.* 24, 1–8. doi: 10.1016/j.cub.2014.06.046

Ganel, T., Chajut, E., and Algom, D. (2008). Visual coding for action violates fundamental psychophysical principles. *Curr. Biol.* 18, 599–601. doi: 10.1016/j.cub.2008.04.052

Ganel, T., and Goodale, M. A. (2003). Visual control of action but not perception requires analytical processing of object shape. *Nature* 426, 664–667. doi: 10.1038/nature02156

Ganel, T., and Goodale, M. A. (2014). Variability-based Garner interference for perceptual estimations but not for grasping. *Exp. Brain Res.* 232, 1751–1758. doi: 10.1007/s00221-014-3867-3

Gentilucci, M., Daprati, E., Toni, I., Chieffi, S., and Saetti, M. C. (1995). Unconscious updating of grasp motor program. *Exp. Brain Res.* 105, 291–303.

Goldenberg, G., Hentze, S., and Hermsdörfer, J. (2004). The effect of tactile feedback on pantomime of tool use in apraxia. *Neurology* 63, 1863–1867. doi: 10.1212/01.wnl.0000144283.38174.07

Goodale, M. A., Jakobson, L. S., and Keillor, J. M. (1994a). Differences in the visual control of pantomimed and natural grasping movements. *Neuropsychologia* 32, 1159–1178. doi: 10.1016/0028-3932(94)90100-7

Goodale, M. A., Meenan, J. P., Bulthoff, H. H., Nicolle, D. A., Murphy, K. J., and Racicot, C. I. (1994b). Separate neural pathways for the visual analysis of object shape in Perception and prehension. *Curr. Biol.* 4, 604–610. doi: 10.1016/s0960-9822(00)00132-9

Goodale, M. A., Milner, A. D., Jakobson, L. S., and Carey, D. P. (1991). A neurological dissociation between perceiving objects and grasping them. *Nature* 349, 154–156. doi: 10.1038/349154a0

Heath, M., Holmes, S. A., Mulla, A., and Binsted, G. (2012). Grasping time does not influence the early adherence of aperture shaping to Weber's law. *Front. Hum. Neurosci.* 6:332. doi: 10.3389/fnhum.2012.00332

Hermsdorfer, J., Li, Y., Randerath, J., Goldenberg, G., and Johannsen, L. (2012). Tool use without a tool: kinematic characteristics of pantomiming as compared to actual use and the effect of brain damage. *Exp. Brain Res.* 218, 201–214. doi: 10.1007/s00221-012-3021-z

Hermsdörfer, J., Terlinden, G., Mühlau, M., Goldenberg, G., and Wohlschläger, A. M. (2007). Neural representations of pantomimed and actual tool use: evidence from an event-related fMRI study. *NeuroImage* 36, 109–118.

Hesse, C., and Franz, V. H. (2010). Grasping remembered objects: exponential decay of the visual memory. *Vis. Res.* 50, 2642–2650. doi: 10.1016/j.visres.2010.07.026

Holm, S. (1979). A simple sequentially rejective multiple test procedure. *Scand. J. Stat.* 6, 65–70.

Holmes, S. A., Lohmus, J., McKinnon, S., Mulla, A., and Heath, M. (2013). Distinct visual cues mediate aperture shaping for grasping and pantomime-grasping tasks. *J. Mot. Behav.* 45, 431–439. doi: 10.1080/00222895.2013.818930

Holmes, S. A., Mulla, A., Binsted, G., and Heath, M. (2011). Visually and memory-guided grasping: aperture shaping exhibits a timedependent scaling to Weber's law. *Vis. Res.* 51, 1941–1948. doi: 10.1016/j.visres.2011.07.005

Humphreys, G., and Riddoch, J. (2013). *A Case Study in Visual Agnosia Revisited: To See But Not To See*, 2nd Edn. Hove: Psychology Press.

Isa, T. (2019). Dexterous hand movements and their recovery after central nervous system injury. *Annu. Rev. Neurosci.* 42, 315–335. doi: 10.1146/annurev-neuro-070918-050436

Jakobson, L. S., Archibald, Y. M., Carey, D. P., and Goodale, M. A. (1991). A kinematic analysis of reaching and grasping movements in a patient recovering from optic ataxia. *Neuropsychologia* 29, 803–809. doi: 10.1016/0028-3932(91)90073-H

James, T. W., Culham, J., Humphrey, G. K., Milner, A. D., and Goodale, M. A. (2003). Ventral occipital lesions impair object recognition but not object-directed grasping: an fMRI study. *Brain* 126, 2463–2475. doi: 10.1093/brain/awg248

Jeannerod, M., Dicety, J., and Michel, F. (1994). Impairment of grasping movements following a bilateral posterior parietal lesion. *Neuropsychologia* 12, 369–380. doi: 10.1016/0028-3932(94)90084-1

Jeannerod, M., and Jacobb, P. (2005). Visual cognition: a new look at the two-visual systems model. *Neuropsychologia* 43, 301–312. doi: 10.1016/j.neuropsychologia.2004.11.016

Karnath, H. O., Ruter, J., Mandler, A., and Himmelbach, M. (2009). The anatomy of object recognition – visual form agnosia caused by medial occipitotemporal stroke. *J. Neurosci.* 29, 5854–5862. doi: 10.1523/JNEUROSCI.5192-08

Karok, S., and Newport, R. (2010). The continuous updating of grasp in response to dynamic changes in object size, hand size and distractor proximity. *Neuropsychologia* 48, 3891–3900. doi: 10.1016/j.neuropsychologia.2010.10.006

Kopiske, K. K., Bruno, N., Hesse, C., Schenk, T., and Franz, V. H. (2016). The functional subdivision of the visual brain: is there a real illusion effect on action? A multi-lab replication study. *Cortex* 79, 130–152. doi: 10.1016/j.cortex.2016.03.020

Koul, A., Soriano, M., Tversky, B., Becchio, C., and Cavallo, A. (2019). The kinematics that you do not expect: integrating prior information and kinematics to understand intentions. *Cognition* 182, 213–219. doi: 10.1016/j.cognition.2018.10.006

Kravitz, D. J., Saleem, K. S., Baker, C. I., and Mishkin, M. (2011). A new neural framework for visuospatial processing. *Nat. Rev. Neurosci.* 12, 217–230. doi: 10.1038/nrn3008

Löhr-Limpens, M., Göhringer, F., Schenk, T., and Hesse, C. (2020). Grasping and perception are both affected by irrelevant information and secondary tasks: new evidence from the Garner paradigm. *Psychol. Res.* 84, 1269–1283. doi: 10.1007/s00426-019-01151-z

Löwenkamp, C., Gartner, W., HJaus, I. D., and Franz, V. H. (2015). Semantic grasping escapes Weber's law. *Neuropsychologia* 70, 235–245. doi: 10.1016/j.neuropsychologia.2015.02.037

MacDonald, S. N., and Culham, J. C. (2015). Do human brain areas involved in visuomotor actions show a preference for real tools over visually similar non-tools? *Neuropsychologia.* 77, 35–41. doi: 10.1016/j.neuropsychologia.2015.08.004

McMahan, A. (2003). "Immersion, engagement, and presence: a method for analyzing 3-D video games," in *The Video Game Theory Reader*, eds M. J. P. Wolf, and B. Perron (New York, NY: Routledge), 67–86.

Milner, A. D., and Goodale, M. A. (2006). *The Visual Brain in Action*, 2nd Edn. New York, NY: Oxford University Press.

Manzone, J., Jazi, S. D., Whitwell, R. L., and Heath, M. (2017). Biomechanical constraints do not influence pantomime-grasping adherence to Weber's law: A reply to Utz et al. (2015). *Vision Res.* 130, 31–35. doi: 10.1016/j.visres.2016.09.018

Navon, G., and Ganel, T. (2020). Consciously monitored grasping is vulnerable to perceptual intrusions. *Conscious. Cogn.* 85:103019. doi: 10.1016/j.concog.2020.103019

Norman, D. A., and Shallice, T. (1986). "Attention to action," in *Consciousness and Self-Regulation*, eds R. J. Davidson, G. E. Schwartz, and D. Shapiro (Boston, MA: Springer), doi: 10.1007/978-1-4757-0629-1_1

Ozana, A., and Ganel, T. (2018a). Dissociable effects of irrelevant context on 2D and 3D grasping. *Atten. Percept. Psychophys.* 80, 564–575. doi: 10.3758/s13414-017-1443-1

Ozana, A., and Ganel, T. (2018b). Weber's law in 2D and 3D grasping. *Psychol. Res.* 83, 977–988. doi: 10.1007/s00426-017-0913-3

Parikh, P. J., Fine, J. M., and Santello, M. (2020). Dexterous object manipulation requires context-dependent sensorimotor cortical interactions in humans. *Cereb. Cortex* 30, 3087–3101. doi: 10.1093/cercor/bhz296

Perenin, M. T., and Rossetti, Y. (1996). Grasping without form discrimination in a hemianopic field. *Neuroreport* 7, 793–797. doi: 10.1097/00001756-199602290-00027

Przybylski, L., and Kroliczak, G. (2017). Planning functional grasps of simple tools invokes the hand-independent praxis representation network: an fMRI study. *J. Int. Neuropsychol. Soc.* 23, 108–120. doi: 10.1017/s1355617716001120

Quarona, D., Koul, A., Ansuini, C., Pascolini, L., Cavallo, A., and Becchio, C. (2020). A kind of magic: enhanced detection of pantomimed grasps in professional magicians. *Q. J. Exp. Psychol.* 73, 1092–1100. doi: 10.1177/1747021820918533

Rice, N. J., Tunik, E., Cross, E. S., and Grafton, S. T. (2007). Online grasp control is mediated by the Contralateral hemisphere. *Brain Res.* 1175C, 76–84. doi: 10.1016/j.brainres.2007.08.009

Rinsma, T., van der Kamp, J., Dicks, M., Canal-Bruland, R. (2017). Nothing magical: pantomimed grasping is controlled by the ventral system. *Exp. Brain Res.* 235, 1823–1833. doi: 10.1007/s00221-016-4868-1

Rizzolatti, G., and Matelli, M. (2003). Two different streams form the dorsal visual system: anatomy and functions. *Exp. Brain Res.* 153, 146–157. doi: 10.1007/s00221-003-1588-0

Rosenbaum, D. A., Meulenbroek, R. J., Vaughan, J., and Jansen, C. (2001). Posture-based motion planning: applications to grasping. *Psychol. Rev.* 108, 709–734. doi: 10.1037/0033-295X.108.4.709

Säfström, D., and Edin, B. B. (2004). Task requirements influence sensory integration during grasping in humans. *Learn. Mem.* 11, 356–363. doi: 10.1101/lm.71804

Säfström, D., and Edin, B. B. (2008). Prediction of object contact during grasping. *Exp. Brain Res.* 190, 265–277. doi: 10.1007/s00221-008-1469-7

Schenk, T. (2012). No dissociation between perception and action in Patient DF when haptic feedback is withdrawn. *J. Neurosci.* 32, 2013–2017. doi: 10.1523/JNEUROSCI.3413-11.2012

Shallice, T., and Burgess, P. (1993). "Supervisory control of action and thought selection," in *Attention: Selection, Awareness, and Control: A Tribute to Donald Broadbent*, eds A. D. Baddeley, and L. Weiskrantz (Oxford: Clarendon Press/Oxford University Press), 171–187.

Smeets, J. B., and Brenner, E. (1999). A new view on grasping. *Mot. Control* 3, 237–271. doi: 10.1123/mcj.3.3.237

Smeets, J. B. J., Kleijn, E., van der Meijden, M., and Brenner, E. (2020). Why some size illusions affect grip aperture. *Exp. Brain Res.* 238, 969–979. doi: 10.1007/s00221-020-05775-1

Striemer, C. L., Enns, J. T., and Whitwell, R. L. (2019). Visuomotor adaptation in the absence of input from early visual cortex. *Cortex* 115, 201–215. doi: 10.1016/j.cortex.2019.01.022

Styrkowiec, P. P., Nowik, A. M., and Króliczak, G. (2019). The neural underpinnings of haptically guided functional grasping of tools: an fMRI study. *NeuroImage* 194, 149–162. doi: 10.1016/j.neuroimage.2019.03.043

Tunik, E., Frey, S. T., and Grafton, S. H. (2005). Virtual lesions of the anterior intraparietal area disrupt goal-dependent on-line adjustments of grasp. *Nat. Neurosci.* 8, 505–511. doi: 10.1038/nn1430

Volcic, R., and Domini, F. (2018). The endless visuomotor calibration of reach-to-grasp actions. *Sci. Rep.* 8:14803. doi: 10.1038/s41598-018-33009-6

Weidner, R., Boers, F., Mathiak, K., Dammers, J., and Fink, G. R. (2010). The temporal dynamics of the muller-lyer illusion. *Cereb. Cortex* 20, 1586–1595. doi: 10.1093/cercor/bhp217

Weigelt, C., and Bock, O. (2007). Adaptation of grasping responses to distorted object size and orientation. *Exp. Brain Res.* 181, 139–146. doi: 10.1007/s00221-007-0911-6

Westwood, D. A., Chapman, C. D., and Roy, E. A. (2000). Pantomimed actions may be controlled by the ventral visual stream. *Exp. Brain Res.* 130, 545–548. doi: 10.1007/s002219900287

Westwood, D. A., Danckert, J. A., Servos, P., and Goodale, M. A. (2002). Grasping two-dimensional and three-dimensional objects in visual-form agnosia. *Exp. Brain Res.* 144, 262–267. doi: 10.1007/s00221-002-1068-y

Whitwell, R. L., Buckingham, G., Enns, J. T., Chouinard, P. A., and Goodale, M. A. (2016). Rapid decrement in the effects of the Ponzo display dissociates action and perception. *Psychon. Bull. Rev.* 23, 1157–1163. doi: 10.3758/s13423-015-0975-4

Whitwell, R. L., Ganel, T., Byrne, C. M., and Goodale, M. A. (2015a). Real-time vision, tactile cues, and visual form agnosia: removing haptic feedback from a "natural" grasping task induces pantomime-like grasps. *Front. Hum. Neurosci.* 9:216. doi: 10.3389/fnhum.2015.00216

Whitwell, R. L., Milner, A. D., Cavina-Pratesi, C., Barat, M., and Goodale, M. A. (2015b). Patient DF's visual brain in action: visual feedforward control in visual form agnosia. *Vis. Res.* 110, 265–276. doi: 10.1016/j.visres.2014.08.016

Whitwell, R. L., and Goodale, M. A. (2009). Updating the programming of a precision grip is a function of recent history of available feedback. *Exp. Brain Res.* 194, 619–629. doi: 10.1007/s00221-009-1737-1

Whitwell, R. L., Goodale, M. A., Merritt, K. E., and Enns, J. T. (2018). The Sander parallelogram illusion dissociates action and perception despite control for the litany of past confounds. *Cortex* 98, 163–176. doi: 10.1016/j.cortex.2017.09.013

Whitwell, R. L., Lambert, L. M., and Goodale, M. A. (2008). Grasping future events: explicit knowledge of the availability of visual feedback fails to reliably influence prehension. *Exp. Brain Res.* 188, 603–611. doi: 10.1007/s00221-008-1395-8

Whitwell, R. L., Milner, A. D., Cavina-Pratesi, C., Byrne, C. M., and Goodale, M. A. (2014). DF's visual brain in action: the role of tactile cues. *Neuropsychologia* 55, 41–50. doi: 10.1016/j.neuropsychologia.2013.11.019

Whitwell, R. L., Sperandio, I., Buckingham, G., Chouinard, P. A., and Goodale, M. A. (2020). Grip constancy but not perceptual size constancy survives lesions of early visual cortex. *Curr. Biol.* 30, 3680.e5–3686.e5.

Whitwell, R. L., Striemer, C. L., Nicolle, D. A., and Goodale, M. A. (2011). Grasping the non-conscious: preserved grip scaling to unseen objects for immediate but not delayed grasping following a unilateral lesion to primary visual cortex. *Vis. Res.* 51, 908–924. doi: 10.1016/j.visres.2011.02.005

Conflict of Interest: The authors declare that the research was conducted in the absence of any commercial or financial relationships that could be construed as a potential conflict of interest.

frontiers
in Neuroscience

ORIGINAL RESEARCH
published: 12 January 2021
doi: 10.3389/fnins.2020.591898

Humans Can Visually Judge Grasp Quality and Refine Their Judgments Through Visual and Haptic Feedback

Guido Maiello[1]†, Marcel Schepko[1]†, Lina K. Klein[1], Vivian C. Paulun[1] and Roland W. Fleming[1,2]*

[1] Department of Experimental Psychology, Justus Liebig University Giessen, Giessen, Germany, [2] Center for Mind, Brain and Behavior, Justus Liebig University Giessen, Giessen, Germany

How humans visually select where to grasp objects is determined by the physical object properties (e.g., size, shape, weight), the degrees of freedom of the arm and hand, as well as the task to be performed. We recently demonstrated that human grasps are near-optimal with respect to a weighted combination of different cost functions that make grasps uncomfortable, unstable, or impossible, e.g., due to unnatural grasp apertures or large torques. Here, we ask whether humans can consciously access these rules. We test if humans can explicitly judge grasp quality derived from rules regarding grasp size, orientation, torque, and visibility. More specifically, we test if grasp quality can be inferred (i) by using visual cues and motor imagery alone, (ii) from watching grasps executed by others, and (iii) through performing grasps, i.e., receiving visual, proprioceptive and haptic feedback. Stimuli were novel objects made of 10 cubes of brass and wood (side length 2.5 cm) in various configurations. On each object, one near-optimal and one sub-optimal grasp were selected based on one cost function (e.g., torque), while the other constraints (grasp size, orientation, and visibility) were kept approximately constant or counterbalanced. Participants were visually cued to the location of the selected grasps on each object and verbally reported which of the two grasps was best. Across three experiments, participants were required to either (i) passively view the static objects and imagine executing the two competing grasps, (ii) passively view videos of other participants grasping the objects, or (iii) actively grasp the objects themselves. Our results show that, for a majority of tested objects, participants could already judge grasp optimality from simply viewing the objects and imagining to grasp them, but were significantly better in the video and grasping session. These findings suggest that humans can determine grasp quality even without performing the grasp—perhaps through motor imagery—and can further refine their understanding of how to correctly grasp an object through sensorimotor feedback but also by passively viewing others grasp objects.

Keywords: grasping, visual grasp selection, precision grip, shape, material, motor imagery, action observation

Edited by:
Luigi F. Cuturi,
Italian Institute of Technology (IIT), Italy

Reviewed by:
Hua-Chun Sun,
The University of Sydney, Australia
Robert Leslie Whitwell,
Western University, Canada

****Correspondence:***
Guido Maiello
guido_maiello@yahoo.it

† These authors share first authorship

Specialty section:
This article was submitted to
Perception Science,
a section of the journal
Frontiers in Neuroscience

Received: *05 August 2020*
Accepted: *16 November 2020*
Published: *12 January 2021*

Citation:
Maiello G, Schepko M, Klein LK,
Paulun VC and Fleming RW (2021)
Humans Can Visually Judge Grasp
Quality and Refine Their Judgments
Through Visual and Haptic Feedback.
Front. Neurosci. 14:591898.
doi: 10.3389/fnins.2020.591898

INTRODUCTION

When we try to grasp objects within our field of view, we rarely fail. We almost never miss the object or have it slip out of our hands. Thus, humans can very effectively use their sense of sight to select where and how to grasp objects. Yet for any given object, there are numerous ways to place our digits on the surface. Consider a simple sphere of 10 cm diameter and ∼300 cm^2 surface area. If we coarsely sample the surface in regions of 3 cm^2 (a generous estimate of the surface of a fingertip) there are approximately 100 surface locations on which to place our digits. Even when considering simple two-digit precision grips, which employ only the thumb and forefinger, there are ∼10,000 possible digit configurations that could be attempted. How do humans visually select which of these configurations is possible and will lead to a stable grasp?

To answer this question, in recent work (Klein et al., 2020) we asked participants to grasp 3D polycube objects made of different materials (wood and brass) using a precision grip. Even with these objects—geometrically more complex than a simple sphere—participants consistently selected only a handful of grasp configurations, with different participants selecting very similar grasps. This suggests that a common set of rules constrains how people visually select where to grasp objects. We formalized this observation, following (Kleinholdermann et al., 2013), by constructing a computational model that takes as input the physical stimuli, and outputs optimal grasp locations on the surface of the objects. Specifically, we constructed a set of optimality functions related to the size, shape, and degrees of freedom of the human hand, as well as to how easily an object can be manipulated after having been grasped. Model predictions closely agreed with human data, demonstrating that actors choose near-optimal grasp locations following this set of rules.

The strongest constraint for two-digit grasps, included in this computational framework, requires surface normals at contact locations to be approximately aligned (a concept known as force closure; Nguyen, 1988). Fingertip configurations that do not fulfill this constraint, e.g., with thumb and forefinger pushing on the same side of an object, cannot lift and manipulate the object. Indeed successful human grasps never fail to meet the force closure constraint (Kleinholdermann et al., 2013; Klein et al., 2020). The other constraints we implemented as optimality functions relate to:

Natural grasp axis: humans exhibit a preferred hand orientation for precision grip grasping, known as the natural grasp axis (Roby-Brami et al., 2000; Lederman and Wing, 2003; Schot et al., 2010; Voudouris et al., 2010), which falls within the midrange of possible hand and arm joint angles. Grasps rotated away from the natural grasp axis may result in uncomfortable (or impossible) hand/arm configurations that require extreme joint angles. Since these extreme joint angles should be avoided (Rosenbaum et al., 2001), optimal grasps should exhibit minimum misalignment with the natural grasp axis.

Grasp aperture: When free to employ any multi-digit grasp, participants select precision grip grasps only when the required distance between finger and thumb at contact (the "grasp aperture") is smaller than 2.5 cm (Cesari and Newell, 1999). As grasp size increases, humans progressively increase the number of digits employed in a grasp. Therefore, optimal two-digit precision grips should exhibit grasp apertures below 2.5 cm.

Minimum torque: grasping an object far from its center of mass results in high torques, which may cause the object to rotate when manipulated (Goodale et al., 1994; Lederman and Wing, 2003; Eastough and Edwards, 2006; Lukos et al., 2007; Paulun et al., 2016). Large gripping forces would be required to counteract high torques and prevent the object from rotating. Thus, optimal grasps should have minimum torque.

Object visibility: when grasping an object, the hand might occlude part of an object from view. This could be detrimental for subsequent object manipulation, and indeed humans exhibit spatial biases in their grasping behavior which are consistent with avoiding object occlusions (Paulun et al., 2014; Maiello et al., 2019). Therefore, optimal grasps should minimize the portion of an object occluded from view.

Whereas the force closure constraint is necessary and immutable, the relative importance given to the other four constraints varies with object properties (e.g., mass) and across participants.

Given the computational costs, it seems relatively unlikely that the brain fully computes these optimality functions for every possible grasp. Nevertheless, our previous findings suggest that humans can employ visual information to estimate these constraints and guide grasp selection. As a further test of our framework for understanding human grasp selection, here we ask whether human participants can explicitly report relative grasp optimality (i.e., which of two candidate grasps would be closer to optimal). We further ask whether observers can judge grasp optimality using vision alone, or whether executing a grasp is necessary to do so.

If participants were indeed better at judging grasp optimality when executing grasps, this might suggest that tactile (Johansson and Westling, 1984) and proprioceptive feedback from our arm and hand (Rosenbaum et al., 2001; Lukos et al., 2013) plays a role in evaluating grasp quality. Humans may employ these sources of feedback to learn that certain hand configurations are uncomfortable, or that one grasp requires more force than another to pick up the same object.

Additionally, participants might also be able to visually assess the characteristics of their own movements, such as the speed and trajectory of the limb. Previous work has in fact demonstrated that humans can access visual information of grasping kinematics. For example, human participants can estimate the size (Campanella et al., 2011; Ansuini et al., 2016) and weight (Podda et al., 2017) of unseen objects by observing the reach to grasp movements performed by others. These sources of visual information are known to play a strong role in grasp planning and execution, as removing them changes the kinematics of grasping movements (Connolly and Goodale, 1999), and even simply observing others execute grasping tasks can improve one's own grasping performance (Buckingham et al., 2014). We therefore, ask how much these sources of visual information might contribute to participant judgements of grasp optimality. Specifically, we test whether grasp quality can be inferred from watching grasps executed by others. If this were the case, then perhaps vision and proprioception may be redundant sources of information about grasp quality, which could aid humans in linking vision and motor control in action planning.

To test whether humans can explicitly judge grasp quality, in Experiment 1 we asked participants to report which of two candidate grasps on an object is best, first using vision alone (vision session), and then also by attempting both grasps on the object, one after the other (grasping session). To test whether visual information about the grasping movements plays a role in judging grasp quality, in Experiment 2a we asked a new set of participants to repeat a subset of key conditions from Experiment 1, while we video-recorded their grasping movements. Finally, in Experiment 2b we showed these recorded movements to yet another set of participants (video session), and asked them to judge grasp quality from the videos of grasps executed by participants from Experiment 2a.

MATERIALS AND METHODS

Participants

We recruited 21 naïve and right-handed participants [16 female, 5 male; mean (range) age: 24 (19–32) years] for Experiment 1, 25 naïve and right-handed participants [17 female, 8 male; mean (range) age: 23 (20–26)] for Experiment 2a, and 25 naïve and right-handed participants [18 female, 7 male; mean (range) age: 24 (19–36)] for Experiment 2b. Participants were staff and students from Justus Liebig University Giessen, Germany. In return for their participation, volunteers were paid 8 EURO per hour. Participants reported healthy upper extremities and normal or corrected to normal vision. All provided written informed consent. All procedures were approved by the local ethics committee of Justus Liebig University Giessen (Lokale Ethik—Kommission des Fachbereichs 06, LEK—FB06; application number: 2018-0003) and adhered to the tenets of the declaration of Helsinki.

Apparatus

All Experiments (1, 2a, 2b) were programmed in Matlab version 2018a. Participants were seated at a table with a mounted chin rest in a brightly lit room. **Figure 1** shows a schematic of the setup. In all experiments, during the vision (**Figure 1A**) and grasping sessions (**Figure 1B**), subjects positioned their heads in the chinrest before each trial. Stimulus objects were positioned 34 cm in front of the participant. At this predefined position, a turntable allowed the experimenter to precisely set object orientation. In the grasping sessions, participants were instructed to grasp the objects and move them to a target location shifted 23 cm to the right side from the initial object location along the horizontal axis, at a distance of 40 cm relative to the participant. The starting position for the right thumb and index finger was 24 cm to the right and 22 cm in front of the participant. In grasping sessions, objects were grasped with a precision grip at two predetermined locations. A ZED Mini stereo camera (Stereolabs) was attached to the front of the forehead rest to record (720p, 30 fps) grasping movements in Experiments 2a and 2b. To record videos, a simple recording program was written in C++, using the ZED SDK, and called from within the Matlab environment. The camera orientation was adjustable along the frontal axis and fixed at a downwards tilt angle of 25° to capture the whole movement sequence. During the experiment, participants did not see the camera due to its position right in front of their forehead (**Figure 1B**). In Experiment 2b (**Figure 1C**), videos were presented on an Asus VG248QE monitor (24″, resolution = 1,920×1,080 pixel) at 60 Hz, positioned at a distance of 40 cm from the observers.

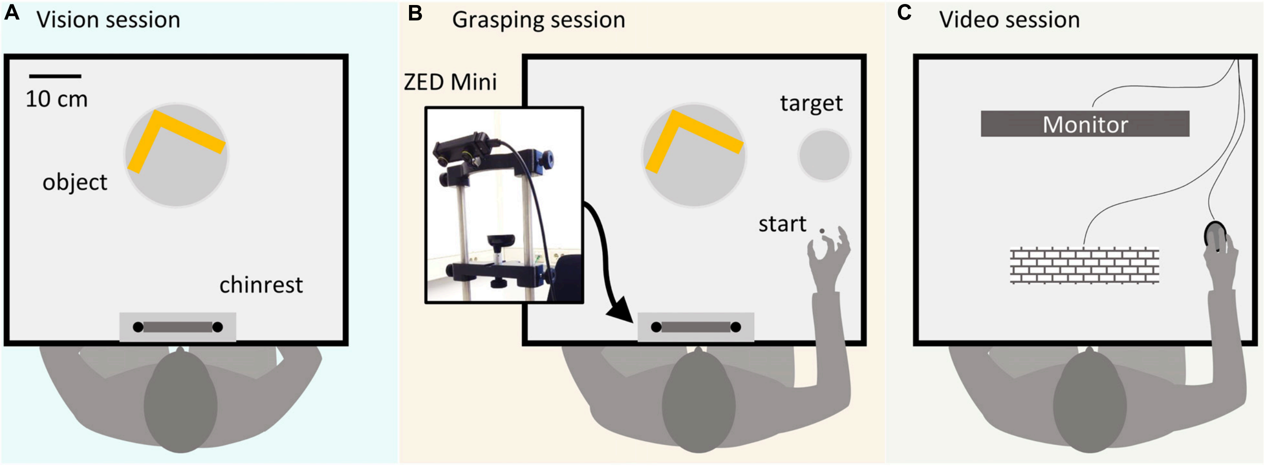

FIGURE 1 | Schematic representation of the experimental setup. **(A)** In the vision sessions participants passively viewed objects and evaluated the relative optimality of preselected grasps without executing the grasps. **(B)** In the grasping sessions, participants executed grasps prior to judging the grasp quality. A ZED Mini stereo camera positioned above the participant's forehead recorded the grasping movements in Experiments 2a and 2b. **(C)** In the video session, participants from Experiment 2b viewed recordings of grasps executed by participants from Experiment 2a on a computer monitor.

Experiment 1

Stimuli

In Experiment 1, we employed 16 3D objects (4 shapes, 4 material configurations), each made of 10 cubes (2.5^3 cm^3) of beech wood or brass. Objects with the same shape but different material configuration varied in mass (light wooden objects: 97 g, heavy wood/brass objects: 716 g) and mass distribution. These objects were the same, and were presented at the same orientations, as described in a previous study (Klein et al., 2020). For each of the objects, we selected pairs of grasps, one near-optimal and one sub-optimal, according to one of four grasp optimality criteria: natural grasp axis; optimal grasp aperture; minimum torque; optimal visibility. These criteria were mathematically defined as in our previous work (Klein et al., 2020). For each of these optimality criteria, we selected pairs of near-optimal and sub-optimal grasps on four of the 16 objects, while maintaining the other optimality criteria approximately constant across the grasp pair or counterbalanced across objects. **Figure 2A** shows one example object in which we selected one near-optimal and one sub-optimal grip with regard to grasp aperture. **Figure 2B** shows the optimality values for both grasps following each of the optimality criteria, and the difference in optimality between the two grasps. The difference in grasp optimality between pairs of grasps on all 16 objects for each of the four grasp optimality criteria is shown in **Figure 2C**. The selected grasp pairs were marked on the objects with colored stickers glued onto the objects' surface. Thumb grasp locations were marked in either blue or green (randomly assigned to the near-optimal and sub-optimal grasps). Index finger locations were marked in yellow. All objects and selected grasp pairs are shown in **Supplementary Figures 1–4**.

Procedure

Experiment 1 consisted of a vision session followed by a grasping session. In each session, all objects were presented in random order. In a single trial of either session, participants were instructed to judge which of the two predefined grasps marked on the object was better. No specific definition of grasp quality was given to participants. In the vision session, no physical contact with the objects was allowed. Participants were instructed to imagine both grasp movements, one after the other in predefined but random order, and then verbally to report which of the two grasps they thought was best. In the grasping session, participants executed both grasps and verbally reported which grasp was best. Participants were instructed to perform imagined and real grasps with a precision grip, i.e., using only thumb and index finger.

Prior to the experiment, participants were introduced to the objects. All stimuli were laid out on a table, the meaning of the stickers was explained, and participants were instructed to view (but not touch) the objects from all angles. Participants were familiarized with the weight of beech wood and brass by placing a wooden bar and a brass bar in sequence on the participants' outstretched palm for a few seconds. Between trials of both sessions, and between grasps within one trial, we ensured

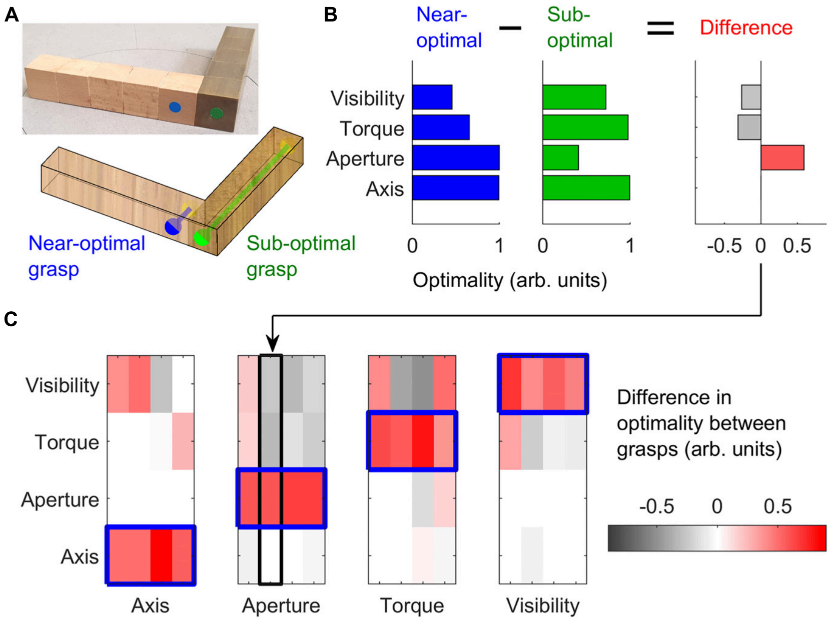

FIGURE 2 | Stimulus selection. **(A)** One example object in which we selected one optimal (blue) and one sub-optimal (green) grasp with respect to grasp aperture. The right side of the object is made of brass, the left side of beech wood. Blue and green dots represent thumb contact locations; the index finger is to be placed on the opposing surface. The blue grasp requires a small (2.5 cm) grip aperture, and is thus optimal with respect to grasp aperture. The green grasp requires a large grip aperture (12.5 cm) and is thus sub-optimal. **(B)** For the two selected grasps in panel **(A)**, we plot the optimality of the grasps (in normalized, arbitrary units) for each of the 4 optimality criteria, and the difference in optimality between grasps. **(C)** The difference in grasp optimality is shown for all pairs of grasps selected on all 16 objects, 4 per optimality criteria. Red indicates the selected near-optimal grasp is better than the selected sub-optimal grasp. Each column corresponds to one of the 16 objects employed in the study. The object and grasps in panel **(A)** correspond to the second column of the Aperture subplot in panel **(C)**.

that participants did not see the experimenter manipulating the objects by asking participants to keep their eyes closed until the objects were positioned.

In the vision session, once the stimulus was positioned at the starting location at its specific orientation, participants (with their head positioned on the chinrest) were instructed to open their eyes and visually explore the object. The experimenter then instructed the participants to imagine executing one of the two grasps (the green or the blue, randomly selected by the experimental script). Participants were asked to imagine reaching toward the object, placing their thumb and index at the marker locations, picking up the object using a precision grip, and moving it to the target location. Once participants indicated that they had finished imagining the first grasp movement, the experimenter instructed them to imagine executing the other. Once they had finished imagining both grasps, they were asked to report which was best, with no time limit. Throughout the whole vision session, participants were instructed to keep both hands on their thighs to prevent them from attempting pantomime grasps.

In the grasping session, on each trial participants positioned their head on the chinrest, and their thumb and index finger at the starting location. Once the stimulus was positioned, participants opened their eyes and the experimenter specified which grasp to attempt first (green or blue, in random order to minimize trial order effects; Maiello et al., 2018). Once the participant reported they were ready, an auditory cue specified the beginning of the grasping movement. Participants were required to reach, grasp, pick up and move the object onto the goal location, and return their hand to the starting position, all within 3 s. Prior to the second grasp, the experimenter positioned the current object back on its starting location while participants kept their eyes closed. Once the object was positioned, the procedure was repeated for the second grasp.

Experiments 2a and 2b

Experiment 2a was a replication of Experiment 1, except that we only employed a subset of the conditions and we recorded participants' grasp movements during the grasping session using the ZED mini stereo camera. The primary purpose of Experiment 2a was thus to capture the video recordings necessary for Experiment 2b. Compared to Experiment 2a, Experiment 2b contained an additional experimental session where participants evaluated grasp quality from the videos of participants from Experiment 2a.

Stimuli

In Experiments 2a and 2b we employed only 6 objects out of the 16 employed in Experiment 1. This subset of conditions, shown in **Supplementary Figure 5**, was selected so that participants would be at chance performance in the vision condition and significantly above chance in the grasping condition.

Procedure

The procedure of Experiment2a was identical to that of Experiment 1, except with fewer conditions.

In contrast to Experiment 1 and 2a, Experiment 2b consisted of three sessions: first a vision, then a video session, followed by a grasping session. The first (vision) and third (grasping) sessions were identical to the first and second sessions of Experiment 2a. In the video session of Experiment 2b, participants were shown videos of participants from Experiment 2a grasping the objects at the predefined grasp locations. Participants across Experiments 2a and 2b were yoked: each participant from Experiment 2b saw and evaluated the grasps from only one participant from Experiment 2a. The videos were taken from the left lens of the Zed mini stereo camera. Participants sat in front of a computer monitor.

On each trial, a dialogue box informed subjects which of the two grasps (green or blue) they would be viewing first. Participants started the video with a mouse click. Once the first grasp video was shown, a dialogue box informed participants they would be viewing the second grasp, and once again, participants started the video. Each video was shown only once. After participants had viewed both videos, they reported, via mouse click, which of the two grasps was better.

Analyses

Data analysis was performed in Matlab version R2018a. The dependent measure for all analyses was the proportion of trials in which the model-optimal grasp was rated as "better," which we refer to as "Percent correct grasp optimality judgments." Differences from chance performance and between group means were evaluated via unpaired and paired t-tests, as appropriate ($p < 0.05$ were considered statistically significant). We also report the 95% highest density interval (95% HDI) of the difference from chance or between group means, obtained via Bayesian estimation (Kruschke, 2013) using the Matlab Toolbox for Bayesian Estimation by Nils Winter. We compute effect size as $\mu - Chance/\sigma$ in case of differences from chance, and as $\mu_{G1-G2}/\sigma_{G1-G2}$ in case of differences between group means. As we are interested in fairly moderate effects (Cohen, 1988), we define a region of practical equivalence (ROPE) on effect size from −0.4 to 0.4. In cases where no statistically significant difference is observed using frequentist hypothesis testing, we use this ROPE to assess how credible the null hypothesis is that there exist no meaningful differences from chance or between group means (Kruschke, 2011). In such cases, we report the effect size and percentage of its posterior distribution that falls within the ROPE.

RESULTS

Experiment 1: Participants Can Report Whether Grasps Are Optimal Through Vision Alone, and Perform Better When Allowed to Execute the Grasps

In Experiment 1, we asked participants to perform imagined and real grasps on 16 objects and to report which of two predefined grasp locations was best. **Figure 3A**, shows that participants were significantly above chance at judging grasp optimality

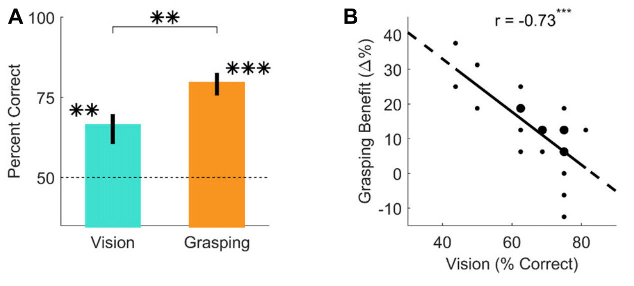

FIGURE 3 | Judgments of grasp optimality using vision and grasping. **(A)** Percent correct grasp optimality judgments for the vision session (left), and the grasping session (right), averaged across objects, and participants. Error bars indicate 95% bootstrapped confidence intervals of the mean. Chance performance is 50% correct (dotted line). **(B)** The grasping benefit (delta percent) as a function of the performance in the vision session, for each individual participant. The size of each dot represents the number of occurrences for each data point (one occurrence for small dots, two for large dots). Black line is best fitting linear regression line. $^{**}p < 0.01$; $^{***}p < 0.001$.

when using vision alone [$t(20) = 6.63$, $p = 1.9{*}10^{-06}$; 95% HDI = (11, 22)] and also when physically executing the grasps [$t(20) = 15.79$, $p = 9.3{*}10^{-13}$; 95% HDI = (25, 33)]. Additionally, participant judgements significantly improved in the grasping session compared to the vision session [$t(20) = 5.14$, $p = 5{*}10^{-05}$; 95% HDI = (8, 19)]. Percent correct grasp optimality judgments for individual objects, grouped by optimality conditions, are shown in **Supplementary Figures 1–4**. Note that we do not compare performance across optimality conditions as we did not equate difficulty across conditions, and even within the same condition task difficulty and performance could vary markedly. **Figure 3B** further shows that participants who performed poorly in the vision session gained the most from physically executing the grasps: there was a strong, inverse relationship between grasping benefit[1] and performance in the vision session ($r = -0.73$, $p = 2{*}10^{-4}$).

Experiment 2: Visual and Proprioceptive Information During Grasping Are Redundant for Evaluating Grasp Optimality

The results from Experiment 1 suggest that participants are better at judging grasp quality when they perform the grasp. However, Experiment 1 leaves open whether the performance increase is due to the sensorimotor or visual feedback during grasp. In Experiment 2, we tested whether visual cues from real grasp movements were sufficient to improve grasp optimality judgements. In Experiment 1, performance varied across optimality criteria and individual objects. Therefore, we selected the subset of conditions from Experiment 1 that showed the largest difference between the vision and grasping session.

Figure 4A shows that for these conditions, participants were at chance in the vision session [$t(20) = 0.5$, $p = 0.62$; 95% HDI = (-8, 13), effect size = 0.11, 88% in ROPE], above chance when physically executing the grasps [$t(20) = 10.25$, $p = 2.1{*}10^{-09}$; 95% HDI = (29, 40)], and performance in the grasping session was significantly improved compared to the vision session [$t(20) = 4.81$, $p = 1.1{*}10^{-4}$; 95% HDI = (19, 46)].

In Experiment 2a we replicated the results from Experiment 1 on this subset of conditions (**Figure 4B**): participants were at chance in the vision session [$t(24) = 1.88$, $p = 0.073$; 95% HDI = (-1, 12)], effect size = 0.38, 53% in ROPE), above chance when physically executing the grasps [$t(24) = 7.27$, $p = 1.7{*}10^{-07}$; 95% HDI = (18, 33)], and performance in the grasping session was significantly improved compared to the vision session [$t(24) = 3.51$, $p = 0.0018$; 95% HDI = (8, 32)]. During the grasping sessions of Experiment 2 we also recorded videos of the participants executing the grasps from approximately the participants' viewpoint. Example videos are shown in the **Supplementary Material**.

In Experiment 2b, participants performed a vision, a video, and a grasping session on the same conditions employed in Experiment 2a. Critically, in the video condition participants judged grasp optimality on videos of participants from Experiment 2a grasping objects at optimal and sub-optimal locations.

Similarly to Experiment 2a, **Figure 4C** shows that in Experiment 2b, participants were at chance in the vision session [$t(24) = -1.19$, $p = 0.25$; 95% HDI = (-11, 4), effect size = -0.24, 81% in ROPE]. Conversely, participants were significantly above chance in both the video [$t(24) = 4.58$, $p = 1.2{*}10^{-4}$; 95% HDI = (10, 26)] and grasping sessions [$t(24) = 6.41$, $p = 1.3{*}10^{-06}$; 95% HDI = (15, 29)]. Compared to the vision session, performance was significantly improved in both the vision [$t(24) = 4.23$, $p = 3{*}10^{-04}$, 95% HDI = (10, 32)] and grasping sessions [$t(24) = 6.35$, $p = 1.4{*}10^{-06}$, 95% HDI = (17, 35)]. Finally, performance in the video and grasping sessions was equivalent [$t(24) = 0.92$, $p = 0.36$; 95% HDI = (-6, 16)], effect size = 0.18, 83% in ROPE). Percent correct grasp optimality judgments for individual objects and optimality conditions for both Experiments 2a and 2b are shown in **Supplementary Figure 5**.

It is also worth noting that in Experiment 2b, the grasping session was always performed last, so the exposure to grasp videos could conceivably have helped the judgments made in the grasping session. To test this possibility, we contrasted performance in the grasping session from Experiment 2b, with performance in the grasping session from Experiment 2a. Performance in the grasping sessions was equivalent across experiments [$t(24) = 0.68$, $p = 0.50$; 95% HDI = (-13, 7), effect size = 0.14, 90% in ROPE], suggesting that the grasp observation session did not improve the decision-making that comes out of physically performing the grasps.

DISCUSSION

When grasping objects guided by vision, humans select finger contact points that are near-optimal according to several physics- and biomechanics-based constraints (Kleinholdermann et al., 2013; Klein et al., 2020). Whether these constraints are explicitly

---

[1] Grasping benefit was defined as: $\%Correct_{Grasping} - \%Correct_{Vision}$.

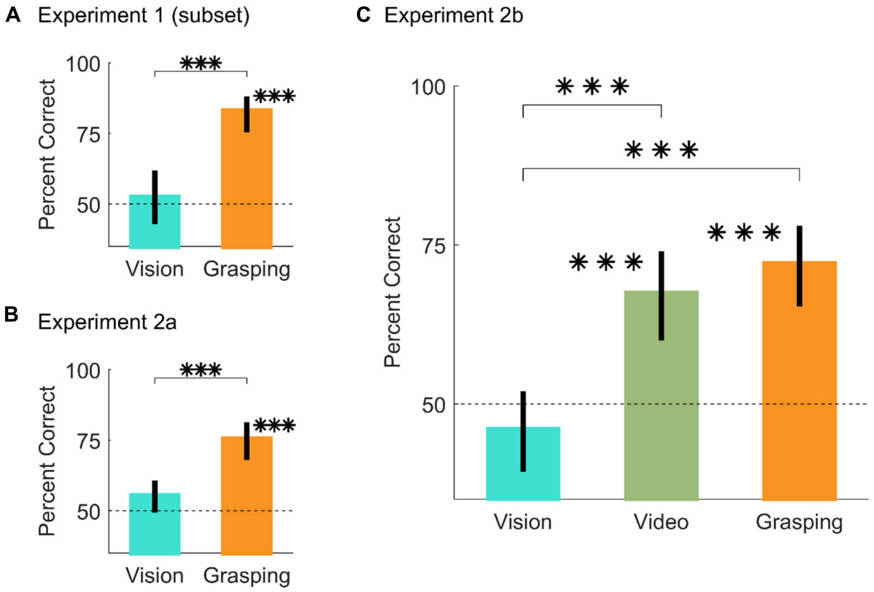

FIGURE 4 | Results from Experiment 2. **(A,B)** Percent correct grasp optimality judgments for vision and grasping sessions, averaged across objects, and participants, for **(A)** the subset of conditions from Experiment 1 that drives the difference between vision and grasping, and **(B)** the same subset of conditions replicated in Experiment 2a. **(C)** Percent correct grasp optimality judgments for vision, video, and grasping sessions, averaged across objects and participants, for Experiment 2b. In all panels, error bars are 95% bootstrapped confidence intervals of the mean and chance performance is 50% correct (graydotted line). ***$p < 0.001$.

computed in the brain is unknown. Here, we demonstrate that humans can explicitly judge which of two potential grasps on an object is best, based on each of these constraints.

In our study, participants could distinguish near-optimal from sub-optimal grasp locations using vision alone, i.e., without physically executing grasps, presumably using motion imagery. This well aligns with the notion that motor imagery, the mental simulation of a motor task, relies on similar neural substrates as action planning and execution. For example, it is well-established that simulated actions take the same time as executed ones (Decety et al., 1989; Jeannerod, 1995). This temporal similarity has also been shown in a task akin to the current study. Frak et al. (2001) asked participants to determine whether contact points marked on a cylindrical object placed at different orientations would lead to easy, difficult, or impossible grasps, without grasping the object. The time to make these estimates varied with object orientation and task difficulty, and closely matched the time taken to perform the grasps. These temporal matches hint that imagined and real actions might rely on similar neural computations. Indeed it has been shown that motor imagery recruits many of the same visuomotor areas of the brain, from early visual cortex (Pilgramm et al., 2016; Zabicki et al., 2016; Monaco et al., 2020), throughout the dorsal stream and the parietal lobe leading to primary motor cortex M1 (Hétu et al., 2013), that are directly involved in action planning and execution (Hardwick et al., 2018).

In Experiment 1 of our study, judgements of grasp optimality improved when participants were required to execute the grasps, and this improvement was strongest in participants who performed poorly using vision alone. What drove this improvement? Since the grasping session always came after the vision session, it is possible that the improvement in the grasping session could be due to participants learning the task or having gained familiarity with the objects. This is unlikely, however, since we did not provide participants with any feedback they might have used to learn the task, and we found no evidence of learning within the single sessions (see **Supplementary Figures 6, 7**). In the grasping sessions, participants were asked to grasp, lift and place the object at a goal location within 3s. However, they had unlimited time to plan the grasps prior to each trial. The planning stage in the grasping sessions was thus similar to the vision sessions. Therefore, in both sessions participants could build hypotheses about which grasp should be easier to execute, but only in the grasping sessions could they test these hypotheses against their own sensorimotor feedback. Specifically, if participants needed to make corrective changes once a movement had been initiated, it is possible that the difference between this event and the original motor intention could have reached consciousness and improved their judgements. However, previous research has shown that the recalibration of reach-to-grasp movements through haptic feedback occurs outside of perceptual awareness (Mon-Williams and Bingham, 2007). If participants could not consciously access the corrections to their original motor plans, crucial clues to indicate that a grasp was sub-optimal could be provided by tactile feedback from object slippage (Johansson and Westling, 1984), the need to apply greater grip forces than anticipated (Lukos et al., 2013), or proprioceptive feedback indicating awkward joint configurations (Rosenbaum et al., 2001).

Tactile and proprioceptive feedback were not the only sources of information that could have aided judgements in the grasping session. Participants could also visually assess the characteristics of their own movements, such as the speed and trajectory of the limb. These sources of visual information are known to play a strong role in grasp execution, as removing them changes the kinematics of grasping movements (Connolly and Goodale, 1999). Additionally, even if visual information from object roll during grasps does not influence the calibration of digit placement and force control (Lukos et al., 2013), lifting without visual feedback does impair fingertip force adaptation (Buckingham and Goodale, 2010; Buckingham et al., 2011). We therefore, wondered whether these sources of visual information alone could aid judgements of grasp optimality.

In Experiment 2, we indeed found that viewing videos of other participants grasping near-optimal and sub-optimal grasps was sufficient for observers to reach the same level of performance at reporting which grasp was best as when actually executing grasps. This does not mean that in the grasping sessions participants did not rely on tactile and proprioceptive feedback. It suggests instead, that visual and tactile/proprioceptive feedback may be redundant sources of information in evaluating grasp quality. This could help explain how humans are able to exploit action observation more generally. For example, humans are able to acquire useful information, such as object size and weight, by simply observing the movement kinematics of others (Bingham, 1987; Hamilton et al., 2007; Campanella et al., 2011; Ansuini et al., 2016; Podda et al., 2017). Additionally, observing others execute grasping tasks, particularly when they make errors, can improve one's own grasping performance (Buckingham et al., 2014). Observing one's own grasps, particularly when making errors, could thus link visual and tactile/proprioceptive information about grasp quality. This in turn would allow us to learn how best to grasp a novel object by simply looking at someone else grasping it.

Limitations and Future Directions

Our findings reinforce the notion that motor imagery and action observation play an important role in learning complex motor tasks (Gatti et al., 2013). For this reason, motor imagery and action observation have also shown promise in aiding and strengthening motor rehabilitation techniques in a variety of neurological conditions (Sharma et al., 2006; Mulder, 2007; de Lange et al., 2008; Zimmermann-Schlatter et al., 2008; Malouin et al., 2013; Mateo et al., 2015). Within this context, our model-driven method of selecting optimal—and particularly sub-optimal—grasps could be used to guide and strengthen mental imagery and action observation techniques for motor rehabilitation. For example, patients could be made to imagine, observe, and execute grasps to object locations, selected through our modeling approach, which contain the most useful information for re-learning grasping movements.

In the vision session of Experiment 1, participants were above chance at judging grasp optimality for a majority of objects (10 out of 16), but not for all. This is likely due to our procedure for selecting pairs of near-optimal and sub-optimal grasps, which was not designed to equate task difficulty across objects and conditions. Yet what makes one pair of grasps more or less visually distinguishable in terms of optimality? This could be related to how humans encode the different constraints on grasp quality through vision. Misjudgments for the pair of grasps shown in **Figure 2** might be due, for example, to inaccuracies in visually estimating the length of the grasp aperture with respect to the span of our hand, or to inaccuracies in judging the exact location of the object's center of mass from visual 3D shape and material cues. A potential approach to test this hypothesis would be to extend our model to be image computable, i.e., able to derive the constraints on grasp selection directly from images of the objects. If the image processing stages of model were designed to mimic those of the human visual system (e.g., Chessa et al., 2016; Maiello et al., 2020) we might then expect the model to begin making the same misjudgments as human participants.

Even in the grasping sessions, however, in about 20% of trials participants did not agree with the model predictions. Does this mean participants could not access the information about grasp quality? We believe it is more likely that the model predictions are incomplete. For example, the model does not take into account that for some grasps with high torques, the objects might rotate and come to rest against a participants' palm, stabilizing an otherwise potentially unstable grasp. Additionally, in the current work we did not account for the different importance given by individual participants to the different constraints (Klein et al., 2020). Inspect for example the data from the last panel of **Supplementary Figure 2**. Even though the selected sub-optimal grasp has much larger grasp aperture than the selected near-optimal grasp, the sub-optimal grasp has marginally less torque. Thus, if some participants gave much greater importance to the torque constraint, this might explain why their responses disagreed with model predictions. Finally, to avoid biasing participants toward our expected results, we explicitly abstained from providing participants with a precise definition of grasp quality. However, this means different participants might have interpreted the instructions differently. The concept of a "better" grasp may have been interpreted in many ways, such as easier, faster, more accessible, or more comfortable. It is thus possible that different criteria may lead to different judgments, and it will be important in future research to link these subjective dimensions of grasp quality to objective measures of grasping performance.

In Experiment 2, we found that action observation and action execution yielded equivalent accuracies. However, it remains unknown whether the accuracy is equivalent across these two conditions because an "action observation system" treats them equivalently, or because there are two systems operating, one based on action observation and one based on action execution and efference copy, for example, which can inform the decision-making process. Nevertheless, the videos from Experiment 2 could provide some further insight into which visual cues participants were exploiting to determine grasp optimality during action observation. For example, in **Supplementary Video 1** an observer might notice the different time it takes the participant to lift the same object with two different grasps, or the slight wobbling of the object when grasped in the uncomfortable hand orientation. In **Supplementary Video 2**, a prominent visual cue comes from the initial failure in computing a successful trajectory to the sub-optimal grasp. A quantitative analysis of the grasping kinematics contained in these videos, using for example novel image based tracking algorithms (Mathis et al., 2018), may reveal the exact nature of the visual information human participants exploit during action observation and execution. The full video dataset from Experiment 2, as well as all other data from the study, are made freely available through the Zenodo repository (doi: 10.5281/zenodo.4382477).

Finally, our approach could be further developed to investigate the neural underpinning of visual grasp selection. The current study demonstrates how, through the computational framework described in Klein et al. (2020), we can identify grasps on arbitrary objects that isolate the individual components of grasp selection. In future studies, these unique grasp configurations could be employed as stimuli for targeted investigations of brain activity, making it possible to pinpoint the neural loci of each of the visuomotor computations underlying grasp planning and execution.

CONCLUSION

We show that humans are capable of judging the relative optimality between different possible grasps on an object. For a majority of tested objects and grasp configurations, human participants could perform these judgments using vision alone, and refined their estimates of grasp quality using visual and proprioceptive feedback during grasp execution. These abilities are likely a key component of how humans visually select grasps on objects. Remaining challenges will be to identify where and how grasp optimality is learned and computed in the brain in order to guide grasp planning and execution.

DATA AVAILABILITY STATEMENT

The datasets and analysis scripts generated for this study can be found in the online Zenodo repository (doi: 10.5281/zenodo.4382477).

ETHICS STATEMENT

The studies involving human participants were reviewed and approved by the Lokale Ethik—Kommission des Fachbereichs 06, LEK—FB06. The patients/participants provided their written informed consent to participate in this study.

AUTHOR CONTRIBUTIONS

GM, MS, LK, VP, and RF conceived and designed the study. GM and MS collected the data. GM analyzed the data. All authors wrote the manuscript.

FUNDING

This research was supported by the DFG (IRTG-1901: "The Brain in Action" and SFB-TRR-135: "Cardinal Mechanisms of Perception," and project PA 3723/1-1), and an ERC Consolidator Award (ERC-2015-CoG-682859: "SHAPE"). GM was supported by a Marie-Skłodowska-Curie Actions Individual Fellowship (H2020-MSCA-IF-2017: "VisualGrasping" Project ID: 793660).

ACKNOWLEDGMENTS

This article is based on MS master's thesis.

SUPPLEMENTARY MATERIAL

The Supplementary Material for this article can be found online at: https://www.frontiersin.org/articles/10.3389/fnins.2020.591898/full#supplementary-material

Supplementary Figure 1 | Percent correct grasp optimality judgments, computed across participants from Experiment 1, for the four individual objects in the natural grasp axis conditions. In each panel, the top object demonstrates the approximate viewpoint of a participant. Thumb locations for selected grasps were marked on the objects in green or blue. The position of the opposing index finger was marked in yellow. The color code only served to mark and identify the grasps for participants, and was purposely unrelated to the grasp optimality. The middle and bottom object show the near-optimal and sub-optimal grasps, respectively, with the objects rotated solely for illustrative purposes, to better show the selected grasp locations. Error bars represent 95% bootstrapped confidence intervals.

Supplementary Figure 2 | | As **Supplementary Figure 1**, except for the four individual objects in the grasp aperture conditions.

Supplementary Figure 3 | As **Supplementary Figure 1**, except for the four individual objects in the minimum torque conditions.

Supplementary Figure 4 | As **Supplementary Figure 1**, except for the four individual objects in the object visibility conditions.

Supplementary Figure 5 | As **Supplementary Figures 1–4**, except for the six individual objects employed in Experiments 2a and 2b.

Supplementary Figure 6 | Participant performance (percent correct grasp optimality judgments) as a function of trial number for Experiment 1. Dots are the mean performance across observers; error bars represent 68% bootstrapped confidence intervals. Dotted lines are best fitting regression lines through the data. We found no significant correlations between trial number and task performance in either the Vision Session (r = 0.052, p = 0.34), nor the Grasping Session (r = −0.041, p = 0.45). There is thus no evidence that performance improved with more practice and more familiarity with the task and objects.

Supplementary Figure 7 | Percent correct grasp optimality judgments as a function of trial number for the six objects from Experiment 2a. In the six small panels, dots are performance, computed across participants, for each of the six objects ordered as in **Supplementary Figure 5**. The final panel shows the average across objects. Error bars represent 68% bootstrapped confidence intervals. Dotted lines are best fitting regression lines through the data. The analysis in **Supplementary Figure 6** averages across participants based on trial number. Thus, different objects contribute to the accuracy computed at each trial number. The large variance in accuracy across objects might thus hide learning effects. The smaller number of conditions in Experiment 2 allows us to investigate potential learning effects at the level of individual objects. We observed a significant positive correlation between trial number and task performance in the Vision Session only for the U shaped object (second panel, r = 0.93, p = 0.0069;

all other correlations $p > 0.1$). Even for this object, this correlation was likely spurious, as it did not replicate in the data from Experiment 2b ($r = 0.18$, $p = 0.74$). Across objects (rightmost panel), we also found no significant correlations between trial number and task performance in either the Vision Session ($r = 0.061$, $p = 0.72$), nor the Grasping Session ($r = -0.13$, $p = 0.44$). There is therefore no evidence that performance improved with more practice and more familiarity with the task and objects.

Supplementary Video 1 | Representative participant from Experiment 2a executing near-optimal (left) and sub-optimal (right) grasps for one object belonging to the natural grasp axis conditions.

Supplementary Video 2 | Representative participant from Experiment 2a executing near-optimal (left) and sub-optimal (right) grasps for one object belonging to the object visibility conditions.

REFERENCES

Ansuini, C., Cavallo, A., Koul, A., D'Ausilio, A., Taverna, L., and Becchio, C. (2016). Grasping others' movements: rapid discrimination of object size from observed hand movements. *J. Exp. Psychol. Hum. Percept. Perform.* 42, 918–929. doi: 10.1037/xhp0000169

Bingham, G. P. (1987). Kinematic form and scaling: further investigations on the visual perception of lifted weight. *J. Exp. Psychol. Hum. Percept. Perform.* 13, 155–177. doi: 10.1037/0096-1523.13.2.155

Buckingham, G., and Goodale, M. A. (2010). Lifting without seeing: the role of vision in perceiving and acting upon the size weight illusion. *PLoS One* 5:e9709. doi: 10.1371/journal.pone.0009709

Buckingham, G., Ranger, N. S., and Goodale, M. A. (2011). The role of vision in detecting and correcting fingertip force errors during object lifting. *J. Vis.* 11:4. doi: 10.1167/11.1.4

Buckingham, G., Wong, J. D., Tang, M., Gribble, P. L., and Goodale, M. A. (2014). Observing object lifting errors modulates cortico-spinal excitability and improves object lifting performance. *Cortex* 50, 115–124. doi: 10.1016/j.cortex.2013.07.004

Campanella, F., Sandini, G., and Morrone, M. C. (2011). Visual information gleaned by observing grasping movement in allocentric and egocentric perspectives. *Proc. R. Soc. B Biol. Sci.* 278, 2142–2149. doi: 10.1098/rspb.2010.2270

Cesari, P., and Newell, K. M. (1999). The scaling of human grip configurations. *J. Exp. Psychol. Hum. Percept. Perform.* 25, 927–935. doi: 10.1037/0096-1523.25.4.927

Chessa, M., Maiello, G., Bex, P. J., and Solari, F. (2016). A space-variant model for motion interpretation across the visual field. *J. Vis.* 16:12. doi: 10.1167/16.2.12

Cohen, J. (1988). *Statistical Power Analysis for the Behavioral Sciences*, 2nd Edn. Abingdon: Routledge.

Connolly, J. D., and Goodale, M. A. (1999). The role of visual feedback of hand position in the control of manual prehension. *Exp. Brain Res.* 125, 281–286. doi: 10.1007/s002210050684

de Lange, F. P., Roelofs, K., and Toni, I. (2008). Motor imagery: a window into the mechanisms and alterations of the motor system. *Cortex* 44, 494–506. doi: 10.1016/j.cortex.2007.09.002

Decety, J., Jeannerod, M., and Prablanc, C. (1989). The timing of mentally represented actions. *Behav. Brain Res.* 34, 35–42. doi: 10.1016/S0166-4328(89)80088-9

Eastough, D., and Edwards, M. G. (2006). Movement kinematics in prehension are affected by grasping objects of different mass. *Exp. Brain Res.* 176, 193–198. doi: 10.1007/s00221-006-0749-3

Frak, V., Paulignan, Y., and Jeannerod, M. (2001). Orientation of the opposition axis in mentally simulated grasping. *Exp. Brain Res.* 136, 120–127. doi: 10.1007/s002210000583

Gatti, R., Tettamanti, A., Gough, P. M., Riboldi, E., Marinoni, L., and Buccino, G. (2013). Action observation versus motor imagery in learning a complex motor task: a short review of literature and a kinematics study. *Neurosci. Lett.* 540, 37–42. doi: 10.1016/j.neulet.2012.11.039

Goodale, M. A., Meenan, J. P., Bülthoff, H. H., Nicolle, D. A., Murphy, K. J., and Racicot, C. I. (1994). Separate neural pathways for the visual analysis of object shape in perception and prehension. *Curr. Biol.* 4, 604–610. doi: 10.1016/S0960-9822(00)00132-9

Hamilton, A. F., Joyce, D. W., Flanagan, J. R., Frith, C. D., and Wolpert, D. M. (2007). Kinematic cues in perceptual weight judgement and their origins in box lifting. *Psychol. Res.* 71, 13–21. doi: 10.1007/s00426-005-0032-4

Hardwick, R. M., Caspers, S., Eickhoff, S. B., and Swinnen, S. P. (2018). Neural correlates of action: comparing meta-analyses of imagery, observation, and execution. *Neurosci. Biobehav. Rev.* 94, 31–44. doi: 10.1016/j.neubiorev.2018.08.003

Hétu, S., Grégoire, M., Saimpont, A., Coll, M.-P., Eugène, F., Michon, P.-E., et al. (2013). The neural network of motor imagery: an ALE meta-analysis. *Neurosci. Biobehav. Rev.* 37, 930–949. doi: 10.1016/j.neubiorev.2013.03.017

Jeannerod, M. (1995). Mental imagery in the motor context. *Neuropsychologia* 33, 1419–1432. doi: 10.1016/0028-3932(95)00073-C

Johansson, R. S., and Westling, G. (1984). Roles of glabrous skin receptors and sensorimotor memory in automatic control of precision grip when lifting rougher or more slippery objects. *Exp. Brain Res.* 56, 550–564. doi: 10.1007/BF00237997

Klein, L. K., Maiello, G., Paulun, V. C., and Fleming, R. W. (2020). Predicting precision grip grasp locations on three-dimensional objects. *plos Comput. Biol.* 16:e1008081. doi: 10.1371/journal.pcbi.1008081

Kleinholdermann, U., Franz, V. H., and Gegenfurtner, K. R. (2013). Human grasp point selection. *J. Vis.* 13:23. doi: 10.1167/13.8.23

Kruschke, J. K. (2011). Bayesian assessment of null values via parameter estimation and model comparison. *Perspect. Psychol. Sci.* 6, 299–312. doi: 10.1177/1745691611406925

Kruschke, J. K. (2013). Bayesian estimation supersedes the t test. *J. Exp. Psychol. Gen.* 142, 573–603. doi: 10.1037/a0029146

Lederman, S. J., and Wing, A. M. (2003). Perceptual judgement, grasp point selection and object symmetry. *Exp. Brain Res.* 152, 156–165. doi: 10.1007/s00221-003-1522-5

Lukos, J., Ansuini, C., and Santello, M. (2007). Choice of contact points during multidigit grasping: effect of predictability of object center of mass location. *J. Neurosci.* 27, 3894–3903. doi: 10.1523/JNEUROSCI.4693-06.2007

Lukos, J. R., Choi, J. Y., and Santello, M. (2013). Grasping uncertainty: effects of sensorimotor memories on high-level planning of dexterous manipulation. *J. Neurophysiol.* 109, 2937–2946. doi: 10.1152/jn.00060.2013

Maiello, G., Chessa, M., Bex, P. J., and Solari, F. (2020). Near-optimal combination of disparity across a log-polar scaled visual field. *PLoS Comput. Biol.* 16:e1007699. doi: 10.1371/journal.pcbi.1007699

Maiello, G., Paulun, V. C., Klein, L. K., and Fleming, R. W. (2018). The sequential-weight illusion. *I-Perception* 9:204166951879027. doi: 10.1177/2041669518790275

Maiello, G., Paulun, V. C., Klein, L. K., and Fleming, R. W. (2019). Object visibility, not energy expenditure, accounts for spatial biases in human grasp selection. *I-Perception* 10:204166951982760. doi: 10.1177/2041669519827608

Malouin, F., Jackson, P. L., and Richards, C. L. (2013). Towards the integration of mental practice in rehabilitation programs. A critical review. *Front. Hum. Neurosci.* 7:576. doi: 10.3389/fnhum.2013.00576

Mateo, S., Di Rienzo, F., Bergeron, V., Guillot, A., Collet, C., and Rode, G. (2015). Motor imagery reinforces brain compensation of reach-to-grasp movement after cervical spinal cord injury. *Front. Behav. Neurosci.* 9:234. doi: 10.3389/fnbeh.2015.00234

Mathis, A., Mamidanna, P., Cury, K. M., Abe, T., Murthy, V. N., Mathis, M. W., et al. (2018). DeepLabCut: markerless pose estimation of user-defined body parts with deep learning. *Nat. Neurosci.* 21, 1281–1289. doi: 10.1038/s41593-018-0209-y

Monaco, S., Malfatti, G., Culham, J. C., Cattaneo, L., and Turella, L. (2020). Decoding motor imagery and action planning in the early visual cortex: overlapping but distinct neural mechanisms. *NeuroImage* 218:116981. doi: 10.1016/j.neuroimage.2020.116981

Mon-Williams, M., and Bingham, G. P. (2007). Calibrating reach distance to visual targets. *J. Exp. Psychol. Hum. Percept. Perform.* 33, 645–656. doi: 10.1037/0096-1523.33.3.645

Mulder, T. H. (2007). Motor imagery and action observation: cognitive tools for rehabilitation. *J. Neural Transm.* 114, 1265–1278. doi: 10.1007/s00702-007-0763-z

Nguyen, V.-D. (1988). Constructing force- closure grasps. *Int. J. Robot. Res.* 7, 3–16. doi: 10.1177/027836498800700301

Paulun, V. C., Gegenfurtner, K. R., Goodale, M. A., and Fleming, R. W. (2016). Effects of material properties and object orientation on precision grip kinematics. *Exp. Brain Res.* 234, 2253–2265. doi: 10.1007/s00221-016-4631-7

Paulun, V. C., Kleinholdermann, U., Gegenfurtner, K. R., Smeets, J. B. J., and Brenner, E. (2014). Center or side: biases in selecting grasp points on small bars. *Exp. Brain Res.* 232, 2061–2072. doi: 10.1007/s00221-014-3895-z

Pilgramm, S., de Haas, B., Helm, F., Zentgraf, K., Stark, R., Munzert, J., et al. (2016). Motor imagery of hand actions: decoding the content of motor imagery from brain activity in frontal and parietal motor areas: MVPA of imagined hand movements. *Hum. Brain Map.* 37, 81–93. doi: 10.1002/hbm.23015

Podda, J., Ansuini, C., Vastano, R., Cavallo, A., and Becchio, C. (2017). The heaviness of invisible objects: predictive weight judgments from observed real and pantomimed grasps. *Cognition* 168, 140–145. doi: 10.1016/j.cognition.2017.06.023

Roby-Brami, A., Bennis, N., Mokhtari, M., and Baraduc, P. (2000). Hand orientation for grasping depends on the direction of the reaching movement. *Brain Res.* 869, 121–129. doi: 10.1016/S0006-8993(00)02378-7

Rosenbaum, D. A., Meulenbroek, R. J., Vaughan, J., and Jansen, C. (2001). Posture-based motion planning: applications to grasping. *Psychol. Rev.* 108, 709–734. doi: 10.1037/0033-295X.108.4.709

Schot, W. D., Brenner, E., and Smeets, J. B. J. (2010). Posture of the arm when grasping spheres to place them elsewhere. *Exp. Brain Res.* 204, 163–171. doi: 10.1007/s00221-010-2261-z

Sharma, N., Pomeroy, V. M., and Baron, J.-C. (2006). Motor imagery: a backdoor to the motor system after stroke? *Stroke* 37, 1941–1952. doi: 10.1161/01.STR.0000226902.43357.fc

Voudouris, D., Brenner, E., Schot, W. D., and Smeets, J. B. J. (2010). Does planning a different trajectory influence the choice of grasping points? *Exp. Brain Res.* 206, 15–24. doi: 10.1007/s00221-010-2382-4

Zabicki, A., de Haas, B., Zentgraf, K., Stark, R., Munzert, J., and Krüger, B. (2016). Imagined and executed actions in the human motor system: testing neural similarity between execution and imagery of actions with a multivariate approach. *Cereb. Cortex* 27, 4523–4536. doi: 10.1093/cercor/bhw257

Zimmermann-Schlatter, A., Schuster, C., Puhan, M. A., Siekierka, E., and Steurer, J. (2008). Efficacy of motor imagery in post-stroke rehabilitation: a systematic review. *J. NeuroEng. Rehabil.* 5:8. doi: 10.1186/1743-0003-5-8

Conflict of Interest: The authors declare that the research was conducted in the absence of any commercial or financial relationships that could be construed as a potential conflict of interest.

frontiers
in Psychology

ORIGINAL RESEARCH
published: 13 January 2021
doi: 10.3389/fpsyg.2020.599125

Convergent and Distinct Effects of Multisensory Combination on Statistical Learning Using a Computer Glove

Christopher R. Madan[1,2] and Anthony Singhal[2,3]*

[1] School of Psychology, University of Nottingham, Nottingham, United Kingdom, [2] Department of Psychology, University of Alberta, Edmonton, AB, Canada, [3] Neuroscience and Mental Health Institute, University of Alberta, Edmonton, AB, Canada

Learning to play a musical instrument involves mapping visual + auditory cues to motor movements and anticipating transitions. Inspired by the serial reaction time task and artificial grammar learning, we investigated explicit and implicit knowledge of statistical learning in a sensorimotor task. Using a between-subjects design with four groups, one group of participants were provided with visual cues and followed along by tapping the corresponding fingertip to their thumb, while using a computer glove. Another group additionally received accompanying auditory tones; the final two groups received sensory (visual or visual + auditory) cues but did not provide a motor response—all together following a 2 × 2 design. Implicit knowledge was measured by response time, whereas explicit knowledge was assessed using probe tests. Findings indicate that explicit knowledge was best with only the single modality, but implicit knowledge was best when all three modalities were involved.

Keywords: sequence learning, multimodal, implicit knowledge, finger tapping, computer glove

Edited by:
Luigi F. Cuturi,
Italian Institute of Technology (IIT), Italy

Reviewed by:
Roberto Arrighi,
University of Florence, Italy
Luca Turella,
University of Trento, Italy

****Correspondence:***
Christopher R. Madan
christopher.madan@nottingham.ac.uk

Specialty section:
This article was submitted to Cognition, a section of the journal Frontiers in Psychology

Received: *26 August 2020*
Accepted: *22 December 2020*
Published: *13 January 2021*

Citation:
Madan CR and Singhal A (2021) Convergent and Distinct Effects of Multisensory Combination on Statistical Learning Using a Computer Glove. Front. Psychol. 11:599125. doi: 10.3389/fpsyg.2020.599125

INTRODUCTION

Much of human behavior relies on the ability to make predictions based on integrating multisensory input to support multi-dimensional actions and decisions. This is a key component for the control of hand motor commands, such as reaching, grasping, and object manipulation. For example, first learning to play a musical instrument involves several distinct components, such as the mapping of visual or auditory cues to motor movements and being able to anticipate the transition to the next motor movement. Initial experiences involve following along with a predetermined sequence of visual and auditory cues. Later on, this process can be planned from rehearsal or creatively reflexive. More generally, many everyday behaviors can be examined as motor command sequences that transition through a broad statistical structure (see Baldwin et al., 2008).

Several standard experimental paradigms are related to this type of learning, such as the serial reaction time task (SRTT) and artificial grammar learning (AGL). Briefly, the SRTT involves making repeated button presses following visual instructions, where the sequences are either fixed or random (Nissen and Bullemer, 1987; Karni et al., 1995, 1998; Robertson, 2007; Clark and Ivry, 2010; DeCoster and O'Mally, 2011; Schwarb and Schumacher, 2012; Stefanescu et al., 2013). In contrast, AGL involves learning implicit rules of a probabilistic transition structure, based on a finite state machine, and is used as a model of language acquisition (Reber, 1967; Perruchet and Pacteau, 1990; Reber et al., 1996; Pothos, 2007; Erickson et al., 2016), though similar procedures have also been used to study memory for sequences (Reed and Johnson, 1994; Jones and Pashler, 2007; Bornstein and Daw, 2012; Schuck et al., 2012; Altmann, 2016). Both of these paradigms, however, miss an important component relative to the skill acquisition involved in real-world behaviors: Conventional SRTT only uses fixed or random sequences, but does not have implicit rules; artificial grammar has implicit rules but does not involve sequences of motor commands. Moreover, it remains an open and important question as to whether statistical learning operates via separate modality-specific mechanisms compared to a single high-level integrated system that is multi-modal in nature (Mitchel et al., 2014).

While some prior studies have sought to integrate both SRTT and AGL procedures (Hunt and Aslin, 2001), we were particularly interested in the influence of multisensory cues and the role of motor commands in implicit and explicit statistical learning tasks. Our design was based on the idea that a general central system would need to optimally integrate visual and auditory information for both implicit and explicit components of a statistical motor-learning paradigm, whereas a set of modality-specific systems might vary in their influences on motor learning.

Participants were presented with visual instructions to tap a specified fingertip with their thumb, with sequences of finger taps designed to follow a probabilistic transition structure, as shown in **Figure 1**. Transitions were designed such that some transitions were more likely, e.g., ring finger is most likely to be followed by index finger, but that all finger taps occurred equally often. Reaction time was measured using a computer glove that detected when finger taps occurred before advancing to the next instruction, allowing us to measure *implicit knowledge* of the probabilistic transitions as the experiment progressed. Participants were periodically also asked to predict the next finger tap, providing a measure of *explicit knowledge* of the probabilistic transitions. A second group of participants received both visual and auditory instructions, where a pure tone additionally accompanied the visual instruction. This comparison group allowed us to examine how additional sensory information can help or hinder learning.

A third and fourth group of participants were not permitted to make motor movements based on the instructions, and were instead explicitly asked to only observe the instructions while keeping their hands flat on the table in front of them. The timing of the instructions for these participants was yoked to participants in the prior two groups, who did make motor movements based on the finger tap instructions. These participants, however, were still probed for their knowledge of the probabilistic transitions, allowing us to examine the contribution of motor movements, i.e., enactment, to explicit knowledge of the transition structure.

In summary, by varying the learning cues presented to each group of participants, we will compare how multimodal sensorimotor information may enhance or impair learning of probabilistic sequences, in comparison to the idea of modality specificity, where unimodal information is sufficient. Furthermore, here we included both implicit and explicit tests of task knowledge, allowing for the measurement of potential of trade-offs between learning systems.

MATERIALS AND METHODS

Participants

A total of 90 young adults (64 female; aged 18–35) participated for a \$10 (Canadian) honorarium. Participants were recruited using ads posted around the University of Alberta campus. All participants were right handed (laterality quotient: M = 89.4, SD = 9.1), measured using the Edinburgh Handedness Inventory (Oldfield, 1971). Informed written consent was obtained from all participants prior to beginning the study, which was approved by the University of Alberta Institutional Review Board.

Participants were excluded for being ambidextrous (laterality < 70; $N = 4$), having insufficient English fluency (i.e., had difficulty understanding the task instructions; $N = 1$); tapping along while being in one of the Observe groups ($N = 3$), or had particularly slow response times (> 3 SD; $N = 2$). A total of 80 participants were included in the reported analyses.

Procedure

Participants were randomly assigned to one of four groups, following a 2 × 2 design. Participants either wore a glove and followed the finger taps presented on the screen (Glove, "G"), or passively observed the finger tap images with presentation times yoked to another participant (Observe, "O"). Additionally, finger tap presentation screens were either accompanied by a coinciding tone (Tone, "T"), or were silent without any auditory cues (Silent, "S"). Thus, the four groups were Glove + Tone (GT), Glove + Silent (GS), Observe + Tone (OT), and Observe + Silent (OS).

The task consisted of 16 sequences (blocks) of 145 items/trials (i.e., finger tap instructions) each, for a total of 2,320 trials. Finger tap instructions remained on the screen until the appropriate tap was made, and were immediately followed by the following trial upon the tap occurring. An example of a sequence of trials is shown in **Figure 1A**. Transitions between the finger tap instructions are shown in **Figures 1B,C**. Briefly, finger tap sequences were constructed such that (a) instructions never sequentially repeated, (b) no transitions were deterministic, and (c) all instructions occurred equally often. See the caption of **Figure 1** for further details.

For the participants in a Glove groups, a Peregrine glove (Iron Will Innovations Canada Inc., Lloydminster, AB) was used to detect finger tap responses. Participants' non-dominant (left) hand was measured so the correct glove size (small, medium, or large) could be used. The glove is designed for use with computer gaming and as such only left-handed gloves are produced by the manufacturer. The design intention is for the glove to be worn on the user's off-hand and replace a computer keyboard, with their dominant hand uses a computer mouse. However, in the current study the dominant hand was not involved in the experimental task.

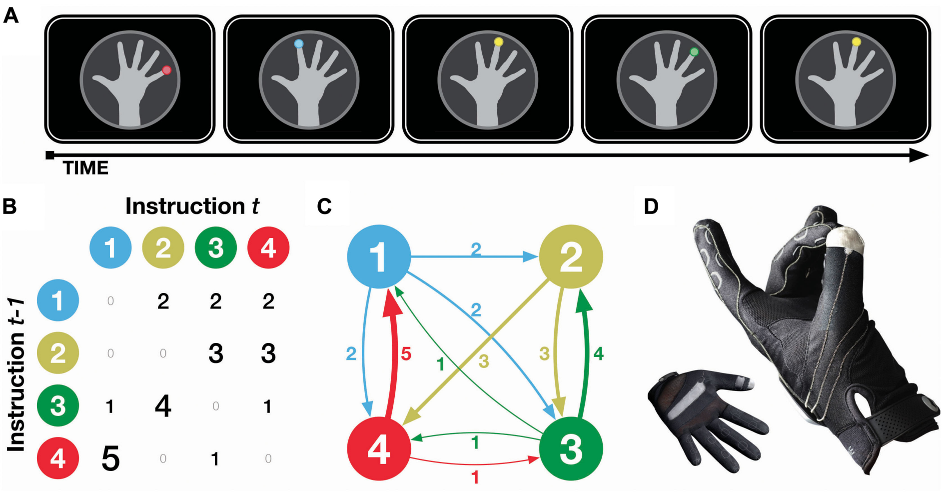

Instruction t-1 \ Instruction t	1	2	3	4
1	0	2	2	2
2	0	0	3	3
3	1	4	0	1
4	5	0	1	0

FIGURE 1 | Experimental procedure. **(A)** Illustration of task design, **(B,C)** matrix and finite state schematics, and **(D)** photos of computer glove input device. Transition values and line weights correspond to the proportion (out of every six occurrences), that finger tap instruction *t - 1* will be followed by instruction *t*. Note that finger taps were never sequentially repeated (i.e., *t - 1* and *t* are never the same), nor are any transitions deterministic (i.e., no 6 s in the matrix). All fingertips occurred equally often overall (i.e., all marginals are 6/6).

A short practice task preceded the experiment to test that participants were able to successfully make finger taps that registered on the computer. In the main task, finger tap instructions remained on the computer screen until the response was made. For participants in the Observe groups, instruction presentation times were yoked to a unique participant in the corresponding Glove group, to match for presentation durations diminishing over the course of the experiment as the glove participants learned the transition probabilities. Participants were asked to keep their hands flat on the table and explicitly instructed to not make movements based on the finger tap instructions and to only imagine the movements.

Every 30–35 trials, participants were prompted to predict which finger tap instruction would occur next. Participants were shown a row of the four finger images, with the numbers 1, 3, 5, and 7 displayed below them. Participants were asked to press the corresponding key on the computer keyboard to make their prediction. The experiment had a total of 72 explicit probe tests.

For participants in the Tone groups, each of the four fingers was additionally associated with pure tones with frequencies of 220, 440, 880, or 1,760 Hz (i.e., "A" note across four octaves). Tones were presented for the first 100 ms of each finger tap instruction—participants were instructed that tones would occur with the onset of each finger tap instruction, but were not informed that these would be redundant with the instructions. The mapping of finger (e.g., index finger) to tone was counterbalanced across participants. It is well established that differences in pitch (i.e., frequency) influence perceived loudness (Stevens, 1934; Robinson and Dadson, 1956; Molino, 1973); however, for these frequencies, differences in perceived loudness have been shown to be minimal (ISO-226, 2003; Glasberg and Moore, 2006). Mean loudness of the tones was measured at the approximate position of the participants' head using a Dawe Sound Level Meter 1400G (Dawe Instruments Ltd., London, United Kingdom) and was between 60 and 70 dB for the 4 tones. Participants in the Silent groups experienced the same visual presentation but did not receive any auditory cues.

RESULTS

Explicit Knowledge

Explicit knowledge of the statistical learning was measured as accuracy on the probe tests, where participants were asked to predict the next finger tap instruction. Predictions of the highest likelihood response were scored as correct, not necessarily based on the instruction that occurred next. As there were 72 explicit probe tests throughout the experiment, we divided the overall experimental task into quarters of four blocks each, rather than the 16 sequence blocks, such that there would be a sufficient number of trials in each unit of analysis. As such, there are 18 explicit probes per experiment quarter.

Accuracy on the explicit probe tests was analyzed using a 2 (Glove) × 2 (Tone) × 16 (Block) mixed ANOVA. As expected, accuracy on these probe trials improved across blocks [$F(3, 76) = 7.13$, $p = 0.009$, $\eta_p^2 = 0.086$] as shown in **Figure 2**, confirming that participants were acquiring explicit knowledge of the task, not procedural learning of the transition probabilities (discussed below; see **Figure 3**). The between-groups main effects and most interactions were non-significant; only the Block × Glove × Tone interaction was significant [$F(1, 76) = 4.70$, $p = 0.033$, $\eta_p^2 = 0.058$].

Here we conducted a 2 (Glove) × 2 (Tone) between-group ANOVA on the explicit probe accuracy from the first quarter of the task (i.e., blocks 1–4), following from a simple main effects approach. We observed a significant Glove × Tone interaction [$F(1, 76) = 5.61$, $p = 0.020$, $\eta_p^2 = 0.066$]. Results

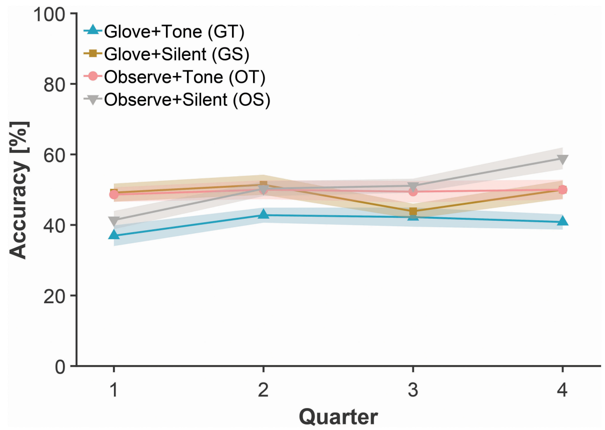

FIGURE 2 | Mean accuracy in explicit probe tests for each group across quarters of the experimental task. Shaded bands represent standard error of the mean, adjusted for inter-individual differences.

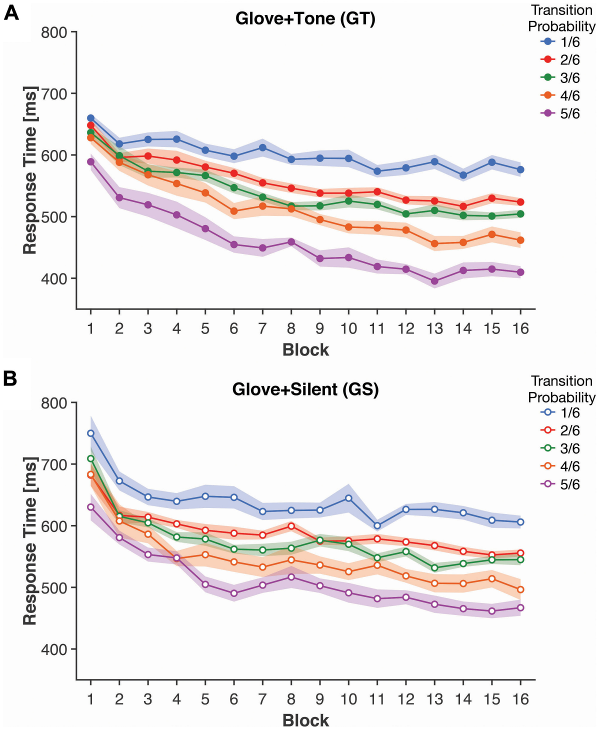

FIGURE 3 | Mean response times for each transition probability and block, for both **(A)** Glove + Tone (GT) and **(B)** Glove + Silent (GS) groups. Shaded bands represent standard error of the mean, adjusted for inter-individual differences.

indicate that participants who had either the glove or the tones, but not both, performed best [mean (SEM) accuracy—GT: 36.9% (2.9); GS: 49.2% (2.6); OT: 48.6% (2.1); OS: 41.4% (2.6)]. A comparable 2 × 2 between-groups ANOVA was conducted on the last quarter of the task (i.e., blocks 13–16). Here we observed significant main effects of Glove [$F(1, 76) = 5.49$, $p = 0.022$, $\eta_p^2 = 0.067$] and Tone [$F(1, 76) = 5.49$, $p = 0.022$, $\eta_p^2 = 0.067$], but no significant interaction [$p = 0.97$].

We then examined the change between the first and last quarters using paired-samples *t*-tests for each group. Mean accuracy improved, but the improvement was nominal in magnitude for all groups except for the Observe + Silent group—where the improvement was more definite [mean (SEM) accuracy—GT: 40.8% (2.1); GS: 50.0% (2.6); OT: 50.0% (2.8); OS: 58.9% (3.1); three *p*'s > 0.05, except OS: $t(19) = 3.43$, $p = 0.003$, Cohen's $d = 1.03$].

Implicit Knowledge

Implicit knowledge of the statistical learning was measured as the response time (RT) for the finger tap responses; as such, this analysis only applies to participants that wore the computer glove (GT and GS groups). Here we calculated the mean response time for trials based on their Transition Probability [1, 2, 3, 4, or 5 (out of 6)]; response times are shown in **Figure 3**.

Response times was initially analyzed as a 2 [Tone: Tone (Group GT) vs. Silent (Group GS)] × 16 (Block) × 5 (Transition Probability) mixed ANOVA. Here we observed a significant effect of Block [$F(15, 570) = 29.76$, $p < 0.001$, $\eta_p^2 = 0.439$], with faster response times as participants progressed through the experiment. The main effect of Transition Probability was also significant [$F(4, 152) = 51.12$, $p < 0.001$, $\eta_p^2 = 0.574$], with faster responses for the higher probability transitions. The Block × Transition Probability interaction was also significant [$F(60, 2{,}280) = 2.58$, $p < 0.001$, $\eta_p^2 = 0.064$] and was investigated with further ANOVAs following from a simple main effects approach. However, we did not observe a significant main effect of Tone [$F(1, 38) = 2.56$, $p = 0.12$, $\eta_p^2 = 0.063$] nor were any interaction effects including tone statistically significant [all *p*'s > 0.1].

To further characterize the interaction, we conducted two additional ANOVAs. The first ANOVA averaged the response times across the first four blocks (i.e., blocks 1–4) and was examined as a 2 (Tone) × 5 (Transition Probability) mixed ANOVA. The factor of Tone was included as a planned factor as multisensory learning was the focus of the study. Response time was significantly faster for higher Transition Probability [$F(2, 88) = 15.92$, $p < 0.001$, $\eta_p^2 = 0.295$]. Response times were 98.0 ms faster for the highest probability transitions than the lowest probability transitions. This finding was expected and also suggests that RT reflects initial learning of the transition structure. However neither the main effect of Tone [$F(1, 38) = 1.02$, $p = 0.32$, $\eta_p^2 = 0.026$] nor the interaction [$F(2, 88) = 0.41$, $p = 0.69$, $\eta_p^2 = 0.011$] was significant—indicating that addition of a tone was not faciliatory initially.

A similar 2 × 5 mixed ANOVA was conducted based on the last four blocks (i.e., blocks 13–16). The effect of Transition Probability on response times persisted [$F(2, 88) = 72.48$, $p < 0.001$, $\eta_p^2 = 0.656$] and increased in magnitude relative to the first blocks [$F(3, 108) = 12.05$, $p < 0.001$, $\eta_p^2 = 0.241$] (directly compared through a *post hoc* analysis), demonstrating continued learning of the task structure. Response times were 160.5 ms faster for the highest than the lowest probability transitions. The interaction with tone remained non-significant [$F(2, 88) = 0.51$, $p = 0.63$, $\eta_p^2 = 0.013$], however, the main effect of tone was significant in the last four blocks [$F(1, 38) = 4.56$, $p = 0.039$, $\eta_p^2 = 0.107$], where participants who received the auditory cues had a mean response time that was 41.6 ms faster—potentially indicating a facilitatory effect of the additional cues. Admittedly, this effect is relatively weak and was examined as a planned comparison, rather than in follow-up to an interaction involving tone from the full ANOVA that included all blocks.

DISCUSSION

The purpose of this study was to examine the relationship between auditory and visual input on implicit and explicit measures of a statistical motor-learning paradigm as it applies to hand motor commands. The primary question of multi-modality vs. modality specificity in statistical learning has been debated in the literature with some research strongly supporting the idea of multiple neural systems (Conway and Christiansen, 2005) and other research favoring the existence of a domain-general learning system (Kirkham et al., 2002). Our study uniquely contrasted a motor-learning paradigm with an observation paradigm for finger-movement sequences that were presented visually, with and without accompanying auditory tones that paired a specific pitch with a particular finger movement. The results showed two main findings, one related to explicit measures of statistical motor-learning and one related to implicit measures. Each will be discussed in turn, followed by a general discussion of our results within the larger framework of modality specificity vs. domain generality in statistical learning.

Our first result was that when auditory tones were paired with the visual movement cues, explicit probe performance decreased in the tapping task (i.e., Group GS > GT) but increased in the observation task (i.e., Group OT > OS). That is, the tones appeared to distract overt motor performance, but enhance performance associated with passive observation. Interestingly, this was only observed in early blocks of the task, and was attenuated in later blocks. One possible explanation for these findings is that in the tone groups, the task consisted of three input modalities for action (visual, auditory, movement), but only two were present for observation (visual, auditory). It is well known that auditory stimuli can be arousing (Eason et al., 1969; Paus et al., 1997), with both enhancing (Driver and Spence, 1998) and distracting effects (Escera et al., 2000). Thus, in the early blocks of our study, the movement (Glove + Tone; GT) group may have been optimally supported by a relatively simple visual-to-motor representation that was not available in the Observe + Tone (OT) group. This may have been related to diminished performance due to an information overload not essentially required (i.e., redundant) for the tapping task. On the other hand, the Observe + Tone group lacked the kinesthetic input afforded in the Glove + Tone group, and here the addition of more sensory input may have aided observation performance. While it has been shown that action observation can support motor learning (Mattar and Gribble, 2005), in our study, the observation groups (OT and OS) did not contain movement observation, but rather an observed *static* visual representation of the subsequent finger transition to be learned. Thus a combination of multisensory (visual-auditory) cues may have benefited the declarative task in the observation groups but not in the movement groups where the auditory information was redundant (Kalyuga et al., 1999). Interestingly, these effects disappeared in the last four blocks of the task suggesting that at some point in the skill-learning process (Fitts, 1964), the respective distracting and beneficial effects were no longer implicated in performance. Indeed, probe accuracy improved across blocks with the largest improvements occurring in the Glove + Tone (3.9%) and Observe + Silent (17.5%) groups. Thus, with repeated trials, the group with the least information input (Observe + Silent) became more like all the other groups that were richer in encoding input.

The second main finding was that the glove response times improved with successive trial blocks such that the last four blocks were faster than the first four blocks (**Figure 3**). However, in the last four blocks, the presence of auditory tones decreased response times in the finger-tapping task compared to the silent group. Thus the presence of tones enhanced the implicit measure of motor learning, perhaps reflecting the progression of knowledge of the task from a more conscious representation in the earlier blocks to something more automatic in later blocks (Masters, 1992). This idea is consistent with the explicit Glove + Tone group results discussed above where the distracting effects of the tones on the probe task disappeared in later trials compared to earlier ones. It has been shown that the implicit motor learning of a sequence can be improved 12 h following an intervening explicit memory task. The authors argue that this effect is due to off-line procedural improvements subserved by a fundamental dissociation between explicit-declarative and implicit-procedural memory systems, and neuroplasticity (Brown and Robertson, 2007). Presumably the hippocampus is a key player in the declarative memory circuit (Eichenbaum, 2000), whereas motor learning of a sequence involves many pre-motor and motor areas that decrease in their activity as learning progresses (Toni et al., 1998). Furthermore, Schendan et al. (2003) showed that both explicit and implicit measures of SRTT was associated with hippocampal/medial-temporal-lobe activation suggesting that procedural learning is also subserved by a memory system that *overlaps* with declarative memory. Such an overlap might be the reason that we found a link between the effects of the auditory tones on both the explicit and implicit measures in the motor-learning task. It is additionally worth considering, however, that the synchronous auditory and visual cues may have increased the saliency of the visual cues, following from the well-known pip-and-pop effect (Van der Burg et al., 2008). This could be evaluated in an additional group where the visual and auditory cues are both still presented, but with an offset in their presentation. If the response time improvements related to the auditory tones are attenuated, this would provide further specificity in how the multisensory cues were combined, such that the synchronicity of presentation was relevant—and potentially shares the same attentional processing as the pip-and-pop effect.

While we describe the non-glove groups as "Observe" as this is what we can assess behaviorally—that is, they did not make any overt motor movements, the instructions were more precisely asking them to engage in movement imagery (i.e., "Imagine" as a group descriptor). Several studies have shown that motor/movement imagery involves engaging similar networks of brain regions as actual movements (Lotze et al., 2003; Lotze and Cohen, 2006; Madan and Singhal, 2012; Hardwick et al., 2018; Kline et al., 2020). The intention here was to minimize actual movements as the experimental manipulation, but still encourage active engagement in the presented finger-tapping sequences through movement imagery and not allowing participants' minds to wander. As the participants in the Observe groups performed comparably to the Glove groups in the explicit knowledge test, and on average were numerically better, it does seem that the Observe participants were engaged in the task and did learn sequences.

Taken together, here we found that participants that only had to observe visual cues performed best in the explicit probe tests—with both enactment and additional auditory tones distracting from explicit knowledge. In contrast, when evaluating implicit knowledge (as measured by glove RT), we found that the additional auditory cues were *beneficial* to performance. These findings indicate that explicit knowledge of the statistical learning was best with only the single modality, but implicit knowledge was best when all three modalities were involved. Moreover, the results demonstrated a clear main effect of transition probability on response time and hastening of response time as learning accumulated (**Figure 3**).

Regarding the domain generality vs. modality-specificity of statistical learning, our results support the latter in the case of a motor-learning paradigm. Frost et al. (2015) has proposed a theoretical model to account for sensory modality effects on statistical learning with both separate and shared systems, particularly between auditory and visual inputs. A key concept in this model is that a brain region like the medial temporal lobe could support computational generality in statistical learning as it does for memory (Bogaerts et al., 2016), but this circuit will still have unique connections with individual sensory cortices that support modality-specific representations (Frost et al., 2015). On the basis of our findings, we argue in favor of this theoretical approach, and suggest that it can easily accommodate our observations in the motor-learning domain for hand motor commands that demonstrate both a convergence and a dissociation of modality effects on explicit and implicit measures of statistical learning.

The computer glove procedure used here generally worked well, while also being sufficiently different than more established procedures used in AGL and SRTT studies. However, future work may want to include a computer keyboard or response pad group as a comparison to the computer glove and also include a random-sequence control group to allow for distinct estimates of practice and learning effects. These findings add to the growing literature demonstrating different mechanisms underlying explicit and implicit knowledge, convergent with the notion of multiple distinct systems supporting motor skill learning (e.g., Clark and Ivry, 2010).

DATA AVAILABILITY STATEMENT

The raw data supporting the conclusions of this article will be made available by the authors, without undue reservation, to any qualified researcher.

ETHICS STATEMENT

The studies involving human participants were reviewed and approved by the University of Alberta Institutional Review Board. The patients/participants provided their written informed consent to participate in this study.

AUTHOR CONTRIBUTIONS

CM implemented the experiment, oversaw data collection, analyzed the data, and wrote the first draft of the manuscript. Both authors conceptualized the study, edited the manuscript, and approved the final draft.

FUNDING

This research was supported by funding from Natural Sciences and Engineering Research Council (NSERC) of Canada, through a Discovery award to AS and an Alexander Graham Bell Canada Graduate Scholarships-Doctoral (CGS-D) fellowship to CM. The Peregrine gloves were lent to CM by Iron Will Innovations Canada Inc., for research purposes.

ACKNOWLEDGMENTS

We would like to thank Christopher Donoff, Emily Armstrong, and Kathryn Lambert for assistance with data collection.

REFERENCES

Altmann, G. T. M. (2016). Abstraction and generalization in statistical learning: implications for the relationship between semantic types and episodic tokens. *Philos. Transact. R. Soc. B* 372:20160060. doi: 10.1098/rstb.2016.0060

Baldwin, D., Andersson, A., Saffran, J., and Meyer, M. (2008). Segmenting dynamic human action via statistical structure. *Cognition* 106, 1382–1407. doi: 10.1016/j.cognition.2007.07.005

Bogaerts, L., Siegelman, N., and Frost, R. (2016). Splitting the variance of statistical learning performance: a parametric investigation of exposure duration and transitional probabilities. *Psychon. Bull. Rev.* 23, 1250–1256. doi: 10.3758/s13423-015-0996-z

Bornstein, A. M., and Daw, N. D. (2012). Dissociating hippocampal and striatal contributions to sequential prediction learning. *Eur. J. Neurosci.* 35, 1011–1023. doi: 10.1111/j.1460-9568.2011.07920.x

Brown, R. M., and Robertson, E. M. (2007). Inducing motor skill improvements with a declarative task. *Nat. Neurosci.* 10, 148–149. doi: 10.1038/nn1836

Clark, D., and Ivry, R. B. (2010). Multiple systems for motor skill learning. *Wiley Interdiscip. Rev.* 1, 461–467. doi: 10.1002/wcs.56

Conway, C. M., and Christiansen, M. H. (2005). Modality-constrained statistical learning of tactile, visual, and auditory sequences. *J. Exp. Psychol.* 31, 24–39. doi: 10.1037/0278-7393.31.1.24

DeCoster, J., and O'Mally, J. (2011). Specific sequence effects in the serial reaction time task. *J. Motor Behav.* 43, 263–273. doi: 10.1080/00222895.2011.574171

Driver, J., and Spence, C. (1998). Crossmodal attention. *Curr. Opin. Neurobiol.* 8, 245–253. doi: 10.1016/s0959-4388(98)80147-5

Eason, R. G., Harter, M. R., and White, C. T. (1969). Effects of attention and arousal on visually evoked cortical potentials and reaction time in man. *Physiol. Behav.* 4, 283–289. doi: 10.1016/0031-9384(69)90176-0

Eichenbaum, H. (2000). A cortical-hippocampal system for declarative memory. *Nat. Rev. Neurosci.* 1, 41–50. doi: 10.1038/35036213

Erickson, L. C., Kaschak, M. P., Thiessen, E. D., and Berry, C. A. S. (2016). Individual differences in statistical learning: conceptual and measurement issues. *Collabra* 2:14. doi: 10.1525/collabra.41

Escera, C., Alho, K., Schröger, E., and Winkler, I. (2000). Involuntary attention and distractibility as evaluated with event-related brain potentials. *Audiol. Neurotol.* 5, 151–166. doi: 10.1159/000013877

Fitts, P. M. (1964). "Perceptual-motor skill learning," in *Categories of Human Learning*, ed. A. W. Melton (Amsterdam: Elsevier), 243–285. doi: 10.1016/b978-1-4832-3145-7.50016-9

Frost, R., Armstrong, B. C., Siegelman, N., and Christiansen, M. H. (2015). Domain generality versus modality specificity: the paradox of statistical learning. *Trends Cogn. Sci.* 19, 117–125. doi: 10.1016/j.tics.2014.12.010

Glasberg, B. R., and Moore, B. C. J. (2006). Prediction of absolute thresholds and equal-loudness contours using a modified loudness model. *J. Acoust. Soc. Am.* 120, 585–588. doi: 10.1121/1.2214151

Hardwick, R. M., Caspers, S., Eickhoff, S. B., and Swinnen, S. P. (2018). Neural correlates of action: comparing meta-analyses of imagery, observation, and execution. *Neurosci. Biobehav. Rev.* 94, 31–44. doi: 10.1016/j.neubiorev.2018.08.003

Hunt, R. H., and Aslin, R. N. (2001). Statistical learning in a serial reaction time task: access to separable statistical cues by individual learners. *J. Exp. Psychol.* 130, 658–680. doi: 10.1037/0096-3445.130.4.658

ISO-226 (2003). *Normal Equal-Loudness Level Contours*. Geneva: International Organization for Standardization.

Jones, J., and Pashler, H. (2007). Is the mind inherently forward looking? comparing prediction and retrodiction. *Psychon. Bull. Rev.* 14, 295–300. doi: 10.3758/bf03194067

Kalyuga, S., Chandler, P., and Sweller, J. (1999). Managing split-attention and redundancy in multimedia instruction. *Appl. Cogn. Psychol.* 13, 351–371. doi: 10.1002/(sici)1099-0720(199908)13:4<351::aid-acp589<3.0.co;2-6

Karni, A., Meyer, G., Jezzard, P., Adams, M. M., Turner, R., and Ungerleider, L. G. (1995). Functional MRI evidence for adult motor cortex plasticity during motor skill learning. *Nature* 377, 155–158. doi: 10.1038/377155a0

Karni, A., Meyer, G., Rey-Hipolito, C., Jezzard, P., Adams, M. M., Turner, R., et al. (1998). The acquisition of skilled motor performance: fast and slow experience-driven changes in primary motor cortex. *Proc. Natl. Acad. Sci. U.S.A.* 95, 861–868. doi: 10.1073/pnas.95.3.861

Kirkham, N. Z., Slemmer, J. A., and Johnson, S. P. (2002). Visual statistical learning in infancy: evidence for a domain general learning mechanism. *Cognition* 83, B35–B42. doi: 10.1016/s0010-0277(02)00004-5

Kline, A., Pittman, D., Ronsky, J., and Goodyear, B. (2020). Differentiating the brain's involvement in executed and imagined stepping using fMRI. *Behav. Brain Res.* 394:112829. doi: 10.1016/j.bbr.2020.112829

Lotze, M., and Cohen, L. G. (2006). Volition and imagery in neurorehabilitation. *Cogn. Behav. Neurol.* 19, 135–140. doi: 10.1097/01.wnn.0000209875.56060.06

Lotze, M., Scheler, G., Tan, H.-R. M., Braun, C., and Birbaumer, N. (2003). The musician's brain: functional imaging of amateurs and professionals during performance and imagery. *NeuroImage* 20, 1817–1829. doi: 10.1016/j.neuroimage.2003.07.018

Madan, C. R., and Singhal, A. (2012). Motor imagery and higher-level cognition: four hurdles before research can sprint forward. *Cogn. Proces.* 13, 211–229. doi: 10.1007/s10339-012-0438-z

Masters, R. S. W. (1992). Knowledge, knerves and know-how: the role of explicit versus implicit knowledge in the breakdown of a complex motor skill under pressure. *Br. J. Psychol.* 83, 343–358. doi: 10.1111/j.2044-8295.1992.tb02446.x

Mattar, A. A. G., and Gribble, P. L. (2005). Motor learning by observing. *Neuron* 46, 153–160. doi: 10.1016/j.neuron.2005.02.009

Mitchel, A. D., Christiansen, M. H., and Weiss, D. J. (2014). Multimodal integration in statistical learning: evidence from the McGurk illusion. *Front. Psychol.* 5:407. doi: 10.3389/fpsyg.2014.00407

Molino, J. A. (1973). Pure-tone equal-loudness contours for standard tones of different frequencies. *Percept. Psychophys.* 14, 1–4. doi: 10.3758/bf03198606

Nissen, M. J., and Bullemer, P. (1987). Attentional requirements of learning: evidence from performance measures. *Cogn. Psychol.* 19, 1–32. doi: 10.1016/0010-0285(87)90002-8

Oldfield, R. C. (1971). The assessment and analysis of handedness: the Edinburgh inventory. *Neuropsychologia* 9, 97–113. doi: 10.1016/0028-3932(71)90067-4

Paus, T., Zatorre, R. J., Hofle, N., Caramanos, Z., Gotman, J., Petrides, M., et al. (1997). Time-related changes in neural systems underlying attention and arousal during the performance of an auditory vigilance task. *J. Cogn. Neurosci.* 9, 392–408. doi: 10.1162/jocn.1997.9.3.392

Perruchet, P., and Pacteau, C. (1990). Synthetic grammar learning: implicit rule abstraction or explicit fragmentary knowledge? *J. Exp. Psychol.* 119, 264–275. doi: 10.1037/0096-3445.119.3.264

Pothos, E. M. (2007). Theories of artificial grammar learning. *Psychol. Bull.* 133, 227–244. doi: 10.1037/0033-2909.133.2.227

Reber, A. S. (1967). Implicit learning of artificial grammars. *J. Verbal Learn. Verbal Behav.* 6, 855–863. doi: 10.1016/s0022-5371(67)80149-x

Reber, P. J., Knowlton, B. J., and Squire, L. R. (1996). Dissociable properties of memory systems: differences in the flexibility of declarative and nondeclarative knowledge. *Behav. Neurosci.* 110, 861–871. doi: 10.1037/0735-7044.110.5.861

Reed, J., and Johnson, P. (1994). Assessing implicit learning with indirect tests: determining what is learned about sequence structure. *J. Exp. Psychol.* 20, 585–594. doi: 10.1037/0278-7393.20.3.585

Robertson, E. M. (2007). The serial reaction time task: implicit motor skill learning? *J. Neurosci.* 27, 10073–10075. doi: 10.1523/jneurosci.2747-07.2007

Robinson, D. W., and Dadson, R. S. (1956). A re-determination of the equal-loudness relations for pure tones. *Br. J. Appl. Phys.* 7, 166–181. doi: 10.1088/0508-3443/7/5/302

Schendan, H. E., Searl, M. M., Melrose, R. J., and Stern, C. E. (2003). An fMRI study of the role of the medial temporal lobe in implicit and explicit sequence learning. *Neuron* 37, 1013–1025. doi: 10.1016/s0896-6273(03)00123-5

Schuck, N. W., Gaschler, R., and Frensch, P. A. (2012). Implicit learning of what comes when and where within a sequence: the time-course of acquiring serial position-item and item-item associations to represent serial order. *Adv. Cogn. Psychol.* 8, 83–97. doi: 10.2478/v10053-008-0106-0

Schwarb, H., and Schumacher, E. H. (2012). Generalized lessons about sequence learning from the study of the serial reaction time task. *Adv. Cogn. Psychol.* 8, 165–178. doi: 10.2478/v10053-008-0113-1

Stefanescu, M. R., Thürling, M., Maderwald, S., Wiestler, T., Ladd, M. E., Diedrichsen, J., et al. (2013). A 7t fMRI study of cerebellar activation in sequential finger movement tasks. *Exp. Brain Res.* 228, 243–254. doi: 10.1007/s00221-013-3558-5

Stevens, S. S. (1934). The attributes of tones. *Proc. Natl. Acad. Sci. U.S.A.* 20, 457–459. doi: 10.1073/pnas.20.7.457

Toni, I., Krams, M., Turner, R., and Passingham, R. E. (1998). The time course of changes during motor sequence learning: a whole-brain fMRI study. *NeuroImage* 8, 50–61. doi: 10.1006/nimg.1998.0349

Van der Burg, E., Olivers, C. N. L., Bronkhorst, A. W., and Theeuwes, J. (2008). Pip and pop: nonspatial auditory signals improve spatial visual search. *J. Exp. Psychol.* 34, 1053–1065. doi: 10.1037/0096-1523.34.5.1053

Conflict of Interest: The authors declare that the research was conducted in the absence of any commercial or financial relationships that could be construed as a potential conflict of interest.

frontiers
in Psychology

MINI REVIEW
published: 09 February 2021
doi: 10.3389/fpsyg.2021.614471

Reach-to-Grasp: A Multisensory Experience

Sonia Betti, Umberto Castiello and Chiara Begliomini*

Department of General Psychology, University of Padova, Padova, Italy

The reach-to-grasp movement is ordinarily performed in everyday living activities and it represents a key behavior that allows humans to interact with their environment. Remarkably, it serves as an experimental test case for probing the multisensory architecture of goal-oriented actions. This review focuses on experimental evidence that enhances or modifies how we might conceptualize the “multisensory” substrates of prehension. We will review evidence suggesting that how reach-to-grasp movements are planned and executed is influenced by information coming from different sensory modalities such as vision, proprioception, audition, taste, and olfaction. The review closes with some considerations about the predominant role of the multisensory constituents in shaping prehensile behavior and how this might be important for future research developments, especially in the rehabilitative domain.

Keywords: multisensory integration, kinematics, grasping, sensory perception, reach-to-grasp

Edited by:
Ivan Camponogara,
New York University Abu Dhabi,
United Arab Emirates

Reviewed by:
Guido Maiello,
Justus Liebig University
Giessen, Germany
Vonne Van Polanen,
KU Leuven, Belgium

Correspondence:
Chiara Begliomini
chiara.begliomini@unipd.it

Specialty section:
This article was submitted to
Cognition,
a section of the journal
Frontiers in Psychology

Received: *06 October 2020*
Accepted: *18 January 2021*
Published: *09 February 2021*

Citation:
Betti S, Castiello U and Begliomini C (2021) Reach-to-Grasp: A Multisensory Experience. Front. Psychol. 12:614471. doi: 10.3389/fpsyg.2021.614471

INTRODUCTION

The notion that senses are better conceptualized as interrelated modalities rather than independent channels is supported by several studies, providing evidence for common neural and psychological mechanisms for the processing of multisensory information (e.g., Graziano and Gross, 1993; Driver and Spence, 1998; Spence et al., 2000; Doyle and Walker, 2002). The creation of a unitary percept of objects is one of the classic roles attributed to multisensory integration (Newell, 2004). Indeed, we are able to recognize a mug not only by looking at it but also, for example, by touching it when it is out of view. Similarly, we can recognize a robin redbreast relying on visual information about its size, shape, and colors, but also by hearing its song.

In humans, most of the research conducted on crossmodal integration has typically focused on perceptual integration, studying this phenomenon by using arbitrary responses (e.g., reaction times, saccadic eye movements). Less clear are the effects of multisensory coding during more natural tasks, such as upper limb tasks, where actions are performed in three-dimensional space. Indeed, different sensory modalities are used in concert not only to perceive objects but also to represent actions (Fogassi and Gallese, 2004). In this respect, a fundamental role of multisensory integration is to help in the planning and execution of actions. In fact, most of the actions we perform daily rely on sensory information and, to act appropriately, we often have to process information coming from more than one sensory modality in parallel. The act of kicking a ball, for example, requires the integration of visual, proprioceptive, and tactile modalities. Writing is another example of an action that, to be accomplished accurately, requires the integration of visual, proprioceptive, and tactile information. In addition, recognizing and understanding what other individuals are doing depends on multimodal information (Fogassi and Gallese, 2004). As an example, by hearing the sound made by the flowing water into a glass, we are able to reasonably recognize the act of pouring even without seeing the acting individual. Thus, information arriving through different and multiple sensory modalities can greatly facilitate the retrieval of the representation of a given object, acting individual, or a given action in our brain.

To date, crossmodal links between vision, audition, sense of touch, and proprioception have been extensively documented for grasping an object with hands (Johansson and Westling, 1984; Klatzky et al., 1987, 2000; Klatzky and Lederman, 1988; Goodwin et al., 1998; Jenmalm et al., 2000; van Beers et al., 2002; Patchay et al., 2003, 2006; Sober and Sabes, 2003; Aziz-Zadeh et al., 2004; Gazzola et al., 2006; Zahariev and MacKenzie, 2007; Etzel et al., 2008; Castiello et al., 2010). Here we present a series of studies that demonstrate crossmodal links between vision and other modalities (audition, olfaction and proprioception) during grasping. Prehensile actions are one of the most frequent behavior we perform and represent a remarkable experimental test case to probe the multisensory nature of our behavior. Specifically, in virtue of the well-characterized kinematics profile of reach-to-grasp movements (Castiello and Ansuini, 2009; Jeannerod, 2009) and of the detailed and multifaced information that it can provide, we mainly focus on the contributions coming from the study of grasp kinematics to reveal its multisensory nature. The results indicate a strong multisensory effect on the posture assumed by the hand during a visually guided reach-to-grasp movement, which is also evident at the level of action planning.

THE ROLE OF TACTILE INFORMATION

How tactile information influences grasping kinematics has been first explored by presenting targets of different dimensions either in visual or haptic modality (Chieffi and Gentilucci, 1993), and asking participants to judge their size and position. Results show that the sensory modality did not affect size estimation for the large target, whereas small stimuli tended to be underestimated when judged relying on tactile information. Adopting a similar approach, Camponogara and Volcic (2019a,b, 2020) recently showed how the role of the sensory modality changes over time when the right hand grasps an object which is perceived through vision, or haptically, with the left hand. When only haptic information was available, wider grip aperture and earlier initiation characterized hand preshaping, whereas the final phase of the action was slower. Conversely, vision appeared to be more relevant for the final phases of the movement, where the hand approaches the object and on-line visual feedback becomes more crucial. Visuo-haptic information made the action more efficient and precise, with the grip aperture becoming less variable and the movement execution faster.

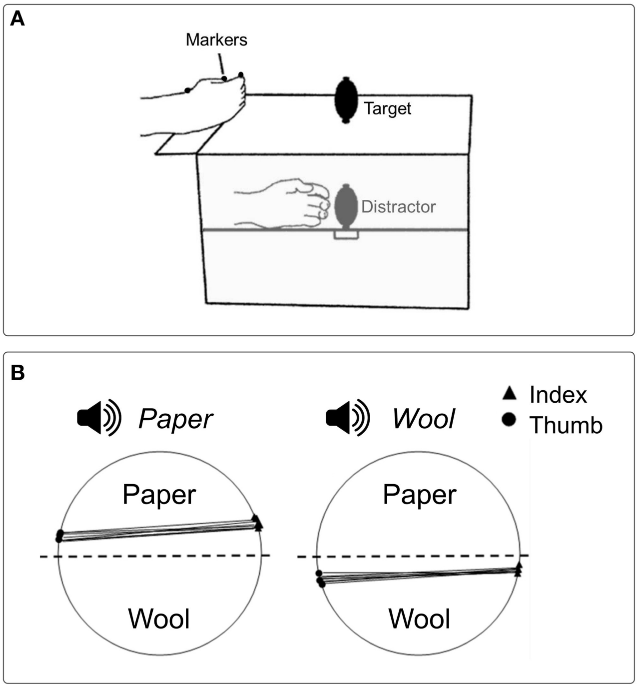

FIGURE 1 | (A) Schematic representation of the experimental setup used in Patchay et al. (2003) to study how haptic and proprioceptive inputs coming from an unseen distractor grasped by a non-reaching hand influenced reach-to-grasp actions toward a visual target performed by the other hand. Both the target and the distractor occupied spatially coincident locations, and the distractor could have a smaller or greater size relative to the target. **(B)** Graphical representation of contact points for the index finger and thumb from a representative participant in Castiello's et al. (2010) study, where the influence of contact sound on grasping actions was investigated. A sound congruent with the material covering one of the two parts of a visual target made participants more likely to grasp the object from the surfaced covered by the same material (e.g., paper, wool).

The effect of tactile information on grasping kinematics has been documented also in terms of competing information: Gentilucci et al. (1998) asked participants to reach and grasp visually presented objects presented in different sizes with one hand, while holding another unseen object (i.e., distractor) of different sizes (smaller or greater than the target) in the other hand. The main finding was that the size of the distractor did affect the kinematics of the grasping executed with the other hand: in particular, maximal hand aperture decreased and increased when the distractor was smaller and larger than the visual target-object, respectively. However, the effect of tactile information was observed only when the visual target-object was small and manipulation was performed using the right hand. This rendered unclear what caused the effect. These results have been confirmed and extended with a similar paradigm (Patchay et al., 2003, 2006), showing that maximum hand aperture for the visual target was proportional to the dimension of the distractor, which was manipulated proprioceptively with the other hand (**Figure 1A**). Analogous patterns were observed when the distractor was manipulated with either the left or the right hand. Noticeably, the effect of tactile information occurred only when the distractor was actively grasped; the effect was absent when the non-reaching hand received passive tactile and proprioceptive stimulation.

Overall these findings show that exploring large or small object activates the movement parameterization which corresponds to the size of that object, i.e., big and small hand aperture, respectively, indicating that the selection of the appropriate "grasp" motor plan for interacting with an object can be based on tactile cues. Therefore, the mechanism underlying the guidance of actions is not only sensitive to the information conveyed via vision but also via the sense of touch. Subsequent studies suggested that the contribution of tactile information better emerges when the inputs coming from the sensory channels disagree: while in conditions of congruency between perceptual inputs (e.g., vision and touch) the benefit of adding tactile information over vision only is almost negligible, in case of a mismatch between sensory inputs a larger variability in performance is observed (Pettypiece et al., 2010).

However, the interaction between vision and touch extends beyond grasp kinematics: for example, studies on haptic "memory" demonstrate that the weight of a previously manipulated target affects forces employed to grasp subsequent objects (Johansson and Westling, 1988; van Polanen and Davare, 2015), and changes the haptically perceived object weight independently of its visual appearance (Maiello et al., 2018). Similarly, presenting asynchronous visual and haptic feedback during object lifting can alter both force scaling and haptic weight perception (van Polanen et al., 2019).

THE ROLE OF AUDITORY INFORMATION

When using hands to manipulate objects and to interact with surfaces we generate contact sounds, providing important information concerned with the interaction between the moving effectors and the acted upon object. In particular, the contact sound signals both functional consequences and completion of manipulative actions. For instance, the "crash" sound associated with our hands breaking a walnut can be considered as a contact sound. Upon hearing the "crash," we become aware of having broken the shell, thus, we stop the walnut handling, and we bring the husk to our mouth.

Zahariev and MacKenzie (2007) have focused on the role played by contact sounds in hand grasping by asking participants to perform reach-to-grasp actions toward a visual target (i.e., a wooden cube) either in the absence or in the presence of a "virtual" contact sound, delivered when digits entered the space immediately surrounding the object. Participants were informed in advance whether a contact sound was delivered or not, and the main finding was shorter movement time for the contact sound compared to the no contact sound trials. This result was taken as an evidence of the effect that auditory information might exert on the organization of hand grasping movements. However, the specific reason of why the presence of a contact sound reduced reach duration leaving unchanged hand kinematics was unclear. Furthermore, the delivered contact sound corresponded to the sound of a cork popping out of bottle, a sound which is not normally generated when touching a wooden block. Therefore, the nature of the effect caused by the contact sound remained unexplained.

A subsequent investigation addressed this issue by adopting a similar procedure (Castiello et al., 2010). Here the sound produced by the digits while making contact with objects covered with different materials (i.e., aluminum, paper, wool) was presented before or during the execution of grasping actions performed toward objects covered with the same materials, either in conditions of congruency (e.g., paper sound for grasping a paper object) or incongruency (e.g., paper sound for grasping a wool object). A neutral condition (e.g., a synthetic sound) was also included. The foremost result was that the contact sound delivered either at the beginning or during the movement did affect kinematics. Specifically, both reach duration and the time of hand closure around the visual target decreased when the administered contact sound corresponded to the sound generated by the forthcoming contact with that visual target. Whereas, when the administered contact sound differed from that associated with the interaction between the hand and the visual target, both reach duration and the time of hand closure around the target increased. Therefore, hearing sounds generated during the end part of the action, when the hand touched the visual target-object, had the ability to modulate the "grasp" motor plan selected for that specific target depending on the level of correspondence between the contact sound and the sound produced at touch. Further support to this proposal comes from a second experiment (Castiello et al., 2010). Following a similar procedure, participants were requested to grasp a visual target with the upper and the lower part covered with different materials (e.g., wool and paper, respectively). Also in this case, the task was performed in the presence of a contact sound associated with the material covering one of the two parts of the visual target (e.g., "touching-wool" sound or "touching-paper" sound). Noticeably, when the presented contact sound was "touching- wool" and "touching-paper," the probability that participants grasped the visual-target object by the wool and the paper surface increased above chance (**Figure 1B**). How the sound produced by the target object can affect grasping planning has been investigated also by Sedda et al. (2011). In their study, participants had to infer the size of a grasping target relying on the sound produced by placing it within the reaching area, while visual information was varied from trial to trial. The results indicated that participants were able to infer the size of the object, with or without visual information available. The influence of auditory information on action has been demonstrated also in for action observation, showing how the activity of the mirror system can be evoked not only by seeing goal-directed hand actions (di Pellegrino et al., 1992) but also by hearing the sound produced by those actions (Aziz-Zadeh et al., 2004; Fadiga et al., 2005). Activity within the human mirror system has been investigated during the observation of hand actions, while sounds -which could have been either congruent or incongruent with that produced by the observed action- were presented. The results showed enhanced mirror activity in conditions of congruence between visual and auditory stimulation, suggesting that mechanisms similar to those typical for speech perception can arise (Alaerts et al., 2009). Altogether, these findings demonstrate that selection of the "grasp" motor plan to be performed to interact with an object can be influenced by sounds, extending the sensitivity of the mechanism underlying the guidance of actions to the auditory information.

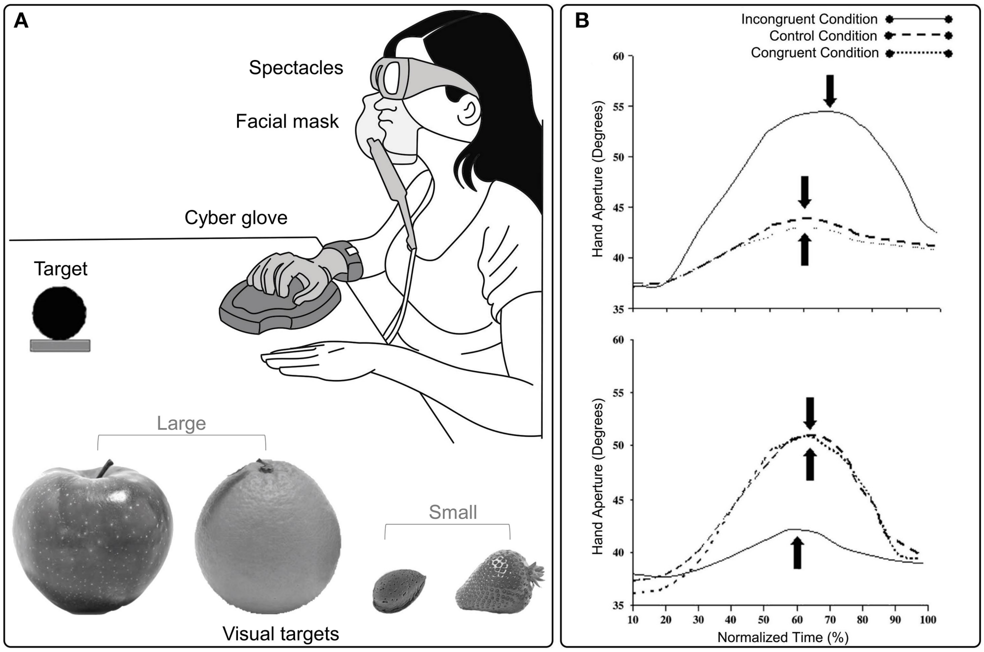

FIGURE 2 | (A) The experimental set up and examples of visual targets used in Castiello's et al. (2006) study, in which the existence of cross-modal links between olfaction and vision during grasping movements was investigated. **(B)** Graphical representation of the amplitude and the time (filled arrow) of maximum hand aperture for small (upper panel) and large (lower panel) targets in congruent, incongruent and control odor conditions. The time course of maximum hand aperture is expressed in terms relative to the overall reach duration (%). The amplitude and time of maximum hand aperture is, respectively, greater and delayed for an action toward a small target when olfactory information evokes an object requiring an incongruent large grasp. Conversely, when an action toward a large target is coupled with olfactory information evoking an incongruent small object, maximum hand aperture is smaller and anticipated. Hand aperture reported in the plots is averaged across trials and subjects for each experimental condition.

THE ROLE OF CHEMOSENSORY INFORMATION

An aspect which has been largely neglected in terms of the multisensory processes underlying hand grasping movements concerns chemosensory information. To date, only few studies considered reach-to-grasp movements performed toward a visual target-object in the presence of olfactory cues (Castiello et al., 2006; Tubaldi et al., 2008a,b). In these studies, the olfactory stimulus delivered during the grasping action could evoke an object of a smaller or larger dimension than the visual target-object (**Figure 2A**). This manipulation affected the both the amplitude and the time of maximum hand aperture (i.e., the maximum distance between the thumb and index finger; **Figure 2B**). In more detail, if the olfactory stimulus evoked an object smaller than the target-object, then the maximum hand aperture was smaller and anticipated in time than when no odor was delivered. If the olfactory stimulus evoked an object larger than the target-object, then the maximum hand aperture was larger and delayed in time than when grasping occurred in the absence of olfactory information (Castiello et al., 2006).

Altogether, the results of these studies indicate that the "size" of an odor influenced the kinematic profile of a reach-to-grasp movement. Crucially, the motor plan evoked by the odor is surprisingly fine grained and when elicited can modulate kinematics patterns both in terms of individual fingers movements and synergic movement amongst digits (Santello and Soechting, 1998). More recently, research on the effect of chemosensory information on reach-to-grasp has been extended to flavor (Parma et al., 2011a,b). In these studies, participants were asked to drink a sip of fruit flavored solution and then reach and grasp a fruit of different size positioned in front of them. The size of the objects (fruit) evoked by the flavor and the size of the visual target could be similar or different in size, and therefore elicit a different kind of grasping. For example, participants could drink a sip of strawberry juice and then reach and grasp an orange: in this case, while the size of the strawberry elicits a precision grip (i.e., the opposition of thumb and index finger), the size of the orange requires a whole-hand grip (i.e., opposition of the thumb to all the other fingers) to be grasped. Overall, the results highlighted how congruence and incongruence between flavor and target size affected kinematic parameters such as the maximum hand aperture. In more detail, a significantly smaller grip aperture was observed when the act of grasping the orange was preceded by a size-incongruent (e.g., strawberry flavored solution) than when it was preceded by a size-congruent (e.g., apple flavored solution) stimulation or water (i.e., control condition). Further, maximum hand aperture was more size attuned when the act of grasping the orange was grasped preceded by a size-congruent stimulation (e.g., orange flavored solution) than when it was grasped preceded by a size-incongruent (e.g., strawberry flavored solution) or water stimulation. The pattern highlighted is in line with studies exploring how interfering perceptual information can modulate grasping components (Castiello, 1999; Patchay et al., 2003, 2006), showing that when considering chemosensory information in combination with visual information, a condition of mismatch can affect the planning and execution of visually guided reach-to-grasp movements (Parma et al., 2011a,b). Rossi et al. (2008) further investigated the role of olfaction in grasping showing that smell can affect the excitability of muscles typically involved in the grasping movement. By means of Transcranial Magnetic Stimulation (TMS) they showed that evoked motor potentials for First Dorsal Interosseous (FDI) and the Abductor Digiti Minimi (ADM) can be modulated by food and non-food odors while participants observed a grasping task. However, this motor facilitation effect was evident only in case of congruence between odor and target of the observed grasping action.

CONCLUSION

This review presents the hand as a theoretical vehicle for understanding the multisensory nature of prehensile actions. The hand, an organ through which we explore our social and objective world, is integral to test the multisensory architecture of action. Unveiling how multisensory integration does shape our action not only has important implications for a full understanding of action planning and on-line control, but can also advance knowledge and applications in the fields of motor learning (Sigrist et al., 2013; Luan et al., 2020) and in the development of multisensory wearable systems for rehabilitation of missing or impaired functions (Shull and Damian, 2015). In our daily life we constantly perceive stimuli in their multimodal -rather than unimodal- forms, ending up with multimodal information that shapes and facilitates our actions toward the surrounding world. However, how multiple senses differentially contribute to the formation of a coherent representation of the world and shape our motor behavior is still an under-investigated aspect in motor control research. Nonetheless, the advantage of employing multimodal information overcoming the specific advantage of each modality critically emerges in the development of rehabilitative applications for the replacement or augmentation of impaired functions. Furthermore, deeply comprehending how multisensory integration works in motor control may play a crucial role for the implementation of "tomorrows" hands. It might be surprising that throughout the history of humanoid robot production, attempts to design robots with functional hands have been met with little success. And if the hands are the gateway to the world, it is clear that contemporary research is not yet in a position to provide us with any robots with meaningful active relations. The motor skills of today's best robots are indeed limited in comparison to animals and humans. But, if one were to come about, it would have to behave itself not as a deliberative and precisely calculating machine, but as skillful and dynamic entity in constant adjustment with its environment. A robot of this kind should approximate a reasonable spectrum of different multisensory motor capabilities. The challenge is to determine how multisensory functions can be integrated into meaningful architectures and to test their functional limits. Overall the findings summarized here could also act as a ground for novel motor rehabilitation approaches, exploiting interaction phenomena linking multisensory perception and action in human cognitive and motor system.

AUTHOR CONTRIBUTIONS

SB, UC, and CB identified the topic, performed the literature overview, and wrote the manuscript. All authors contributed to the article and approved the submitted version.

FUNDING

This study was supported by a grant from MIUR (Dipartimenti di Eccellenza DM 11/05/2017 no. 262) to the Department of General Psychology.

REFERENCES

Alaerts, K., Swinnen, S. P., and Wenderoth, N. (2009). Interaction of sound and sight during action perception: evidence for shared modality-dependent action representations. *Neuropsychologia* 47, 2593–2599. doi: 10.1016/j.neuropsychologia.2009.05.006

Aziz-Zadeh, L., Iacoboni, M., Zaidel, E., Wilson, S., and Mazziotta, J. (2004). Left hemisphere motor facilitation in response to manual action sounds. *Eur. J. Neurosci.* 19, 2609–2612. doi: 10.1111/j.0953-816X.2004.03348.x

Camponogara, I., and Volcic, R. (2019a). Grasping adjustments to haptic, visual, and visuo-haptic object perturbations are contingent on the sensory modality. *J. Neurophysiol.* 122, 2614–2620. doi: 10.1152/jn.00452.2019

Camponogara, I., and Volcic, R. (2019b). Grasping movements toward seen and handheld objects. *Sci. Rep.* 9:3665. doi: 10.1038/s41598-018-38277-w

Camponogara, I., and Volcic, R. (2020). Integration of haptics and vision in human multisensory grasping. *Cortex*. 135, 173–185. doi: 10.1101/2020.05.12.090647

Castiello, U. (1999). Mechanisms of selection for the control of hand action. *Trends Cogn. Sci.* 3, 264–271. doi: 10.1016/S1364-6613(99)01346-7

Castiello, U., and Ansuini, C. (2009). "Kinematic assessment of grasping," in *Sensorimotor Control of Grasping: Physiology and Pathophysiology*, eds. D. A. Nowak and J. Hermsdörfer (Cambridge: Cambridge University Press), 20–32. doi: 10.1017/CBO9780511581267.003

Castiello, U., Giordano, B. L., Begliomini, C., Ansuini, C., and Grassi, M. (2010). When ears drive hands: the influence of contact sound on reaching to grasp. *PLoS ONE* 5:e12240. doi: 10.1371/journal.pone.0012240

Castiello, U., Zucco, G. M., Parma, V., Ansuini, C, and Tirindelli, R. (2006). Cross-modal interactions between olfaction and vision when grasping. *Chem. Senses* 31, 665–671. doi: 10.1093/chemse/bjl007

Chieffi, S., and Gentilucci, M. (1993). Coordination between the transport and the grasp components during prehension movements. *Exp. Brain Res.* 94, 471–477. doi: 10.1007/BF00230205

di Pellegrino, G., Fadiga, L., Fogassi, L., Gallese, V., and Rizzolatti, G. (1992). Understanding motor events: a neurophysiological study. *Exp. Brain Res.* 91, 176–180. doi: 10.1007/BF00230027

Doyle, M. C., and Walker, R. (2002). Multisensory interactions in saccade target selection: Curved saccade trajectories. *Exp. Brain Res.* 142, 116–130. doi: 10.1007/s00221-001-0919-2

Driver, J., and Spence, C. (1998). Crossmodal attention. *Curr. Opin. Neurobiol.* 8, 245–253. doi: 10.1016/S0959-4388(98)80147-5

Etzel, J. A., Gazzola, V., and Keysers, C. (2008). Testing simulation theory with cross-modal multivariate classification of fMRI data. *PLoS ONE* 3:e3690. doi: 10.1371/journal.pone.0003690

Fadiga, L., Craighero, L., and Olivier, E. (2005). Human motor cortex excitability during the perception of others' action. *Curr. Opin. Neurobiol.* 15, 213–218. doi: 10.1016/j.conb.2005.03.013

Fogassi, L., and Gallese, V. (2004). "Action as a Binding Key to Multisensory Integration," in *The Handbook of Multisensory Processes*, eds. G. A. Calvert, C. Spence, and B. E. Stein (Cambridge, MA, US: MIT Press), 425–441.

Gazzola, V., Aziz-Zadeh, L., and Keysers, C. (2006). Empathy and the somatotopic auditory mirror system in humans. *Curr. Biol.* 16, 1824–1829. doi: 10.1016/j.cub.2006.07.072

Gentilucci, M., Daprati, E., and Gangitano, M. (1998). Haptic information differentially interferes with visual analysis in reaching-grasping control and in perceptual processes. *Neuro Report* 9, 887–891. doi: 10.1097/00001756-199803300-00023

Goodwin, A. W., Jenmalm, P., and Johansson, R. S. (1998). Control of grip force when tilting objects: effect of curvature of grasped surfaces and applied tangential torque. *J. Neurosci.* 18, 10724–10734. doi: 10.1523/JNEUROSCI.18-24-10724.1998

Graziano, M. S. A., and Gross, C. G. (1993). A bimodal map of space: somatosensory receptive fields in the macaque putamen with corresponding visual receptive fields. *Exp. Brain Res.* 97, 96–109. doi: 10.1007/BF00228820

Jeannerod, M. (2009). "The study of hand movements during grasping. A historical perspective," in *Sensorimotor Control of Grasping: Physiology and Pathophysiology*, eds. D. A. Nowak and J. Hermsdörfer (Cambridge: Cambridge University Press), 127–140. doi: 10.1017/CBO9780511581267.011

Jenmalm, P., Dahlstedt, S., and Johansson, R. S. (2000). Visual and tactile information about object-curvature control fingertip forces and grasp kinematics in human dexterous manipulation. *J. Neurophysiol.* 84, 2984–2997. doi: 10.1152/jn.2000.84.6.2984

Johansson, R. S., and Westling, G. (1984). Roles of glabrous skin receptors and sensorimotor memory in automatic control of precision grip when lifting rougher or more slippery objects. *Exp. Brain Res.* 56, 550–564. doi: 10.1007/BF00237997

Johansson, R. S., and Westling, G. (1988). Coordinated isometric muscle commands adequately and erroneously programmed for the weight during lifting task with precision grip. *Exp. Brain Res.* 71, 59–71. doi: 10.1007/BF00247522

Klatzky, R. L., and Lederman, S. J. (1988). "The Intelligent Hand," in *Psychology of Learning and Motivation*, ed. G. H. Bower (San Diego: Academic Press), 121–151. doi: 10.1016/S0079-7421(08)60027-4

Klatzky, R. L., Lederman, S. J., and Reed, C. (1987). There's more to touch than meets the eye: the salience of object attributes for haptics with and without vision. *J. Exp. Psychol. Gen.* 116, 356–369. doi: 10.1037/0096-3445.116.4.356

Klatzky, R. L., Pai, D. K., and Krotkov, E. P. (2000). Perception of material from contact sounds. *Presence Teleoperators Virtual Environ.* 9, 399–410. doi: 10.1162/105474600566907

Luan, M., Maurer, H., Mirifar, A., Beckmann, J., and Ehrlenspiel, F. (2020). Multisensory action effects facilitate the performance of motor sequences. *Atten. Percept. Psychophys.* doi: 10.3758/s13414-020-02179-9. [Epub ahead of print].

Maiello, G., Paulun, V. C., Klein, L. K., and Fleming, R. W. (2018). The sequential-weight illusion. *Percept* 9:2041669518790275. doi: 10.1177/2041669518790275

Newell, F. N. (2004). "Cross-modal object recognition," in *The Handbook of Multisensory Processes*, eds. G. A. Calvert, C. Spence, and B. E. Stein (Cambridge, MA, US: MIT Press), 123–139.

Parma, V., Ghirardello, D., Tirindelli, R., and Castiello, U. (2011a). Grasping a fruit. Hands do what flavour says. *Appetite* 56, 249–254. doi: 10.1016/j.appet.2010.12.013

Parma, V., Roverato, R., Ghirardello, D., Bulgheroni, M., Tirindelli, R., and Castiello, U. (2011b). When flavor guides motor control: an effector independence study. *Exp. Brain Res.* 212, 339–346. doi: 10.1007/s00221-011-2733-9

Patchay, S., Castiello, U., and Haggard, P. (2003). A cross-modal interference effect in grasping objects. *Psychon. Bull. Rev.* 10, 924–931. doi: 10.3758/BF03196553

Patchay, S., Haggard, P., and Castiello, U. (2006). An object-centred reference frame for control of grasping: effects of grasping a distractor object on visuomotor control. *Exp. Brain Res.* 170, 532–542. doi: 10.1007/s00221-005-0240-6

Pettypiece, C. E., Goodale, M. A., and Culham, J. C. (2010). Integration of haptic and visual size cues in perception and action revealed through cross-modal conflict. *Exp. Brain Res.* 201, 863–873. doi: 10.1007/s00221-009-2101-1

Rossi, S., Capua, A. D., Pasqualetti, P., Ulivelli, M., Fadiga, L., Falzarano, V., et al. (2008). Distinct olfactory cross-modal effects on the human motor system. *PLoS ONE* 3:e1702. doi: 10.1371/journal.pone.0001702

Santello, M., and Soechting, J. F. (1998). Gradual molding of the hand to object contours. *J. Neurophysiol.* 79, 1307–1320. doi: 10.1152/jn.1998.79.3.1307

Sedda, A., Monaco, S., Bottini, G., and Goodale, M. A. (2011). Integration of visual and auditory information for hand actions: preliminary evidence for the contribution of natural sounds to grasping. *Exp. Brain Res.* 209, 365–374. doi: 10.1007/s00221-011-2559-5

Shull, P. B., and Damian, D. D. (2015). Haptic wearables as sensory replacement, sensory augmentation and trainer – a review. *J. Neuro Eng. Rehabil.* 12:59. doi: 10.1186/s12984-015-0055-z

Sigrist, R., Rauter, G., Riener, R., and Wolf, P. (2013). Augmented visual, auditory, haptic, and multimodal feedback in motor learning: a review. *Psychon. Bull. Rev.* 20, 21–53. doi: 10.3758/s13423-012-0333-8

Sober, S. J., and Sabes, P. N. (2003). Multisensory integration during motor planning. *J. Neurosci.* 23, 6982–6992. doi: 10.1523/JNEUROSCI.23-18-06982.2003

Spence, C., Pavani, F., and Driver, J. (2000). Crossmodal links between vision and touch in covert endogenous spatial attention. *J. Exp. Psychol. Hum. Percept. Perform.* 26, 1298–1319. doi: 10.1037/0096-1523.26.4.1298

Tubaldi, F., Ansuini, C., Demattè, M. L., Tirindelli, R., and Castiello, U. (2008a). Effects of olfactory stimuli on arm-reaching duration. *Chem. Senses* 33, 433–440. doi: 10.1093/chemse/bjn010

Tubaldi, F., Ansuini, C., Tirindelli, R., and Castiello, U. (2008b). Odours grab his hand but not hers. *Perception* 37, 1886–1889. doi: 10.1068/p6286

van Beers, R. J., Baraduc, P., and Wolpert, D. M. (2002). Role of uncertainty in sensorimotor control. *Philos. Trans. R. Soc. Lond. B. Biol. Sci.* 357, 1137–1145. doi: 10.1098/rstb.2002.1101

van Polanen, V., and Davare, M. (2015). Sensorimotor memory biases weight perception during object lifting. *Front. Hum. Neurosci.* 9:700. doi: 10.3389/fnhum.2015.00700

van Polanen, V., Tibold, R., Nuruki, A., and Davare, M. (2019). Visual delay affects force scaling and weight perception during object lifting in virtual reality. *J. Neurophysiol.* 121, 1398–1409. doi: 10.1152/jn.00396.2018

Zahariev, M. A., and MacKenzie, C. L. (2007). Grasping at 'thin air': multimodal contact cues for reaching and grasping. *Exp. Brain Res.* 180, 69–84. doi: 10.1007/s00221-006-0845-4

Conflict of Interest: The authors declare that the research was conducted in the absence of any commercial or financial relationships that could be construed as a potential conflict of interest.

frontiers in Psychology

ORIGINAL RESEARCH
published: 12 February 2021
doi: 10.3389/fpsyg.2021.612558

Role of Tactile Noise in the Control of Digit Normal Force

Abdeldjallil Naceri[1]*, **Yasemin B. Gultekin**[2,3], **Alessandro Moscatelli**[4,5] **and Marc O. Ernst**[6]*

[1] Advanced Robotics Department, Italian Institute of Technology, Genoa, Italy, [2] Neurobiology of Vocal Communication, Werner Reichardt Centre for Integrative Neuroscience, University of Tübingen, Tübingen, Germany, [3] Functional Imaging Laboratory, German Primate Center, Leibniz Institute for Primate Research, Göttingen, Germany, [4] Department of Systems Medicine and Centre of Space Biomedicine, University of Rome Tor Vergata, Rome, Italy, [5] Laboratory of Neuromotor Physiology, Istituto di Ricovero e Cura a Carattere Scientifico (IRCCS) Fondazione Santa Lucia, Rome, Italy, [6] Applied Cognitive Psychology, Faculty for Computer Science, Engineering, and Psychology, Ulm University, Ulm, Germany

Whenever we grasp and lift an object, our tactile system provides important information on the contact location and the force exerted on our skin. The human brain integrates signals from multiple sites for a coherent representation of object shape, inertia, weight, and other material properties. It is still an open question whether the control of grasp force occurs at the level of individual fingers or whether it is also influenced by the control and the signals from the other fingers of the same hand. In this work, we approached this question by asking participants to lift, transport, and replace a sensorized object, using three- and four-digit grasp. Tactile input was altered by covering participant's fingertips with a rubber thimble, which reduced the reliability of the tactile sensory input. In different experimental conditions, we covered between one and three fingers opposing the thumb. Normal forces at each finger and the thumb were recorded while grasping and holding the object, with and without the thimble. Consistently with previous studies, reducing tactile sensitivity increased the overall grasping force. The gasping force increased in the covered finger, whereas it did not change from baseline in the remaining bare fingers (except the thumb for equilibrium constraints). Digit placement and object tilt were not systematically affected by rubber thimble conditions. Our results suggest that, in each finger opposing thumb, digit normal force is controlled locally in response to the applied tactile perturbation.

Keywords: grasping, manipulation, tactile perturbation, normal force, tactile object

OPEN ACCESS

Edited by:
Simone Toma,
Arizona State University, United States

Reviewed by:
Qiushi Fu,
University of Central Florida, United States
Yen-Hsun Wu,
Arizona State University, United States

Correspondence:
Abdeldjallil Naceri
abdeldjallil.naceri@iit.it
Marc O. Ernst
marc.ernst@uni-ulm.de

Specialty section:
This article was submitted to Perception Science, a section of the journal Frontiers in Psychology

Received: *01 October 2020*
Accepted: *08 January 2021*
Published: *12 February 2021*

Citation:
Naceri A, Gultekin YB, Moscatelli A and Ernst MO (2021) Role of Tactile Noise in the Control of Digit Normal Force. Front. Psychol. 12:612558. doi: 10.3389/fpsyg.2021.612558

INTRODUCTION

It is possible to grasp the same object in an infinite number of ways, due to the multiple combinations of digit placement on the object and the level of force exerted by each digit. Grasping and manipulating an object requires that the central nervous system masters this redundancy in degrees of freedom (Bernshtein, 1967; Naceri et al., 2014, 2017). Sensory feedback from proprioception, touch, and other modalities such as vision plays a key role in the control of grasping. In particular, tactile feedback is conveyed by afferent fibers that respond to the deformation of the mechanoreceptors in the skin. Cutaneous mechanoreceptors provide information concerning the timing of the contact, the location of the contact area on the skin, and the direction and amplitude of the contact force (Johansson and Flanagan, 2008). In addition to sensory feedback, finger force control is achieved in an anticipatory fashion during grasping tasks, by taking into account prior knowledge of the object and the internalized model of our body (Johansson and Westling, 1984; Westling and Johansson, 1984; Johansson and Flanagan, 2008).

A crucial point for understanding grasping is to uncover the coordination of the different digits, and the integration of cutaneous information from each of them, for motor control. Edin et al. (1992) investigated how the precision grip is regulated with respect to the individual digits. The authors studied precise grasping (two-finger grasping using the thumb and index fingers) while varying the friction coefficient independently at each digit, by changing the contact surfaces. The digit touching the most slippery surface exerted less tangential force than the digit touching the surface with the high friction. Consequently, the safety margins were similar at the two digits. During digital nerve block, large, and variable safety margins were employed, i.e., in absence of feedback, the finger-tip forces were not related to surface properties. Burstedt et al. (1999) extend the previous study to tripod grasping, i.e., three-digit grasping using index, middle finger, and thumb. The two studies reported that digit normal forces were adjusted locally when changing the frictional conditions at fingertip contact. Aoki et al. (2007) investigated the same research question for five-digit grasps using a similar experimental method and paradigm. Specifically, they manipulated the digit contact friction using either low friction (rayon paper) or high friction (sandpaper) independently for each digit giving 32 possible combinations (Aoki et al., 2007). They observed nonlocal force changes (between digit control), when the friction coefficient was changed in at least three digits.

A fourth study, which used a similar paradigm as the aforementioned study, revealed a similar within and between digit normal force regulation during five-digit grasps (McIsaac et al., 2009). This latter study concluded that multidigit force responses to texture, which was revealed by the studies referenced earlier, are not obligatory and instead suggested that the behavioral context of a task ought to be considered when inferring general principles of multidigit force coordination.

As indicated above, the nature of force control during grasping tasks is still unclear. The referenced studies investigated the modulation of a precision grip under different frictional conditions at the fingertips. All these studies used a manipulandum that constrained digit location due to the fixed location of force transducers. However, digit locations play a major role in influencing the modulation of the digit forces (Burstedt et al., 1999; Fu et al., 2010; Naceri et al., 2014).

In this study, the tactile input to different fingertips was perturbed by asking participants to wear a rubber thimble, which reduced the reliability of the tactile signal and changed the friction coefficient between finger and object (Kinoshita, 1999). First, we investigated whether the normal force exerted by each digit varies when wearing a rubber thimble. Additionally, we evaluated whether the thimble modulates the contact force locally, i.e., the force exerted by the covered finger, or globally, when grasping with three and four digits. We exploited the technical advantages of an innovative sensorized object to study the above question during unconstrained hand grasping (Naceri et al., 2017). In each trial, participants were required to grasp, lift, transport, and replace the sensorized object. Due to the design of the sensorized object, in each trial, participants could freely choose the location of the digits on the object. We considered two possible motor strategies, where force is controlled either independently within each digit or simultaneously across digits. In the former, we expect that wearing the thimble might increase or decrease grip force without affecting the adjacent noncovered finger. In the across digit normal-force regulation, we expect a synergistic increase or decrease across the adjacent noncovered fingers. The thumbs' normal force should be equal to the sum of normal forces of the opposing fingers in order to achieve a stable grasp. We hypothesize that in three-digit grasps, there is a within-digit control. Moreover, for four-digit grasping, synergic effects may occur between fingers (Santello et al., 2013). Therefore, in four-digit grasps, we expect between-digit force control rather than within-digit force control.

METHOD

Participants

Twenty-eight right-handed participants took part in the experiment (13 females, 15 males; age 27 ± 5 years of age, and mean ± standard deviation). Participants received course credit or were paid 7 €/h for their participation. Ten out of 28 participants participated in more than one condition with the thimble covering a different number of fingers; at least 48 h passed between two conditions. Six participants participated in all conditions. All participants had no history of neurological or motor deficits. The testing procedures were approved by the ethics committee of Bielefeld University and were conducted in accordance with the guidelines of the Declaration of Helsinki for research involving human participants. Informed written consent was obtained from all participants involved.

Experimental Setup

With the TACtile-sensorized Object (TACO), we are able to record the position and the normal force exerted by each finger on its sensorized surface, while it allows participants to freely choose the position for digit placement on the object, thus enabling unconstrained grasping (Schürmann et al., 2011). For details on using this device for gasping studies, see also Naceri et al. (2017). For this study, an additional force/torque sensor was integrated in the center of the TACO to additionally record the net torque and force vectors (see below). The TACO has a cuboid shape [length (l) = 170 mm; height (h) = 85 mm; width (w) = 55 mm], while the two opposing sides used for grasping were sensorized with four high-speed tactile sensor modules (Schürmann et al., 2011), named "Myrmex"—two on each side (Schürmann et al., 2012). Each Myrmex module provides a 16×16 tactile sensor array on an area of 80×80 mm^2, has a sampling rate of up to 1.9 kHz, and a spatial resolution of 5 mm (the size of one sensor element). That is, the TACO consisted of 512 tactels on each side. The Myrmex sensors were covered with conductive foam in order to increases the dynamic range of the sensor to match the contact pressure during grasping (Schürmann et al., 2012). The TACO allows us to simultaneously record the center of pressure and the normal force exerted by each digit. The device was calibrated using a force gauge with a force ranging from 0 to 25 N. During the calibration, we varied the cross-sectional area of the gauge tip from 10 to 50 mm^2 with a step of 20 mm^2 to account for the differences in size of participants' fingertips. The six-axis force/torque sensor that was added in the center of the TACO was the "Mini40" from ATI.

Two metallic plates were fixed on both sides of the force/torque sensor through its threaded insert. Each metallic plate was then attached to one side of the TACO using four screws. The force/torque sensor allowed us to record the net forces and net torques of participants' grasp.

During the experiment, participants looked through a mirror onto the haptic scene. The mirror occluded the participants' hands and the TACO from sight thus removing any visual feedback about their hand location and grasp. The mirror faced a computer monitor (21-in. CRT-computer monitor SONY CPDG520 with a resolution of 1280–1024 pixels and refresh rate of 100 Hz) that we used to display the visual stimulus. The visual stimulus consists of a rectangular cuboid, with the same dimensions of the TACO. Participants wore liquid-crystal shutter glasses (CrystalEyes^{TM}) providing binocular disparity (**Figure 1a**).

The TACO was attached to two PHANToM^{TM} (SensAble Technologies) force-feedback devices to track its position and allow force/torque perturbations to be applied during the holding phase of the trial (**Figure 1b**). The sampling rate of the PHANToM^{TM} was 1 kHz, allowing a precise position match between the virtual visual simulation and the physical TACO object. The total mass of TACO was 0.850 kg. Due to the constraints imposed by the two PHANToM^{TM} devices, the TACO had 5 degrees of freedom: translation along the x, y, and z directions, and rotation along the yaw ($\boldsymbol{\alpha}$) and roll ($\boldsymbol{\delta}$) axis. The 3D position and the rotations around the yaw and roll axis of the TACO were tracked using the PHANToM^{TM} devices.

Procedure

Participants sat on a chair with adjustable height. Before the start of the grasping movement, participants received an auditory "GO" signal, instructing them to grasp the TACO and to move it from the start to the end location behind a virtual bar, as illustrated in **Figure 1c**. They were asked to move the object smoothly and to place it in the end position in a similar orientation as it was picked up back at the beginning of the trial. A simulated rectangular cuboid was displayed on the CRT via the mirror with matched size and in the same location as the TACO. To provide participants with feedback, the virtual cuboid changed its color from red to purple as if it collided with the virtual bar (**Figure 1b**, upper left panel). After participants placed the TACO on the table, they received a second auditory signal prompting them to release the TACO and the experimenter stopped data recording. The next auditory signal instructed participants to replace the TACO back to the starting position for the next trial (**Figure 1c**). In different experiments, participants were instructed to grasp the TACO with three or four digits (thumb-index-middle digits, thumb-index-middle-ring digits). Fingers not involved in the task were extended and taped to a splint made of cardboard to prevent them from contacting the TACO. The finger placements on the TACO were self-chosen (grasping without constraints). There were different grasping conditions depending on how many fingers opposing the thumb were covered with a rubber thimble made from three layers of a nitrile glove, starting from none (control condition), to one, two, or three. Each trial lasted ∼10 s from grasp onset to the end. Fourteen trials were conducted for each condition. Each experimental session consisted of one condition involving the glove together with the baseline condition with no finger covered by a glove. The order of the experimental and control condition was randomly assigned to the participants. The total duration of the experimental session was approximately 15 min. There were two grasp conditions (three-digit grasp and four-digit grasp) and thus giving four glove conditions for the three-digit grasps: (1) no glove, (2) index finger covered, (3) middle finger covered, and (4) index and middle fingers covered and eight glove conditions for the four-digit grasps: (1) no glove, (2) index finger, (3) covered, (4) middle finger covered, (4) ring finger covered, (5) index and middle fingers covered, (6) index and ring fingers covered, (7) middle and ring fingers covered, and (8) index, middle, and ring fingers covered.

Data Processing and Analysis

Using the TACO device, we measured the values of normal force (F) for each finger and their positions on the surface of the device, determined by the horizontal (CoP_x) and vertical center of pressures (CoP_y) independently for each finger. We set the center of the TACO as the origin of the coordinate system (0, 0, 0). The CoP_x and CoP_y were defined as the location of the global maximum of the activated region of tactels for each fingers' region on the sensor matrix. The force measurements were converted from arbitrary units to Newtons using the lookup table generated during calibration. The calibration table was obtained with a resolution of ± 0.2 N. Digit locations, normal forces, and the position and orientation of the TACO were recorded and processed with a second-order Butterworth low-pass filter with 10 Hz cutoff frequency (**Figure 2**). In the following, we analyzed the average values of CoP_x and CoP_y during the transport phase of the TACO (i.e., the CoP values recorded between time t_0 and time t_1 in **Figure 2**).

For each digit contact with its CoP, we determined the force vector $F = (F_x, F_y, F_z)$ giving the direction and magnitude of the contact force. In the TACO reference frame (**Figure 4B**), F_z is the normal force F^n, F_x, and F_y are the tangential force components: $F^t = (F_x{}^2 + F_y{}^2)^{1/2}$, that are parallel to the TACO's contact surface.

To satisfy a stable grasp of the TACO, the force produced by the thumb must be equal to the sum of the normal forces of the opposing digits:

$$\sum\nolimits_{\boldsymbol{i=T,\,I,\,M,\,R,\,L}} \boldsymbol{F_i^n} = \boldsymbol{0}, \tag{1}$$

The sum of the absolute digit normal forces represents the total grip force applied by the participant.

The two PHANToM^{TM} devices did not support the weight of TACO. Hence, the sum of digits' load force, $\sum F_i^t$, must be equal

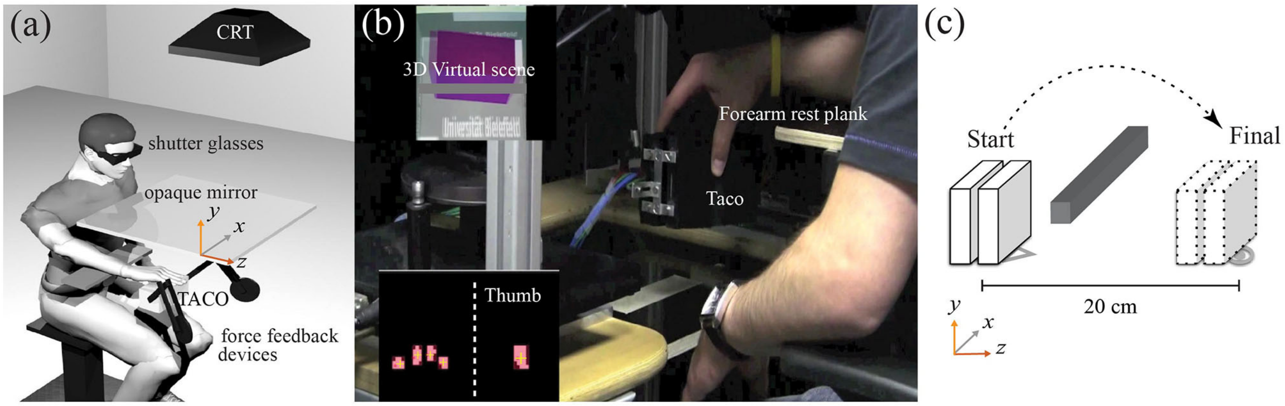

FIGURE 1 | Experimental setup. **(a)** Participants binocularly viewing the mirror image of the visual scene. **(b)** The TACO attached to the PHANToMTM force feedback devices. On the top left, the 3D virtual scene, the purple cube color indicates to the participants that the TACO collided the gray horizontal bar (red color otherwise). On the bottom left, the TACO output image with a yellow cross represents digit center of pressures (CoPs). **(c)** The TACO initial and final target and its desired trajectory.

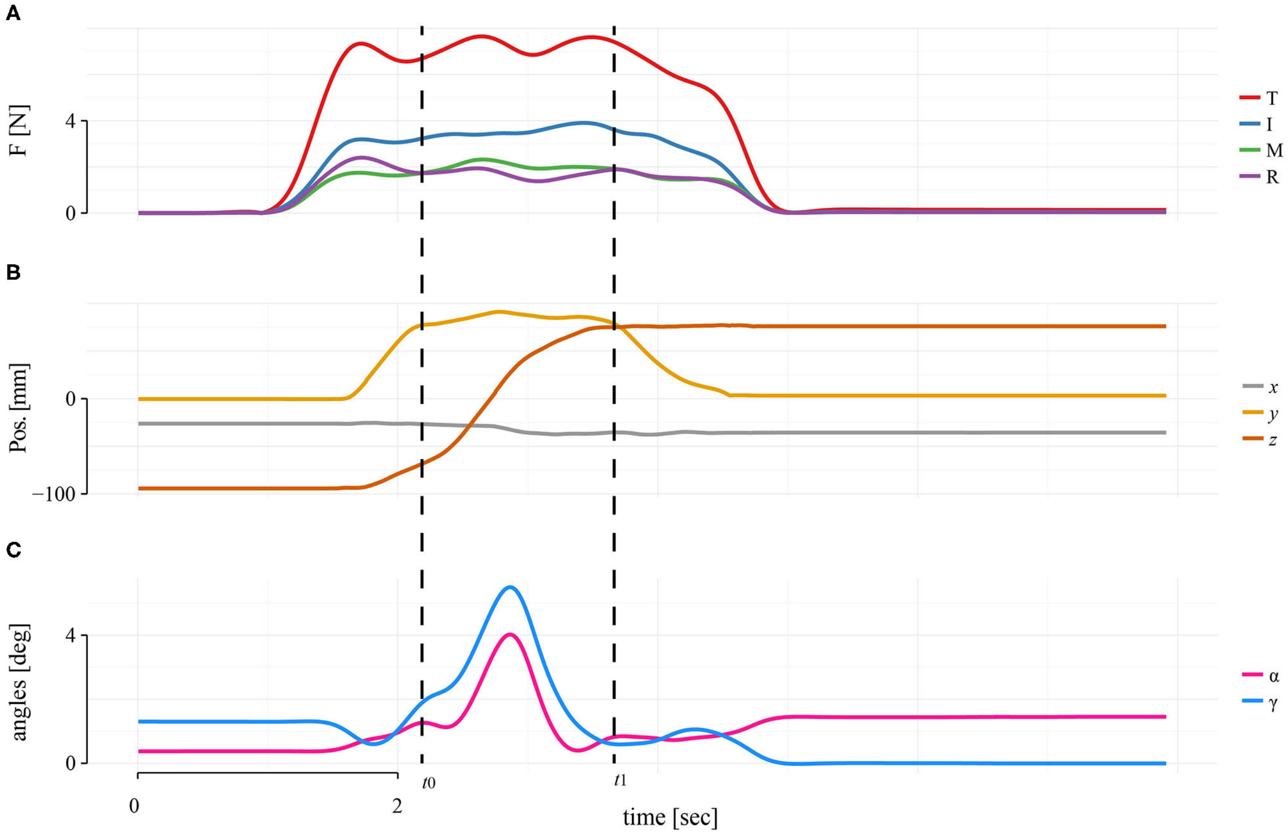

FIGURE 2 | Single trial of a representative participant in four digits in baseline condition. **(A)** Force profiles for each digit. **(B)** TACO coordinates. **(C)** TACO orientations. Dashed lines represent the transporting phase, which is the interval between t_0 and t_1, where all dependent variables were quantified and averaged.

to the TACO load force when the object is stationary (i.e., when there are no additional inertial forces):

$$\sum_{i=T,\,I,\,M,\,R,\,L} F_i^t = -\mathrm{mg}, \tag{2}$$

where m is the TACO's mass and g is the gravity.

Finally, the friction constraints must be satisfied. Specifically, the force F must be inside the friction cone:

$$F_i^t < \mu F_i^n, \tag{3}$$

where μ is friction coefficient.

Statistical Analysis

The aim of this study is to evaluate whether normal forces are adjusted either independently for each digit or whether there is a coupling such that the normal forces of some digits are regulated jointly (synergetically), in response to the sensory feedback perturbance when covering individual fingers with a rubber thimble. By means of multivariable linear mixed models (LMMs), we evaluated the systematic variation in the normal force and analyzed whether there are synergetic variations between different digits under the different conditions. The digit normal force "$\boldsymbol{y}$" (**Eq. 4**) was modeled individually for each digit as a linear combination of the experimental variables (referred to as the fixed-effect linear predictors $\boldsymbol{X\beta}$), the random variability between participants (the random-effect predictors, Zb), and the residual random error ε (Bates et al., 2015).

The LMM equation has the following form:

$$\boldsymbol{y} \;=\; \boldsymbol{\beta_1}\mathrm{CoP_x} \;+\; \boldsymbol{\beta_2}\mathrm{G} \;+\; \boldsymbol{\beta_3}\mathrm{CoP_xG} \;+\; \boldsymbol{Zb} \;+\; \boldsymbol{\varepsilon} \tag{4}$$

The matrix of fixed-effect predictors, $\boldsymbol{X}$, included the following predictors: glove condition G ($G = 1$ if any of the fingers was covered with the thimble, and $G = 0$ otherwise), the $\mathrm{CoP}_{x,y}$ of the index, the middle and the ring fingers normalized to thumb, and the interaction factor between $\mathrm{CoP}_{x,y}$ and glove condition G (**Figure 3**). We evaluated the effect of each digit by testing the significance of the corresponding single fixed-effect parameters β_1, β_2, and the interaction β_3 with the Likelihood Ratio (LR) test (Pinheiro and Bates, 2000). The LR test compares the maximized log-likelihood functions of two nested models, M1 and M0, with and without the parameter of interest. Under the null hypothesis that the simpler model M0 is better than M1, the LR has a large-sample χ_1^2 distribution (Bolker et al., 2009; Moscatelli et al., 2012). The dummy variable G has value 1 if *at least one* of the fingers was covered with the glove and 0 otherwise. Therefore, the parameter β_2 in **Eq. (4)** allowed us to estimate the influence of the covered finger on the noncovered fingers (see **Figure 6**).

Next, by using the LMM, we evaluated the effect of the glove perturbation (G) and the position CoP of all fingers on the orientation yaw ($\boldsymbol{\alpha}$) and roll ($\boldsymbol{\gamma}$) of the TACO object:

$$\boldsymbol{\alpha} \;=\; \boldsymbol{\eta_1}\mathrm{CoP_x} \;+\; \boldsymbol{\eta_2}\mathrm{G} \;+\; \boldsymbol{\eta_3}\mathrm{CoP_xG} \;+\; \boldsymbol{Zb} \;+\; \boldsymbol{\varepsilon} \tag{5}$$

and

$$\boldsymbol{\gamma} \;=\; \boldsymbol{\theta_1}\mathrm{CoP_x} \;+\; \boldsymbol{\theta_2}\mathrm{G} \;+\; \boldsymbol{\theta_3}\mathrm{CoP_xG} \;+\; \boldsymbol{Zb} \;+\; \boldsymbol{\varepsilon}. \tag{6}$$

With this, we could evaluate whether changes of the digit normal forces that were triggered by perturbing the tactile input at each finger would also lead to significant effects on the orientation of the TACO object during the transport phase.

Predictions

In this study, we expect two possible outcomes concerning the control of the digit normal forces: either participants adjusted the grip and normal forces of each digit independently in response to the tactile perturbation (**Figures 4C,D**), i.e., there is a selective adjustment of normal force in the perturbed finger(s) compared with baseline (**Figures 4C,D**). Alternatively, there might be a (synergetic) link between the force adjustment of multiple digits even when only some of them are tactilely perturbed (**Figures 4E,F**), such that the force adjustment occurs across multiple perturbed and nonperturbed fingers. The force variations at single finger can be due to the tactile perturbation from one side and the finger placements with respect to thumb from the other side. In order to exclude (reduce) the effect of force increase due to finger placements with respect to the thumb, we included the distance-normalized CoPs of the fingers to thumb into the LMM (**Figure 3**).

What complicates the differentiation between these alternative hypotheses is that also under the hypothesis of independent control of finger forces, the nonperturbed fingers might change slightly when the force exerted by the perturbed finger changes in order to meet the stable grasp constraints (**Eq. 1**), i.e., if the force exerted by the perturbed finger decreases, the forces exerted by the other fingers opposing the thumb must increase such that the sum of all normal forces remains zero. For both hypothesis, we may find arguments that the normal force of the perturbed finger(s) might decrease or increase in response to the tactile manipulation. Since the sensitivity of the tactile input is decreased by the rubber thimble, we may speculate that the force might increase to compensate for the reduced input. Alternatively, we may speculate that the unreliable tactile input induced by the rubber thimble might lead to a decrease in force because the feedback for grasp control is less reliable.

RESULTS

Three-Digit Grasp

Before analyzing the forces exerted by each finger during three-digit grasping, we evaluated the overall grip force of the grasp and we report on the peak of the grip force. Participants produced the lowest peak grip force in the baseline condition (no glove), whereas they exerted the largest peak grip force when covering both fingers opposing the thumb, the index, and middle fingers. For the conditions with only one finger covered (index or middle finger), the result for the peak grip force was in-between: the peak grip force was slightly larger than baseline when covering the middle finger. When covering the index finger, the peak grip force was slightly higher compared with covering the middle finger but lower than the peak grip force with both fingers covered (**Figure 5**).

In order to get better insight on force control within single finger, we analyze the force contribution of each finger (mean values within transporting phase between t_0 and t_1) to the overall grip force. **Figure 6** shows the force difference between the baseline condition (no glove) and the condition when at least one finger is covered (i.e., index or/and middle). When one of the two fingers opposing the thumb was covered during the three-digit grasps, the results using LMM revealed a significantly higher mean finger force compared with baseline for the covered finger (i.e., for the index in index-covered condition and the middle finger in the middle-covered condition). In contrast, there was nonsignificant effect of the noncovered finger (i.e., of the

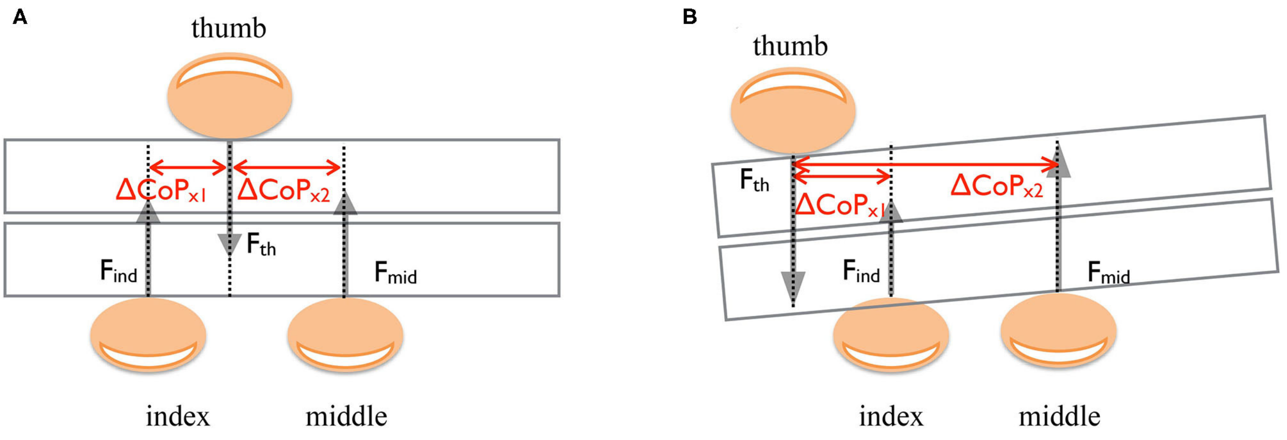

FIGURE 3 | Schema illustrates digit horizontal placements normalized to the thumb, forces, and the TACO orientation in three digits grasp. **(A)** An example of grasp configuration when the thumb is located right between the index and middle fingers. **(B)** Grasp configuration example when the thumb is shifted left of the index and middle fingers.

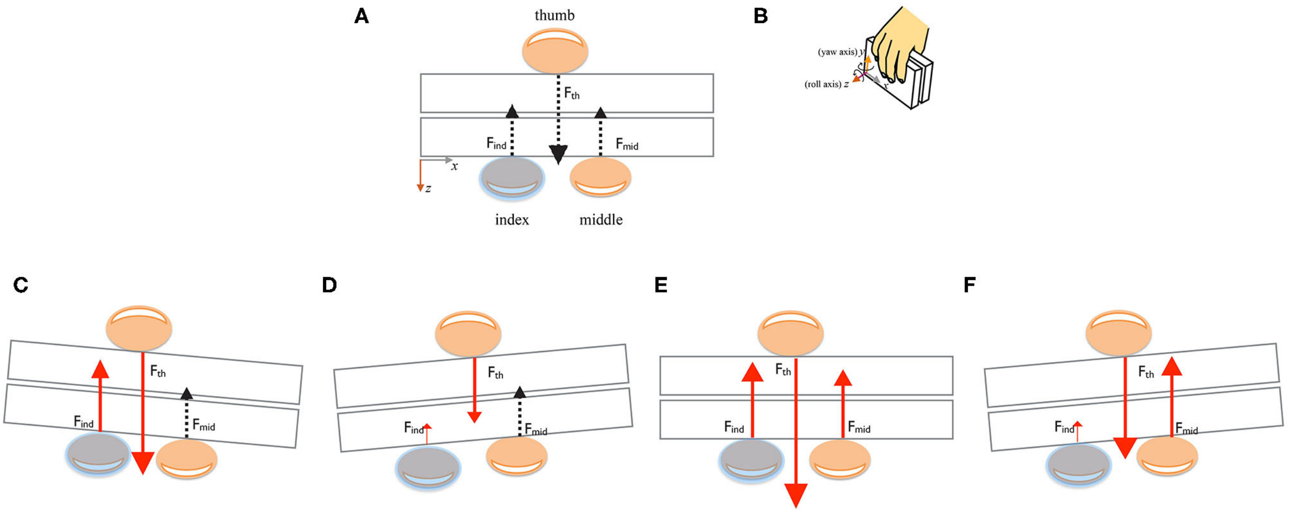

FIGURE 4 | Experimental predictions using three-digit grasp as an example. **(A)** Digit horizontal placements, forces, and TACO position in the baseline condition. **(B)** 3D layout of the human hand grasping the TACO and 3D axes showing the TACO's 5 degrees of freedom. **(C,D)** Predictions for local digit normal force regulation with force increase and decrease of the covered finger, respectively. Black dashed arrow indicates digit normal force of noncovered finger did not change significantly. **(E,F)** Between digit normal force regulations with force increase and decrease at the covered finger, respectively, and the tactile perturbation significantly affecting the noncovered adjacent finger.

middle finger in index-covered condition or the index finger in the middle-covered condition) compared with baseline regarding the produced normal force. In the condition with both digits covered, we found a significant increase in finger force for both digits relative to baseline. These results indicate that the tactile perturbation significantly increased the produced finger force selectively for the digits covered.

Next, we explored the horizontal placement of the fingers on the TACO. To this end, we compared the fingers' horizontal positions relative to the thumb for the glove and the baseline conditions. **Figure 7** shows the difference in CoP_x between the baseline condition (no glove) and the condition when at least one finger is covered (i.e., index and/or middle). We found a significant variation in digit placement in the glove condition compared with baseline only for the index finger when both index and middle fingers were covered. The rest of the conditions were not significant (**Figure 7**); thus, these results indicate that the variation in digit placements cannot fully account for the effects found for the digit normal forces. Finally, we have to mention that there was no significant effect ($p > 0.05$) relative to the baseline condition in any of the conditions with different fingers covered on the vertical placement of the fingers (CoP_y). Therefore, CoP_y was not included as a predictor in **Eqs. (4–6)**.

Next, we analyze participants' grasp performance by investigating the yaw and roll angles of the TACO during the transport phase evaluating the mean (quantified within

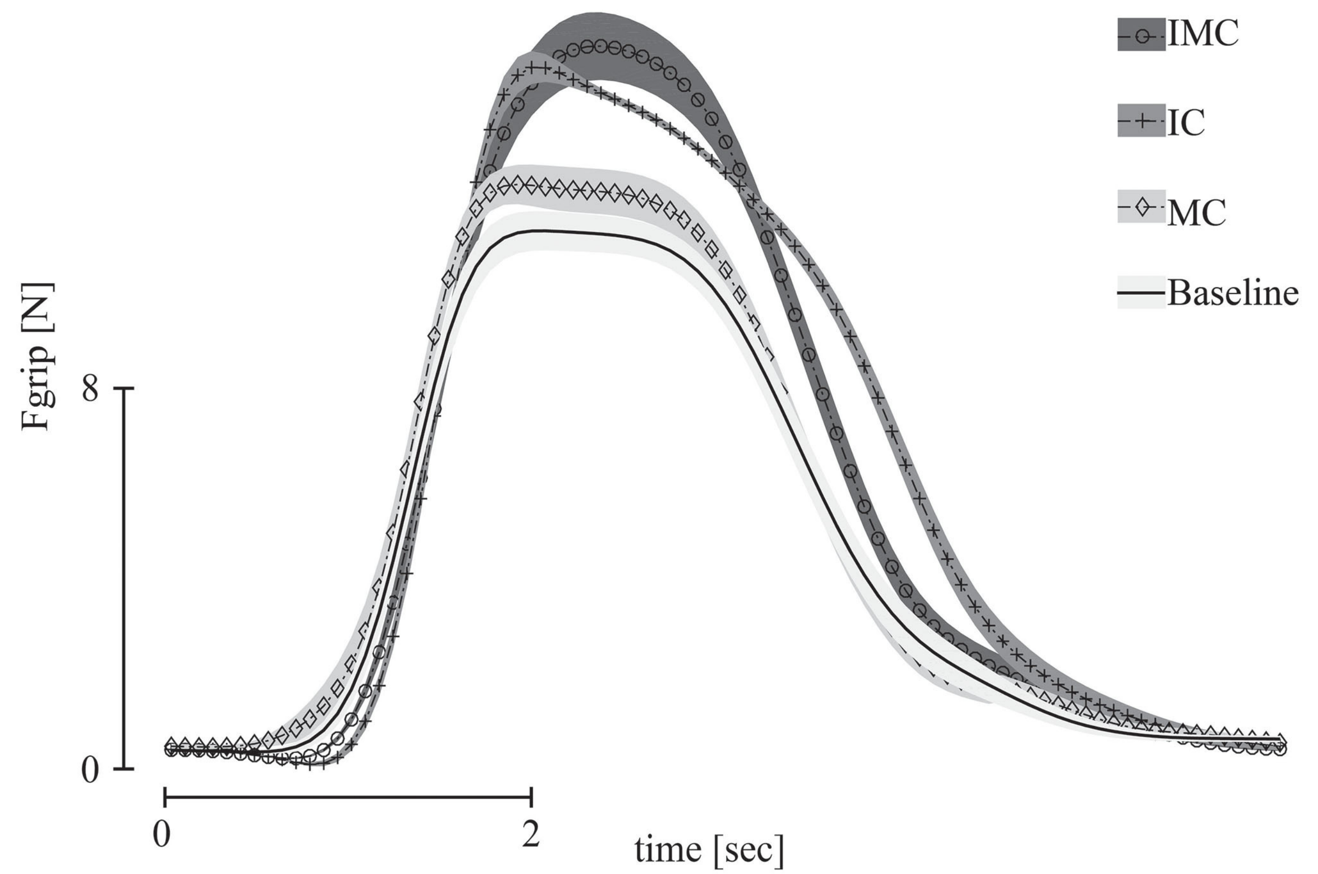

FIGURE 5 | Grip force profiles in all glove conditions in three-digit grasp for all participants.

transport time window) orientation of the TACO. Participants kept the TACO relatively straight during transport and there was no significant difference of the mean orientation between the baseline and any of the glove conditions on the TACO orientations [likelihood ratio test; α-IC: $\chi^2_{(1)} = 0.61$, $p = 0.44$; MC: $\chi^2_{(1)} = 1.48$, $p = 0.22$; IMC: $\chi^2_{(1)} = 0.22$, $p = 0.64$, γ-IC: $\chi^2_{(1)} = 0.98$, $p = 0.32$; MC: $\chi^2_{(1)} = 3.16$, $p = 0.08$; IMC: $\chi^2_{(1)} = 0.22$, $p = 0.64$]. **Figure 8** shows a top view of the experimental scene indicating averages across participants for the mean orientation of the TACO in yaw together with the mean normal force produced by each digit. This figure provides a schematic overview on the distribution of the mean normal forces across the fingers together with the horizontal digit placement on the TACO.

Four-Digit Grasp

In this experiment, participants were grasping the TACO with four fingers—three fingers opposing the thumb—and either none, one, two, or three of the fingers opposing the thumb could be covered by the rubber thimble. Similar to the previous experiment, the present results of all conditions revealed a significant increase in the mean force of the finger or the fingers covered with the rubber thimble, while the other noncovered finger(s) did not differ significantly from baseline. This is shown in **Figure 9** which for all fingers opposing the thumb depicts the difference in peak force averaged across participants between the experimental condition with at least one finger covered and the baseline with no finger covered. These results indicate that the tactile perturbation introduced significantly increased the digit force selectively for the covered finger also during four-digit grasps, similar as it did for three-digit grasps.

Next, we explored how the fingers' horizontal positions varied relative to the thumb $\Delta\mathrm{CoP}_x$ in the experimental conditions with tactile perturbation when compared with baseline ($\Delta\mathrm{CoP}_{x,\mathrm{exp}}$ – $\Delta\mathrm{CoP}_{x,\mathrm{baseline}}$, **Figure 10**). The patterns of observed changes in the placement of the fingers on the object seem meaningful for achieving a stable grasp with the altered digit forces reported above, which can be best seen in **Figure 11**. **Figure 11** (top view) shows the average values across participants of the (mean values within transporting phase between t_0 and t_1) orientation of the TACO object (yaw angle) and the exerted digit normal forces for the fingers placed on the object. Thus, this figure provides an overview on the patterns of finger placement and forces when the tactile input was manipulated in the different conditions. For example, **Figures 10**, **11** show that we observed significant changes for the placement of all fingers to the right (top view) when the index finger was covered. The changes in finger

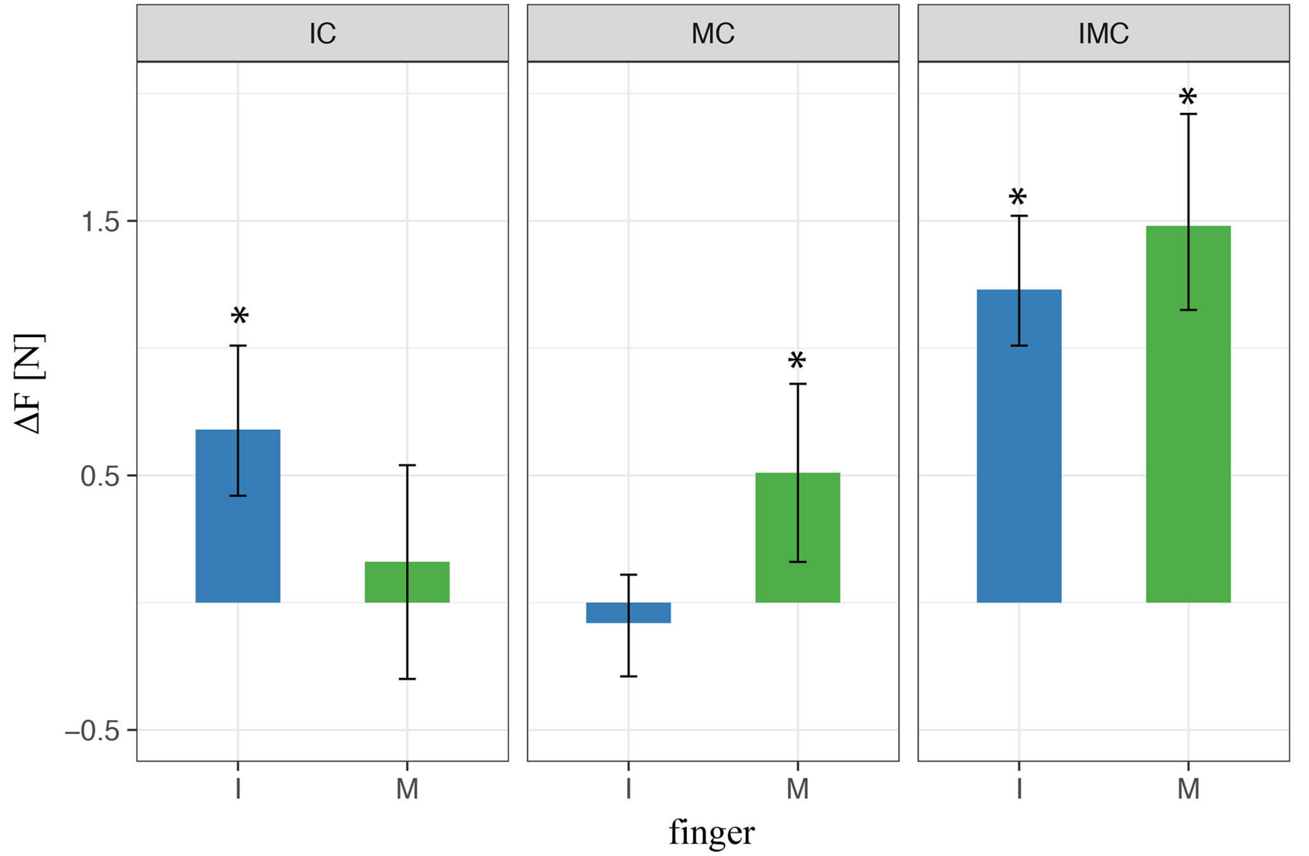

FIGURE 6 | LMM results of digit normal forces in three-digit grasp. * indicate statistical significance determined by LMM analysis.

placement counteract the higher digit force of the index finger that would otherwise induce an increased torque. Similarly, when the middle finger was covered which in baseline is typically placed left of the thumb, the placement of all fingers was slightly shifted to the left to counteract the higher forces of the middle finger when covered thus to not induce an unnecessary torque. The other patterns of changes in digit placement when perturbing the tactile input are also consistent with the notion of torque reduction due to an increased force in the covered digits. That is participants know or have learned over trials how to best reposition their fingers on the object to reduce torque when the grip forces are increased due to the tactile manipulation.

In order to investigate whether the torque due to increased digit forces was completely compensated by the adjustment of the placement of the fingers on the object, we analyzed the orientation (mean values of yaw and roll within transporting phase between t_0 and t_1) of the TACO object during the movement.

In general, participants kept the TACO object pretty straight in the glove condition compared with the baseline such that there was no significant effect of glove condition on its orientation [likelihood ratio test; α-IC: $\chi^2_{(1)} = 3.05$, $p = 0.08$; MC: $\chi^2_{(1)} = 0.64, p = 0.43$; RC: $\chi^2_{(1)} = 3.63, p = 0.06$; IMC $\chi^2_{(1)} = 0.14$, $p = 0.71$; IRC: $\chi^2_{(1)} = 0.05, p = 0.83$; MRC: $\chi^2_{(1)} = 2.23$, $p = 0.14$; IMRC: $\chi^2_{(1)} = 0.73$, $p = 0.39$, γ-IC: $\chi^2_{(1)} = 0.36$, $p = 0.55$; MC: $\chi^2_{(1)} = 0.37, p = 0.54$; RC: $\chi^2_{(1)} = 0.27, p = 0.61$; IMC $\chi^2_{(1)} = 0.36$, $p = 0.55$; IRC: $\chi^2_{(1)} = 0.35, p = 0.55$; MRC: $\chi^2_{(1)} = 2.35, p = 0.11$; IMRC: $\chi^2_{(1)} = 0.74$, $p = 0.39$]. There was also no difference in the orientation of the TACO between the experimental and the baseline condition, indicating that the torque due to increased digit forces was counteracted well by the repositioning of the fingers. **Figure 11** shows a top view of the experimental scene indicating averages across participants for the mean orientation of the TACO in yaw together with the mean normal force produced by each digit. This figure provides a schematic overview on the distribution of the mean normal forces across the fingers together with the horizontal digit placement on the TACO.

DISCUSSION

In this work, we revisited the impact of tactile input on the modulation of the grip force during unconstrained grasping. All previous studies were conducted using constrained grasping. As in our previous studies, we found that digit normal forces are crucially altered by digit placements. In the present study, participants had to lift, transport, and replace the TACO with

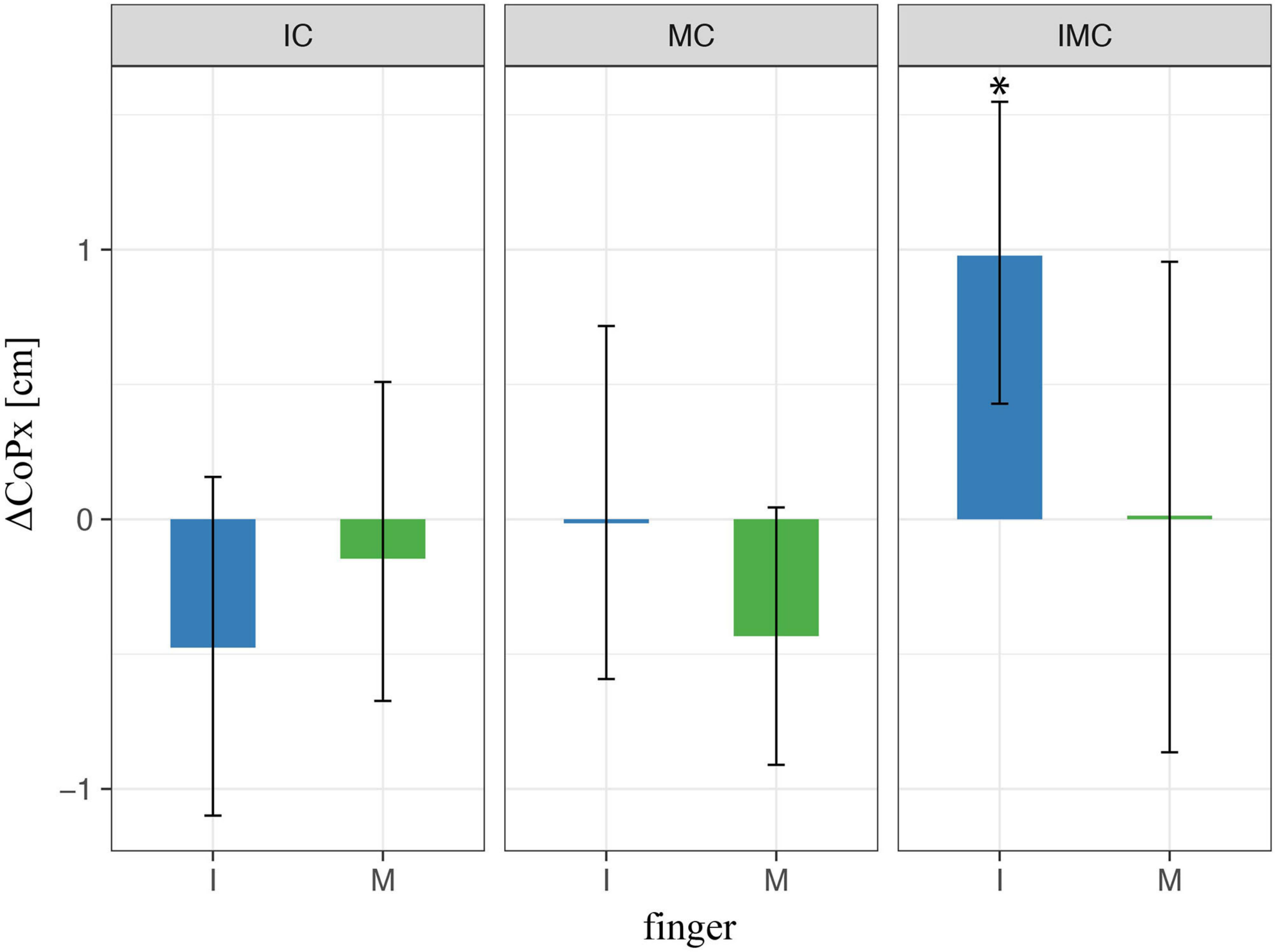

FIGURE 7 | LMM results of digit initial horizontal placements (CoPs) in three-digit grasp. * indicate statistical significance determined by LMM analysis.

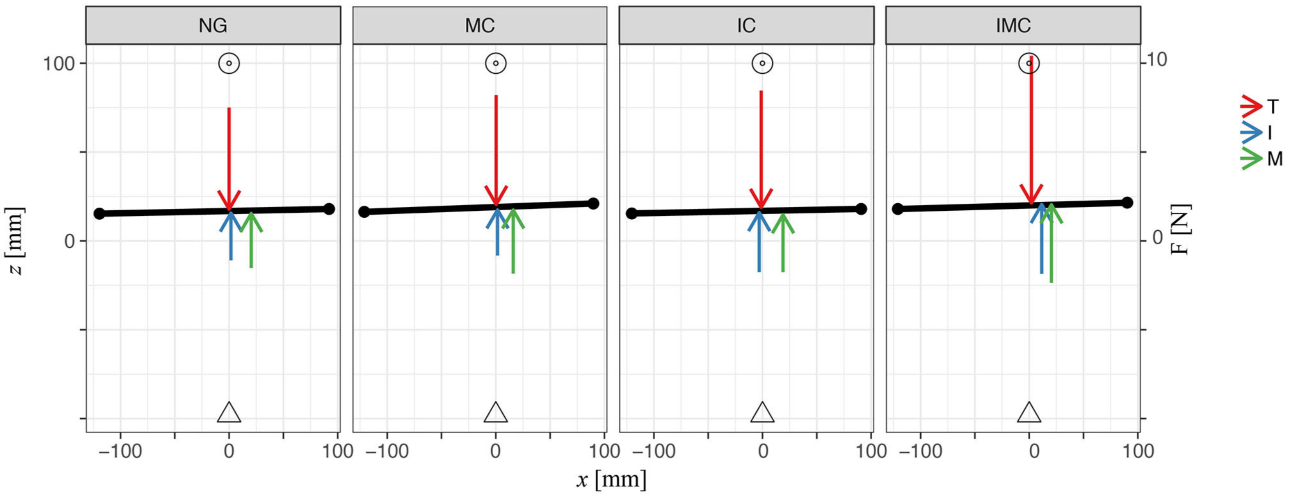

FIGURE 8 | Plot illustrates average values across participants of digit normal forces, horizontal initial placements on the TACO, and the TACO yaw angle four digits within all glove conditions in three-digit grasp. Triangle represents the TACO start location, and circles represent the TACO target location.

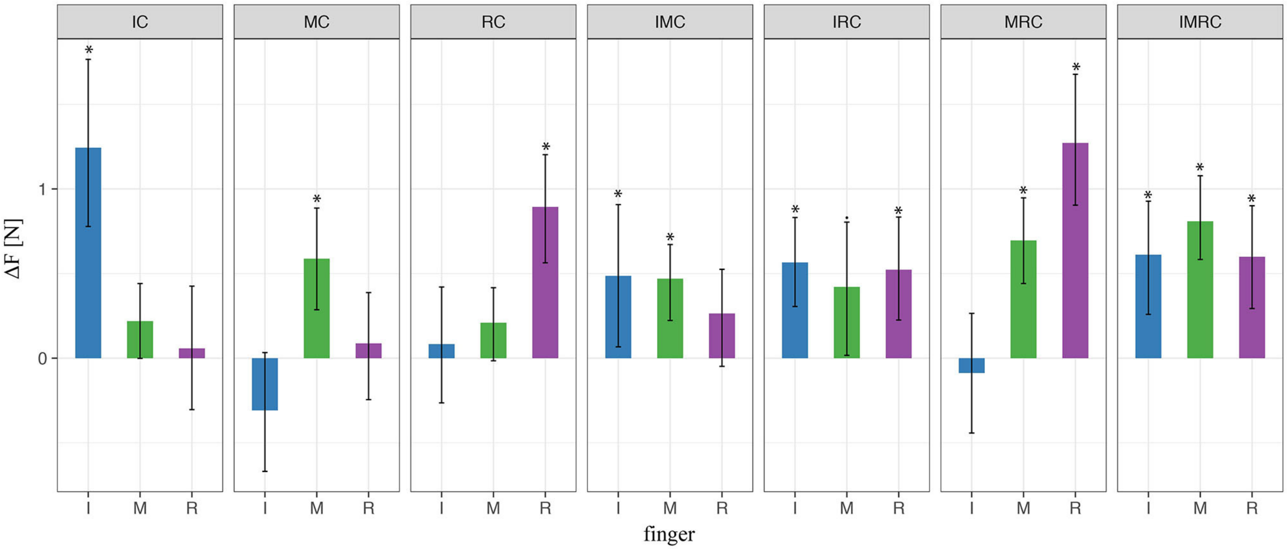

FIGURE 9 | LMM results of digit normal forces in four-digit grasp. * indicate statistical significance determined by LMM analysis.

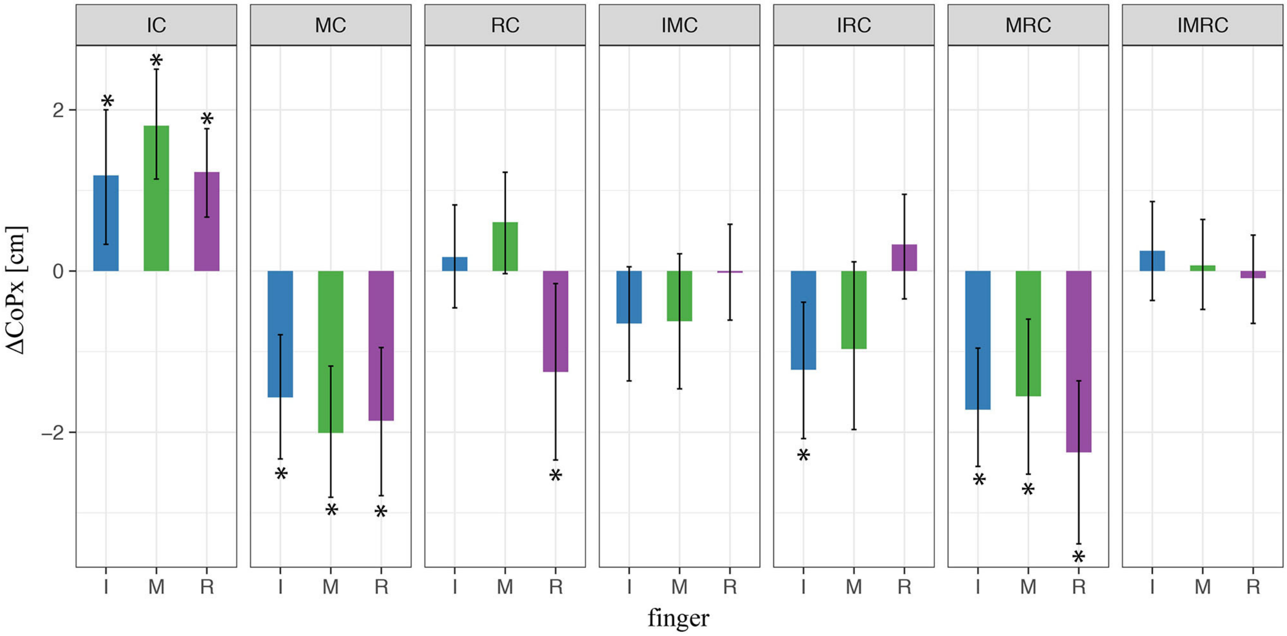

FIGURE 10 | LMM results of digit initial horizontal placements (CoPs) in four-digit grasp. * indicate statistical significance determined by LMM analysis.

either three- and four-digit unconstrained grasp. Fingertips were covered with a rubber thimble depending on the experimental conditions. Overall, we recorded digit normal force changed locally when perturbing at least one finger opposing the thumb in three- and four-digit unconstrained grasp. Moreover, there was no systematic effect of glove condition on digit placements and the TACO tilt. Our results confirm and extend previous studies on local digit friction perturbation in two-, three-, and five-digit constrained grasp.

Overall Grip Force Adjustment

Grip force was larger when fingers were covered with the rubber thimble compared with the baseline condition. This motor behavior is in accordance with previous studies that perturbed tactile input by changing the surface texture (Johansson and Westling, 1984; Burstedt et al., 1999; Aoki et al., 2007) or by asking participants to wear a glove (Kinoshita, 1999). Specifically, it has been shown that grip force increased with decrease of object friction between digit and object in order to maintain stability

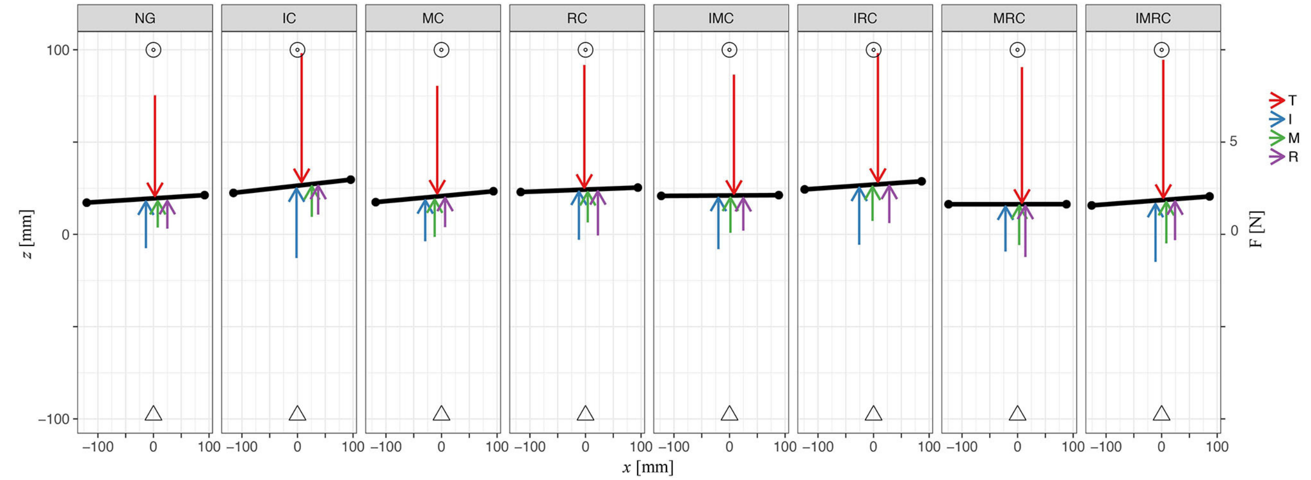

FIGURE 11 | Plot illustrates average values across participants of digit normal forces, horizontal initial placements on the TACO, and the TACO yaw angle four digits within all glove conditions in four-digit grasp. Triangle represents the TACO start location, and circles represent the TACO target location.

of an object (Johansson and Westling, 1984). The latter results were also confirmed by a study of Cadoret and Smith (1996) which showed that participants relied on the friction between digit and the grasped object to optimally modulate the grip force. The normal forces of the thumb and the opposing finger varied in a synergistic manner to increase the safety margin during the transport phase of the grasped object.

Instead, a reduction in the grip force was reported when perturbing tactile input using local anesthesia (Carteron et al., 2016). Specifically, Carteron et al. (2016) recorded a significant drop in the grip force when applying anesthesia at least in one of the digits involved in the grasp. Covering the fingers with the glove did not completely abolish cutaneous information at fingertips which is mainly responsible for generating an adequate safety margin at the individual fingers (Augurelle et al., 2003). However, this dual effect of covering the skin would not change the interpretation of the main finding, that is, the system responds to this perturbation at the level of individual digit.

Digit Normal Force Control and Synergies

At the individual digit, when covering at least one finger only, the digit normal force changed in both covered and noncovered finger(s), but it reached significance level only for the covered finger(s). The latter result indicates that digit normal force changed locally at the fingers opposing the thumb. Similar observation was found in two-digit (Edin et al., 1992) and three-digit constrained grasp (Burstedt et al., 1999). To achieve a stable grasp in our experimental paradigm, thumb normal force should be equal to the sum of normal forces of the opposing fingers (see section "Methods"). Due to this mechanical constraint, the covered opposing finger(s) regulated locally the normal force that consequently altered the thumb. This latter was confirmed by looking at the TACO yaw and roll rotation angles that did not significantly varied with the force sharing that changed across conditions. Therefore, our results suggest that digit normal forces were adjusted locally for the covered and noncovered fingers whereas force increase at the covered finger altered the thumb normal force (opposing finger) as consequence of the task mechanical constraints. This latter result was also observed and reported in Carteron et al. (2016) where they used local anesthesia to disable cutaneous information that decrease the overall grip force. This latter work reported no synergistic motor behavior between fingers at the level of normal forces opposing the thumb which somehow underscore our obtained results to some extent. However, Aoki et al. (2007) examined the role of tactile input on the grip force modulation during five-digit constrained grasp and observed that varying friction condition between digits and the grasped object elicit force adjustment at both the stimulated and unstimulated digits.

The force sharing distribution among digits is also unconstrained due to the redundancy in degrees of freedom in terms of digit locations and forces (Friedman and Flash, 2007; Naceri et al., 2014, 2017). Indeed, distribution of digit normal forces was quite different between participants and they could still achieve a stable grasp. Considering this variability between participants, the local effect of the glove at the stimulated finger(s) persisted in all conditions. Previous studies on precision grip control showed that the magnitude of digit normal forces was regulated locally, within the perturbed digits, in two- and three-digit constrained grasp (Edin et al., 1992; Burstedt et al., 1999). The latter studies suggested that digit normal forces changes in parallel at all digits engaged in the grasping and manipulation tasks. It has been suggested that fast afferent fibers at fingertips (FA I) plays a role in triggering the controller of digit normal force due changes in the friction conditions between fingertip and the object signals in tactile afferents from fingers (Johansson and Westling, 1987). The local changes at frictional condition at fingertips play a role at triggering the digit force controller individually, which consequently scaled the overall grip force. Moreover, this overall change at the grip force due to the local frictional changes at each digit indicates that participants integrated the frictional condition at the covered fingers used in the grasping task. Especially, it has been shown that participants use frictional information from previous trials to scale the force output in anticipatory fashion to the frictional conditions at fingertips (Edin et al., 1992; Cole and Johansson, 1993; Johansson and Flanagan, 2009).

The friction of dry skin is characterized by relatively low and pressure-independent friction coefficients similar to the case of dry friction of rough solids whereas moist or wet skin shows high friction coefficients that strongly increase with decreasing contact pressure and are determined by the shear properties of wet skin (Derler and Gerhardt, 2012). The frictional behavior at the single digit tends to be extremely complex, and it might require complex models to understand such a behavior (Adams et al., 2013). This complexity is mainly due to several factors such as the unusual contact mechanics associated with fingerprint ridges and the relatively large number of sweat glands under these ridges (Adams et al., 2013). In the dry state, a finger pad has a coefficient of friction that is comparable with glassy polymers. However, sustained sliding on a smooth impermeable countersurface triggers the process of the secretion of moisture from the sweat glands causing the coefficient of friction to increase by about an order of magnitude to values comparable with elastomers, which can also exhibit contact areas close to the nominal values due to the deformability of the surface asperities. Covering the fingers with a rubber thimble might have triggered the process of the secretion of moisture from the sweat glands leading to the increase of skin friction of the covered finger which consequently caused the local adaptation of the normal force to friction change between fingertips and the grasped object.

Previous studies on prehension synergies reported the exitance of trade-offs between synergies at the two assumed hierarchical levels: thumb-opposing fingers and between opposing fingers (Gorniak et al., 2007, 2009; Sun et al., 2011; Wu et al., 2012). These studies evaluated the motor synergy at those levels using method of computation of synergy index. For instance, high variance of both thumb and opposing finger forces for the same performance variables leads to an increase of synergy index, whereas the same force variance at the individual fingers leads to a decrease of synergy index. Previous studies made by Gorniak et al. (2009) and Wu et al. (2012) did not observe any motor synergy when evaluating the synergy index. In our study, no clear motor synergy coordination was recorded between fingers (opposing the thumb) when covering at least one finger with a rubber thimble. The latter might be explained by a decrease of synergy index at the individual finger level as found in previous studies.

Variability in Digit Placements

Participants tend to largely variate their digit placements when allowing them to freely choose the placement of their digits (Friedman and Flash, 2007; Fu et al., 2010; Naceri et al., 2017). Moreover, trial-to-trial variability in digit horizontal locations alters the modulation of the grip force (Naceri et al., 2014) and load force (Burstedt et al., 1999; Fu et al., 2010). In our experimental task, participants could freely choose their digit placements on the object leading to infinite combinations of digit position forces in order to achieve a stable grasp. Based on these observations, we included the normalized digit horizontal placements to thumb in our fitting model of digit normal forces in order to reduce CoPs' noise effect.

In this experiment, digit horizontal initial placements significantly varied and altered the digit normal forces. These changes in initial digit horizontal locations reflect trial-to-trial variability and also condition-to-condition variability and not within trial variability since participants did not regrasp the TACO during the holding phase. In other words, participants did not control systematically digit positions in order to adjust the grip force, despite the effect of digit positions on the grip force. This latter effect was explained by idiosyncratic grasping strategies (Naceri et al., 2017). In spite of the variability in digit horizontal placements, digit normal forces was significantly regulated at the covered finger(s).

The TACO's rotation angles (roll and yaw) and digit initial placements were not affected by the glove, as shown in the result section. This latter agrees with what is found in Burstedt et al. (1999), where also the manipulandum tilt and digit locations were not affected by the changing friction between fingertips and the grasped object. In contrast, local anesthesia at the individual digit altered the object tilt (Carteron et al., 2016). Indeed, using gloves or a surface texture for instance to change local friction condition at fingertip contacts does not induce motor deficit as does local anesthesia. Importantly, the recorded normal force was affected by either above methods used to perturb the tactile input at fingertips.

CONCLUSION

In summary, our results suggest that perturbing tactile gloves increased the overall grip force in order to provide and ensure a stable grasp, despite that the produced force is higher than the one required for the task. Digit normal forces were adjusted locally between fingers opposing the thumb when covered using the glove. The force increase adjustment at the covered finger(s) altered the thumb normal force since this latter digit mechanically contributes 50% to the overall grip force. There were no systematic effects across participants by glove conditions on the digit initial placements and TACO rotation angles. This latter effect is due to the fact these variables could vary between participants as well as between trials within participants.

DATA AVAILABILITY STATEMENT

The raw data supporting the conclusions of this article will be made available by the authors, without undue reservation, to any qualified researcher.

ETHICS STATEMENT

The studies involving human participants were reviewed and approved by Ethics committee of Bielefeld University. The patients/participants provided their written informed consent to participate in this study.

AUTHOR CONTRIBUTIONS

AN and ME conceived and designed the study and coordinated the scientific and technical aspects of this work. YG conducted the experiments and data processing. AN and YG analyzed, processed data, and prepared the figures. AN, YG, AM, and ME wrote the manuscript. AN, AM and ME supervised the study. All authors contributed to the article and approved the submitted version.

FUNDING

This work was partially supported by the Italian Ministry of Health (Ricerca Corrente, IRCCS Fondazione Santa Lucia) and by the European Commission under IP grant no. 248587 THE Hand Embodied, by the European Commission under IP grant no. 601165 WEARable HAPtics, and by the DFG Center of Excellence EXC 277: Cognitive Interaction Technology (CITEC).

ACKNOWLEDGMENTS

We thank Prof. Helge Ritter and Prof. Edin Benoni for their useful comments and discussion on the current work.

REFERENCES

Adams, M. J., Johnson, S. A., Lefèvre, P., Lévesque, V., Hayward, V., André, T., et al. (2013). Finger pad friction and its role in grip and touch. *J. R. Soc. Interface* 10:20120467. doi: 10.1098/rsif.2012.0467

Aoki, T., Latash, M. L., and Zatsiorsky, V. M. (2007). Adjustments to local friction in multifinger prehension. *J. Motor Behav.* 39, 276–290. doi: 10.3200/JMBR.39.4.276-290

Augurelle, A.-S., Smith, A. M., Lejeune, T., and Thonnard, J.-L. (2003). Importance of cutaneous feedback in maintaining a secure grip during manipulation of hand-held objects. *J. Neurophysiol.* 89, 665–671. doi: 10.1152/jn.00249.2002

Bates, D., Mächler, M., Bolker, B., and Walker, S. (2015). Fitting linear mixed-effects models using lme4. *J. Stat. Softw.* 67, 1–48. doi: 10.18637/jss.v067.i01

Bernshtein, N. A. (1967). *The Co-ordination and Regulation of Movements*. Oxford: Pergamon.

Bolker, B. M., Brooks, M. E., Clark, C. J., Geange, S. W., Poulsen, J. R., Stevens, M. H. H., et al. (2009). Generalized linear mixed models: a practical guide for ecology and evolution. *Trends Ecol. Evol.* 24, 127–135. doi: 10.1016/j.tree.2008.10.008

Burstedt, M. K., Flanagan, J. R., and Johansson, R. S. (1999). Control of grasp stability in humans under different frictional conditions during multidigit manipulation. *J. Neurophysiol.* 82, 2393–2405. doi: 10.1152/jn.1999.82.5.2393

Cadoret, G., and Smith, A. M. (1996). Friction, not texture, dictates grip forces used during object manipulation. *J. Neurophysiol.* 75, 1963–1969. doi: 10.1152/jn.1996.75.5.1963

Carteron, A., McPartlan, K., Gioeli, C., Reid, E., Turturro, M., Hahn, B., et al. (2016). Temporary nerve block at selected digits revealed hand motor deficits in grasping tasks. *Front. Hum. Neurosci.* 10:596. doi: 10.3389/fnhum.2016.00596

Cole, K. J., and Johansson, R. S. (1993). Friction at the digit-object interface scales the sensorimotor transformation for grip responses to pulling loads. *Exp. Brain Res.* 95, 523–532. doi: 10.1007/BF00227146

Derler, S., and Gerhardt, L.-C. (2012). Tribology of skin: review and analysis of experimental results for the friction coefficient of human skin. *Tribol. Lett.* 45, 1–27. doi: 10.1007/s11249-011-9854-y

Edin, B. B., Westling, G., and Johansson, R. S. (1992). Independent control of human fingertip forces at individual digits during precision lifting. *J. Physiol.* 450, 547–564. doi: 10.1113/jphysiol.1992.sp019142

Friedman, J., and Flash, T. (2007). Task-dependent selection of grasp kinematics and stiffness in human object manipulation. *Cortex* 43, 444–460. doi: 10.1016/S0010-9452(08)70469-6

Fu, Q., Zhang, W., and Santello, M. (2010). Anticipatory planning and control of grasp positions and forces for dexterous two-digit manipulation. *J. Neurosci.* 30, 9117–9126. doi: 10.1523/JNEUROSCI.4159-09.2010

Gorniak, S. L., Zatsiorsky, V. M., and Latash, M. L. (2007). Hierarchies of synergies: an example of two-hand, multi-finger tasks. *Exp. Brain Res.* 179, 167–180. doi: 10.1007/s00221-006-0777-z

Gorniak, S. L., Zatsiorsky, V. M., and Latash, M. L. (2009). Hierarchical control of static prehension: I. Biomechanics. *Exp. Brain Res.* 193, 615–631. doi: 10.1007/s00221-008-1662-8

Johansson, R. S., and Flanagan, J. R. (2008). "Tactile sensory control of object manipulation in humans," in: eds. E. Gardner and J.H. Kass, The Senses: A Comprehensive Reference, Vol. 6 (Amsterdam: Elsevier), 67–86.

Johansson, R. S., and Flanagan, J. R. (2009). Coding and use of tactile signals from the fingertips in object manipulation tasks. *Nat. Rev. Neurosci.* 10, 345–359. doi: 10.1038/nrn2621

Johansson, R. S., and Westling, G. (1984). Roles of glabrous skin receptors and sensorimotor memory in automatic control of precision grip when lifting rougher or more slippery objects. *Exp. Brain Res.* 56, 550–564. doi: 10.1007/BF00237997

Johansson, R. S., and Westling, G. (1987). Signals in tactile afferents from the fingers eliciting adaptive motor responses during precision grip. *Exp. Brain Res.* 66, 141–54. doi: 10.1007/BF00236210

Kinoshita, H. (1999). Effect of gloves on prehensile forces during lifting and holding tasks. *Ergonomics* 42, 1372–1385. doi: 10.1080/001401399185018

McIsaac, T. L., Santello, M., Johnston, J. a, Zhang, W., and Gordon, A. M. (2009). Task-specific modulation of multi-digit forces to object texture. *Exp. Brain Res.* 194, 79–90. doi: 10.1007/s00221-008-1671-7

Moscatelli, A., Mezzetti, M., and Lacquaniti, F. (2012). Modeling psychophysical data at the population-level: the generalized linear mixed model. *J. Vis.* 12, 1–17. doi: 10.1167/12.11.26

Naceri, A., Moscatelli, A., Haschke, R., Ritter, H., Santello, M., and Ernst, M. O. (2017). Multi-digit force control during unconstrained grasping in response to object perturbations. *J. Neurophysiol.* 117:2025–2036. doi: 10.1152/jn.00546.2016

Naceri, A., Moscatelli, A., Santello, M., and Ernst, M. O. (2014). "Coordination of multi-digit positions and forces during unconstrained grasping in response to object perturbations," in: *2014 IEEE Haptics Symposium (HAPTICS)* (Houston, TX: IEEE), 35–40.

Pinheiro, J., and Bates, D. (2000). *Mixed-Effects Models in S and S-PLUS*. New York, NY: Springer.

Santello, M., Baud-Bovy, G., and Jörntell, H. (2013). Neural bases of hand synergies. *Front. Comput. Neurosci.* 7:23. doi: 10.3389/fncom.2013.00023

Schürmann, C., Koiva, R., Haschke, R., and Ritter, H. (2011). "A modular high-speed tactile sensor for human manipulation research," in *World Haptics Conference (WHC)* (Istanbul: IEEE), 339–344. doi: 10.1109/WHC.2011.5945509

Schürmann, C., Koiva, R., Haschke, R., and Ritter, H. (2012). "Analysis of human grasping under task anticipation using a tactile book," in *IEEE-RAS International Conference on Humanoid Robots* (Osaka: IEEE), 773–778. doi: 10.1109/HUMANOIDS.2012.6651607

Sun, Y., Park, J., Zatsiorsky, V. M., and Latash, M. L. (2011). Prehension synergies during smooth changes of the external torque. *Exp. Brain Res.* 213:493. doi: 10.1007/s00221-011-2799-4

Westling, G., and Johansson, R. S. (1984). Factors influencing the force control during precision grip. *Exp. Brain Res.* 53, 277–284. doi: 10.1007/BF00238156

Wu, Y.-H., Zatsiorsky, V. M., and Latash, M. L. (2012). Static prehension of a horizontally oriented object in three dimensions. *Exp. Brain Res.* 216, 249–261. doi: 10.1007/s00221-011-2923-5

Conflict of Interest: The authors declare that the research was conducted in the absence of any commercial or financial relationships that could be construed as a potential conflict of interest.

frontiers in Psychology

ORIGINAL RESEARCH
published: 22 March 2021
doi: 10.3389/fpsyg.2021.638780

Motor Imagery Training of Reaching-to-Grasp Movement Supplemented by a Virtual Environment in an Individual With Congenital Bilateral Transverse Upper-Limb Deficiency

Joanna Mencel[1]*, *Anna Jaskólska*[1], *Jarosław Marusiak*[1], *Łukasz Kamiński*[1], *Marek Kurzyński*[2], *Andrzej Wołczowski*[3], *Artur Jaskólski*[1] and *Katarzyna Kisiel-Sajewicz*[1]

[1] Department of Kinesiology, Faculty of Physiotherapy, University School of Physical Education in Wrocław, Wrocław, Poland, [2] Department of Systems and Computer Networks, Faculty of Electronics, Wrocław University of Science and Technology, Wrocław, Poland, [3] Department of Fundamental Cybernetics and Robotics, Institute of Computer Engineering, Control and Robotics, Wrocław University of Science and Technology, Wrocław, Poland

Edited by:
Luigi F. Cuturi,
Italian Institute of Technology (IIT), Italy

Reviewed by:
John E. Downey,
University of Chicago, United States
Pavel Bobrov,
Institute of Higher Nervous Activity
and Neurophysiology (RAS), Russia

***Correspondence:**
Joanna Mencel
joanna.mencel@awf.wroc.pl

Specialty section:
This article was submitted to
Movement Science and Sport
Psychology,
a section of the journal
Frontiers in Psychology

Received: 07 December 2020
Accepted: 03 March 2021
Published: 22 March 2021

Citation:
Mencel J, Jaskólska A, Marusiak J, Kamiński Ł, Kurzyński M, Wołczowski A, Jaskólski A and Kisiel-Sajewicz K (2021) Motor Imagery Training of Reaching-to-Grasp Movement Supplemented by a Virtual Environment in an Individual With Congenital Bilateral Transverse Upper-Limb Deficiency. Front. Psychol. 12:638780. doi: 10.3389/fpsyg.2021.638780

This study explored the effect of kinesthetic motor imagery training on reaching-to-grasp movement supplemented by a virtual environment in a patient with congenital bilateral transverse upper-limb deficiency. Based on a theoretical assumption, it is possible to conduct such training in this patient. The aim of this study was to evaluate whether cortical activity related to motor imagery of reaching and motor imagery of grasping of the right upper limb was changed by computer-aided imagery training (CAIT) in a patient who was born without upper limbs compared to a healthy control subject, as characterized by multi-channel electroencephalography (EEG) signals recorded before and 4, 8, and 12 weeks after CAIT. The main task during CAIT was to kinesthetically imagine the execution of reaching-to-grasp movements without any muscle activation, supplemented by computer visualization of movements provided by a special headset. Our experiment showed that CAIT can be conducted in the patient with higher vividness of imagery for reaching than grasping tasks. Our results confirm that CAIT can change brain activation patterns in areas related to motor planning and the execution of reaching and grasping movements, and that the effect was more pronounced in the patient than in the healthy control subject. The results show that CAIT has a different effect on the cortical activity related to the motor imagery of a reaching task than on the cortical activity related to the motor imagery of a grasping task. The change observed in the activation patterns could indicate CAIT-induced neuroplasticity, which could potentially be useful in rehabilitation or brain-computer interface purposes for such patients, especially before and after transplantation. This study was part of a registered experiment (ID: NCT04048083).

Keywords: mental training, reaching, grasping, EEG, amelia, neuroplasticity, transplantation

INTRODUCTION

Motor imagery is defined as the conscious, mental simulation of an action without any body movement (Jeannerod, 1994; Jeannerod and Decety, 1995). Imaging studies have shown that the motor imagery of movement and an execution of movements share overlapping brain areas including the primary motor cortex, supplementary motor area, superior and inferior parietal lobules, dorsal and ventral premotor cortices, prefrontal cortex, inferior frontal gyrus, superior temporal gyrus, sensory cortex, anterior cingulate gyrus, basal ganglia, and cerebellum (Decety et al., 1994; Jeannerod and Decety, 1995; Stephan et al., 1995; Fadiga et al., 1999; Gerardin et al., 2000; Hanakawa et al., 2003; Solodkin et al., 2004; Avanzino et al., 2015). There are two main types of motor imagery: kinesthetic, which can be defined as mentally feeling oneself moving one's own body parts, and visual, which can be described as mentally seeing another person moving his/her body parts. Most authors agree that the kinesthetic approach to imagery is more effective and produces higher levels of physiological responses (Ranganathan et al., 2004; Harris and Hebert, 2015). Motor imagery plays an important role in motor skill learning (Mokienko et al., 2013; Cabral-Sequeira et al., 2016; Sobierajewicz et al., 2016) and rehabilitation (Mulder, 2007; Ietswaart et al., 2011; Harris and Hebert, 2015). It is also used in the brain-computer interface field (Ortner et al., 2012; Mokienko et al., 2013; Teo and Chew, 2014).

The effectiveness of motor imagery is related to training-induced neuroplasticity, as the brain has the capacity to adapt to both internal and external stimuli (Merzenich et al., 2014; Marins et al., 2019). Mental training, as well as physical training, is a stimulus that can induce activity-dependent neuroplasticity (Di Rienzo et al., 2014; Ballesteros et al., 2018). On one hand, motor imagery is known to be a useful approach for rehabilitation in patients with altered body image such as those with spinal cord injuries (Saadah and Melzack, 1994) or those with peripheral lesions, including amputees (Ersland et al., 1996; Lotze et al., 2001). The efficacy of motor imagery in reducing phantom limb pain has also been assessed (Harris and Hebert, 2015). On the other hand, there have been cases of people with congenital limb deficiencies and altered body image (Melzack et al., 1997; Gallagher et al., 1998; Brugger et al., 2000), whose phantom sensations of nonexistent body parts have been reported by many authors (Melzack et al., 1997; Brugger et al., 2000), whereas this phenomenon was disproved by the study of others (Montoya et al., 1997; Flor et al., 1998; Reilly and Sirigu, 2011). Montoya et al. (1997) showed that the homuncular organization of the somatosensory cortex in subjects with congenital limb atrophy is similar to that in healthy subjects. There were also no significant differences between the locations of the cortical maps and the distances between the hand digits, lower lip, and toes in such patients compared to healthy controls. Flor et al. (1998) confirmed no reorganization of the lower lip map in the primary somatosensory cortex of subjects with congenital limb deficiency and further suggested the presence of a silent representation of the missing limb in such patients. Additionally, it has been shown that the neural representation of tools and hands appears to be virtually the same in individuals born without hands as in healthy people (Striem-Amit et al., 2017), as well as the spatial arrangement and functional properties of brain areas specialized in the processing of observed actions for the hand (Vannuscorps et al., 2018).

Excluding our previous publication (Kurzynski et al., 2017), we did not find any other literature regarding the use of motor imagery training in patients born without upper limbs, nor any information about the use of any kind of training in these patients. Motor imagery recruits high-level brain processes involved in motor behavior and could be one of the few that can be used in these patients. If training results in training-dependent neuroplasticity, it may be possible to transplant the limbs in these patients in the future. Currently, it seems impossible, but it is not the first time that motor imagery training is used in such unusual situations (Guillot and Debarnot, 2019), and many authors agree that it should be conducted in situations, where traditional therapeutic techniques cannot be implemented. Therefore, we evaluated whether kinesthetic motor imagery training of upper-limb movement (specifically, a functional reaching-to-grasp movement) could promote neuroplasticity in the sensorimotor cortex in a congenitally amputated patient, which could be especially important in the context of transplant surgery. We employed a virtual environment in which movements that were imagined during training were visualized to support the training effect after the importance of the role of visual feedback was proven (Ramachandran and Altschuler, 2009). In this paper, we describe cortical activity associated with the motor imagery of reaching (MIR) and the motor imagery of grasping (MIG) by a patient with a congenital bilateral transverse upper-limb deficiency compared with that of a healthy control subject, as characterized by electroencephalography (EEG) signals recorded before computer-aided imagery training (CAIT) and after 4, 8, and 12 weeks of training. In addition to the neurophysiological method of CAIT evaluation (EEG), we decided to apply a subjective assessment of the imageries' vividness using a 10-cm visual analog scale (VAS) after Guillot and Collet (2005) reported that questionnaires and self-report ratings are reliable psychometric methods for evaluating the quality of motor imagery in healthy subjects. This has never been researched in patients born without upper limbs; however, in healthy people, the spatial patterns of neural activity within the motor cortices assessed by fMRI reflect the individual vividness of imaged tasks (Zabicki et al., 2019).

The aims of this study were (i) to evaluate whether cortical activity related to MIR and MIG of the right upper limb was changed by CAIT in a patient with congenital bilateral transverse upper-limb deficiency and a healthy control subject and (ii) to compare the effects of CAIT on the motor imagery of two different mental tasks: reaching and grasping.

We focused on an analysis of event-related potentials (ERP amplitude, the amplitude of negative potential) after their sensitivity to mental and physical practice was proven (Ranganathan et al., 2004; Allami et al., 2014) and (ii) sources of ERP localization.

MATERIALS AND METHODS

Subjects

The test participant (hereinafter, the patient) was a woman with congenital bilateral transverse upper-limb deficiency who lacked upper limbs at the glenohumeral joint level. The control participant (hereinafter, the control) was a woman with an average body build and no history of neurological, muscular, or skeletal disorders. Both subjects were between 27 and 30 years of age.

The participants were informed about the nature of the experiment, and they provided written consent to participate. The study was approved by the Ethical Committee of the University School of Physical Education in Wroclaw and was conducted in accordance with the Declaration of Helsinki.

Experimental Procedures

The participants received 12 weeks of motor imagery training supplemented by a virtual environment (CAIT). The 12-week training duration was chosen to provoke long-term changes in the nervous system, as suggested by Schuster et al. (2011). Before the training (PRE) and after 4, 8, and 12 weeks of CAIT (POST4, POST8, and POST12, respectively), the subjects participated in the measurement sessions (**Figure 1**).

Computer-Aided Imagery Training

The CAIT involved mental training in reaching-to-grasp movements supplemented by the computer visualization of movements provided by a special headset (Sony HMZ-T1 model). The visualization software was coded specifically for this experiment (for details, see Kurzynski et al., 2017). The main task during the CAIT was to kinesthetically imagine the execution of reaching-to-grasp movements without any overt movement or muscle activation (Mizuguchi et al., 2011). We chose the kinesthetic approach for motor imagery training to achieve a physiological response (Ranganathan et al., 2004), and thus potentially provoke neuroplasticity. A virtual reality environment was used for two main reasons: first, to facilitate the motor imagery and make it easier for the patient and, second, to serve as a form of virtual afferent information to create the illusion of possessing a real upper limb. This kind of stimulation could arouse sensations incompatible with a sensory body plan (Guterstam et al., 2011).

During each training session, small vibrating devices were attached to the skin above the trapezius muscle of both subjects and to the first dorsal interosseous muscle of the control to obtain additional sensory information and to elucidate movements. The first vibration was delivered when the subject approached the object to be grasped (a book) with the virtual limb to emphasize the end of the reaching phase, and the second vibration was delivered at the beginning of the grasping phase. The vibration frequency and force were adjusted to the individual subjects' sensations and remained at the lowest detectable level.

Training Procedure (CAIT)

During each training session, the subjects were seated in a comfortable chair. The vibrating devices were attached to the skin above the chosen muscles by the same experienced physiotherapist. The patient with only the lower limbs, as well as the healthy control, both touched a real book (always the same book, similar to that presented in the computer animation) to feel the weight of the book, its size, and its surface. The subjects also observed during the CAIT that the location of the book was always the same at approximately 0.14 m away.

While sitting in the experimental chair and wearing a headset, the subject was instructed to relax the body and mind (i.e., to not think about anything in particular). Instruction was then given to perform the mental reaching and precise grasping of the book using the thumb and four fingers with computer animation.

Instructions were given to the subjects at the beginning of each training session, and the subjects performed three practice trials according to the instructions. Instruction was then discontinued, and the subjects performed 30 trials of mental movements, wherein the signal for the start of a trial was equal to the start of the computer animation. Each training session consisted of 30 trials of the task of reaching to grasp (three sets, 10 trials in each set) for the left and right upper limbs separately. There was a 20-s rest between trials, a 3-min rest between sets, and a 15-min rest between sides (right and left upper limb). Each training session took 52 min. A total of 36 training sessions were conducted over 12 weeks (three times a week for 12 weeks).

Measurement Sessions

All measurements were performed during four sessions, denoted herein as PRE (before CAIT), POST4 (after 4 weeks of CAIT), POST8 (after 8 weeks of CAIT), and POST12 (after 12 weeks of CAIT). Each session consisted of a short introductory period to familiarize the subjects with the tasks to be performed, followed

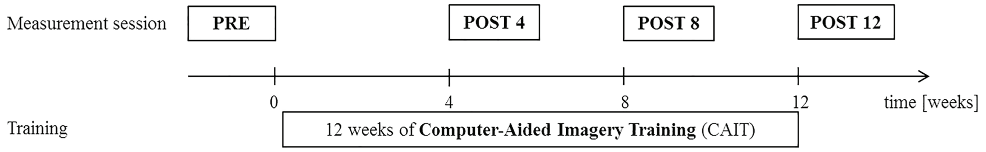

FIGURE 1 | Scheme of the experimental protocol consisting of four measurement sessions (PRE, POST4, POST8, and POST12) and 12 weeks of computer-aided imagery training (CAIT).

by two motor imagery (MI) tasks: MIR of the right upper limb and MIG of the right hand, with a short break between the two tasks. The subjects were seated comfortably with their eyes open, and their role was to imagine kinesthetically reaching with the right upper limb for a book (the first task) and then to imagine kinesthetically grasping the book (the second task). Each task was repeated 20 times to achieve a sufficient number of trials for further analysis while avoiding fatigue. The protocol for the MI tasks was the same for both tasks. A single tone was the signal to start the imagery, and a double tone was the signal to stop and relax. The subjects did not receive any additional stimuli (visual or tactile stimuli) during the recordings. The time between the single and double tones (i.e., the time for one imagery trial) was 8 s, and the rest time between trials was 10 s. During one trial of the MIR task, the subject was asked to imagine the reaching task upon hearing the single tone and mentally reaching the goal (the book, with its location similar to that used during CAIT) and then to stop the MIR task and wait for another single tone (or an earlier double tone to relax and then another single tone to repeat the MIR task). Each trial of the MIG task lasted exactly 8 s, during which the subject was asked to imagine grasping the book with a force sufficient to lift it upon hearing a single tone and to stop upon hearing a double tone.

During each session (before and after 4, 8, and 12 weeks of training), immediately after EEG data recording, the vividness of the imagination (the ability to create images characterized by a high level of complexity and detail) of the reaching and grasping tasks was evaluated. We used a VAS ranging from 0 = very hard to feel to 10 = very easy to feel.

EEG Data Recording

EEG data were recorded continuously using Ag/AgCl electrodes from 128 scalp electrodes relative to a vertex reference, using the BioSemi Active-two system (Biosemi Inc., Amsterdam, the Netherlands). The electrodes were placed according to the BioSemi-designed Equiradial system and partially overlapped with an extended International 10–20 system (Oostenveld and Praamstra, 2001) using a nylon electrode cap. The EEG signals were amplified with a bandpass of 0–128 Hz and sampled at 2048 Hz. The impedance between each electrode and the skin was displayed on a computer monitor to inspect the quality of the connection. If a particular electrode showed high impedance, an adjustment was made, such as applying pressure or adding more conducting gel (Electro-gel™, Electro-Cap International Inc., Eaton, OH) to improve the connection. The EEG data recording did not begin until the impedance for all electrodes was below 5 kΩ.

The subjects were instructed to maintain a stable body position and to avoid eye blinking, teeth biting, and head movements during the trials. Minimal eye blinking and body adjustments were allowed during rest periods between trials and tasks. All possible aural and visual sources of distraction were minimized.

EEG Data Processing and Analysis

The EEG signal data were analyzed using the Brain Electrical Source Analysis 6.1 software (BESA, MEGIS Software GmbH, Gräfelfing, Germany). During offline processing, the EEG signal was downsampled to 512 Hz (Decimator, Biosemi Inc.), visually inspected, and filtered using high (50 Hz) and low (0.53 Hz) filters as well as a notch filter at 50 Hz. Although the subjects were instructed not to perform blinking, biting, or head movements, these activities occasionally occurred, and recordings that included these activities were excluded from further analysis. We calculated the intraclass correlation coefficient (ICC) to determine the intra-rater reliability for the patient and the control for both conditions (two tasks: MIR and MIG), and for four measurement time points (PRE, POST4, POST8, and POST12). We noted poor (less than 0.4; according to Cicchetti, 1994) ICC for the patient and the MIG task, fair ICC for the patient and the MIR task, and excellent ICC for the control (for both tasks). To obtain the ERP, the EEG signals associated with the MIR and MIG tasks for each subject were trigger-averaged using a single tone as the trigger. A 2-s-long time window was chosen for this purpose (where 0 was the time of the single tone and indicated that the subject should start the MI task), with an interval of −100 to 0 ms used for baseline correction. Artifact-free, averaged-referenced trial data were used for further analysis, specifically 16, 14, 15, and 12 trials for the reaching task and 17, 15, 15, and 12 trials over four sessions for the grasping task for the patient (from PRE to POST12); and 19, 20, 15, and 17 trials for the reaching task and 20, 19, 19, and 17 trials over four sessions for the grasping task for the control (from PRE to POST12). Two parameters were calculated to quantify CAIT-induced cortical signal alterations: ERP amplitude and ERP sources.

The ERP amplitudes [the value of the negative potential's peak, NP (μV)] were obtained from the following regions related to planning and execution of movements using four electrodes within each region: the contralateral-to-the-task (above the left hemisphere), prefrontal cortex (area of F3), contralateral sensorimotor cortex (area of C3), ipsilateral-to-the-task (above the right hemisphere) prefrontal cortex (area of F4), and the ipsilateral sensorimotor cortex (area of C4). The data are presented as mean values with standard deviations, as well as topographic maps of scalp potentials.

Subsequent analysis consisted of reconstruction of the regional sources' locations of the ERP based on the 2-s-long averaged file but limited to the time of the ERP. BESA's discrete multiple source analysis method (Scherg and Berg, 1996) was used separately for this purpose for each subject, task, and session. Details on selected features of this method that have the power to transform the EEG signal from the scalp back into the brain structures were described by Scherg et al. (2019). The number of sources was determined based on a principal component analysis (PCA) conducted using the BESA software of the data corresponding to the time when the residual value (unexplained by the dipole data) was less than 10% (Hoshiyama et al., 1997). According to Scherg (1992), PCA provides an *a priori* objective estimate of the lowest number of possible sources, which, together with the assumption of RV < 10%, allowed us to quantitatively analyze the number of sources between the subjects, sessions, and tasks. The source locations were estimated using a four-shell ellipsoidal head model. The location of each source was determined in the Talairach standard brain space (x, y, and z coordinates) and transformed to a Brodmann area (BA) in Talairach Daemon (Talairach Client 2.4.2), as presented in Tables.

RESULTS

Vividness of Motor Imagery of Reaching for the Patient and Control

The vividness of the MIR for the patient was high (8.7, 8.4, 9.3, and 7.8) during the four measurement sessions from PRE to POST12. The vividness of the MIR for the control was high during the PRE, POST4, and POST12 sessions, but lower during the POST8 measurement session (9.4, 7, 5.5, and 9.2 for PRE, POST4, POST8, and POST12, respectively).

ERP Analysis Related to Motor Imagery of Reaching for Patient

The results showed that in the contralateral prefrontal cortex and sensorimotor cortexes of both hemispheres, the ERP amplitude related to the MIR decreased with CAIT and increased only in the ipsilateral prefrontal cortex as a result of CAIT for the patient (**Figure 2**). The ERP amplitudes had relatively similar values in each of the four regions during the POST4 and POST8 sessions. Higher values above the prefrontal cortices of both hemispheres and lower values above the sensorimotor cortices above the right and left hemispheres were observed after completion of the training period (POST12; **Figure 2**).

ERP Analysis Related to Motor Imagery of Reaching for Control

The mean values of the ERP amplitude in the contralateral- and ipsilateral-to-the-task sensorimotor cortexes were similar for all the measurement sessions for the control, i.e., they did not change noticeably over the training period (**Figure 2**). Unstable trends in the mean value of ERP amplitudes were observed in the prefrontal cortices of both hemispheres, with similarly high values observed during the PRE and POST8 sessions, but with low values observed during the POST4 session and after completion of the training period (POST12).

Location of Regional ERP Sources Related to Motor Imagery of Reaching

The results (**Table 1**) show that the number of ERP sources related to the MIR the right upper limb for the patient did not change over the course of the training. However, the location did change. The ERP sources for the patient related to the MIR task were located in the frontal lobe, the anterior cingulate cortex of the right hemisphere (BA 32), the middle temporal gyrus of the left hemisphere, and the occipital cortex of the right and left hemispheres (BA 18 and BA 19). After the full training period, the ERP sources were located in the dorsolateral prefrontal cortex of both hemispheres (BA 9, BA 10, and BA 46), the posterior cingulate cortex of the left hemisphere (BA 23), and the premotor cortex (BA 8) of the right hemisphere. The number of ERP sources related to MI reaching the control (**Table 1**) decreased over the course of training from 5 (PRE) to 3 (POST12). After the training period, the sources of the

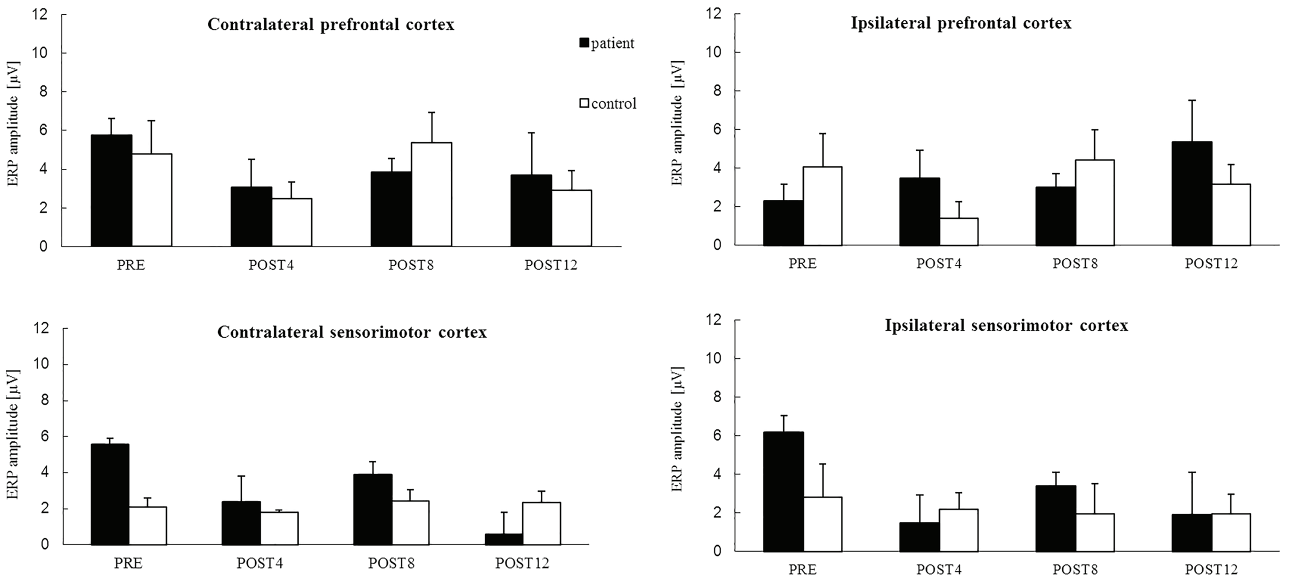

FIGURE 2 | The mean value of ERP amplitude [*−1 (µV)] related to the motor imagery of reaching for the right upper limb from four channels in: the contralateral prefrontal cortex (above the **left** hemisphere) – area of standard "F3" channel, ipsilateral prefrontal cortex (above the **right** hemisphere) – area of standard "F4" channel, and contralateral sensorimotor cortex – area of standard "C3" channel and ipsilateral sensorimotor cortex – area of standard "C4" channel for the patient (black color) and control subject (white color) for sessions before 12 weeks of computer-aided imagery training (PRE) and after intervals of 4 weeks each (POST4, POST8, and POST12).

TABLE 1 | Location (x, y, and z coordinates) of the regional sources of the ERP related to MIR of the patient (on the left side in the table) and control subject (on the right side in the table) expressed in lobe, Brodmann areas (BAs), or other from four measurement sessions (PRE, POST4, POST8, and POST12).

Patient MIR	No.	x	y	z	Lobe/BAs/ other	Control MIR	No.	x	y	z	Lobe/BAs/ other
PRE	1	77.5	−10	−12	Frontal lobe	PRE	1	3	−22	26.6	23
	2	9.3	16.6	44.9	32		2	8.4	−79	−19	18
	3	−23	−98	−21	18		3	66.1	−29	0.5	22
	4	52.6	−90	4.7	19		4	44.7	54.3	33.5	9
	5	−68	−52	−4.2	21		5	−19	−4	50.8	6
POST4	1	24.7	22.9	−6.1	13	POST4	1	−0.2	−11	7	Thalamus
	2	19.1	−43	36.7	31		2	−47	56.2	21.7	10
	3	−47	−92	−20	Posterior lobe		3	52.6	39.9	26.8	46
	4	58.8	−70	−34	Posterior lobe		4	48.4	−49	−7.5	37
	5	−34	13.3	60.4	6		5	−61	23.9	19.1	45
POST8	1	5.7	−40	39.5	31	POST8	1	−47	48	23.6	46
	2	25.8	−61	7.2	30		2	53.5	44.6	−5.7	47
	3	−57	−26	58.1	Parietal lobe		3	3	−64	10.7	30
	4	−67	−67	3	37		4	59.1	40.9	28.8	46
	5	−57	48.6	21.6	46						
	6	73.5	−17	14.9	42						
POST12	1	−1.4	−59	14.4	23	POST12	1	2.6	−19	31	23
	2	7.2	18	50.4	8		2	−56	20	52.2	8
	3	48.3	58.8	21.6	10		3	41.6	66.1	18.3	10
	4	−60	27	40.9	9						
	5	64.9	32.7	24.5	46						

A negative x coordinate value indicates location in the left hemisphere, while a positive x coordinate value indicates location in the right hemisphere.

ERP of the MIR were localized in the premotor cortex of the left hemisphere (BA 8), the dorsolateral prefrontal cortex of the right hemisphere, and the posterior cingulate cortex of the right hemisphere (POST12). Topographic maps of EEG during MIR for the patient and the control are presented in **Figure 3**.

Vividness of Motor Imagery of Grasping for the Patient and Control

The vividness of the MIG for the patient was 4.8, 6.2, 5, and 8 during the four measurement sessions from PRE to POST12. The vividness of the MIG was higher for the control (9.9, 8.2, 8.9, and 9.9) for the PRE, POST4, POST8, and POST12 sessions, respectively.

ERP Analysis Related to Motor Imagery of Grasping for the Patient

The results show that the ERP amplitudes related to the MIG increased with CAIT for both the patient and control in each of the four regions (**Figure 4**) except for the ipsilateral prefrontal cortex for the POST8 measurement session. For the contralateral and ipsilateral prefrontal cortices, the mean values were approximately twice as high after the full CAIT period (POST12) before training. Increases in the ERP amplitudes for the sensorimotor cortexes of the right and left hemispheres were observed after 4 weeks of training (POST4) and remained higher in subsequent measurement sessions (POST8 and POST12) than those before training (PRE). During the POST4 and POST8 sessions, the ERP amplitudes were slightly higher for the sensorimotor cortexes above the right and left hemispheres than for the prefrontal cortices of both hemispheres.

ERP Analysis Related to Motor Imagery of Grasping for Control

The mean values of the ERP amplitudes for the prefrontal and sensorimotor cortexes above the right and left hemispheres did not change after the first 4 weeks of training (from PRE to POST4) for the control (**Figure 4**). Similar values were observed for the prefrontal cortexes above the right and left hemispheres, while similar but slightly lower values were observed for the sensorimotor cortexes above the right and left hemispheres. Changes in the ERP amplitudes were observed after 8 weeks of training and were different for the prefrontal and sensorimotor cortices of both hemispheres. The ERP amplitudes of the prefrontal cortexes of both hemispheres increased greatly after 8 weeks of training (POST8), but decreased to lower values than before the training period after 12 weeks (POST12). The ERP amplitudes of the contralateral sensorimotor cortex remained similar throughout the training period (albeit with an increase noted at POST8) and doubled for the sensorimotor cortex above the right hemisphere by the end of the training period (POST12) in comparison to those in the PRE session.

Location of Regional ERP Sources Related to Motor Imagery of Grasping

The number of ERP sources related to MI for grasping the right hand (**Table 2**) for the patient increased from four (PRE, POST4, and POST8) to five after the training. Before the training, the sources were located in the temporal lobe of the left hemisphere, the dorsolateral prefrontal cortex of the left hemisphere, and above the right hemisphere in the precuneus and occipital cortex. After the full training period, they were

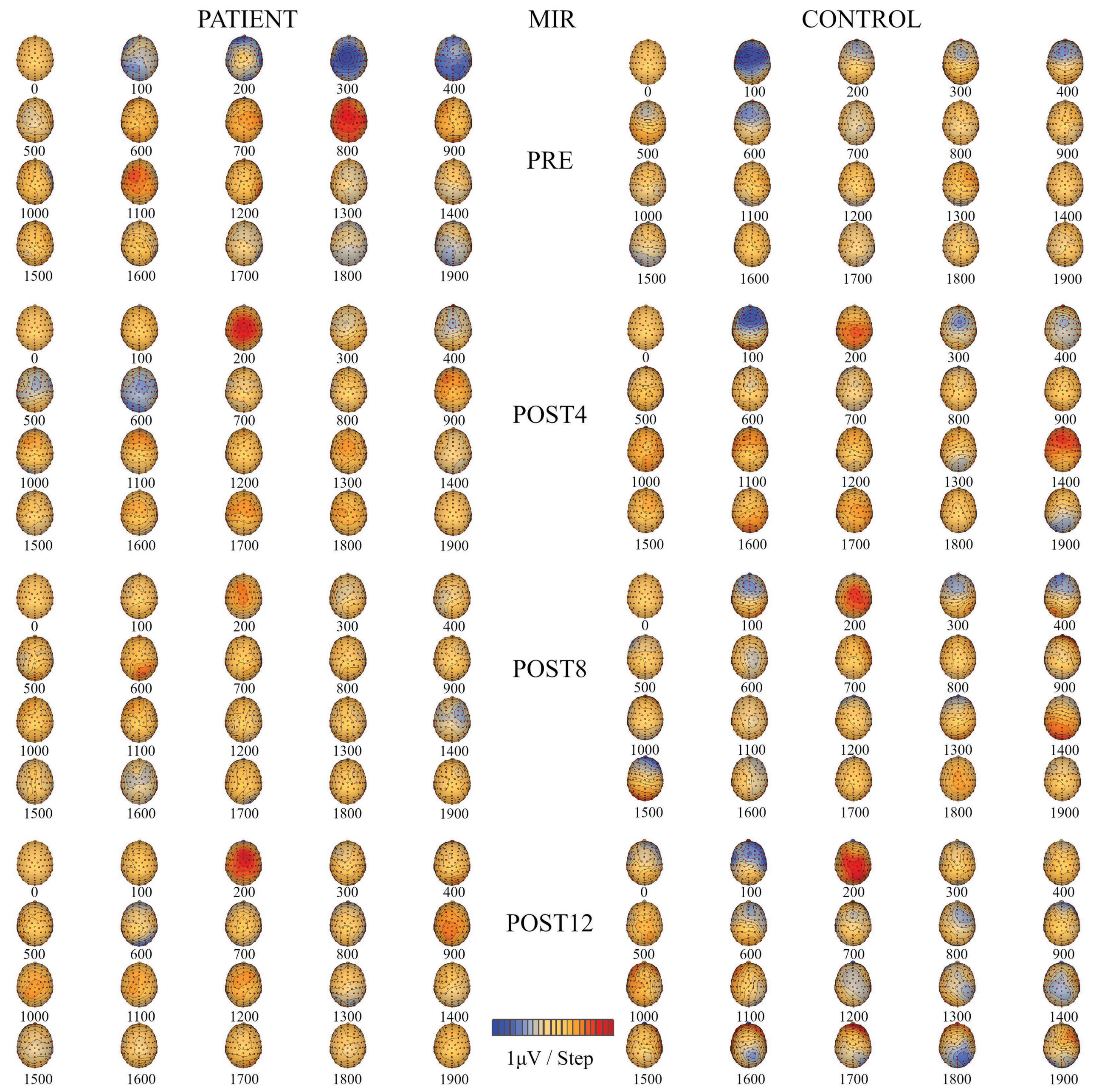

FIGURE 3 | Topographic maps of electroencephalography (EEG) during motor imagery of reaching (MIR) of the right upper limb for the patient **(left)** and the control subject **(right)** for four measurement sessions (PRE, POST4, POST8, and POST12).

located in the premotor cortex, posterior lobe, occipital cortex of the left hemisphere, dorsolateral prefrontal cortex of the right hemisphere, and thalamus. For the control, the number of ERP sources related to the MIG task decreased after CAIT from six (PRE) to four (POST12) and were eventually located in the primary sensory cortex (BA 2) of the left hemisphere, dorsolateral prefrontal cortex, occipital cortex, and limbic lobe of the right hemisphere (**Table 2**). Topographic maps of EEG during MIG for the patient and the control are presented in **Figure 5**.

DISCUSSION

MI is a cognitive process and a dynamic state during which the representation of a specific motor action is internally activated without any motor output (Jeannerod and Decety, 1995). In other words, MI is a part of motor action related to the planning of voluntary movements. They share overlapping structures of the brain, which explains why learning effects occur after MI training and why mental practice facilitates

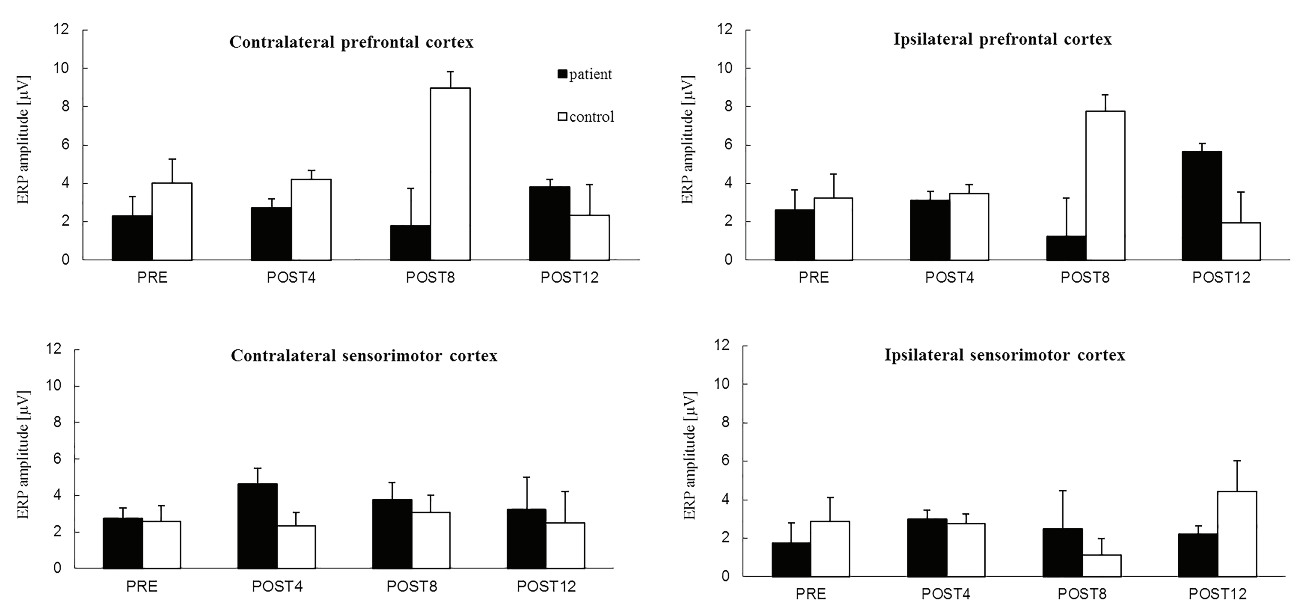

FIGURE 4 | The mean value of ERP amplitude [*−1 (µV)] related to motor imagery of grasping of the right hand from four channels in: the contralateral prefrontal cortex (above **left** hemisphere) – area of standard "F3" channel and ipsilateral prefrontal cortex (above **right** hemisphere) – area of standard "F4" channel, contralateral sensorimotor cortex – area of standard "C3" channel and ipsilateral sensorimotor cortex – area of standard "C4" channel for the patient (black color) and the control subject (white color) for the session before 12 weeks of computer-aided imagery training (PRE) and after intervals of 4 weeks (POST4, POST8, and POST12).

performance (Drickstein et al., 2004; Ranganathan et al., 2004; Allami et al., 2014; Avanzino et al., 2015; Sobierajewicz et al., 2016). In the present study, 12 weeks of training in the kinesthetic MI of a reaching-to-grasp task with a virtual environment (CAIT) was used for the first time in a congenitally amputated patient to evoke training-related changes in cortical activity as a result of neuroplasticity.

Our experiment shows that CAIT can be conducted in patients born without upper limbs with higher vividness of imagery for reaching than for grasping tasks. Our results confirm that CAIT can change the brain activation patterns in areas related to motor planning and the execution of reaching and grasping movements, and that the effect was more pronounced in the patient than in the control. These results show that CAIT has a different effect on the cortical activity related to the MI of a reaching task than on the cortical activity related to the MI of a grasping task, which could be partially related to the different sensorimotor and visuomotor transformations required for reaching and grasping tasks (Kandel et al., 2000). In this study, we chose to use mental training for a task involving reaching to grasp a book, because this type of movement is frequently used in daily life and is commonly used in healthy people. This gave us the opportunity to compare the effect of training on cortex activity between a congenitally amputated patient and a healthy control.

Effects of Computer-Aided Imagery Training on Cortical Activity Related to the Motor Imagery of Reaching

The effects of 12 weeks of CAIT were observed in the contralateral (left) and ipsilateral (right) prefrontal and sensorimotor cortices in the patient but only in the prefrontal cortices of both hemispheres of the control. The ERP amplitudes of the sensorimotor cortices of both hemispheres in the patient decreased after the full training period and approached values similar to those of the control, for which they were stable throughout the whole training period (i.e., they did not change as a result of the training). Greater variability in ERP amplitudes over time was noted for the prefrontal cortices of both hemispheres for the patient and control. The ERP amplitudes for these areas, except for the ipsilateral prefrontal cortex, decreased after the entire training period.

The effects of training on the ERP source locations were different for the patient than for the control. In the control, we observed a reduction in the number of ERP sources located in the premotor cortex of the left hemisphere, dorsolateral prefrontal cortex, and posterior cingulate cortex of the right hemisphere. For the patient, the number of sources did not change, but the areas became more specific than those observed for the healthy control, namely: the premotor cortex of the right hemisphere, the dorsolateral prefrontal cortex of both hemispheres, and the left posterior cingulate cortex. These findings are consistent with those reported in several previous studies (Glover et al., 2012; Hétu et al., 2013; Pilgramm et al., 2016) in healthy subjects, indicating that planning a reaching task without a grasping part could be easier to achieve by mental training in people who were born without arms. This could be related to the fact that planning of this task as a part of goal-directed movement is based on visual information regarding the target location (Kandel et al., 2000). According to Sober and Sabes (2003), the first stage of planning of goal-directed reaching mainly relies on visual information, accounting for approximately 80% of the process with only 20% for proprioception.

Additionally, planning of the reaching requires not only visual information about the target location, but also information about the position of the upper limb – especially the position of the proximal muscles – to prepare motor commands related to the direction of movement. Reilly and Sirigu (2011) found that changes in motor cortex representation of the upper limb in individuals born without arms depend on the level of the missing part of the limb, where more proximal parts are less changed. This could explain our results regarding the observed training-related changes in cortical activity related to the MIR. Additionally, Binkofski et al. (2001) showed that activity in various areas of the frontal cortex is related to motor imagery in the context of its trajectory, which corresponds to the MIR. This could explain why in our study, ERP sources were frequently located in the frontal cortex for each measurement session for both the patient and control (areas such as BA 6, BA 8, BA 9, BA 10, or BA 46). After the entire training period, most of the ERP sources were located in the frontal lobe (BA 8 and BA 10) for the control and four out of five ERP sources (BA 8, BA 9, BA 10, and BA 46) for the patient.

Effects of Computer-Aided Imagery Training on Cortical Activity Related to Motor Imagery of Grasping

The training increased the ERP amplitudes related to the MIG for the prefrontal and sensorimotor cortices of the right and left hemispheres in the patient. The number of ERP sources also increased from four to five as a result of the training, and were located in the premotor cortex, occipital cortex, posterior lobe of the left hemisphere, right dorsolateral prefrontal cortex, and thalamus. The localization of ERP sources corresponded to the areas noted by Glover et al. (2012). The authors identified large networks of brain structures related to the online control of the execution of goal-directed movement. This included the sensorimotor cortex, cerebellum, supramarginal gyrus, and superior parietal lobule. In our study, after the entire training period, the ERP source was localized in the sensory cortex (BA 2) only in the control. We found that the effects of training were smaller for the control. It is well known that the parameters of an object that should be grasped (such as weight and size) are essential in the planning phase of grasping as a part of goal-directed movement (Kandel et al., 2000). This could explain why ERP sources were often localized in the visual cortex (BA 17, BA 18, and BA 19) in both the patient and control. The ERP amplitudes for the prefrontal cortices of both hemispheres and the contralateral sensorimotor cortex remained stable (except for higher values during POST8), while the ERP amplitude of the ipsilateral sensorimotor cortex increased over the full course of the period for the control. After the training (POST12), the ERP sources were located in the primary sensory cortex of the left hemisphere, dorsolateral prefrontal cortex, and occipital cortex of the right hemisphere in the control. The different effects of CAIT on the sensorimotor cortices of both hemispheres (the increase in the patient and decrease in the control) could be related to the inhibition of movement that occurs during MI in healthy people (Solodkin et al., 2004; Kasess et al., 2008), which may not be the case in a congenitally amputated patient.

TABLE 2 | Location (x, y, and z coordinates) of regional sources of the ERP related to MIG of the right side of the patient (on the left side in the table) and control subject (on the right side in the table), expressed in lobe or BAs from four measurement sessions (PRE, POST4, POST8, and POST12).

PATIENT MIG	No.	x	y	z	Lobe/BAs/ other	CONTROL MIG	No.	x	y	z	Lobe/BAs/ other
PRE	1	−46	57.6	14.5	10	PRE	1	−3.4	−2.8	5.1	White matter
	2	31.7	35.6	33.5	9		2	38.8	−64	1.5	37
	3	3.1	−21	47.7	31		3	−36	−39	13.8	41
	4	−67	−66	−12	Temporal lobe		4	−42	48.1	40.3	9
							5	56.4	2.8	26.8	6
							6	−35	−74	57.9	Parietal lobe
POST4	1	−4.9	−21	25.8	23	POST4	1	7.2	−15	4.6	Thalamus
	2	61.8	39.4	23.4	46		2	−48	52.5	22.1	10
	3	65.2	−70	−11	19		3	52.1	43.7	29	46
	4	44.4	53.4	24.7	10		4	41.2	−72	−7.9	19
	5	−62	−77	3.8	37		5	−65	16.2	34.3	9
							6	−26	9.1	50.6	6
							7	48.2	−46	−11	37
POST8	1	28.5	−79	6.6	18	POST8	1	−2	33.7	−1.3	24
	2	−5.1	−22	41.6	31		2	−6.9	−67	26.9	31
	3	−35	1	−17	38		3	41.2	52.5	12.7	10
	4	59.2	43.2	24.8	46		4	−46	43.8	3	46
	5	−45	−98	5.1	19		5	−1.3	−8.9	43.9	24
POST12	1	11.8	−17	6.1	Thalamus	POST12	1	−61	−24	37.4	2
	2	−8.1	43.9	41.3	8		2	12.8	−66	3.5	18
	3	45.2	58.4	29.7	10		3	21.5	34.9	32.1	9
	4	−59	−61	−28	Posterior lobe		4	15.4	−13	32.8	Limbic lobe
	5	−39	−88	40.1	19						

The negative value of the x coordinate indicates location in the left hemisphere, while a positive value of the x coordinate indicates location in the right hemisphere.

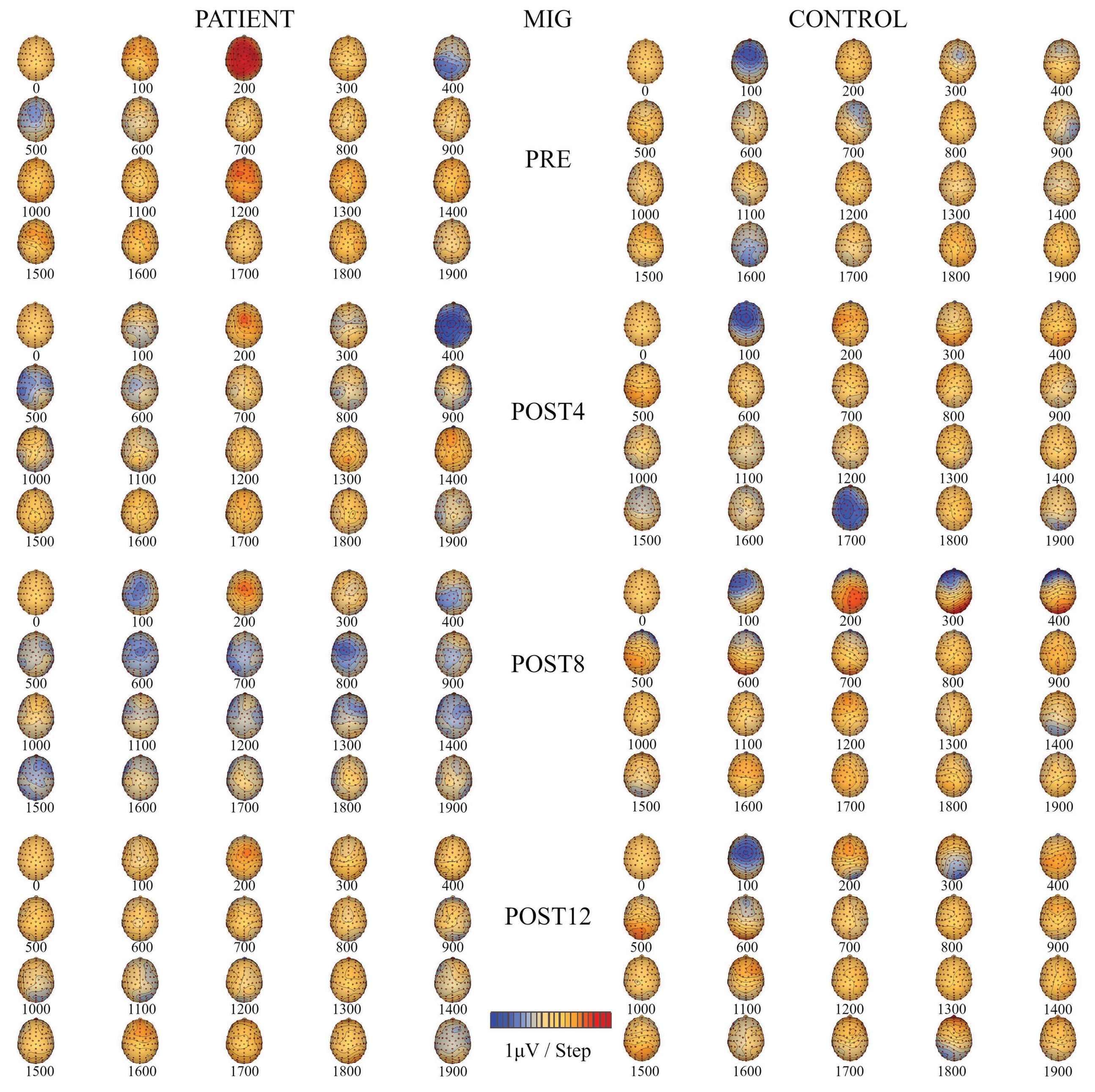

FIGURE 5 | Topographic maps of EEG during motor imagery of grasping (MIG) of the right hand for the patient **(left)** and the control subject **(right)** for four measurement sessions (PRE, POST4, POST8, and POST12).

Comparison of the Effects of Computer-Aided Imagery Training on Cortical Activity Related to Different Tasks (Motor Imagery of Reaching vs. Motor Imagery of Grasping)

Our results show that training had a smaller effect on the MIR (with a high level of vividness of imagery before the training that remained stable during the training period) and larger effects on the MIG (where the vividness of imagery was increased with training) in the patient. These findings can be compared to those of Williams et al. (2002), who reported that the vividness of imagery is associated with the level of neural activation in motor and related areas. These results could also be related to a greater familiarity with the reaching task for the patient who used to perform this type of action with her lower limbs. The MIG is a much more difficult task. However, with the support of applied training with virtual sensory feedback, the cortical activity related to this task increased. Our results also show that CAIT had different effects on the activity of the sensorimotor cortices of both hemispheres – as expressed in terms of the ERP amplitudes related to the MIR – compared to those for the MIG. The activity of the sensorimotor cortices of both hemispheres decreased during MIR as a result of training and increased during MIG. The ERP amplitudes of the sensorimotor cortices of the right and left hemispheres in the control were stable except for an increase in the right sensorimotor cortex after the full training period. The training increased ERP amplitudes in the prefrontal cortices of both hemispheres and for both tasks in the patient (except for the contralateral prefrontal cortex during MIG after 12 weeks of training). The effects of CAIT on the ERP amplitudes in the control were observed only for the prefrontal cortices of the right and left hemispheres and were different for the MIR task (unstable trends) than for the MIG task (increased during the POST8 session and then decreased by half after the full training period). Similarly, Allami et al. observed greater effects of MI training on frontal lobe activity, especially over the premotor cortex. CAIT also had different effects on ERP sources related to MIR and MIG tasks. The number of sources did not change for the patient during the MIR task, but the locations changed to more specific ones – similar to those for the healthy control. For the MIG task, an increase in ERP amplitudes was accompanied by an increase in the number of sources. Our results are consistent with those of an fMRI study of reaching and grasping tasks, in which Glover et al. (2012) reported activity in different brain areas related to pre-movement planning of reaching and online control that was more specific to the neural control of grasping tasks. Their results showed that these two tasks could involve different sub-processes of planning, which could explain, in part, why CAIT had different effects on those tasks in our study.

In our study, smaller effects of CAIT were observed on the ERP amplitude in the control, but the number of sources was reduced for the MIR and MIG tasks. This could be a result of the optimization of cortical activity related to the tasks after CAIT in the control.

CONCLUSION

Although our study obtained results from only one patient and one control subject, our results confirm that 12 weeks of CAIT on a reaching-to-grasp task produced more notable cortical changes in a patient with congenital bilateral transverse upper-limb deficiency than in a healthy control subject. For the patient, training had smaller effects on the MIR and greater effects on the MIG. The larger number of ERP amplitude sources for the MIR and MIG tasks in the congenitally amputated patient indicates that the MIR and grasping at the cortical level was modulated by a higher number of areas of the brain in the patient than in the control. The changes observed in the activation patterns indicate CAIT-induced neuroplasticity.

Despite the study's novel findings, there are certain limitations that are mainly related to the case study's characteristics, such as issues of reliability, validity, and the problem of determining the real causes of the described effects. The major limitation of our study is that our results were obtained from only one patient and one healthy control subject, which prevents generalization of the results.

Nevertheless, this study presents an unusual situation of using mental training that can be used in patients with congenital limb deficiency. This has never been reported before and opens up the possibility of upper-limb transplantation in such patients in the future if the effects of training-induced neuroplasticity would be confirmed by studies with larger sample sizes.

DATA AVAILABILITY STATEMENT

The raw data supporting the conclusion of this article will be made available by Principal Investigator K. Kisiel-Sajewicz (grant number DEC-2011/03/B/NZ7/00588) on reasonable request.

ETHICS STATEMENT

The studies involving human participants were reviewed and approved by Ethical Committee of the University School of Physical Education in Wrocław, Poland. The patients/participants provided their written informed consent to participate in this study.

AUTHOR CONTRIBUTIONS

KK-S, AnJ, JMa, ArJ, MK, and AW contributed conception and design of the study. JMe and KK-S wrote the first draft of the manuscript. ŁK collected EEG data under supervision of KK-S. ŁK conducted training. All authors contributed to manuscript revision, read, and approved the submitted version.

FUNDING

This work was supported by grant no. DEC-2011/03/B/NZ7/00588 from the National Science Centre of the Republic of Poland.

ACKNOWLEDGMENTS

We thank the subjects that participated in the study, and Lukasz Szumowski for technical support during the acquisition of the data.

REFERENCES

Allami, N., Brovelli, A., Hamzaoui, M., Regragui, F., Paulignan, Y., and Boussaoud, D. (2014). Neurophysiological correlates of visuo-motor learning through mental and physical practice. *Neuropsychologia* 55, 6–14. doi: 10.1016/j.neuropsychologia.2013.12.017

Avanzino, L., Gueugneau, N., Bisio, A., Ruggeri, P., Papaxanthis, C., and Bove, M. (2015). Motor cortical plasticity induced by motor learning through mental practice. *Front. Behav. Neurosci.* 9:105. doi: 10.3389/fnbeh.2015.00105

Ballesteros, S., Voelcker-Rehage, C., and Bherer, L. (2018). Editorial: cognitive and brain plasticity induced by physical exercise, cognitive training, video games, and combined interventions. *Front. Hum. Neurosci.* 12:169. doi: 10.3389/fnhum.2018.00169

Binkofski, F., Amunts, K., Stephan, K. M., Posse, S., Schormann, T., Freund, H. J., et al. (2001). Broca's region subserves imagery of motion: a combined cytoarchitectonic and fMRI study. *Hum. Brain Mapp.* 11, 273–285. doi: 10.1002/1097-0193(200012)11:4<273::aid-hbm40>3.0.co;2-0

Brugger, P., Kollias, S. S., Muri, R., Crelier, G., Hepp-Reymond, M. C., and Regard, M. (2000). Beyond re-membering: phantom sensations of congenitally absent limbs. *PNAS* 97, 6167–6172. doi: 10.1073/pnas.100510697

Cabral-Sequeira, A. S., Coelho, D. B., and Teixeira, L. A. (2016). Motor imagery training promotes motor learning in adolescents with cerebral palsy: comparison between left and right hemiparesis. *Exp. Brain Res.* 234, 1515–1524. doi: 10.1007/s00221-016-4554-3

Cicchetti, D. V. (1994). Guidelines, criteria, and rules of thumb for evaluating normed and standardized assessment instruments in psychology. *Psychol. Assess.* 6, 284–290. doi: 10.1037/1040-3590.6.4.284

Decety, J., Perani, D., Jeannerod, M., Bettinardi, V., Tadary, B., Woods, R., et al. (1994). Mapping motor representations with PET. *Nature* 371, 600–602. doi: 10.1038/371600a0

Di Rienzo, F., Collet, C., Hoyek, N., and Guillot, A. (2014). Impact of neurologic deficits on motor imagery: a systematic review of clinical evaluations. *Neuropsychol. Rev.* 24, 116–147. doi: 10.1007/s11065-014-9257-6

Drickstein, R., Dunsky, A., and Marcovitz, E. (2004). Motor imagery for gait rehabilitation in post-stroke hemiparesis. *Phys. Ther.* 84, 1167–1177. doi: 10.1093/ptj/84.12.1167

Ersland, L., Rosen, G., Lundervold, A., Smievoll, A. I., Tillung, T., Sundberg, H., et al. (1996). Phantom limb "fingertapping" causes primary motor cortex activation: an fMRI study. *Neuroreport* 8, 207–210. doi: 10.1097/00001756-199612200-00042

Fadiga, L., Buccino, G., Craighero, L., Fogassi, L., Gallese, V., and Pavesi, G. (1999). Corticospinal excitability is specifically modulated by motor imagery: a magnetic stimulation study. *Neuropsychologia* 37, 147–158. doi: 10.1016/s0028-3932(98)00089-x

Flor, H., Elbert, T., Mühlnickel, W., Pantev, C., Wienbruch, C., and Taub, E. (1998). Cortical reorganization and phantom phenomena in congenital and traumatic upper-extremity amputees. *Exp. Brain Res.* 119, 205–212. doi: 10.1007/s002210050334

Gallagher, S., Butterworth, G. E., Lew, A., and Cole, J. (1998). Hand-mouth coordination, congenital absence of limb and evidence for innate body schemas. *Brain Cogn.* 38, 53–65. doi: 10.1006/brcg.1998.1020

Gerardin, E., Sirigu, A., Lehericy, S., Poline, J. B., Gaymard, B., Marsault, C., et al. (2000). Partially overlapping neural networks for real and imagined hand movements. *Cereb. Cortex* 10, 1093–1104. doi: 10.1093/cercor/10.11.1093

Glover, S., Wall, M. B., and Smith, A. T. (2012). Distinct cortical networks support the planning and online control of reaching-to-grasp in human. *Eur. J. Neurosci.* 35, 909–915. doi: 10.1111/j.1460-9568.2012.08018.x

Guillot, A., and Collet, C. (2005). Contribution from neurophysiological and psychological methods to the study of motor imagery. *Brain Res. Rev.* 50, 387–397. doi: 10.1016/j.brainresrev.2005.09.004

Guillot, A., and Debarnot, U. (2019). Benefits of motor imagery for human space flight: a brief review of current knowledge and future applications. *Front. Physiol.* 10:396. doi: 10.3389/fphys.2019.00396

Guterstam, A., Petkova, V. I., and Ehrsson, H. H. (2011). The illusion of owning a third arm. *PLoS One* 6:e17208. doi: 10.1371/journal.pone.0017208

Hanakawa, T., Immisch, I., Toma, K., Dimyan, A. M., Van Gelderen, P., and Hallett, M. (2003). Functional properties of brain areas associated with motor execution and imagery. *J. Neurophysiol.* 89, 989–1002. doi: 10.1152/jn.00132.2002

Harris, J. E., and Hebert, A. (2015). Utilization of motor imagery in upper limb rehabilitation: a systematic scoping review. *Clin. Rehabil.* 29, 1092–1107. doi: 10.1177/0269215514566248

Hétu, S., Grégoire, M., Saimpont, A., Coll, M. P., Eugène, F., Michon, P. E., et al. (2013). The neural network of motor imagery: an ALE meta-analysis. *Neurosci. Biobehav. Rev.* 37, 930–949. doi: 10.1016/j.neubiorev.2013.03.017

Hoshiyama, M., Kakigi, R., Berg, P., Koyama, S., Kitamura, Y., and Shimojo, M., et al. (1997). Identification of motor and sensory brain activities during unilateral finger movement: spatiotemporal source analysis of movement-associated magnetic fields. *Exp. Brain Res.* 115, 6–14. doi:10.1007/PL00005685

Ietswaart, M., Johnston, M., Dijkerman, H. C., Joice, S., Scott, C. L., MacWalter, R. S., et al. (2011). Mental practice with motor imagery in stroke recovery: randomized controlled trial of efficacy. *Brain* 134, 1373–1386. doi: 10.1093/brain/awr077

Jeannerod, M. (1994). Mental imagery in the motor context. *Neuropsychologia* 33, 1419–1432.

Jeannerod, M., and Decety, J. (1995). Mental motor imagery: a window into the representational stages of action. *Curr. Opin. Neurobiol.* 5, 727–732. doi: 10.1016/0959-4388(95)80099-9

Kandel, E. R., Schwartz, J. H., and Jessell, T. M. (2000). *Principles of neural science*. New York: McGraw-Hill, Health Professions Division.

Kasess, C. H., Windischberger, C., Cunnington, R., Lanzenberger, R., Pezawas, L., and Moser, R. (2008). The suppressive influence of SMA on MI in motor imagery revealed by fMRI and dynamic causal modeling. *NeuroImage* 40, 828–837. doi: 10.1016/j.neuroimage.2007.11.040

Kurzynski, M., Jaskolska, A., Marusiak, J., Wolczowski, A., Bierut, P., Szumowski, L., et al. (2017). Computer-aided training sensorimotor cortex functions in humans before the upper limb transplantation using virtual reality and sensory feedback. *Comput. Biol. Med.* 87, 311–321. doi: 10.1016/j.compbiomed.2017.06.010

Lotze, M., Flor, H., Grodd, W., Larbig, W., and Birbaumer, N. (2001). Phantom movements and pain. An fMRI study in upper limb amputees. *Brain* 124, 2268–2277. doi: 10.1093/brain/124.11.2268

Marins, T., Rodrigues, E. C., Bortolini, T., Melo, B., Moll, J., and Tovar-Moll, F. (2019). Structural and functional connectivity changes in response to short-term neurofeedback training with motor imagery. *NeuroImage* 194, 283–290. doi: 10.1016/j.neuroimage.2019.03.027

Melzack, R., Israel, R., Lacroix, R., and Schultz, G. (1997). Phantom limbs in people with congenital limb deficiency or amputation in early childhood. *Brain* 120, 1603–1620. doi: 10.1093/brain/120.9.1603

Merzenich, M. M., Van Vleet, T. M., and Nahum, M. (2014). Brain plasticity-based therapeutics. *Front. Hum. Neurosci.* 8:385. doi: 10.3389/fnhum.2014.00385

Mizuguchi, N., Sakamoto, M., Muraoka, T., Nakagawa, K., Kanazawa, S., Nakata, H., et al. (2011). The modulation of corticospinal excitability during motor imagery of actions with objects. *PLoS One* 6:e26006. doi: 10.1371/journal.pone.0026006

Mokienko, O. A., Chervyakov, A. V., Kulikova, S. N., Bobrov, P. D., Chernikova, L. A., Frolov, A. A., et al. (2013). Increased motor cortex excitability during motor imagery in brain-computer interface in trained subjects. *Front. Comput. Neurosci.* 7:168. doi: 10.3389/fncom.2013.00168

Montoya, P., Larbig, W., Grulke, N., Flor, H., Taub, E., and Birbaumer, N. (1997). The relationship of phantom limb pain to other phantom limb phenomena in upper extremity amputees. *Pain.* 72, 87–93. doi: 10.1016/s0304-3959(97)00004-3

Mulder, T. (2007). Motor imagery and action observation: cognitive tools for rehabilitation. *J. Neural Transm.* 114, 1265–1278. doi: 10.1007/s00702-007-0763-z

Oostenveld, R., and Praamstra, P. (2001). The five percent electrode system for high-resolution EEG and ERP measurements. *Clin. Neurophysiol.* 112, 713–719. doi: 10.1016/S1388-2457(00)00527-7

Ortner, R., Irimia, D. C., Scharinger, J., and Guger, C. (2012). A motor imagery based brain-computer interface for stroke rehabilitation. *Stud. Health Technol. Inform.* 181, 319–323. doi: 10.3233/978-1-61499-121-2-319

Pilgramm, S., de Haas, B., Helm, F., Zentgraf, K., Stark, R., Munzert, J., et al. (2016). Motor imagery of hand actions: decoding the content of motor imagery from brain activity in frontal and parietal motor areas. *Hum. Brain Mapp.* 37, 81–93. doi: 10.1002/hbm.23015

Ramachandran, V. S., and Altschuler, E. L. (2009). The use of visual feedback, in particular mirror visual feedback, in restoring brain function. *Brain* 132, 1693–1710. doi: 10.1093/brain/awp135

Ranganathan, V. K., Siemionow, V., Liu, J. Z., Sahgal, V., and Yue, G. H. (2004). From mental power to muscle power-gaining strength by using the mind. *Neuropsychiatrie* 42, 944–956. doi: 10.1016/j.neuropsychologia.2003.11.018

Reilly, K. T., and Sirigu, A. (2011). Motor cortex representation of the upper-limb in individuals born without a hand. *PLoS One* 6:e18100. doi: 10.1371/journal.pone.0018100

Saadah, E. S., and Melzack, R. (1994). Phantom limb experiences in congenital limb-deficient adults. *Cortex* 30, 479–485. doi: 10.1016/S0010-9452(13)80343-7

Scherg, M. (1992). Functional imaging and localization of electromagnetic brain activity. *Brain Topogr.* 5, 103–111. doi: 10.1007/BF01129037

Scherg, M., and Berg, P. (1996). New concepts of brain source imaging and localization. *Electroencephalogr. Clin. Neurophysiol. Suppl.* 46, 127–137.

Scherg, M., Berg, P., Nakasato, N., and Beniczky, S. (2019). Taking the EEG back into the brain: the power of multiple discrete sources. *Front. Neurol.* 10:855. doi: 10.3389/fneur.2019.00855

Schuster, C., Hilfiker, R., Amft, O., Scheidhauer, A., Andrews, B., Butler, J., et al. (2011). Best practice for motor imagery: a systematic literature review on motor imagery training elements in five different disciplines. *BMC Med.* 9:75. doi: 10.1186/1741-7015-9-75

Sober, S. J., and Sabes, P. N. (2003). Multisensory integration during motor planning. *J. Neurosci.* 23, 6982–6992. doi: 10.1523/JNEUROSCI.23-18-06982.2003

Sobierajewicz, J., Przekoracka-Krawczyk, A., Jaśkowski, W., Verwey, W., and van der Lubbe, R. (2016). The influence of motor imagery on the learning of a fine hand motor skill. *Exp. Brain Res.* 235, 305–320. doi: 10.1007/s00221-016-4794-2

Solodkin, A., Hlustik, P., and Chen, E. E. (2004). Small SL. Fine modulation in network activation during motor execution and motor imagery. *Cereb. Cortex* 14, 1246–1255. doi: 10.1093/cercor/bhh086

Stephan, K. M., Fink, G. R., Passingham, R. E., Silbersweig, D., Ceballos-Baumann, A. O., Frith, C. D., et al. (1995). Functional anatomy of the mental representation of upper extremity movements in healthy subjects. *J. Neurophysiol.* 73, 373–386. doi: 10.1152/jn.1995.73.1.373

Striem-Amit, E., Vannuscorps, G., and Caramazza, A. (2017). Sensorimotor-independent development of hands and tools selectivity in the visual cortex. *PNAS* 114, 4787–4792. doi: 10.1073/pnas.1620289114

Teo, W. P., and Chew, E. (2014). Is motor-imagery brain-computer interface feasible in stroke rehabilitation? *PM R* 6, 723–728. doi: 10.1016/j.pmrj.2014.01.006

Vannuscorps, G., Wurm, M. F., Striem-Amit, E., and Caramazza, A. (2018). Large-scale organization of the hand action observation network in individuals born without hands. *Cereb. Cortex* 29, 3434–3444. doi: 10.1093/cercor/bhy212

Williams, S. E., Cumming, J., Ntoumanis, N., Nordin-Bates, S. M., Ramsey, R., and Hall, C. (2002). Further validation and development of the movement imagery questionnaire. *J. Sport Exerc. Psychol.* 34, 621–646. doi: 10.1123/jsep.34.5.621

Zabicki, A., de Haas, B., Zentgraf, K., Stark, R., Munzert, J., and Krüger, B. (2019). Subjective vividness of motor imagery has a neural signature in human premotor and parietal cortex. *NeuroImage* 197, 273–283. doi: 10.1016/j.neuroimage.2019.04.073

Conflict of Interest: The authors declare that the research was conducted in the absence of any commercial or financial relationships that could be construed as a potential conflict of interest.

frontiers
in Neuroscience

HYPOTHESIS AND THEORY
published: 07 April 2021
doi: 10.3389/fnins.2021.646698

Multisensory Integration in Stroke Patients: A Theoretical Approach to Reinterpret Upper-Limb Proprioceptive Deficits and Visual Compensation

Jules Bernard-Espina, Mathieu Beraneck, Marc A. Maier and Michele Tagliabue*

Université de Paris, INCC UMR 8002, CNRS, Paris, France

OPEN ACCESS

Edited by:
Luigi F. Cuturi,
Italian Institute of Technology (IIT), Italy

Reviewed by:
Jacopo Zenzeri,
Italian Institute of Technology (IIT), Italy
Laura Mikula,
York University, Canada

****Correspondence:***
Jules Bernard-Espina
jules.bernard@parisdescartes.fr

Specialty section:
This article was submitted to
Perception Science,
a section of the journal
Frontiers in Neuroscience

Received: *27 December 2020*
Accepted: *04 March 2021*
Published: *07 April 2021*

Citation:
Bernard-Espina J, Beraneck M, Maier MA and Tagliabue M (2021) Multisensory Integration in Stroke Patients: A Theoretical Approach to Reinterpret Upper-Limb Proprioceptive Deficits and Visual Compensation.
Front. Neurosci. 15:646698.
doi: 10.3389/fnins.2021.646698

For reaching and grasping, as well as for manipulating objects, optimal hand motor control arises from the integration of multiple sources of sensory information, such as proprioception and vision. For this reason, proprioceptive deficits often observed in stroke patients have a significant impact on the integrity of motor functions. The present targeted review attempts to reanalyze previous findings about proprioceptive upper-limb deficits in stroke patients, as well as their ability to compensate for these deficits using vision. Our theoretical approach is based on two concepts: first, the description of multisensory integration using statistical optimization models; second, on the insight that sensory information is not only encoded in the reference frame of origin (e.g., retinal and joint space for vision and proprioception, respectively), but also in higher-order sensory spaces. Combining these two concepts within a single framework appears to account for the heterogeneity of experimental findings reported in the literature. The present analysis suggests that functional upper limb post-stroke deficits could not only be due to an impairment of the proprioceptive system per se, but also due to deficiencies of cross-references processing; that is of the ability to encode proprioceptive information in a non-joint space. The distinction between purely proprioceptive or cross-reference-related deficits can account for two experimental observations: first, one and the same patient can perform differently depending on specific proprioceptive assessments; and a given behavioral assessment results in large variability across patients. The distinction between sensory and cross-reference deficits is also supported by a targeted literature review on the relation between cerebral structure and proprioceptive function. This theoretical framework has the potential to lead to a new stratification of patients with proprioceptive deficits, and may offer a novel approach to post-stroke rehabilitation.

Keywords: stroke, eye-hand coordination, maximum likelihood principle, visual compensation, proprioception assessment, multisensory integration

INTRODUCTION

Manual dexterity is highly specialized in humans (Lemon, 2008). Multimodal information from different sensory systems need to be combined to optimally control hand movements. Among them are vision, proprioception, touch, audition and graviception. Goal-oriented upper limb movements are planned and controlled using mainly vision and proprioception, which allow comparison of hand position with the location/orientation of the object to be reached and/or grasped.

In the context of brain lesions, such as in stroke, proprioceptive deficits are common (Connell et al., 2008; Kessner et al., 2016). These deficits significantly contribute to the patients' motor disability and largely determine their degree of recovery (Turville et al., 2017; Zandvliet et al., 2020). Despite the clinical relevance, no consensus exists regarding the neurological assessment of proprioceptive deficits, nor on the rehabilitation strategies (Findlater and Dukelow, 2017). Clinical research studies that investigated and compared various techniques for the assessment of proprioception observed inconsistencies (Dukelow et al., 2012; Gurari et al., 2017; Ingemanson et al., 2019). Attempts to quantify the patients' ability to use vision to compensate for proprioceptive deficits also provided contrasting results depending on the task and on the brain lesion (Darling et al., 2008; Scalha et al., 2011; Semrau et al., 2018; Herter et al., 2019).

In the present non-systematic review, we propose a new analysis and re-classification of assessment techniques commonly used in clinical practice and stroke research. This reinterpretation is based on the theoretical framework provided by the Maximum Likelihood Principle (MLP) and its application in the field of perception and sensorimotor control (Van Beers et al., 1996; Ernst and Banks, 2002; Körding et al., 2007). This theory describes how sensory inputs are optimally combined to generate a coherent movement representation and statistically maximize its precision. Experimental evidence, and its interpretation through this statistical model, suggests that the central nervous system (CNS) reconstructs multiple concurrent representations of the task (Tagliabue and McIntyre, 2008; McGuire and Sabes, 2009; Tagliabue and McIntyre, 2011, 2014). Each of these concurrent representations encodes the information in a specific reference frame, which can be directly associated to a sensory system (e.g., the retinal reference for vision and the joint reference for proprioception) or to a combination of sensory signals (i.e., body-centered, gravito-centered and allocentric references). As a consequence, the information acquired through a sensory channel can be encoded in a reference frame not directly associated to the originating sensory system. This information processing is commonly termed "cross-modal" when the transformations involves two reference frames associated to two different sensory modalities. In the following we will privilege the more generic "cross-reference" term, which accounts for both between-modalities transformations (e.g., proprioceptive to visual) and within-modality transformations (e.g., proprioceptive transformation between different reference frames as the hand or the trunk, or even with respect to external references).

Cross-reference processing appears to take place even when the constraints of the task leaves only one sensory input modality available (Pouget et al., 2002; Sarlegna and Sainburg, 2007; McGuire and Sabes, 2009; Jones and Henriques, 2010; Tagliabue and McIntyre, 2013; Arnoux et al., 2017). It is therefore critical to distinguish between the modality of the sensory inputs provided by the task, and the potential cross-reference sensory processing that ensues during task performance.

The present reinterpretation of the contrasting results reported in the stroke literature is founded on the hypothesis that altered cross-reference processing could form an essential part of what has (perhaps misleadingly) been termed proprioceptive post-stroke deficits.

In the next section, we will describe the standard methods used for the assessment of proprioceptive deficits and visual compensation mechanisms post-stroke. In the following section we will present the multisensory integration theory based on MLP and its application to the most representative clinical tests. Based on the MLP theoretical predictions, in section "Reinterpretation of Experimental Observations About Proprioceptive Deficits and Visual Compensation" we will propose a new stratification for stroke patients which is based on their sensory deficits. In section "Insights From Brain Lesions and Functional Anatomy Studies," we will review lesion-behavior and brain imaging studies in the framework of this novel classification and attempt to relate brain structures to either purely proprioceptive functions or cross-reference processing. In the final section, we will summarize the contribution of this review to neuroscientific and clinical research and describe some specific applications for post-stroke sensory assessment and rehabilitation.

UPPER LIMB PROPRIOCEPTIVE DEFICITS POST-STROKE

Stroke can affect not only motor abilities, but also sensory functions. In particular, proprioceptive deficits can be observed in a large percentage, up to 60%, of individuals following stroke (Connell et al., 2008; Kessner et al., 2016). These impairments are clearly correlated with functional deficits (Scalha et al., 2011; Meyer et al., 2014, 2016; Rand, 2018). In particular, reaching (Zackowski et al., 2004), dexterity (Carlsson et al., 2019), and inter-limb coordination (Torre et al., 2013) appear to be negatively affected by proprioceptive deficits. Moreover, sensory recovery is a predictive factor for functional recovery (Turville et al., 2017; Zandvliet et al., 2020).

Yet, no consensus seems to have emerged regarding proprioceptive assessment methods (Saeys et al., 2012; Simo et al., 2014; Pumpa et al., 2015; Santisteban et al., 2016). For the assessment of upper-limb function, no less than 48 different clinically validated (standardized) measures are used in clinical research (Santisteban et al., 2016). A high discrepancy between studies was found, as only 15 of the 48 outcome measures are used in more than 5% of the studies. In particular, only few studies specifically assess proprioceptive function: the NSA[1], one

---

[1] Nottingham Sensory Assessment.

of the most commonly used standardized scales, was applied in only 0.6% of studies reviewed (Santisteban et al., 2016). Moreover, current clinical practice does not systematically use standardized scales (Saeys et al., 2012; Simo et al., 2014; Pumpa et al., 2015; Santisteban et al., 2016; Matsuda et al., 2019). This lack of consensus is a major shortcoming for meta-analysis of recovery of upper limb function after stroke (Findlater and Dukelow, 2017). Similarly, research examining the ability of patients to compensate for a proprioceptive deficit using vision lack homogeneity. Although empirical evidence suggests that vision is helpful to compensate a proprioceptive deficit (Pumpa et al., 2015), the studies addressing this question are scarce and their methodologies are hardly comparable (Darling et al., 2008; Scalha et al., 2011; Torre et al., 2013; Semrau et al., 2018; Herter et al., 2019).

In the following subsections we will review the assessment techniques currently used in stroke for proprioceptive function, as well as for visual compensation. We will then discuss several studies showing that some of these proprioception and visual compensation tests might lead to different diagnostics. Finally, in the last subsection we will propose a new categorization of these tests with the aim of better understanding the origin of their different outcomes.

Proprioceptive Tests in the Clinical Practice

All existing proprioceptive assessment methods are relevant from a functional point of view, but their differences pose a challenge for their comparability. The commonly used tests, both in clinical practice (Pumpa et al., 2015) and in clinical research are described below:

- **Thumb Localization Test (TLT)**: Assesses the ability of a subject to localize a body part (thumb). The physiotherapist positions the affected arm of the patient who then has to point, without vision, to the affected thumb with the other, less-affected hand (Dukelow et al., 2012; Meyer et al., 2016; Rand, 2018).
- **Up or Down Test (UDT)**: Assesses the ability of a subject to detect joint displacement direction. The physiotherapist moves a joint of the patient whose vision is occluded. The subject is then asked to report the up or down movement direction. This test is part of the FMA-UE[2] and the RASP[3] (Scalha et al., 2011; Saeys et al., 2012; Simo et al., 2014; Rand, 2018; Birchenall et al., 2019; Carlsson et al., 2019; Frenkel-Toledo et al., 2019; Kessner et al., 2019; Pennati et al., 2020; Zandvliet et al., 2020).
- **Mirror Position Test (MPT)**: Assesses the ability of a subject to perceive the angular configuration of a particular joint. The physiotherapist positions a joint of the patient's affected arm in the absence of vision. The patient is then asked to mirror the position with the other, less-affected arm. This task can also be performed using a robotic device. This test is part of the NSA (Connell et al., 2008; Dukelow et al., 2010; Scalha et al., 2011; Iandolo et al., 2014; Ben-Shabat et al., 2015; Meyer et al., 2016; Gurari et al., 2017; Sallés et al., 2017; Findlater et al., 2018; Rinderknecht et al., 2018; Semrau et al., 2018; Herter et al., 2019; Zandvliet et al., 2020).
- **Bimanual Sagittal Matching Test (BSMT)**: Assesses the ability of the patients to reproduce with their free hand the trajectory/position of the affected hand which is passively driven by a robotic device along the sagittal plane (Torre et al., 2013).
- **Within-arm Position Test (WPT)**: Assesses the ability of a subject to perceive the angular configuration of one joint. A robot moves the arm of the patient to a position to be memorized and then back to the initial configuration. Subsequently, the subject is asked to move his/her arm to the remembered position (Dos Santos et al., 2015; Contu et al., 2017; Gurari et al., 2017).
- **Matching to a Visual Image (MV)**: Assesses the ability of a subject to localize in space his/her unseen arm or hand relative to a visual reference. A visual image, that could be a lever or a virtual hand with a given orientation, is shown to the subject. The subject is then asked, without visual feedback, to reproduce the same orientation with his/her hand. The vision of the hand can be occluded by a box covering the hand, or by wearing a virtual reality headset that leaves the subject's hand non-rendered (Turville et al., 2017; Deblock-Bellamy et al., 2018).
- **Threshold Detection Test (TDT)**: Assesses the patient's ability to detect hand displacements of various magnitudes. Using a robotic device, a joint (elbow, wrist, metacarpophalangeal) is first moved from a starting to a reference position. Then, a second movement from the starting position in the same direction, but not with the same amplitude, is operated by the robot. The subject is asked to assess whether the second movement was larger or smaller than first one. The threshold detection value is measured (Simo et al., 2014; De Santis et al., 2015; Rinderknecht et al., 2018; Ingemanson et al., 2019).
- **Finger Proprioception Test (FPT)**: Assesses the patient's ability to detect whether the index finger is aligned (in flexion/extension) with the middle finger. The two fingers are passively moved by a robotic device in a crossing flexion/extension movement. For each finger-crossing movement, the patient is asked to report when the two fingers are directly aligned relative to each other (Ingemanson et al., 2019).
- **Motor Sequences Test (MS)**: Assesses the patient's ability to localize a body part (fingers). The subject is asked to touch with the thumb pad (I) the other finger pads (II, III, IV, V) with eyes closed. Motor sequences with alternating movements between the thumb and the other fingers are used: for example, touching in the following order: I with II, I with III, I with IV, I with V (Scalha et al., 2011).
- **Reaching Test (RT)**: Assesses the patient's ability to localize in space his/her unseen arm relative to a visual reference. A visual target (real or on a screen) is shown and the subject asked to reach to the memorized target, without

---

[2] Fugl-Meyer Assessment for the Upper Extremity.

[3] Rivermead Assessment of Somatosensory Performance.

visual feedback of the reaching hand (Scalha et al., 2011; Elangovan et al., 2019; Valdes et al., 2019).

- **Shape** or **Length Discrimination (SLD)**: Assesses the patient's ability to discriminate object shapes and dimensions without vision. Different objects of familiar geometric shapes, everyday objects or segments of different lengths are presented to the patient whose vision is occluded. Either with passive movements (operated by a robotic device or a physiotherapist) or active movements, the patient interacts with the different objects. The subject is asked to report the perceived shape, object or length (Van de Winckel et al., 2012; De Diego et al., 2013; Metzger et al., 2014; Sallés et al., 2017; Turville et al., 2017; Matsuda et al., 2019; Carlsson et al., 2019).

Although each one of these tests involves proprioception, they are clearly different. For instance, some tests involve one articular chain only (UDT, TDT, WPT), whereas others involve two distinct articular chains (two arms for MPT and TLT or two fingers for FPT and MS). When two articular chains are involved, the patient is either asked to mirror the joint configuration (MPT, FPT), or to point to a body part (e.g., thumb of the affected arm: TLT and MS). It is noteworthy that some other tests do not rely on proprioceptive inputs only, but use visually remembered references (MV, RT, SLD).

Different Proprioceptive Assessments, Different Outcomes

Experimental observations suggest that methodological differences between these tests can lead to different diagnostics (Hirayama et al., 1999; Dukelow et al., 2012; Gurari et al., 2017; Ingemanson et al., 2019). Similarly, the ability of patients to compensate the proprioceptive deficit with vision depends on the task considered (Darling et al., 2008; Scalha et al., 2011; Torre et al., 2013; Semrau et al., 2018; Herter et al., 2019). In the following we will detail and discuss some of the studies reporting differences between proprioceptive assessment techniques for stroke patients.

Within-Arm Position Test (WPT) vs. Mirror Position Test (MPT)

Gurari et al. (2017) characterized the ability of chronic stroke patients and healthy controls to match elbow flexion/extension positions using two approaches: the **MPT** performed with a physiotherapist vs. the **WPT** under robotic control. The large majority of stroke patients showed impairments in the mirror task, but no difference with the control group in the within-arm task. These different outcomes could be due to lateralized sensory deficits observed after stroke (Connell et al., 2008; Kessner et al., 2016) resulting in asymmetries that may affect the between-arms comparison in the mirror task, but not the unilateral within-arm task. A non-exclusive alternative explanation for the difference in performances may reside in stroke lesions that could have damaged brain networks specifically involved in the mirror but not in the within-arm task (Iandolo et al., 2018). This second hypothesis appears supported by the results of Torre et al. (2013), where stroke patients performed the bimanual sagittal matching tests (BSMT). The accomplishment of BSMT does not require mirroring with respect to the body midline of the hand position, because both hands moved along the sagittal plane, close to each other. The precision of the patients in this study is similar to that observed in within-arm tasks (Dos Santos et al., 2015; Contu et al., 2017; Rinderknecht et al., 2018) and appears better than for the MPT (Herter et al., 2019; Ingemanson et al., 2019), suggesting that stroke lesions can affect the sensory processing necessary to mirror the hand position with respect to the body midline without affecting the between-arms communication per se.

Mirror Position Test (MPT) vs. Thumb Localization Test (TLT)

Outcomes of these two tests were only poorly correlated (Kenzie et al., 2017) and could not reliably identify a proprioceptive deficit within the same patients (Dukelow et al., 2012). Estimated prevalence of proprioceptive deficits using these two tests varied by a factor of two (Meyer et al., 2016). A clear difference between the two tasks, which might explain the different outcomes, is the use of a left/right symmetric (MPT) vs. an asymmetric joint configuration in the TLT. Studies on healthy subjects comparing analogous symmetric and asymmetric inter-manual proprioceptive tasks suggest that these tests differ by the way the joint information from the two arms is processed (Arnoux et al., 2017). Stroke lesions may differentially damage brain areas involved in the specific sensory processing characterizing symmetric and asymmetric tasks.

Thumb Localization Test (TLT) and Finger Proprioception Test (FPT) vs. Up or Down Test (UDT)

These comparisons showed poor correlations (Lanska and Kryscio, 2000; Ingemanson et al., 2019), and prevalence of proprioceptive deficits varied by a factor of three (Hirayama et al., 1999). The difference between the unimanual UDT and both the inter-manual TLT and FPT, which uses two fingers of the affected hand, suggests that the different outcomes do not originate from involving only the affected limb. A key difference between these tasks resides in using a single (UDT) vs. two articular chains (TLT and FPT). Research on healthy subjects, comparing analogous proprioceptive tasks, supports differential proprioceptive processing in these two situations (Tagliabue and McIntyre, 2013).

Within-Arm Position Test (WPT) vs. Reaching Test (RT)

Performance errors in the WPT were only poorly correlated with errors in the RT (Darling et al., 2008). This result is most likely due to the obvious difference in sensory modality: the target position is either memorized through proprioception (WPT) or through vision (RT). These tasks have been studied in healthy subjects and been shown to require different sensory processing (Tagliabue and McIntyre, 2011; Tagliabue et al., 2013).

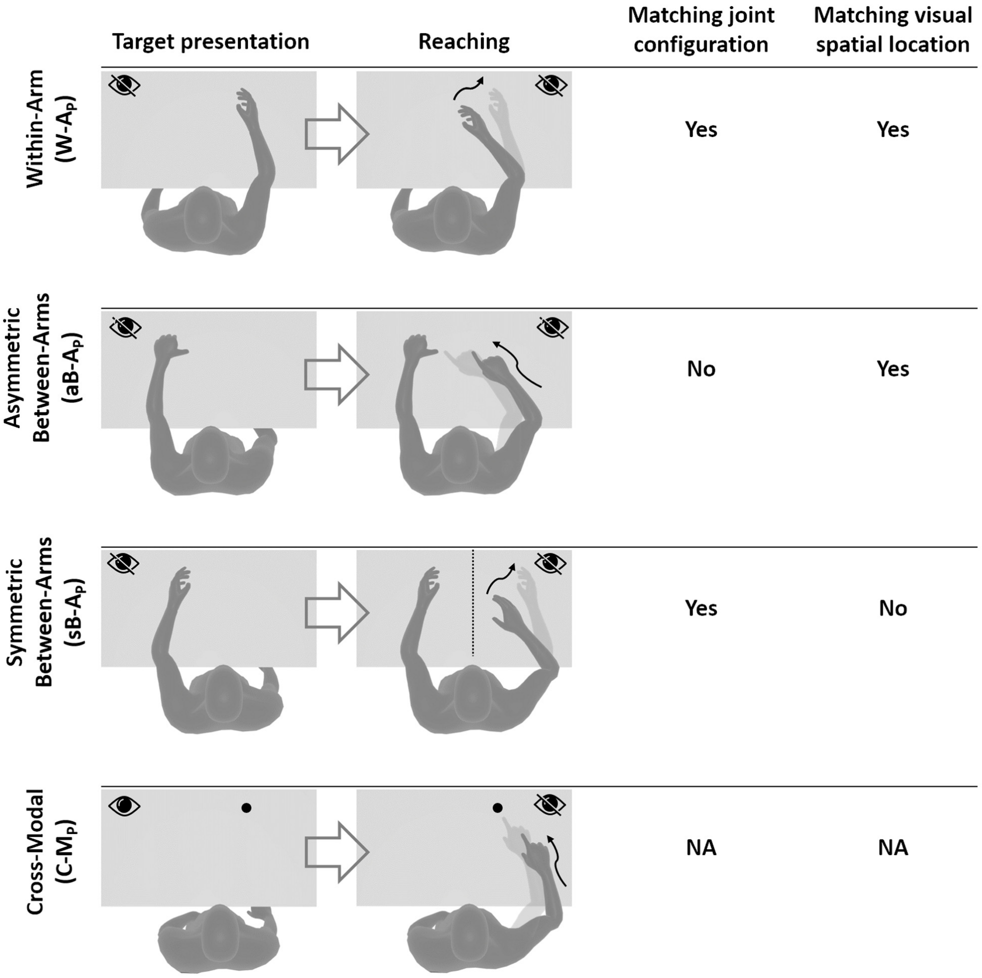

FIGURE 1 | Four categories of proprioceptive assessments. In all represented examples, subjects are asked to, first, perceive a target position and then to reach for it. The last two columns show that the tasks categorization is based on the possibility, or not, to compare the target and effector position in joint and/or retinal space. In the within-arm category (W-A) the patient first perceives and then moves back to the target with the same arm. In the asymmetric between-arms category (aB-A) the location of the target perceived with one hand is subsequently reached with the other hand. In the symmetric between-arms category (sB-A) the patient perceives the target with one hand and mirrors its position with the other hand. In the cross-modal (C-M) category, where the hand and the target do not share the same sensory modality, the patient reaches for a visually memorized target with the unseen hand.

Different Visual Compensation Assessments, Different Outcomes

Several studies tested whether stroke patients could compensate for their proprioceptive deficits by using visual information. The results appear to be very different depending on the task under investigation.

Visual feedback of the hand appears to improve the patient's performance in some tasks, such as the **Motor Sequences Test** (Scalha et al., 2011), and the **Reaching Test** (Darling et al., 2008). On the other hand, in a large-scale study where patients were assessed using a **Mirror Position Test**, up to 80% of patients with proprioceptive deficits were not able to improve their performance when visual feedback of both arms was available (Semrau et al., 2018; Herter et al., 2019). The important difference between Mirror Position Test and both Motor Sequences Test and Reaching Test, is the different way visual information can be used. In both tasks where vision significantly improves performance in patients, the hand (or finger) reaches the same spatial position of the target: the tasks can hence be accomplished by simply matching the visually acquired target position and the visual feedback of the hand (or finger). In the Mirror Position Test in contrast, the patient does not have to reach the spatial location of the target, but its mirror position: the patient must thus "flip," relative to the body midline, the image of the arms to evaluate the task accomplishment. It follows that the ability to use visual information to compensate for proprioceptive deficits in reaching, but not in mirror tasks, could be due to specific difficulties in performing "mirroring" of visual information. Consistent with this interpretation, patients were shown to be able to significantly improve their performance with vision in the Bimanual Sagittal Matching Test which does not require the "mirroring" of visual information, because their hands moved parallel to the sagittal plane and close to each other (Torre et al., 2013).

Categorization of Proprioceptive Assessments

Based on the above observations, we propose here a new categorization of these various proprioceptive tests. We group them into four distinct categories (**within-arm** tasks, **asymmetric between-arms** tasks, **symmetric between-arms**[4] tasks, and **cross-modal** tasks). This categorization is based on the possibility to achieve the tasks by reproducing the joint configuration memorized during the target acquisition and/or by matching the target position in retinal coordinates (**Figure 1**).

Within-Arm tasks require one and the same articular chain to perceive and to reproduce the target position. Thus, proprioceptive information to be remembered (target) and the feedback about the moving hand (effector) originate from the same joints (**Figure 1**, W-A). These tasks can be performed by directly matching the proprioceptive signals corresponding to the target and effector positions (Within-arm Position Test) or by directly comparing two movement signals originating from the same joints (Up or Down Test, Threshold Detection Test). These tasks can also be performed by matching the target and effector position encoded in the retinal reference. Bi-manual matching tests performed along the mid-sagittal plane (BSMT) are also associated to this category, because, as described in sections "Different Proprioceptive Assessments, Different Outcomes" and "Different Visual Compensation Assessments, Different Outcomes," although involving two arms, the experimental results suggest that they are performed by a direct encoding of the information in joint and retinal coordinates, similarly to the within-arm tasks.

Asymmetric Between-Arms tasks involve two articular chains. Typically, the less-affected arm (effector) has to reach the target location perceived with the affected arm (Thumb Location Test, see **Figure 1**, aB-A). These tasks cannot be performed by matching the joint configuration of the affected arm (target) with that of the effector, since they differ at the end of the movement. They can be accomplished, however, by matching the target and effector location encoded in the retinal reference frame. The Motor Sequences test (involving only one arm), as well as the Thumb Location Test, can also be classified in this category since they involve different articular chains (fingers) to perceive the target position and to match it.

Symmetric Between-Arms tasks also involve two articular chains. "Symmetric" refers to the fact that the effector has to "mirror" the target configuration. The articular chains can be the arms (Mirror Position Test, see **Figure 1**, sB-A) or the index and middle fingers (Finger Proprioception Test). At task achievement, the joint configuration of the two articular chains is identical, allowing for direct matching of proprioceptive signals corresponding to the target and effector positions. In contrast, the task cannot be performed in the retinal space, since the target and the effector do not share the same spatial location.

TABLE 1 | Categorization of proprioceptive assessments.

Category	Test
Within-arm (W-A)	Within-arm Position Test (WPT)
	Up or Down Test (UDT)
	Threshold Detection Test (TDT)
	Bimanual Sagittal Matching Test (BSMT)
Asymmetric between-arms (aB-A)	Thumb Localization Test (TLT)
	Motor Sequences Test (MS)
Symmetric between-arms (sB-A)	Mirror Position Test (MPT)
	Finger Proprioception Test (FPT)
Cross-modal (C-M)	Reaching Test (RT)
	Matching to a Visual image (MV)
	Shape/Length Discrimination (SLD)

Cross-Modal Tasks differ from the other three categories in that the target information is given visually (or remembered visually) whereas only proprioceptive information is provided for the effector (the moving hand, **Figure 1**, C-M). Thus, these tasks always require cross-reference sensory processing. For this reason, their categorization based on the direct encoding in the joint and/or retinal space is not fully applicable. Both Reaching Test and Matching to a Visual image share this characteristic. Similar sensory processing could also be involved in the tasks used in Perfetti's neurocognitive approach, such as the Shape or Length Discrimination test.

Overall, this new categorization (summarized in **Table 1**) allows to discriminate the above-mentioned tests in terms of sensory requirements. In the following section, we will present the multisensory integration theory based on MLP and its application to the most representative clinical tests among those reported here.

OPTIMAL MULTISENSORY INTEGRATION THEORY AND STROKE

In this section we will present the MLP and its application to generic target-oriented movements (first subsection). Then we will use this theoretical framework to describe the information processing underlying the proprioceptive assessments according to their categorization (second subsection).

Statistical Optimality in Multisensory Integration for Goal-Oriented Hand Movements

When reaching to grasp an object, visual and proprioceptive sensory information about the target and the hand (effector) is used to control movement execution. In a first step, each sensory modality is encoded in the reference frame of the respective receptors: retinal and joint reference for vision and proprioception, respectively. Several studies have shown that redundant sensory

---

[4] We choose here to refer to this group of tasks as "between-arms," and not bimanual, as the two arms are not used together to sense and move to the target. In contrast, tasks involving only one arm will be referred as "within-arm."

signals are then optimally combined and weighted according to MLP in order to statistically minimize the variability of the estimated movement parameters (Ernst and Banks, 2002).

Figure 2A shows how sensory signals are conceptually processed for goal-oriented upper limb movements. To match the target position with the effector, that is to reach the target with the hand, the latter must be displaced by a distance and in a direction that are represented by the movement vector Δ. To compute Δ, the target and effector positions are compared concurrently in the visual, v, and proprioceptive, p, space (Tagliabue and McIntyre, 2011). This is represented by the following equations of the visual and proprioceptive target-effector comparisons v and p:

$$\begin{aligned} \Delta V &= x_{T,v} - x_{E,v} \\ \Delta P &= x_{T,p} - x_{E,p} \end{aligned} \tag{1}$$

where T and E subscripts indicate an information about the target and the effector, respectively. For each sensory modality, the comparison is characterized by a variance corresponding to the sum of the variances of the target and effector information (Eq. 2).

$$\begin{aligned} \sigma^2_{\Delta V} &= \sigma^2_{T,v} + \sigma^2_{E,v} \\ \sigma^2_{\Delta P} &= \sigma^2_{T,p} + \sigma^2_{E,p} \end{aligned} \tag{2}$$

The MLP predicts that in order to maximize the precision of the estimated movement vector Δ, the concurrent visual and proprioceptive comparisons must be combined (summed), as in Eq. 3.

$$\begin{aligned} \Delta &= w_{\Delta V} \cdot \Delta V + w_{\Delta P} \cdot \Delta P \\ w_{\Delta V} &= \frac{\sigma^2_{\Delta P}}{\sigma^2_{\Delta V} + \sigma^2_{\Delta P}} \\ w_{\Delta P} &= \frac{\sigma^2_{\Delta v}}{\sigma^2_{\Delta V} + \sigma^2_{\Delta P}} \end{aligned} \tag{3}$$

Thus, the movement vector is the weighted sum of the concurrent target-effector comparisons, and each comparison is associated to a weight, $w_{\Delta V}$ and $w_{\Delta P}$, whose value depends on the relative variability of the two comparisons.

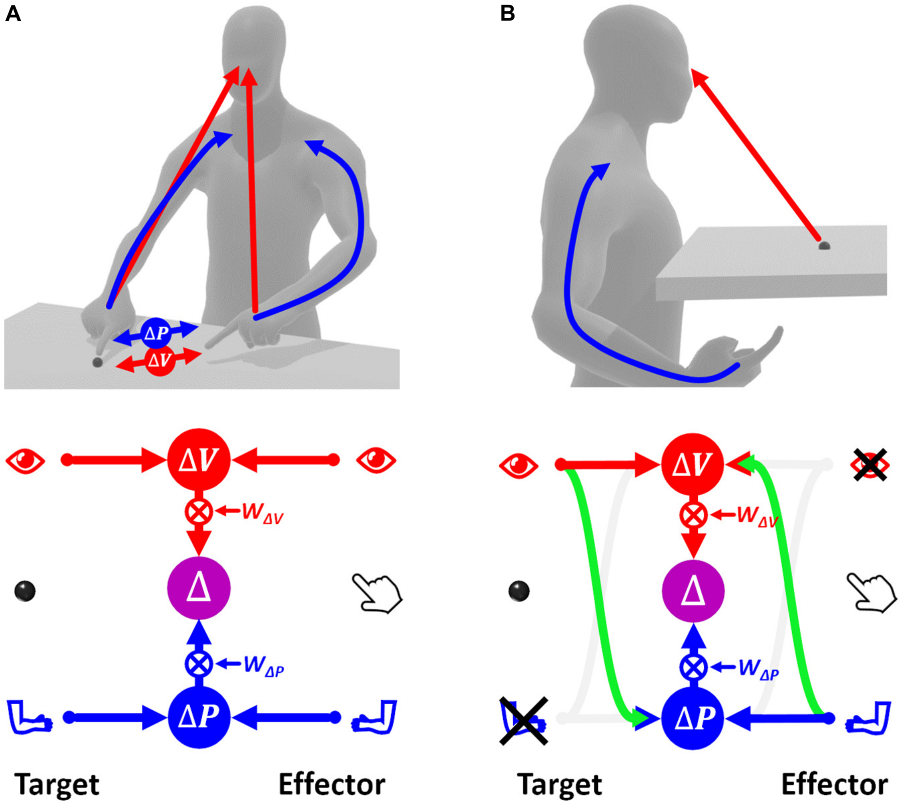

FIGURE 2 | Concurrent Model of sensorimotor integration. In the bottom diagrams the left part represents the target information; the right part represents effector information. Target-effector comparisons are concurrently performed in visual (V) and proprioceptive (P) space. These two comparisons are then combined, using the relative weights w_V and w_P, leading to the optimal estimation of the motor vector. **(A)** Sensory information flow when the hand and target position are perceived through vision and proprioception concurrently. **(B)** Model prediction when the target position is perceived visually and the effector position is sensed through proprioception only. None of the two concurrent comparisons can be computed directly. In this condition, the model postulates occurrence of cross-reference transformations (green curved arrows) between sensory modalities. Blue: proprioceptive information, red: visual information, violet: multimodal visuo-proprioceptive processing.

If this MLP formulation, called "Concurrent Model," is straightforward when both target and effector positions can be perceived through vision and proprioception (**Figure 2A**), the information processing seems more complex when some information is not available, e.g., when the target position can be perceived only visually while the effector position only through proprioception (**Figure 2B**). In this case, none of the two concurrent comparisons can be computed directly, because the target and the effector cannot be perceived through the same sensory modality. However, these comparisons can be performed through two mutually not exclusive possibilities: first, the visually perceived position of the target may be encoded in a proprioceptive space; second, the effector position, provided through proprioception, may be encoded in visual space.

In this condition the variability associated with the two concurrent comparisons is given in Eq. 4 where $\sigma^2_{p\to v}$ and $\sigma^2_{v\to p}$ represent the variance associated with the cross-reference transformations from proprioception to vision, and vice-versa. The indentation is used to facilitate the distinction between the variance associated with the target and effector encoding (the same type of indentation will be used throughout).

$$\begin{array}{llll} & | \quad \text{Target} & | \quad \text{Effector} & \\ \sigma^2_{\Delta V} = \sigma^2_{T,v} & & + \sigma^2_{E,p} + \sigma^2_{p\to v} & \\ \sigma^2_{\Delta P} = \sigma^2_{T,v} + \sigma^2_{v\to p} & & + \sigma^2_{E,p} & \end{array} \tag{4}$$

In contrast to the task represented in **Figure 2A** and Eq. 3, in this condition the two concurrent comparisons are not fully independent, because they are partially computed from the same information. In this case, Eq. 3 must be modified to take into account the covariance between proprioceptive and visual target-effector comparisons, $cov(\triangle P, \triangle V)$ (see **Supplementary Section 1** for details):

$$\begin{aligned} w_{\Delta V} &= \frac{\sigma^2_{\Delta P} - cov(\triangle P, \triangle V)}{\sigma^2_{\Delta V} + \sigma^2_{\Delta P} - 2\cdot cov(\triangle P, \triangle V)} \\ w_{\Delta P} &= \frac{\sigma^2_{\Delta V} - cov(\triangle P, \triangle V)}{\sigma^2_{\Delta V} + \sigma^2_{\Delta P} - 2\cdot cov(\triangle P, \triangle V)} \end{aligned} \tag{5}$$

For the example of **Figure 2B** $cov(\triangle P, \triangle V) = \sigma^2_{T,v} + \sigma^2_{E,p}$, that is the common variance component between $\sigma^2_{\Delta P}$ and $\sigma^2_{\Delta V}$. Therefore, Eq. 5 become:

$$\begin{aligned} w_{\Delta V} &= \frac{\sigma^2_{v\to p}}{\sigma^2_{v\to p} + \sigma^2_{p\to v}} \\ w_{\Delta P} &= \frac{\sigma^2_{p\to v}}{\sigma^2_{v\to p} + \sigma^2_{p\to v}} \end{aligned} \tag{6}$$

It follows that the relative weights between the two concurrent object-effector comparisons depend on the noisiness of the two cross-modal transformations, which is consistent with experimental observations (Burns and Blohm, 2010; Tagliabue et al., 2013).

Application of the Optimal Sensory Integration Theory to Proprioception Assessment Tests

In the following we will show whether the MLP predicts clear differences between the sensory processing necessary to accomplish the tasks depending on their categorization described in the previous section.

In order to be able to represent consistently the type of sensory processing underlying the execution of tasks within these four categories, we will use a slightly modified formulation of the Concurrent Model with respect to the one presented in section above. This formulation, represented in **Figure 3**, explicitly distinguishes between the reference frames in which the sensory signals are natively encoded (the joint, *J*, and the retinal, *R*, reference frames for proprioception and vision, respectively) and the reference frames which correspond to a combination of the original sensory signal about target and response position, with additional sensory information. For instance, the hand position perceived through joint receptors can be encoded with respect to different body parts or even with respect to external references, such as gravity or visual landmarks (Tagliabue and McIntyre, 2014). To refer to this type of indirect sensory encodings we use the generic term "extra-joint," *ExJ*, for proprioception and "extra-retinal," *ExR*, for vision.

Although both visual and proprioceptive information can potentially be encoded in multiple "extra-" reference frames, we have reduced the model formulation to its simplest version

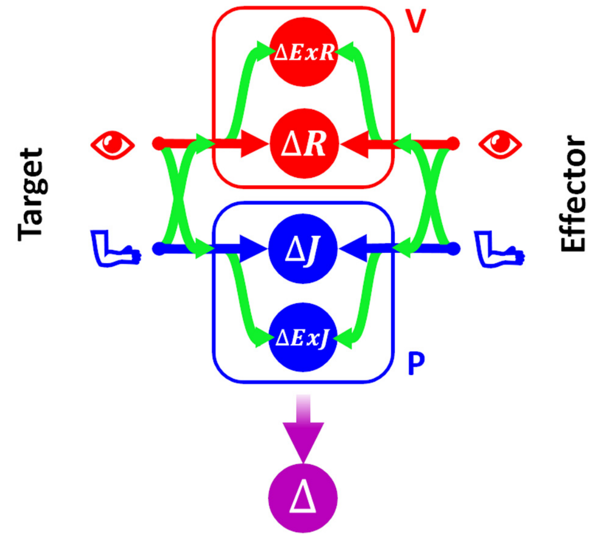

FIGURE 3 | Concurrent Model for proprioceptive assessment tasks. Sensory inputs from the target and the effector are concurrently compared in four reference-frames: retino-centered (Δ*R*), joint-centered (Δ*J*), extra-retinal (Δ*ExR*), and extra-joint (Δ*ExJ*). The visual (red) and proprioceptive (blue) signals are primarily encoded in retino-centered and joint-centered reference frames, respectively, but they can also be encoded in additional "secondary" reference frames not directly associated with the respective receptors. To encode a sensory signal in a secondary reference frame, cross-reference transformations (represented by the curved green arrows) are necessary.

allowing an accurate description of the sensory processing underlying the analyzed tasks. As a consequence, the present formulation of MLP includes four concurrent target-effector comparisons: $\triangle J$, $\triangle R$, $\triangle ExJ$, $\triangle ExR$. In this formulation of the concurrent model the estimation of the motor vector $\triangle$ corresponds to the following weighted sum:

$$\Delta = w_{\Delta J}\Delta J + w_{\Delta ExJ}\Delta ExJ + w_{\Delta R}\Delta R + w_{\Delta ExR}\Delta ExR \tag{7}$$

To represent all possible cross-reference transformations between these four reference frames, this model includes not only the possibility to perform cross-reference transformations between proprioceptive, joint-centered, and visual, retino-centered reference frames ($J \leftrightarrow R$), but also the possibility to encode joint and retinal signals in the extra-joint and extra-retinal reference frames, respectively ($J \rightarrow ExJ$ and $R \rightarrow ExR$).

In the following this statistical model will be used to evaluate, for each of the categories of proprioceptive assessments, the relative weights that must be associated with the four concurrent target-effector comparisons to optimize the precision of the movement vector estimation, Δ. The precise values of the sensory weight and details of the methods used are reported in **Supplementary Sections 2, 3**. In the following paragraphs these results will be only graphically described in the figures representing the information flow theoretically associated with each category of tasks. The analytical equation of the variability of the optimal motor vector estimation predicted by MLP will be reported for each test and will then be quantitatively compared to the results of experimental studies.

Within-Arm Proprioceptive Tasks (W-A*P*)

In this test the memorized target and the effector positions are perceived through the same set of joint sensors. Thus, their position can be compared "directly" in the joint space *J*. All three other concurrent comparisons would require some cross-reference transformation. The variance associated with each of the four concurrent target-response comparisons for the W-A*P* tasks is reported in Eq. 8, where $\sigma^2_{J\rightarrow R}$ is the variance associated with the cross-reference transformation from the joint-centered to the retino-centered reference frame. $\sigma^2_{J\rightarrow ExJ}$, $\sigma^2_{R\rightarrow ExR}$ are the variances corresponding to the intra-modal transformations from joint to extra-joint and from retinal to extra-retinal references, respectively.

$$\begin{aligned}
\sigma^2_{\triangle J} &= \sigma^2_J & &+ \sigma^2_J \\
\sigma^2_{\triangle ExJ} &= \sigma^2_J + \sigma^2_{J\rightarrow ExJ} & &+`\sigma^2_J + \sigma^2_{J\rightarrow ExJ} \\
\sigma^2_{\triangle R} &= \sigma^2_J + \sigma^2_{J\rightarrow R} & &+ \sigma^2_J + \sigma^2_{J\rightarrow R} \\
\sigma^2_{\triangle ExR} &= \sigma^2_J + \sigma^2_{J\rightarrow R} + \sigma^2_{R\rightarrow ExR} & &+ \sigma^2_J + \sigma^2_{J\rightarrow R} + \sigma^2_{R\rightarrow ExR}
\end{aligned} \tag{8}$$

The optimal information flow predicted by MLP is represented in **Figure 4A**: the model predicts no use of the reconstructed representations of the task, and the "exclusive" use of the comparison in the joint space does not require any cross-reference transformation. This phenomenon was clearly shown in unimodal, proprioceptive tasks involving only one arm (Tagliabue and McIntyre, 2011, 2013; Arnoux et al., 2017). The variance of the movement vector estimation corresponding to this optimal sensory processing is

$$\sigma^2_{\triangle} = 2\sigma^2_J \tag{9}$$

Asymmetric Between-Arms Proprioceptive Tasks (aB-A*P*)

The asymmetric configuration of the limb during this test results in the impossibility to achieve the task by simply matching the joint signals from the two arms. Mathematically, this impossibility is represented by a large variance associated with the transformation of the proprioceptive joint signals between the left and right arm: $\sigma^2_{J_{l\rightarrow r}} = \sigma^2_{J_{r\rightarrow l}} \rightarrow \infty$. The variances associated with the four concurrent target-effector comparisons are thus:

$$\begin{aligned}
\sigma^2_{\triangle J} &= \sigma^2_{J_l} + \sigma^2_{J_{l\rightarrow r}} & &+ \sigma^2_{J_r} + \sigma^2_{J_{r\rightarrow l}} \\
\sigma^2_{\triangle ExJ} &= \sigma^2_{J_l} + \sigma^2_{J_l\rightarrow ExJ} & &+ \sigma^2_{J_r} + \sigma^2_{J_r\rightarrow ExJ} \\
\sigma^2_{\triangle R} &= \sigma^2_{J_l} + \sigma^2_{J_l\rightarrow R} & &+ \sigma^2_{J_r} + \sigma^2_{J_r\rightarrow R} \\
\sigma^2_{\triangle ExR} &= \sigma^2_{J_l} + \sigma^2_{J_l\rightarrow R} + \sigma^2_{R\rightarrow ExR} & &+ \sigma^2_{J_r} + \sigma^2_{J_r\rightarrow R} + \sigma^2_{R\rightarrow ExR}
\end{aligned} \tag{10}$$

If we assume that the cross-reference transformations from the left and right arm joints are characterized by the same variance ($\sigma^2_{J_l\rightarrow ExJ} = \sigma^2_{J_r\rightarrow ExJ}$ and $\sigma^2_{J_l\rightarrow R} = \sigma^2_{J_r\rightarrow R}$), the optimal sensory weighting predicted by MLP (**Figure 4B**), consists in encoding the position of the two hands perceived through proprioception in alternative reference frames, including the retinal one, rather than in joint space. This prediction is consistent with experimental observations on healthy subjects suggesting that retinal and external references contribute to the encoding of asymmetric between-arm tasks (Pouget et al., 2002; McGuire and Sabes, 2009; Jones and Henriques, 2010; Tagliabue and McIntyre, 2013; Arnoux et al., 2017). Tagliabue and McIntyre (2013) showed that it is the use of tasks that require asymmetric joint configurations in the above-mentioned studies that led to the visual reconstruction of proprioceptive signals.

The minimal achievable variability of the Δ estimation for these tasks is:

$$\sigma^2_{\triangle} = \sigma^2_{J_r} + \sigma^2_{J_l} + \frac{2\sigma^2_{J\rightarrow R}\sigma^2_{J\rightarrow ExJ}}{\sigma^2_{J\rightarrow R} + \sigma^2_{J\rightarrow ExJ}} \tag{11}$$

Thus in the aB-A*P* tasks, the predicted variability of Δ is higher than for the W-A tasks, as experimentally observed (Tagliabue and McIntyre, 2013; Arnoux et al., 2017).

Symmetric Between-Arms Proprioceptive Tasks (sB-A*P*)

Experiments on healthy subjects have shown that, in contrast to what has been observed for the aB-A*P* tests, the precision of this type of symmetric tasks is very similar to the one observed in within-arm tasks, W-A*P*, and no evidence of visual encoding was

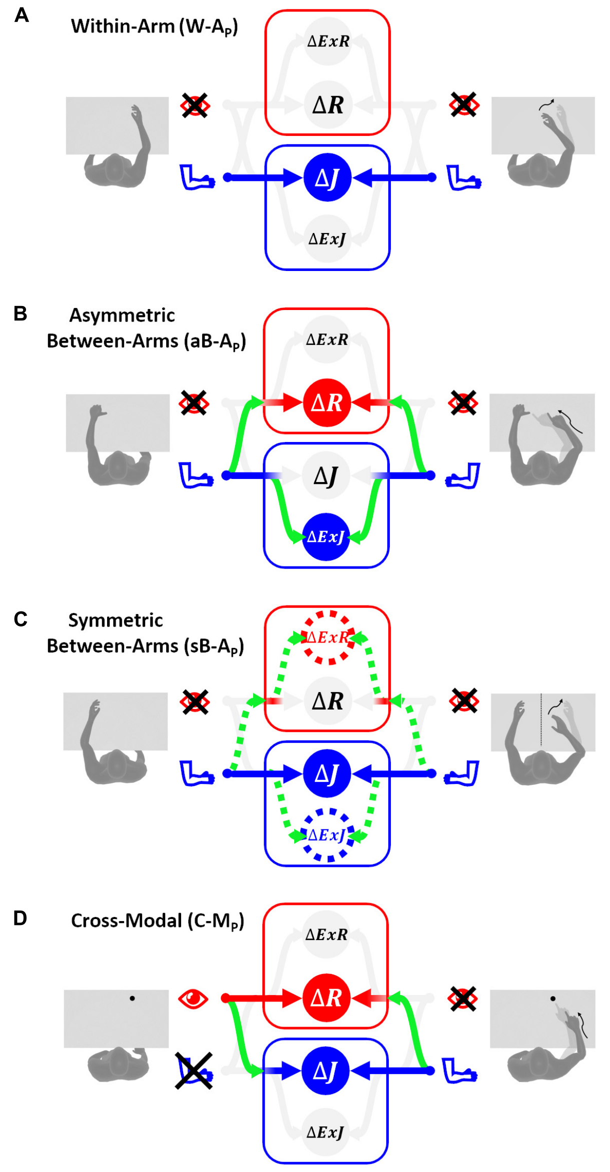

FIGURE 4 | Sensory information flow predicted for proprioceptive tests. The model results are reported separately for the four categories of tests without vision of the arms: **(A)** within-arm task (W-A$_P$), proprioceptive joint signals from the right arm during the target memorization (left column) can be directly compared with proprioceptive joint signals from the same arm during the response phase (right column). **(B)** Asymmetric between-arms task (aB-A$_P$), the task cannot be achieved by simply matching the homologous proprioceptive joint signals from the left and right arm: the use of alternative reference frames and cross-reference transformations (green curved arrows) is necessary. **(C)** Symmetric between-arms task (sB-A$_P$), proprioceptive joint signals from the left arm during the target memorization can theoretically be compared directly with the homologous proprioceptive joint signals from the right arm. However, for patients with inter-hemispheric transformation impairment, indirect comparisons (doted lines) are necessary.
(D) Cross-modal task (C-M$_P$), the target and the effector do not share the same sensory modality. The model prediction in this situation consists in encoding the task in both joint and retinal space by performing the depicted cross-reference transformation. The target-effector comparisons performed in a sensory space associated with a weight close to zero are in pale gray, while those associated with weights significantly larger than zero are in bright colors.

found (Arnoux et al., 2017). These similarities appear to be due to the same joint configuration of the arm holding the target and the arm performing the movement when achieving sB-A$_P$ tasks. Hence, the movement can be controlled by a "direct" comparison between proprioceptive signals from homologous joints of the two limbs (**Figure 4C**).

The variances associated with the four concurrent target-effector comparisons for the mirroring tasks can be expressed as reported in Eq. 12.

$$
\begin{aligned}
\sigma^2_{\triangle J} &= \sigma^2_{J_l} + \sigma^2_{J_{l\to r}} && + \sigma^2_{J_r} + \sigma^2_{J_{r\to l}} \\
\sigma^2_{\triangle ExJ} &= \sigma^2_{J_l} + \sigma^2_{J_l\to ExJ} && + \sigma^2_{J_r} + \sigma^2_{J_r\to ExJ} \\
\sigma^2_{\triangle R} &= \sigma^2_{J_l} + \sigma^2_{J_l\to R} && + \sigma^2_{J_r} + \sigma^2_{J_r\to R} + \sigma^2_{R,Mir} \\
\sigma^2_{\triangle ExR} &= \sigma^2_{J_l} + \sigma^2_{J_l\to R} + \sigma^2_{R\to ExR} && + \sigma^2_{J_r} + \sigma^2_{J_r\to R} + \sigma^2_{R\to ExR}
\end{aligned}
\tag{12}
$$

These equations appear very similar to those describing the asymmetric between-arms tasks (Eq. 10), but there are two important differences, which reflect the different nature of the mirror task and the above-mentioned experimental observations. First, the parameter $\sigma^2_{R,Mir}$ is added to $\sigma^2_{\Delta R}$. This parameter, which is very large ($\sigma^2_{R,Mir} \to \infty$), reflects the impossibility to perform the task directly in retinal space: since the two hands must be in two distinct spatial locations, the task cannot be accomplished by matching the reconstructed image of the two hands on the retina. Second, the possibility of directly comparing proprioceptive signals from the two arms is represented by very low values of the variance associated to the transformation of the joint signals between the left and right arm: $\sigma^2_{J_{l\to r}} = \sigma^2_{J_{r\to l}} \to 0$. However, these parameters have not been removed from the equations to be able to describe the behavior of some of the stroke patients. An increase of the value of $\sigma^2_{J_{l\to r}}$ and $\sigma^2_{J_{r\to l}}$ can indeed be used to represent the observed difficulties of some patients in performing sB-A$_P$ test with respect to the W-A$_P$ tasks (Gurari et al., 2017).

Figure 4C reports the information flow predicted by MLP for two categories of patients: those that have difficulties in performing inter-hemispheric transformations ($\sigma^2_{Jr\leftrightarrow l} > 0$; dashed lines) and those that do not have this problem ($\sigma^2_{J_{r\leftrightarrow l}} \to 0$). For the latter category of patients, the proprioceptive information is encoded in joint space only, as for the within-arm tasks. For the patients with inter-hemispheric transformation issues MLP predicts an encoding of the information also in Extra-Joint and Extra-Retinal space.

Equation 13 reports the minimally achievable variability of the motor vector estimation.

$$
\sigma^2_{\triangle} = \sigma^2_{J_r} + \sigma^2_{J_l} + \frac{2\sigma^2_{Jr\leftrightarrow l}\sigma^2_{J\to ExJ}\left(\sigma^2_{J\to R} + \sigma^2_{R\to ExR}\right)}{(\sigma^2_{J\to R}+\sigma^2_{R\to ExR})(\sigma^2_{J\to ExJ} + \sigma^2_{Jr\leftrightarrow l}) + \sigma^2_{J\to ExJ}\sigma^2_{Jr\leftrightarrow l}}
\to \sigma^2_{J_r} + \sigma^2_{J_l} \tag{13}
$$

In healthy subjects or in patients without inter-hemispheric transformation problems ($\sigma^2_{J_{r\leftrightarrow l}} \to 0$), **Figure 4C** and Eq. 13 suggest that the sensory weighting and the motor vector variance tend to those predicted for the W-A$_P$ tasks (**Figure 4A** and Eq. 9): encoding of the information in joint space only and minimal variability of the responses. This prediction is consistent with the experimentally observed similarities between the performances in sB-A$_P$ and W-A$_P$ tasks for healthy subjects (Tagliabue and McIntyre, 2013; Arnoux et al., 2017) and with the performances of some stroke patients (Herter et al., 2019).

The MLP prediction for stroke patients with a difficulty to compare joint signals from the affected to the less-affected side ($\sigma^2_{Jr\leftrightarrow l} > 0$) appears to provide some interesting insight into the patient's deterioration of performances in the Mirror Position Test, with respect to the Within-arm Position Test (Gurari et al., 2017) discussed in section "Upper Limb Proprioceptive Deficits Post-stroke." Equation 13 shows that the increased variability in the mirror task can be correctly predicted if the noise associated with the inter-hemispheric comparison of the joint signals ($\sigma^2_{Jr\leftrightarrow l}$) is significantly larger than that for healthy patients. In other words, lower performances in patients assessed by the Mirror Position Test could be due to a problem in the neural inter-hemispheric processing and not due to a proprioceptive problem *per se*.

Cross-Modal Tasks (C-M$_P$)

Contrary to the other categories of tasks, C-M$_P$ tasks involve a visually memorized target which the patient has to match with the eyes closed (**Figure 4D**). In these tasks no direct comparison is possible between the target and effector. Thus, cross-reference transformations are strictly necessary. The variability associated with the four concurrent comparisons is:

$$\begin{aligned}
\sigma^2_{\triangle J} &= \sigma^2_R + \sigma^2_{R\to J} + \sigma^2_J \\
\sigma^2_{\triangle ExJ} &= \sigma^2_R + \sigma^2_{R\to J} + \sigma^2_{J\to ExJ} + \sigma^2_J + \sigma^2_{J\to ExJ} \\
\sigma^2_{\triangle R} &= \sigma^2_R + \sigma^2_J + \sigma^2_{J\to R} \\
\sigma^2_{\triangle ExR} &= \sigma^2_R + \sigma^2_{R\to ExR} + \sigma^2_J + \sigma^2_{J\to R} + \sigma^2_{R\to ExR}
\end{aligned} \tag{14}$$

σ^2_R refers to the variability associated with the retinal inputs of the target location. If we assume that the noise associated with the transformation of the sensory signals from retinal to joint space and from joint to retinal space are similar ($\sigma^2_{R\to J} = \sigma^2_{J\to R} = \sigma^2_{J\leftrightarrow R}$), then the sensory weights predicted by the MLP are those represented in **Figure 4D** and the corresponding minimal variance of the estimated movement vector Δ is:

$$\sigma^2_{\triangle} = \sigma^2_J + \sigma^2_R + \frac{\sigma^2_{J\leftrightarrow R}}{2} \tag{15}$$

It follows that degraded performances of stroke patients when performing this category of tasks could be due, not only to a noisy proprioceptive system, but also to difficulties in the encoding of retinal information in joint space or, vice-versa, proprioceptive information in a retinal reference.

Application of the Optimal Sensory Integration Theory to Visual Compensation Tests

The MLP also renders predictions for the visual compensation tests in which stroke patients can use visual feedback to perform the tasks. In the following we will apply the Concurrent Model to the execution of the same four categories of tasks analyzed in the previous section (W-A, aB-A, sB-A, and C-M) but including the availability of visual information about both target and effector position. σ^2_R will be used to refer to the variability associated with the retinal inputs of both target and effector locations.

Within-Arm Visuo-Proprioceptive Tasks (W-A$_{VP}$)

Equations 16 represent the variance associated with the four concurrent comparisons for the within-arm tasks using both proprioceptive and visual information.

$$\begin{aligned}
\sigma^2_{\triangle J} &= \sigma^2_J + \sigma^2_J \\
\sigma^2_{\triangle ExJ} &= \sigma^2_J + \sigma^2_{J\to ExJ} + \sigma^2_J + \sigma^2_{J\to ExJ} \\
\sigma^2_{\triangle R} &= \sigma^2_R + \sigma^2_R \\
\sigma^2_{\triangle ExR} &= \sigma^2_R + \sigma^2_{R\to ExR} + \sigma^2_R + \sigma^2_{R\to ExR}
\end{aligned} \tag{16}$$

The first two equations, representing the proprioceptive comparison in Joint and Extra-Joint space, are identical to those reported for the W-A$_P$ tasks in Eq. 8. The last two equations represent the visual comparison in Retinal and Extra-Retinal space. The target and effector images on the retina can be compared directly. Therefore, the variability of the retinal comparison, $\sigma^2_{\triangle R}$, simply corresponds to the sum of the variability of the retinal information about the target and the effector position. The visual extra-retinal comparison, $\triangle ExR$, on the other hand, must include the terms $\sigma^2_{R\to ExR}$, associated with the transformation from the retinal to the extra-retinal reference frame.

As shown in **Figure 5A**, MLP predicts that for the W-A$_{VP}$ task there would be no sensory encoding in extra-joint or extra-retinal reference. This is due to the fact that, for both visual and proprioceptive modality, the information can be directly compared in the reference frame corresponding to the originating sensory system. The retinal and joint comparisons are weighted as predicted by the standard MLP formulation (Eq. 3), taking into account only the relative variance of the available sources of information (Ernst and Banks, 2002). The variability of the estimation of the movement vector Δ corresponding to this optimal sensory weighting is:

$$\sigma^2_{\triangle} = \frac{2\sigma^2_J\sigma^2_R}{\sigma^2_J + \sigma^2_R} \tag{17}$$

The comparison of these results with the corresponding prediction for the proprioceptive task (Eq. 9) suggests that patients should be able to visually compensate in this category of tasks, independently from their ability to perform cross-reference transformations: $\frac{2\sigma^2_J\sigma^2_R}{\sigma^2_J + \sigma^2_R}$ is always smaller than $2\sigma^2_J$

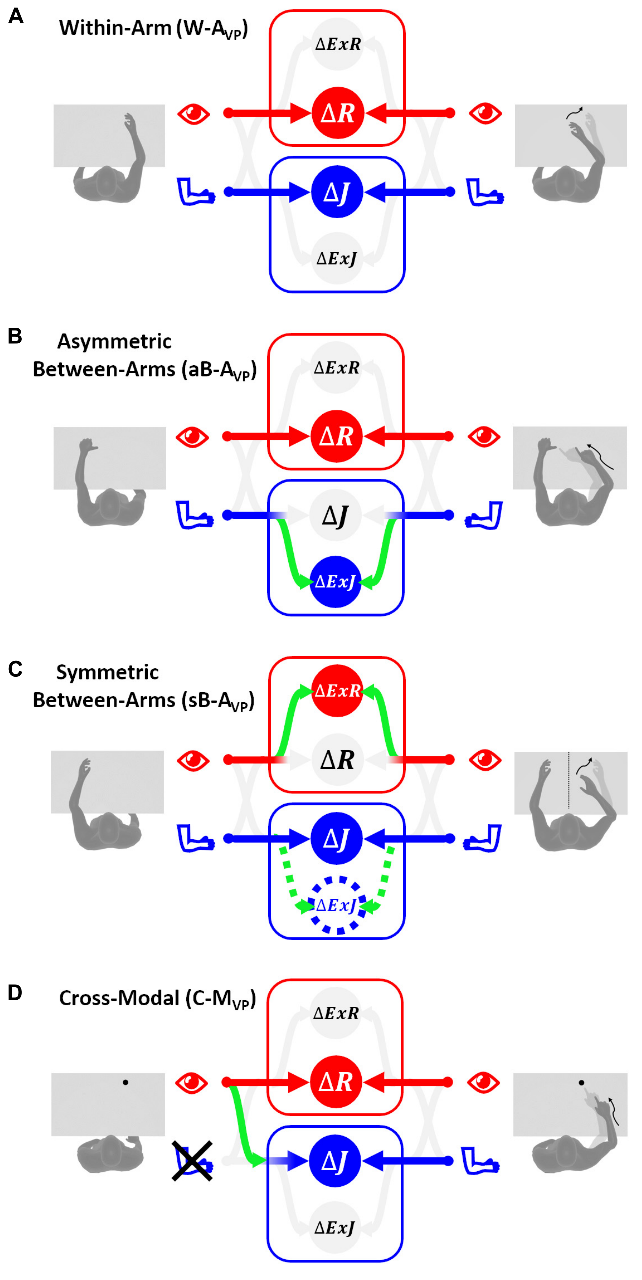

FIGURE 5 | Sensory information flow predicted for visual compensation tests. The model results are reported separately for the four categories of tests with vision: **(A)** within-arm task (W-A$_{VP}$), both proprioceptive and visual signals from the target and the effector can be directly compared in their primary reference frames. **(B)** Asymmetric between-arms task (aB-A$_{VP}$), the proprioceptive target-effector comparison cannot be encoded in the primary joint space, while the visual comparison can be performed directly in the retinal space. **(C)** Symmetric between-arms task (sB-A$_{VP}$), the proprioceptive target-effector comparison is performed directly in the primary joint space only for patients without inter-hemispheric transformation deficits. In order to compare the visual position of the two hands that are far apart, all patients have to encode the retinal signals in some extra-retinal space.
(D) Cross-modal task (C-M$_{VP}$), the proprioceptive target-effector comparison in joint space can be performed through a cross-reference transformation, while visual signals from the target and the reaching movement can be directly compared in retinal space.

and this difference is not affected by the variance of the sensory transformations reported in Eq. 16. This comparison also shows that, the stronger the proprioceptive deficit, the larger will be the advantage provided by using visual information. This prediction is consistent with the observation that stroke patients can compensate through vision for their proprioceptive deficits in this type of tasks (Torre et al., 2013).

Asymmetric Between-Arms Visuo-Proprioceptive Tasks (aB-A$_{VP}$)

In these tasks, as previously explained for the aB-A$_P$ tests, a direct comparison between the proprioceptive information in joint space is not possible ($\sigma^2_{J_{l\leftrightarrow r}} \rightarrow \infty$). On the other hand, target and effector can be compared directly in retinal coordinates because the task achievement corresponds to the matching of their respective positions on the retina. As a consequence, the concurrent comparison for these tasks are associated with the following variances:

$$\begin{aligned}
\sigma^2_{\Delta J} &= \sigma^2_{J_l} + \sigma^2_{J_{l\rightarrow r}} + \sigma^2_{J_r} + \sigma^2_{J_{r\rightarrow l}} \\
\sigma^2_{\Delta ExJ} &= \sigma^2_{J_l} + \sigma^2_{J_l\rightarrow ExJ} + \sigma^2_{J_r} + \sigma^2_{J_r\rightarrow ExJ} \\
\sigma^2_{\Delta R} &= \sigma^2_{R} + \sigma^2_{R} \\
\sigma^2_{\Delta ExR} &= \sigma^2_{R} + \sigma^2_{R\rightarrow ExR} + \sigma^2_{R} + \sigma^2_{R\rightarrow ExR}
\end{aligned} \tag{18}$$

Figure 5B shows that the sensory information flow corresponding to the minimal variability of the aB-A$_{VP}$ task consists, theoretically, in the encoding of proprioceptive information in extra-joint spaces, while visual information is directly encoded in retinal space. Proprioceptive information is not encoded in the joint reference frame, because, as discussed for the corresponding proprioceptive task aB-A$_P$, the comparison in the joint space is not possible. The visual information is not encoded in extra-retinal references, because, although $\triangle ExR$ would be theoretically possible, it would fully covary with $\triangle R$. In other words, the extra-retinal encoding would not provide any additional information over the retinal encoding, and would not contribute to reduce the variance of the motor vector estimate, which is given in Eq. 19.

$$\sigma^2_{\triangle} \rightarrow \frac{2\sigma^2_R(\sigma^2_{J_r} + \sigma^2_{J_l} + 2\sigma^2_{J\rightarrow ExJ})}{\sigma^2_{J_r} + \sigma^2_{J_l} + 2\sigma^2_{J\rightarrow ExJ} + 2\sigma^2_R} \tag{19}$$

The comparison of this result with the one obtained in Eq. 11 for the corresponding proprioceptive task aB-Ap (see the **Supplementary Section 4**), shows that in normal conditions the noisiness of the motor vector estimation in the visuo-proprioceptive task is always smaller than for the proprioceptive task. Thus, MLP predicts for this kind of asymmetric tasks that the patients should be able to compensate their proprioceptive deficits by using vision, consistent with experimental observations (Scalha et al., 2011).

Symmetric Between-Arms Visuo-Proprioceptive Tasks (sB-A$_{VP}$)

For these tasks, the considerations about inter-hemispheric transfer of joint signals presented for the corresponding proprioceptive tasks (sB-A$_P$) remain valid: the value of the $\sigma^2_{J_{r\leftrightarrow l}}$ parameter allows distinguishing patients with problems in comparing joint information from the two arms ($\sigma^2_{J_{r\leftrightarrow l}} > 0$) from healthy subjects and patients not showing this deficit ($\sigma^2_{J_{r\leftrightarrow l}} \rightarrow 0$). The considerations about the impossibility of performing the task by directly comparing the visual feedback about the target and the effector ($\sigma^2_{R,Mir} \rightarrow \infty$) also remain valid.

Equations 20, which describe the variability associated with the four concurrent comparisons for this type of tasks, differ from the analogous equations of the proprioceptive sB-A$_P$ task (Eq. 12), simply by the fact that $\triangle R$ and $\triangle ExR$ are computed from the available retinal information (R) and not through cross-reference transformations of proprioceptive signals ($J \rightarrow R$).

$$\begin{aligned}
\sigma^2_{\triangle J} &= \sigma^2_{J_l} + \sigma^2_{J_{l\rightarrow r}} + \sigma^2_{J_r} + \sigma^2_{J_{r\rightarrow l}} \\
\sigma^2_{\triangle ExJ} &= \sigma^2_{J_l} + \sigma^2_{J_l\rightarrow ExJ} + \sigma^2_{J_r} + \sigma^2_{J_r\rightarrow ExJ} \\
\sigma^2_{\triangle R} &= \sigma^2_{R} + \sigma^2_{R} + \sigma^2_{R,Mir} \\
\sigma^2_{\triangle ExR} &= \sigma^2_{R} + \sigma^2_{R\rightarrow ExR} + \sigma^2_{R} + \sigma^2_{R\rightarrow ExR}
\end{aligned} \tag{20}$$

The optimal weights associated with the four concurrent target-response comparisons are represented in **Figure 5C**. The predicted sensory information flow is reported for patients both with and without inter-hemispheric transformation deficits. The MLP prediction suggests that to achieve optimal performance stroke patients with problems in comparing joint signals from the two arms should encode proprioceptive information in both joint and extra-joint space, and visual information in extra-retinal space only. Patients without inter-hemispheric communication issues, on the other hand, should encode proprioceptive information in joint space only and visual information in extra-retinal references only.

The variability of the optimal motor vector estimation is shown in Eq. 21. The equation reports, first, the prediction for patients with inter-hemispheric transformation deficits ($\sigma^2_{J_{r\leftrightarrow l}} > 0$) and then for patients without problems in comparing the sensory information coming from the two arms ($\sigma^2_{J_{r\leftrightarrow l}} \rightarrow 0$).

$$\begin{aligned}
\sigma^2_{\triangle} &\rightarrow \frac{2(\sigma^2_R + \sigma^2_{R\rightarrow ExR})((\sigma^2_{J_r} + \sigma^2_{J_l})(\sigma^2_{J\rightarrow ExJ} + \sigma^2_{Jr\leftrightarrow l}) + 2\sigma^2_{J\rightarrow ExJ}\sigma^2_{Jr\leftrightarrow l})}{(\sigma^2_{J\rightarrow ExJ} + \sigma^2_{Jr\leftrightarrow l})(\sigma^2_{J_r} + \sigma^2_{J_l} + 2\sigma^2_R + 2\sigma^2_{R\rightarrow ExR}) + 2\sigma^2_{J\rightarrow ExJ}\sigma^2_{Jr\leftrightarrow l}} \\
&\rightarrow \frac{2(\sigma^2_R + \sigma^2_{R\rightarrow ExR})(\sigma^2_{J_r} + \sigma^2_{J_l})}{(2\sigma^2_R + 2\sigma^2_{R\rightarrow ExR}) + (\sigma^2_{J_r} + \sigma^2_{J_l})}
\end{aligned} \tag{21}$$

The comparison of these results with those reported in Eq. 13 for the corresponding proprioceptive task, sB-A$_P$ (see **Supplementary Section 4** for details) suggests different visual compensation mechanism for the patient with and without inter-hemispheric transformation issues. For patients without problems in comparing joint signals from the two arms, the availability of visual information should result in a direct reduction of the noisiness of the estimation of the motor vector. For the patients with problems in comparing joint information from the two arms, the possibility to reduce the noise of the motor vector estimate appears to be more limited and to depend on the relative noisiness associated to cross-reference transformations. The inability observed in some stroke patients to use visual information to improve their performances with respect to analogous proprioceptive tasks (Semrau et al., 2018; Herter et al., 2019) could, therefore, be due to difficulties in performing inter-hemispheric and cross-reference transformations.

Cross-Modal Tasks (C-M$_{VP}$)

As shown in **Figure 5D**, since the target is not perceived proprioceptively, no direct comparison is possible between the target and effector in joint space in this task. Hence a cross-reference transformation ($\sigma^2_{R\rightarrow J}$) would be necessary to make use of the proprioceptive signal on effector position. The variability associated with the four concurrent comparisons is given in Eq. 22.

$$\begin{aligned}
\sigma^2_{\triangle J} &= \sigma^2_{R} + \sigma^2_{R\rightarrow J} + \sigma^2_{J} \\
\sigma^2_{\triangle ExJ} &= \sigma^2_{R} + \sigma^2_{R\rightarrow J} + \sigma^2_{J\rightarrow ExJ} + \sigma^2_{J} + \sigma^2_{J\rightarrow ExJ} \\
\sigma^2_{\triangle R} &= \sigma^2_{R} + \sigma^2_{R} \\
\sigma^2_{\triangle ExR} &= \sigma^2_{R} + \sigma^2_{R\rightarrow ExR} + \sigma^2_{R} + \sigma^2_{R\rightarrow ExR}
\end{aligned} \tag{22}$$

MLP predicts that the optimal solution for this type of tasks is to encode the proprioceptive and visual information directly in joint and retinal space, respectively. The variance of the estimated movement vector corresponding to this optimal solution is given in Eq. 23.

$$\sigma^2_{\triangle} = \frac{\sigma^2_R(2\sigma^2_J + \sigma^2_R + 2\sigma^2_{R\rightarrow J})}{\sigma^2_J + \sigma^2_{R\rightarrow J} + \sigma^2_R} \tag{23}$$

The comparison between this result and the variability of the movement vector estimation in the corresponding proprioceptive task C-M$_P$ of Eq. 15 (see **Supplementary Section 4**) shows that, unless visual information is extremely noisy, its availability should lead to a reduction of the variance of $\triangle$. It follows that, for this category of task, MLP predicts that the patients should show a clear visual compensation of their proprioceptive deficit. This prediction is in agreement with the visual compensation experimentally observed in stroke patients for this category of tasks (Darling et al., 2008; Scalha et al., 2011).

REINTERPRETATION OF EXPERIMENTAL OBSERVATIONS ABOUT PROPRIOCEPTIVE DEFICITS AND VISUAL COMPENSATION

After having described the theoretical sensory information flow underlying the four categories of tasks used to test proprioception and visual compensation, we assess the ability of the model to capture the relevant experimental findings described in the first sections. In order to avoid data overfitting, the number of model parameters is reduced to six: the noise of the joint (σ^2_J) and retinal (σ^2_R) signals and the noise associated to sensory transformations (σ^2_T) in healthy subjects; for patients, three terms representing the noise added to the joint signal of the more affected (N_{J_m}) and less affected arm (N_{J_l}) and to the sensory transformations (N_T) due to the deficit of stroke patients.

For this analysis, we will consider three distinct type of patients: P, with proprioceptive deficits only (N_{J_m} and $N_{J_l} > 0$ and $N_T = 0$); C, with cross-reference processing deficits only (N_{J_m} $N_{J_l} = 0$ and $N_T > 0$); and P+C, with combined proprioceptive and cross-reference processing deficits (N_{J_m}, N_{J_l} and $N_T > 0$). In patients of type P, only the noisiness of the proprioceptive joint signals σ^2_J is increased with respect to healthy subjects. For patients of type C, only the noise associated to the sensory transformation ($\sigma^2_{R\leftrightarrow J}$, $\sigma^2_{R\to ExR}$, $\sigma^2_{J\to ExJ}$, $\sigma^2_{Jr\leftrightarrow l}$) is increased with respect to healthy subjects. For patients of type P+C the noise is increased for both proprioception and transformations.

Figure 6 shows the comparison between the quantitative experimental data found in the literature and the prediction of the MLP model for the four categories of proprioceptive tasks (**Figure 6A**) and for the same four tasks performed using vision to compensate for proprioceptive deficits (**Figure 6B**). In order to be able to apply the model to the whole dataset, the results from different studies have to be comparable. This was achieved through their normalization with respect to a reference task. To be able to perform the normalization, among the numerous studies that can be found in the literature, only those reporting a quantitative comparison between at least two of the four categories of tasks (W-A, sB-A, aB-A, and C-M) could be included in the dataset. Performance data of healthy subjects were retrieved from Van Beers et al. (1996), Ernst and Banks (2002), Butler et al. (2004), Monaco et al. (2010), Tagliabue and McIntyre (2011), Torre et al. (2013), Khanafer and Cressman (2014), Cameron and López-Moliner (2015), Arnoux et al. (2017), Herter et al. (2019), and Marini et al. (2019) and those of stroke patients from Scalha et al. (2011), Torre et al. (2013), Dos Santos et al. (2015), Contu et al. (2017), Gurari et al. (2017), Rinderknecht et al. (2018), Herter et al. (2019), and Ingemanson et al. (2019). Details about the dataset, the fitting algorithm and the quantification of the obtained results are given in **Supplementary Section 5**.

Figure 6 shows that the model predicts very different results for healthy subjects and for the three type of patients (P, C, and P+C), depending on the considered task.

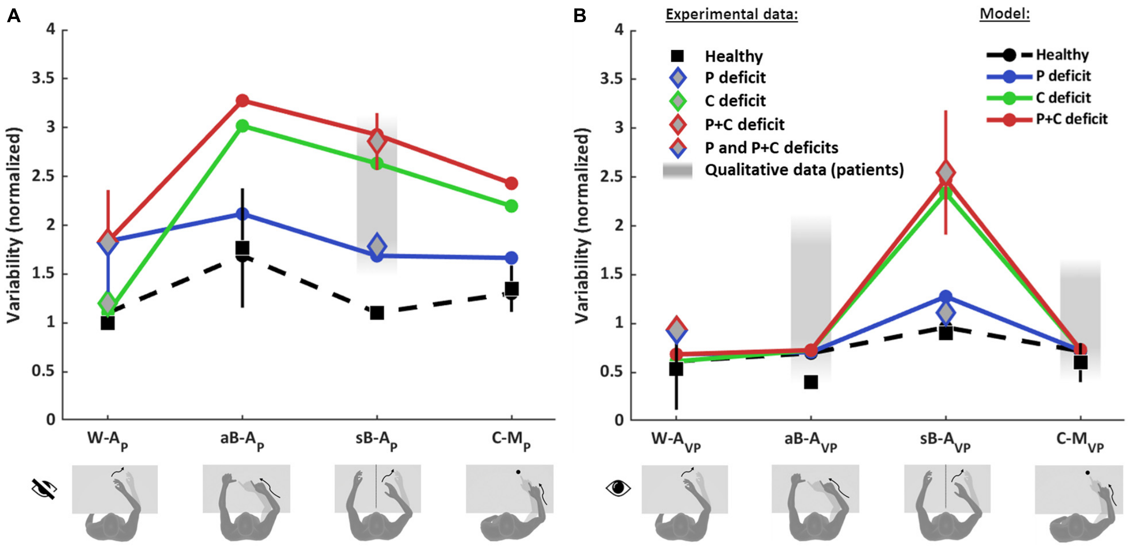

FIGURE 6 | Model predictions and experimental observations for proprioception and visual compensation tests. Data and predictions are reported for the three types of patients: purely proprioceptive deficit (P), cross-reference deficit (C) and mixed proprioceptive and cross reference deficit (P+C), and for healthy subjects. All values are normalized with respect to the variability of healthy subjects in the within-arm proprioceptive task (W-A$_P$). If more than one quantitative study was included in the analysis for a particular task and group of subjects, the mean and standard deviation (vertical whiskers) were used to represent experimental data. Qualitative data from stroke patients (gray filled rectangles) were not used for the fitting. **(A)** Proprioceptive tests. For the W-A$_P$ tasks, the mean of healthy subjects' data is used as reference value for the normalizations. For this tasks, C patients' data can be distinguished from P and P+C patients. For the aB-A$_P$ tasks, only data from healthy subject could be included. For the sB-A$_P$ tasks, both healthy subjects and stroke patients data are available: patients with P deficits perform better and could hence be distinguished from P+C patients. The model results suggest that the data associated to the P+C patients is similar to what is expected also for C patients. The reported qualitative results refer to the same C patients of the W-A$_P$ task. For the C-M$_P$ task, only results from healthy subjects were included. **(B)** Visual compensation tests. For the W-A$_{VP}$ tasks, data from healthy subjects and from stroke patients are reported. For the aB-A$_{VP}$ task, quantitative data were included for healthy subjects. For patients only qualitative observations were found. For the sB-A$_{VP}$ tasks, data from healthy subjects, P patients and P+C patients are reported. The model results suggest that the experimental data associated to P+C patients correspond also to the results expected for C patients. For the C-M$_{VP}$ tasks, as for the asymmetric tasks, quantitative data were found for healthy subjects, but only qualitative observations for patients. Full details about the studies from which the data have been retrieved are reported in **Supplementary Tables 1–4**.

For healthy subjects, MLP reproduces well the experimentally observed modulations of the precision among the eight tasks. In particular, the model correctly predicts that the asymmetric test (aB-A$_{P}$) is the least precise (largest variability) among the proprioceptive tasks (**Figure 6A**) and that the symmetric test (sB-A$_{VP}$) is the less precise among the tasks using vision (**Figure 6B**).

For stroke patients, the results of **Figure 6A** show that the model seems to capture the different experimental data for the within-arm tasks (W-A$_{P}$), suggesting that the heterogeneity of the results would be partially explained by differentiating C patients (Gurari et al., 2017) from P and P+C patients (Dos Santos et al., 2015; Contu et al., 2017; Rinderknecht et al., 2018). For the asymmetric tasks (aB-A$_{P}$), the model predicts a very high variability for the C and P+C patients while the increase with respect to the W-A$_{P}$ task is moderate for P patients. We do not have, however, experimental data to validate the predictions for the patients in this task. For the sB-A$_{P}$ task, the model well captures the heterogeneity of the patients' dataset by distinguishing P patients (Herter et al., 2019) from C and P+C patients (Herter et al., 2019; Ingemanson et al., 2019). Interestingly, this classification is consistent with the fact that P patients were able to visually compensate in the sB-A$_{VP}$ task, whereas C and P+C patients were not able to compensate (Herter et al., 2019). The experimental data represented by a red diamond for sB-A$_{P}$ task were associated with to P+C patients in the fitting procedure, because observations in the literature suggest that P+C patients are more common than C patients. The model prediction suggests, however, that these data could also include C patients. The prediction for the sB-A$_{P}$ task is also consistent with qualitative observations of Gurari et al. (2017) that the same patients that performed without difficulties the W-A$_{P}$ task (classified as C patients) showed significant deficits in a symmetric task. For the cross-modal tasks (C-M$_{P}$), the model predicts that performances of C and P+C patients would be characterized by a variability significantly larger than that of P patients, similarly to the sB-A$_{P}$ task.

Concerning the patients' ability to visually compensate for their proprioceptive deficits (**Figure 6B**), the model predicts that in the W-A$_{VP}$ task all three types of patients (P, C and P+C) should be able to use visual information to improve performance to that of healthy subjects. This prediction is consistent with the experimental observation of Torre et al. (2013) that stroke patients can fully compensate with vision when performing this kind of task, where the information about the target and the effector could be compared directly in both joint and retinal space. For the aB-A$_{VP}$ tasks, the model predicts the same full visual compensation as for the within-arm task. Although we could not find any quantitative experimental results for patients in this type of tasks, the model prediction is coherent with the qualitative observation of Scalha et al. (2011) that patients can significantly improve their performances with vision. For the sB-A$_{VP}$ tasks, the model prediction is very different from the other tasks and it matches the different results obtained by Herter et al. (2019) for patients with low and high levels of visual compensation. The model predictions for this task suggests that the group of patients showing low visual compensation (higher variability) could confound C and P+C patients, although the patients with the ability to visually compensate (lower variability) are probably of type P. For this task, as for the corresponding proprioceptive test sB-A$_{P}$, the model prediction suggests that the experimental data point represented by a red diamond could confound C and P+C patients. For the C-M$_{VP}$ tasks, the same considerations apply as for the aB-A$_{VP}$ task, in terms of model predictions and of matching with qualitative observations.

Altogether, these results suggest that only the W-A$_{P}$ tasks can be considered as "pure proprioception tests." This expression here refers to those tests whose outcome is affected only by deficits of the proprioceptive system, and not by other factors, such as the inability to perform sensory transformations. In contrast, sB-A$_{P}$, aB-A$_{P}$, and C-M$_{P}$ tasks appear to confound proprioceptive deficits and cross-reference transformation deficits, since they are affected by P, C, or P+C deficits. These results also suggest that the visual compensation tests for sB-A$_{VP}$ tasks can assess the patients' ability to perform cross-reference transformations. The reinterpretation of the data of the literature through the MLP framework represented in **Figure 6** additionally suggests that most of the tested stroke patients have mixed P+C deficits (Dos Santos et al., 2015; Contu et al., 2017; Rinderknecht et al., 2018; Herter et al., 2019), but that there are also clear examples of C (Gurari et al., 2017) and P (Herter et al., 2019) categories of patients.

In conclusion, the proposed stratification of patients presented here based on their deficits (P, C, and P+C) appears to be able to explain, and at least partially reconciliate, the different outcomes experimentally obtained with various assessments currently in use in clinical research.

INSIGHTS FROM BRAIN LESIONS AND FUNCTIONAL ANATOMY STUDIES

The neural network responsible for proprioceptive processing seems widely distributed over cortical and subcortical structures (Ben-Shabat et al., 2015; Kessner et al., 2016; Semrau et al., 2018). Beyond the integrity of S1, with a clear impact on proprioception, neural correlates of proprioceptive deficits after stroke remain incompletely understood (Ingemanson et al., 2019). Moreover, no study has yet been undertaken to stratify stroke patients according to the categorization of deficits described in the previous section. However, to probe the clinical potential of this approach we present here a short non-systematic review on brain structures involved in either "pure" proprioceptive perception or cross-reference processing. To that end, we reviewed studies that used functional imaging (fMRI, PET, and EEG after a non-systematic PubMed screening) during proprioceptive and visuo-proprioceptive tasks, as well as imaging-based lesion-symptom mapping (LSM) studies. This should provide a first approximative view on whether brain areas may potentially be dissociated as a function of their involvement in proprioceptive processing according to the described task affordances.

However, there is a caveat: as discussed in the previous section, most stroke patients likely have mixed deficits affecting both proprioception and cross-reference processing. Since a mixed deficit would alter the patients' performances in all task categories (**Figure 6**), only a dedicated protocol would allow dissociating the structures specifically involved in tasks requiring cross-reference processing or not. Unsurprisingly, cortical networks seemed to overlap to a large extent among the reviewed articles, and proprioceptive test categorization did not provide a clear dissociation between the cortical areas activated during tests belonging to one or the other category.

In addition to S1, a number of regions within the posterior parietal cortex (PPC) were identified as critical for proprioceptive perception, assessed with either a W-A$_P$ (Rinderknecht et al., 2018; Kessner et al., 2019) task or a sB-A$_P$ task (Dukelow et al., 2010; Findlater et al., 2016, 2018; Meyer et al., 2016). But the lack of between-task comparisons does not allow for a distinction between the lesions sites affecting primarily the proprioceptive sense *per se* or cross-reference processing. Furthermore, based on these results we cannot conclude whether hemispheric dominance may be related to either proprioception or cross-reference processing.

A comparative approach with different types of tasks is needed to elucidate the sensory deficit and to eventually associate a given sensory deficit to particular brain regions. Unless the study assesses and compares different tasks (Semrau et al., 2018; Herter et al., 2019), or uses functional imaging (Van de Winckel et al., 2012; Ben-Shabat et al., 2015), we cannot draw clear conclusions on which brain areas are important for either sensory function.

According to the presented MLP predictions, we consider W-A$_P$ assessments to be "purely" proprioceptive (**Figure 4A**) in contrast to assessments which involve cross-reference processing (aB-A$_P$, sB-A$_P$, C-M$_P$: see **Figures 4B–D**). We therefore attempted to classify the reviewed functional brain imaging studies accordingly and to probe whether this categorization might result in a processing-specific topological cerebral organization.

"Pure" proprioceptive processing, assessed with a W-A$_P$ tasks seemed to entail primarily the activation of M1 and S1 (Butler et al., 2004; Marini et al., 2019). W-A$_P$ (**Figure 4A**) tasks, the simplest tasks in terms of computational load (see section "Application of the Optimal Sensory Integration Theory to Proprioception Assessment Tests"), are presumably based on simpler networks. In contrast, the mirror task (a sB-A$_P$ task) seem to involve cross-reference processing. And fMRI revealed that a larger brain network was involved compared to W-A$_P$ tasks, with higher activation of the supramarginal gyrus (SMG) and superior temporal gyrus (STG) (Iandolo et al., 2018), in line with Ben-Shabat et al. (2015). In theory, the same mirror task with visual feedback also involves cross-reference processing (sB-A$_{VP}$: **Figure 5C**). An LSM study showed that patients with lesions to the SMG did not improve their performance when adding visual feedback in the mirror test (sB-A$_P$ vs. sB-A$_{VP}$), a result presumably related to cross-reference processing deficit (Semrau et al., 2018). Patients that improved to normal performance with vision, i.e., presumably patients with "pure" proprioceptive deficit (**Figure 6**), had smaller lesions that primarily affected white-matter tracts carrying proprioceptive information rather than lesions in parietal association areas (Semrau et al., 2018). This result is therefore consistent with a specific role of the parietal association areas in cross-reference processing.

Other proprioceptive tasks such as aB-A$_P$ and C-M$_P$, known for the visual encoding of proprioceptive information requiring cross-reference transformations, have also been associated to parietal activation. Pellijeff et al. (2006) showed that the fMRI response was specifically enhanced in the superior parietal lobule (SPL) and Precuneus (medial part of the PPC) in a thumb and chin pointing task requiring an update of the limb posture to achieve the task. Similarly, using PET, Butler et al. (2004) showed a greater activity in the SPL in the C-M$_P$ reaching task. Within the PPC, Grefkes et al. (2002) showed that the activity in the anterior intraparietal sulcus (IPS) was specifically enhanced during tactile object recognition. This task, requiring cross-modal visuo-tactile information transfer, involved the anterior IPS in stroke patients (Van de Winckel et al., 2012).

Overall, these studies tended to show that "pure" proprioceptive processing involves mainly S1, whereas cross-reference processing recruits specifically the parietal associative cortex. **Figure 7** shows the main trends for task-specific involvement that might be read out as: (i) Tasks excluding visual inputs and that do not require cross-reference processing (W-A$_P$) showed a trend for activating preferentially anterior parietal areas (M1, S1). (ii) Tasks excluding visual inputs but requiring cross-reference processing (sB-A$_P$), or for which visual processing requires cross-reference transformations (sB-A$_{VP}$), seemed to entail additional activation of superior temporal and inferior-lateral PPC areas. (iii) Tasks that impose cross-modal processing, for which a visual encoding of the proprioceptive information has been reported in healthy subjects (aB-A$_P$, C-M$_P$: Tagliabue and McIntyre, 2011, 2013), tended to activate the superior-medial PPC areas. There might thus be a gradient

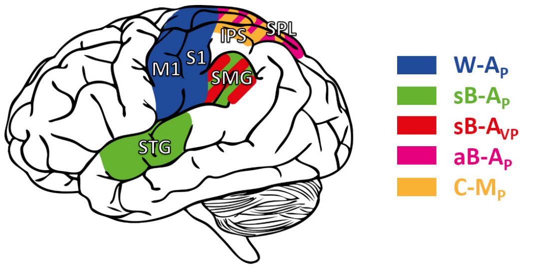

FIGURE 7 | Cortical areas potentially involved in proprioceptive and cross-reference processing. M1, S1: primary motor and somatosensory area, respectively. STG: superior temporal gyrus. Posterior parietal cortex (PPC), including the supramarginal gyrus (SMG), the superior parietal lobule (SPL), and the intraparietal sulcus (IPS). Areas in blue: cortical areas preferentially involved in W-A$_P$, purely proprioceptive tasks (Butler et al., 2004; Iandolo et al., 2018; Marini et al., 2019). Green: enhanced activity when the task requires cross-reference processing in symmetric between-arms tasks (sB-A$_P$) as in Ben-Shabat et al. (2015) and Iandolo et al. (2018); red: in the symmetric between-arms tasks (sB-A$_{VP}$) as in Semrau et al. (2018); purple: in the asymmetric between-arms task (aB-A$_P$) as in Pellijeff et al. (2006); yellow: in cross-modal (C-M$_P$) tasks as in Grefkes et al. (2002), Butler et al. (2004), and Van de Winckel et al. (2012).

within PPC from inferior-lateral to more superior-medial activation with increasing cross-reference processing demands.

DISCUSSION

Here, we present a reinterpretation of proprioceptive post-stroke deficits affecting manual control, and of the ability of patients to compensate for these deficits using vision. This theoretical analysis uses the MLP (Ernst and Banks, 2002) and a new formulation of the "Concurrent Model" for multi-sensory integration (Tagliabue and McIntyre, 2011, 2014). The rationale for this work hinges on the conceptual approach that the sensory space in which the information is encoded is not limited to the sensory system from which the signal originates. This concept is supported by evidence that retinal encoding of purely proprioceptive task-contingent stimuli (i.e., in absence of vision) occurs in some pointing tasks (Pouget et al., 2002; Sarlegna and Sainburg, 2007; McGuire and Sabes, 2009; Jones and Henriques, 2010; Tagliabue and McIntyre, 2013; Arnoux et al., 2017). Hence, it is questionable whether some tasks, traditionally classified as being proprioceptive, can be considered as relying on proprioceptive processing only. Moreover, there is evidence that the efficacy of visual compensation is task-dependent (Scalha et al., 2011; Torre et al., 2013; Semrau et al., 2018; Herter et al., 2019). Therefore, it is also questionable whether different visual compensation tasks imply similar sensory processing.

A Useful Categorization of Proprioceptive Assessments

Applying this concept to clinical proprioceptive deficits and visual compensation tests, we attempt to dissociate purely proprioceptive deficits from those affecting cross-reference processing. We were able to show that tasks described as proprioceptive in clinical practice are likely to involve cross-reference processing. As a consequence, task performances in patients may not specifically depend on a strictly proprioceptive deficit, but may also depend on deficits in performing cross-reference transformations. Clinical and nonclinical methods as well as tasks that assess proprioceptive function and visual compensation have been reviewed and compared through this new conceptual framework. This process led to a new classification of methods for proprioceptive assessments into four categories, which differ by the requirement of performing a task by encoding the information directly in the reference frame associated with sensory receptors: proprioceptive (joint) space and visual (retinal) spaces, respectively. In the first category both visual and proprioceptive information can be encoded in the primary sensory space. The second category includes those tasks in which visual, but not proprioceptive, information can be encoded in the primary sensory space. In the tasks of the third category, proprioceptive, but not visual, information can be encoded in the primary sensory space. The tasks of the fourth category require encoding in non-primary sensory space for both proprioception and vision.

The present analysis suggests that only assessments using a within-arm task represent a "pure" proprioceptive test, because their execution does not require any cross-reference transformation of proprioceptive information. On the contrary, tasks including a between-arms condition, and in particular those that are asymmetric with respect to the body-midline, likely require cross-reference transformations, among which a reconstruction of the task in visual space. As a consequence, these tests do not specifically assess proprioceptive integrity *per se*, but also the ability to perform sensory transformations. Lesion-symptom and functional imaging studies support this hypothesis (Grefkes et al., 2002; Butler et al., 2004; Pellijeff et al., 2006; Van de Winckel et al., 2012; Ben-Shabat et al., 2015; Iandolo et al., 2018; Semrau et al., 2018). The neural network involved in between-arms tasks is wider compared to the network involved in simpler, within-arm, proprioceptive tasks (Ben-Shabat et al., 2015; Iandolo et al., 2018) and includes the PPC which is known to be involved in cross-modal processing (Grefkes et al., 2002; Yau et al., 2015). Moreover, the use of visual information in between-arms mirror (symmetric) tasks might be dependent on the ability to perform cross-reference transformations (Semrau et al., 2018; Herter et al., 2019). Hence, the common practice in neurorehabilitation, to encourage the use of vision for guiding limb movements post-stroke (Pumpa et al., 2015), might be effective when using only one arm or a between-arms asymmetric configuration, but not in the mirror configuration, unless the target is on the body midline (Torre et al., 2013). Since activities of daily living usually involve objects (e.g., grasping), visual feedback on hand position and orientation can often be used to compensate for proprioceptive deficits, as previously suggested (Scalha et al., 2011).

An Enhanced Patient Stratification

According to the present reasoning, the commonly interpreted proprioceptive deficits might often encompass a larger and in part multi-modal spectrum of dysfunctions. Taking cross-reference processing into account in the assessment may potentially provide a more detailed patient stratification. The deficits may be reclassified into three distinct categories: (P) pure proprioceptive deficits, (C) pure cross-reference processing deficits, and (P+C) mixed proprioceptive and cross-reference processing deficit. **Table 2** lists the expected test performance as a function of assessment type and deficit category: although no single test can potentially differentiate these three clinical groups, the different combination of these tests could.

This model has limits, since it focuses on stroke deficits in terms of sensory processing. Other factors can interfere with post-stroke performance in the different type of assessments, which are not taken into account by our model, such as age, hand dominance, target memorization, task workspace (Goble, 2010), active or passive reaching (Gurari et al., 2017), position or movement sense (Semrau et al., 2019). However, it provides a framework which reconciles apparently contradictory results from proprioceptive assessments (Torre et al., 2013; Dos Santos et al., 2015; Contu et al., 2017; Gurari et al., 2017; Rinderknecht et al., 2018; Herter et al., 2019; Ingemanson et al., 2019) and from visual compensation tests (Darling et al., 2008; Scalha et al., 2011; Torre et al., 2013; Semrau et al., 2018; Herter et al., 2019), and it adequately predicts tendencies which fit experimental data (**Figure 6**).

According to the predicted effect of the three type of deficits (P, C, and P+C) on the tests results (**Table 2** and **Figure 6**), the best candidates for stratifying patients, among the assessments that are currently used, would be the combined use of the W-A$_P$ task (eyes closed) and a sB-A$_{VP}$ task (mirror, with visual feedback). Together, these two complementary assessments may help to better stratify patients. In addition to these two methods, adding visual feedback in common proprioceptive tasks (Scalha et al., 2011; Torre et al., 2013; Semrau et al., 2018; Herter et al., 2019; Marini et al., 2019), or using graphesthesia, shape or length discrimination (Van de Winckel et al., 2012; De Diego et al., 2013; Turville et al., 2017) or reaching to visual targets with the unseen hand (Tagliabue and McIntyre, 2011; Elangovan et al., 2019) could help to further explore the complexity of sensorimotor deficits. In the future, to help explore this complexity, robot-assisted tests may enter clinical routine: the tasks are relatively easy and rapid, and 2D robotic manipulators are affordable (Contu et al., 2017; Rinderknecht et al., 2018). Moreover, robotic devices can overcome major limits of current clinical assessment: a quantitative measurement, without ceiling or floor effect, allowing for a more reliable, precise and reproducible evaluation of proprioceptive deficits (Dukelow et al., 2010; Lambercy et al., 2011; Simo et al., 2014; Dos Santos et al., 2015; Contu et al., 2017; Semrau et al., 2017; Deblock-Bellamy et al., 2018; Rinderknecht et al., 2018; Ingemanson et al., 2019).

The proposed stratification of patients may also provide insights about the neural correlates. We would expect that lesions of different brain areas would correspond to the three different categories of deficits. Hypothetically, and informed by the reviewed brain-mapping literature, injury affecting S1 may primarily relate to purely proprioceptive deficits, whereas lesions in the PPC and STG may cause deficits in the ability of performing cross-reference transformations. Patients with mixed deficits would likely tend to have larger lesions affecting both proprioceptive and associative areas. Further lesion-symptom studies examining the correlation of brain lesions in different categories of tasks may offer better identification of brain structures in relation to proprioception or cross-reference processing.

TABLE 2 | Tasks for which the model predicts an impairment (X) depending on the type of deficit present in patients: (P) deficit of purely proprioceptive origin, (C) cross-reference transformation deficit only, and (C+P) combined deficits.

	P	C	P+C
W-A$_P$	X		X
W-A$_{VP}$			
aB-A$_P$	X	X	X
aB-A$_{VP}$			
sB-A$_P$	X	X	X
sB-A$_{VP}$		X	X
C-M$_P$	X	X	X
C-M$_{VP}$			

TABLE 3 | Possible strategies for differential rehabilitation methods depending on the observed sensory deficit: proprioceptive (P), cross-reference (C), and combined (P+C) deficits.

	P	C	P+C
Proprioceptive, within-arm training	X		X
Proprioceptive, between-arm training		X	X
Cross-modal training		X	X
Visual compensation (matching spatial location)	X	X	X
Visual compensation (mirror configuration)	X		

Xs identify appropriate rehabilitation methods.

Application for a More Personalized Rehabilitation Approach

A more accurate stratification of post-stroke patients suffering from proprioceptive deficits should be relevant also for rehabilitation protocols. Given that sensory recovery is a predictor for motor and functional recovery (Bolognini et al., 2016), training of proprioception and cross-reference processing may be key to improve recovery. Currently the effectiveness of sensory rehabilitation is rather weak (Doyle et al., 2010; Findlater and Dukelow, 2017), in part due to heterogeneity in interventions, in outcomes measures (Doyle et al., 2010), and in the precision and reliability of the assessment (Findlater and Dukelow, 2017). A more accurate diagnostic stratification would potentially allow for sensory rehabilitation interventions targeting either proprioception alone, cross-reference processing alone, or both of them; although this would need validation. Adequate training needs to match the symptoms: training restricted to the proprioceptive modality may not address dysfunction in cross-modal processing, and vice versa. **Table 3** summarizes hypothetical treatment options based on the present novel stratification of patients with specific deficits. A more accurate assessment of the different sensory functions could also provide a better assessment of the progress made during rehabilitation.

CONCLUSION

Proprioception is a prerequisite for normal hand function, in particular for reaching, grasping and object manipulation. Using a theoretical approach, based on statistical models of optimal multi-sensory integration, we have reinterpreted post-stroke proprioceptive deficits, as well as the ability of patients to visually compensate for their deficit. The present analyses highlight that proprioceptive control of the hand may be largely affected by the inability to perform cross-reference transformations, that is to process proprioceptive information in order to encode it, not only in joint space, but also in alternative (often visual) reference frames. This finding allowed us to propose an improved classification of post-stroke deficits, which distinguishes between deficits of the proprioceptive system *per se*, deficits of cross-reference processing, and the combined deficits of the former two. This distinction could lead to a new stratification of stroke patients and may result in more personalized rehabilitation plans.

DATA AVAILABILITY STATEMENT

The manuscript presents only experimental data from the literature. All datasets generated for this study are included in the article/**Supplementary Material**, further inquiries can be directed to the corresponding author/s.

AUTHOR CONTRIBUTIONS

MT conceptualized the topic of the manuscript. JB-E wrote the initial draft of the manuscript and prepared the figures. All authors contributed to writing the manuscript, and read and approved the submitted version.

FUNDING

JB-E was supported by a Ph.D. fellowship of the École Doctorale Cerveau-Cognition-Comportement (ED3C, n°158, Sorbonne Université and Université de Paris). This work was supported by the *Centre National d'Etudes Spatiales*, the *Centre National de la Recherche Scientifique* (CNRS), and the *Université de Paris*. This study contributes to the IdEx Université de Paris ANR-18-IDEX-0001.

ACKNOWLEDGMENTS

We wish to thank Martino Trassinelli, from the Institut des Nanosciences de Paris (CNRS – Sorbonne Université), for the useful discussion about constrained optimization methods.

SUPPLEMENTARY MATERIAL

The Supplementary Material for this article can be found online at: https://www.frontiersin.org/articles/10.3389/fnins.2021.646698/full#supplementary-material

REFERENCES

Arnoux, L., Fromentin, S., Farotto, D., Beraneck, M., McIntyre, J., and Tagliabue, M. (2017). The visual encoding of purely proprioceptive intermanual tasks is due to the need of transforming joint signals, not to their interhemispheric transfer. *J. Neurophysiol.* 118, 1598–1608. doi: 10.1152/jn.00140.2017

Ben-Shabat, E., Matyas, T. A., Pell, G. S., Brodtmann, A., and Carey, L. M. (2015). The right supramarginal gyrus is important for proprioception in healthy and stroke-affected participants: a functional mri study. *Front. Neurol.* 6:248. doi: 10.3389/fneur.2015.00248

Birchenall, J., Térémetz, M., Roca, P., Lamy, J. C., Oppenheim, C., Maier, M. A., et al. (2019). Individual recovery profiles of manual dexterity, and relation to corticospinal lesion load and excitability after stroke –a longitudinal pilot study. *Neurophysiol. Clin.* 49, 149–164. doi: 10.1016/j.neucli.2018.10.065

Bolognini, N., Russo, C., and Edwards, D. J. (2016). The sensory side of post-stroke motor rehabilitation. *Restor. Neurol. Neurosci.* 34, 571–586. doi: 10.3233/RNN-150606

Burns, J. K., and Blohm, G. (2010). Multi-sensory weights depend on contextual noise in reference frame transformations. *Front. Hum. Neurosci.* 4:221. doi: 10.3389/fnhum.2010.00221

Butler, A. J., Fink, G. R., Dohle, C., Wunderlich, G., Tellmann, L., Seitz, R. J., et al. (2004). Neural mechanisms underlying reaching for remembered targets cued kinesthetically or visually in left or right hemispace. *Hum. Brain Mapp.* 21, 165–177. doi: 10.1002/hbm.20001

Cameron, B. D., and López-Moliner, J. (2015). Target modality affects visually guided online control of reaching. *Vision Res.* 110, 233–243. doi: 10.1016/j.visres.2014.06.010

Carlsson, H., Ekstrand, E., and Brogårdh, C. (2019). Sensory function, measured as active discriminative touch, is associated with dexterity after stroke. *PM R* 11, 821–827. doi: 10.1002/pmrj.12044

Connell, L. A., Lincoln, N. B., and Radford, K. A. (2008). Somatosensory impairment after stroke: frequency of different deficits and their recovery. *Clin. Rehabil.* 22, 758–767. doi: 10.1177/0269215508090674

Contu, S., Hussain, A., Kager, S., Budhota, A., Deshmukh, V. A., Kuah, C. W. K., et al. (2017). Proprioceptive assessment in clinical settings: evaluation of joint position sense in upper limb post-stroke using a robotic manipulator, edited by françois tremblay. *PLoS One* 12:e0183257. doi: 10.1371/journal.pone.0183257

Darling, W. G., Bartelt, R., Pizzimenti, M. A., and Rizzo, M. (2008). Spatial perception errors do not predict pointing errors by individuals with brain lesions. *J. Clin. Exp. Neuropsychol.* 30, 102–119. doi: 10.1080/13803390701249036

De Diego, C., Puig, S., and Navarro, X. (2013). A sensorimotor stimulation program for rehabilitation of chronic stroke patients. *Restor. Neurol. Neurosci.* 31, 361–371. doi: 10.3233/RNN-120250

De Santis, D., Zenzeri, J., Casadio, M., Masia, L., Riva, A., Morasso, P., et al. (2015). Robot-assisted training of the kinesthetic sense: enhancing proprioception after stroke. *Front. Hum. Neurosci.* 8:1037. doi: 10.3389/fnhum.2014.01037

Deblock-Bellamy, A., Batcho, C. S., Mercier, C., and Blanchette, A. K. (2018). Quantification of upper limb position sense using an exoskeleton and a virtual reality display. *J. Neuroeng. Rehabil.* 15:24. doi: 10.1186/s12984-018-0367-x

Dos Santos, G. L., García Salazar, L. F., Lazarin, A. C., and Russo, T. L. (2015). Joint position sense is bilaterally reduced for shoulder abduction and flexion in chronic hemiparetic individuals. *Topics Stroke Rehabil.* 22, 271–280. doi: 10.1179/1074935714Z.0000000014

Doyle, S., Bennett, S., Fasoli, S. E., and McKenna, K. T. (2010). Interventions for sensory impairment in the upper limb after stroke. *Cochrane Database Syst. Rev.* 2010:CD006331. doi: 10.1002/14651858.CD006331.pub2

Dukelow, S. P., Herter, T. M., Bagg, S. D., and Scott, S. H. (2012). The independence of deficits in position sense and visually guided reaching following stroke. *J. Neuroeng. Rehabil.* 9:72. doi: 10.1186/1743-0003-9-72

Dukelow, S. P., Herter, T. M., Moore, K. D., Demers, M. J., Glasgow, J. I., Bagg, S. D., et al. (2010). Quantitative assessment of limb position sense following stroke. *Neurorehabil. Neural Repair* 24, 178–187. doi: 10.1177/1545968309345267

Elangovan, N., Yeh, I. L., Holst-Wolf, J., and Konczak, J. (2019). "A robot-assisted sensorimotor training program can improve proprioception and motor function in stroke survivors," in *Proceedings of the 2019 IEEE 16th International Conference on Rehabilitation Robotics (ICORR)* (Toronto, ON: IEEE), 660–664. doi: 10.1109/ICORR.2019.8779409

Ernst, M. O., and Banks, M. S. (2002). Humans integrate visual and haptic information in a statistically optimal fashion. *Nature* 415, 429–433. doi: 10.1038/415429a

Findlater, S. E., Desai, J. A., Semrau, J. A., Kenzie, J. M., Rorden, C., Herter, T. M., et al. (2016). Central Perception of Position Sense Involves a Distributed Neural Network – Evidence from Lesion-Behavior Analyses. *Cortex* 79, 42–56. doi: 10.1016/j.cortex.2016.03.008

Findlater, S. E., and Dukelow, S. P. (2017). Upper extremity proprioception after stroke: bridging the gap between neuroscience and rehabilitation. *J. Mot. Behav.* 49, 27–34. doi: 10.1080/00222895.2016.1219303

Findlater, S. E., Hawe, R. L., Semrau, J. A., Kenzie, J. M., Yu, A. Y., Scott, S. H., et al. (2018). Lesion locations associated with persistent proprioceptive impairment in the upper limbs after stroke. *Neuroimage Clin.* 20, 955–971. doi: 10.1016/j.nicl.2018.10.003

Frenkel-Toledo, S., Fridberg, G., Ofir, S., Bartur, G., Lowenthal-Raz, J., Granot, O., et al. (2019). Lesion location impact on functional recovery of the hemiparetic upper limb." edited by mariella pazzaglia. *PLoS One* 14:e0219738. doi: 10.1371/journal.pone.0219738

Goble, D. J. (2010). Proprioceptive acuity assessment via joint position matching: from basic science to general practice. *Phys. Ther.* 90, 1176–1184. doi: 10.2522/ptj.20090399

Grefkes, C., Weiss, P. H., Zilles, K., and Fink, G. R. (2002). Crossmodal processing of object features in human anterior intraparietal cortex: an fmri study implies equivalencies between humans and monkeys. *Neuron* 35, 173–184. doi: 10.1016/s0896-6273(02)00741-9

Gurari, N., Drogos, J. M., and Dewald, J. P. A. (2017). Individuals with chronic hemiparetic stroke can correctly match forearm positions within a single arm. *Clin. Neurophysiol.* 128, 18–30. doi: 10.1016/j.clinph.2016.10.009

Herter, T. M., Scott, S. H., and Dukelow, S. P. (2019). Vision does not always help stroke survivors compensate for impaired limb position sense. *J. Neuroeng. Rehabil.* 16:129. doi: 10.1186/s12984-019-0596-7

Hirayama, K., Fukutake, T., and Kawamura, M. (1999). Thumb localizing test' for detecting a lesion in the posterior column-medial lemniscal system. *J. Neurol. Sci.* 167, 45–49. doi: 10.1016/s0022-510x(99)00136-7

Iandolo, R., Bellini, A., Saiote, C., Marre, I., Bommarito, G., Oesingmann, N., et al. (2018). Neural correlates of lower limbs proprioception: an fmri study of foot position matching. *Hum. Brain Mapp.* 39, 1929–1944. doi: 10.1002/hbm.23972

Iandolo, R., Squeri, V., De Santis, D., Giannoni, P., Morasso, P., and Casadio, M. (2014). "Testing proprioception in intrinsic and extrinsic coordinate systems: is there a difference?," in *Proceedings of the 2014 36th Annual International Conference of the IEEE Engineering in Medicine and Biology Society* (Chicago, IL: IEEE), 6961–6964. doi: 10.1109/EMBC.2014.6945229

Ingemanson, M. L., Rowe, J. R., Chan, V., Riley, J., Wolbrecht, E. T., Reinkensmeyer, D. J., et al. (2019). Neural correlates of passive position finger sense after stroke. *Neurorehabil. Neural Repair* 33, 740–750. doi: 10.1177/1545968319862556

Jones, S. A. H., and Henriques, D. Y. P. (2010). Memory for proprioceptive and multisensory targets is partially coded relative to gaze. *Neuropsychologia* 48, 3782–3792. doi: 10.1016/j.neuropsychologia.2010.10.001

Kenzie, J. M., Semrau, J. A., Hill, M. D., Scott, S. H., and Dukelow, S. P. (2017). A composite robotic-based measure of upper limb proprioception. *J. Neuroeng. Rehabil.* 14:114. doi: 10.1186/s12984-017-0329-8

Kessner, S. S., Bingel, U., and Thomalla, G. (2016). Somatosensory deficits after stroke: a scoping review. *Topics Stroke Rehabil.* 23, 136–146. doi: 10.1080/10749357.2015.1116822

Kessner, S. S., Schlemm, E., Cheng, B., Bingel, U., Fiehler, J., Gerloff, C., et al. (2019). Somatosensory deficits after ischemic stroke: time course and association with infarct location. *Stroke* 50, 1116–1123. doi: 10.1161/STROKEAHA.118.023750

Khanafer, S., and Cressman, E. K. (2014). Sensory integration during reaching: the effects of manipulating visual target availability. *Exp. Brain Res.* 232, 3833–3846. doi: 10.1007/s00221-014-4064-0

Körding, K. P., Beierholm, U., Ma, W. J., Quartz, S., Tenenbaum, J. B., and Shams, L. (2007). Causal inference in multisensory perception." edited by olaf sporns. *PLoS ONE* 2:e943. doi: 10.1371/journal.pone.0000943

Lambercy, O., Robles, A. J., Kim, Y., and Gassert, R. (2011). "Design of a robotic device for assessment and rehabilitation of hand sensory function," in *Proceedings of the 2011 IEEE International Conference on Rehabilitation Robotics* (Zurich: IEEE), 1–6. doi: 10.1109/ICORR.2011.5975436

Lanska, D. J., and Kryscio, R. (2000). Thumb localizing test' for detecting a lesion in the posterior column-medical lemniscal system. *J. Neurol. Sci.* 174, 152–154. doi: 10.1016/s0022-510x(99)00321-4

Lemon, R. N. (2008). Descending pathways in motor control. *Annu. Rev. Neurosci.* 31, 195–218. doi: 10.1146/annurev.neuro.31.060407.125547

Marini, F., Zenzeri, J., Pippo, V., Morasso, P., and Campus, C. (2019). Neural correlates of proprioceptive upper limb position matching. *Hum. Brain Mapp.* 40, 4813–4826. doi: 10.1002/hbm.24739

Matsuda, K., Satoh, M., Tabei, K. I., Ueda, Y., Itoh, A., Ishikawa, H., et al. (2019). Subregional heterogeneity of somatosensory dysfunction in the insula. *J. Neurol. Neurosurg. Psychiatry* 90, 957–958. doi: 10.1136/jnnp-2018-319174

McGuire, L. M. M., and Sabes, P. N. (2009). Sensory transformations and the use of multiple reference frames for reach planning. *Nat. Neurosci.* 12, 1056–1061. doi: 10.1038/nn.2357

Metzger, J. C., Lambercy, O., Califfi, A., Conti, F. M., and Gassert, R. (2014). Neurocognitive robot-assisted therapy of hand function. *IEEE Trans. Haptics* 7, 140–149. doi: 10.1109/TOH.2013.72

Meyer, S., De Bruyn, N., Lafosse, C., Van Dijk, M., Michielsen, M., Thijs, L., et al. (2016). Somatosensory impairments in the upper limb poststroke: distribution and association with motor function and visuospatial neglect. *Neurorehabil. Neural Repair* 30, 731–742. doi: 10.1177/1545968315624779

Meyer, S., Karttunen, A. H., Thijs, V., Feys, H., and Verheyden, G. (2014). How do somatosensory deficits in the arm and hand relate to upper limb impairment, activity, and participation problems after stroke? a systematic review. *Phys. Ther.* 94, 1220–1231. doi: 10.2522/ptj.20130271

Monaco, S., Króliczak, G., Quinlan, D. J., Fattori, P., Galletti, C., Goodale, M. A., et al. (2010). Contribution of visual and proprioceptive information to the precision of reaching movements. *Exp. Brain Res.* 202, 15–32. doi: 10.1007/s00221-009-2106-9

Pellijeff, A., Bonilha, L., Morgan, P. S., McKenzie, K., and Jackson, S. R. (2006). Parietal updating of limb posture: an event-related fmri study. *Neuropsychologia* 44, 2685–2690. doi: 10.1016/j.neuropsychologia.2006.01.009

Pennati, G. V., Plantin, J., Carment, L., Roca, P., Baron, J. C., Pavlova, E., et al. (2020). Recovery and prediction of dynamic precision grip force control after stroke. *Stroke* 51, 944–951. doi: 10.1161/STROKEAHA.119.026205

Pouget, A., Ducom, J. C., Torri, J., and Bavelier, D. (2002). Multisensory spatial representations in eye-centered coordinates for reaching. *Cognition* 83, B1–B11. doi: 10.1016/S0010-0277(01)00163-9

Pumpa, L. U., Cahill, L. S., and Carey, L. M. (2015). Somatosensory assessment and treatment after stroke: an evidence-practice gap. *Aust. Occup. Ther. J.* 62, 93–104. doi: 10.1111/1440-1630.12170

Rand, D. (2018). Proprioception deficits in chronic stroke—upper extremity function and daily living. *Edited by Sliman J. Bensmaia. PLoS One* 13:e0195043. doi: 10.1371/journal.pone.0195043

Rinderknecht, M. D., Lambercy, O., Raible, V., Büsching, I., Sehle, A., Liepert, J., et al. (2018). Reliability, validity, and clinical feasibility of a rapid and objective assessment of post-stroke deficits in hand proprioception. *J. Neuroeng. Rehabil.* 15:47. doi: 10.1186/s12984-018-0387-6

Saeys, W., Vereeck, L., Truijen, S., Lafosse, C., Wuyts, F. P., and Van de Heyning, P. (2012). Influence of sensory loss on the perception of verticality in stroke patients. *Disabil. Rehabil.* 34, 1965–1970. doi: 10.3109/09638288.2012.671883

Sallés, L., Martín-Casas, P., Gironès, X., Durà, M. J., Lafuente, J. V., and Perfetti, C. (2017). A Neurocognitive approach for recovering upper extremity movement following subacute stroke: a randomized controlled pilot study. *J. Phys. Ther. Sci.* 29, 665–672. doi: 10.1589/jpts.29.665

Santisteban, L., Térémetz, M., Bleton, J. P., Baron, J. C., Maier, M. A., and Lindberg, P. G. (2016). Upper limb outcome measures used in stroke rehabilitation studies: a systematic literature review." edited by françois tremblay. *PLoS One* 11:e0154792. doi: 10.1371/journal.pone.0154792

Sarlegna, F. R., and Sainburg, R. L. (2007). The effect of target modality on visual and proprioceptive contributions to the control of movement distance. *Exp. Brain Res.* 176, 267–280. doi: 10.1007/s00221-006-0613-5

Scalha, T. B., Miyasaki, E., Lima, N. M., and Borges, G. (2011). Correlations between motor and sensory functions in upper limb chronic hemiparetics after stroke. *Arq. Neuropsiquiatr.* 69, 624–629. doi: 10.1590/S0004-282X2011000500010

Semrau, J. A., Herter, T. M., Scott, S. H., and Dukelow, S. P. (2017). Inter-rater reliability of kinesthetic measurements with the kinarm robotic exoskeleton. *J. Neuroeng. Rehabil.* 14:42. doi: 10.1186/s12984-017-0260-z

Semrau, J. A., Herter, T. M., Scott, S. H., and Dukelow, S. P. (2018). Vision of the upper limb fails to compensate for kinesthetic impairments in subacute stroke. *Cortex* 109, 245–259. doi: 10.1016/j.cortex.2018.09.022

Semrau, J. A., Herter, T. M., Scott, S. H., and Dukelow, S. P. (2019). Differential loss of position sense and kinesthesia in sub-acute stroke. *Cortex* 121, 414–426. doi: 10.1016/j.cortex.2019.09.013

Simo, L., Botzer, L., Ghez, C., and Scheidt, R. A. (2014). A robotic test of proprioception within the hemiparetic arm post-stroke. *J. Neuroeng. Rehabil.* 11:77. doi: 10.1186/1743-0003-11-77

Tagliabue, M., Arnoux, L., and McIntyre, J. (2013). Keep your head on straight: facilitating sensori-motor transformations for eye–hand coordination. *Neuroscience* 248, 88–94. doi: 10.1016/j.neuroscience.2013.05.051

Tagliabue, M., and McIntyre, J. (2008). *Multiple and Multimodal Reference Frames for Eye-Hand Coordination Program Neuroscience Meeting*. Washington, DC: Society for Neuroscience.

Tagliabue, M., and McIntyre, J. (2011). Necessity is the mother of invention: reconstructing missing sensory information in multiple, concurrent reference frames for eye-hand coordination. *J. Neurosci.* 31, 1397–1409. doi: 10.1523/JNEUROSCI.0623-10.2011

Tagliabue, M., and McIntyre, J. (2013). When kinesthesia becomes visual: a theoretical justification for executing motor tasks in visual space. *Edited by Robert J. van Beers. PLoS One* 8:e68438. doi: 10.1371/journal.pone.0068438

Tagliabue, M., and McIntyre, J. (2014). A modular theory of multisensory integration for motor control. *Front. Comput. Neurosci.* 8:1. doi: 10.3389/fncom.2014.00001

Torre, K., Hammami, N., Metrot, J., Van Dokkum, L., Coroian, F., Mottet, D., et al. (2013). Somatosensory-related limitations for bimanual coordination after stroke. *Neurorehabil. Neural Repair* 27, 507–515. doi: 10.1177/1545968313478483

Turville, M., Carey, L. M., Matyas, T. A., and Blennerhassett, J. (2017). Change in functional arm use is associated with somatosensory skills after sensory retraining poststroke. *Am. J. Occup. Ther.* 71, 7103190070p1-7103190070p9. doi: 10.5014/ajot.2017.024950

Valdes, B. A., Khoshnam, M., Neva, J. L., and Menon, C. (2019). "Robot-aided upper-limb proprioceptive training in three-dimensional space," in *Proceedings of the 2019 IEEE 16th International Conference on Rehabilitation Robotics (ICORR)* (Toronto, ON: IEEE), 121–126. doi: 10.1109/ICORR.2019.8779529

Van Beers, R. J., Sittig, A. C., and Gon, J. J. (1996). How humans combine simultaneous proprioceptive and visual position information. *Exp. Brain Res.* 111, 253–261. doi: 10.1007/BF00227302

Van de Winckel, A., Wenderoth, N., De Weerdt, W., Sunaert, S., Peeters, R., Van Hecke, W., et al. (2012). Frontoparietal involvement in passively guided shape and length discrimination: a comparison between subcortical stroke patients and healthy controls. *Exp. Brain Res.* 220, 179–189. doi: 10.1007/s00221-012-3128-2

Yau, J. M., DeAngelis, J. C., and Angelaki, D. E. (2015). Dissecting neural circuits for multisensory integration and crossmodal processing. *Philos. Trans. R. Soc. B Biol. Sci.* 370:20140203. doi: 10.1098/rstb.2014.0203

Zackowski, K. M., Dromerick, A. W., Sahrmann, S. A., Thach, W. T., and Bastian, A. J. (2004). How do strength, sensation, spasticity and joint individuation relate to the reaching deficits of people with chronic hemiparesis? *Brain* 127, 1035–1046. doi: 10.1093/brain/awh116

Zandvliet, S. B., Kwakkel, G., Nijland, R. H. M., Van Wegen, E. E. H., and Meskers, C. G. M. (2020). Is recovery of somatosensory impairment conditional for upper-limb motor recovery early after stroke? *Neurorehabil. Neural Repair* 34, 403–416. doi: 10.1177/1545968320907075

Conflict of Interest: The authors declare that the research was conducted in the absence of any commercial or financial relationships that could be construed as a potential conflict of interest.

frontiers
in Psychology

ORIGINAL RESEARCH
published: 12 April 2021
doi: 10.3389/fpsyg.2021.597691

Grasping of Real-World Objects Is Not Biased by Ensemble Perception

Annabel Wing-Yan Fan[1], Lin Lawrence Guo[1], Adam Frost[1], Robert L. Whitwell[2], Matthias Niemeier[1] and Jonathan S. Cant[1]*

[1]Department of Psychology, University of Toronto Scarborough, Toronto, ON, Canada, [2]The Department of Psychology, The University of British Columbia, Vancouver, BC, Canada

The visual system is known to extract summary representations of visually similar objects which bias the perception of individual objects toward the ensemble average. Although vision plays a large role in guiding action, less is known about whether ensemble representation is informative for action. Motor behavior is tuned to the veridical dimensions of objects and generally considered resistant to perceptual biases. However, when the relevant grasp dimension is not available or is unconstrained, ensemble perception may be informative to behavior by providing gist information about surrounding objects. In the present study, we examined if summary representations of a surrounding ensemble display influenced grip aperture and orientation when participants reached-to-grasp a central circular target which had an explicit size but importantly no explicit orientation that the visuomotor system could selectively attend to. Maximum grip aperture and grip orientation were not biased by ensemble statistics during grasping, although participants were able to perceive and provide manual estimations of the average size and orientation of the ensemble display. Support vector machine classification of ensemble statistics achieved above-chance classification accuracy when trained on kinematic and electromyography data of the perceptual but not grasping conditions, supporting our univariate findings. These results suggest that even along unconstrained grasping dimensions, visually-guided behaviors toward real-world objects are not biased by ensemble processing.

Keywords: ensemble perception, grasping, perception, electromyography, support vector machine classification, two visual stream hypothesis, action perception dissociation

Edited by:
Simone Toma,
Arizona State University, United States

Reviewed by:
Kazutaka Takahashi,
University of Chicago, United States
Sabrina Hansmann-Roth,
Université de Lille, France

****Correspondence:***
Annabel Wing-Yan Fan
annabel.fan@mail.utoronto.ca

Specialty section:
This article was submitted to Cognition, a section of the journal Frontiers in Psychology

Received: *21 August 2020*
Accepted: *15 March 2021*
Published: *12 April 2021*

Citation:
Fan AW-Y, Guo LL, Frost A, Whitwell RL, Niemeier M and Cant JS (2021) Grasping of Real-World Objects Is Not Biased by Ensemble Perception. Front. Psychol. 12:597691. doi: 10.3389/fpsyg.2021.597691

INTRODUCTION

Ensemble perception refers to the ability of the visual system to extract summary representations of groups of similar objects (ensembles) across various visual domains. For example, observers can accurately report the mean size of an array of different-sized circles, while, paradoxically, providing poor estimates of the size of the individual circles that are biased toward the mean size of the set (Ariely, 2001). This observation has been replicated (Chong and Treisman, 2003; Brady and Alvarez, 2011) and extended to other domains such as spatial position (Alvarez and Oliva, 2008) and orientation (Dakin and Watt, 1997; Parkes et al., 2001), and can be extracted across multiple visual domains in parallel (Emmanouil and Treisman, 2008; Attarha and Moore, 2015; Yörük and Boduroglu, 2020). Ensemble summary statistics are thought to provide the visual system with a means to make computational simplifications, which translates into lower requirements for the storage of visual information, and the preservation of a coherent percept *via* the reduction of artifactual noise that can arise from the loss of spatial resolution with increased eccentricity. In-line with this viewpoint, ensemble perception is refractory to conditions of reduced or dispersed attention (Chong and Treisman, 2005; Alvarez and Oliva, 2008, 2009; Chen et al., 2020), providing "gist" information that can guide subsequent attentional shifts (see review by Alvarez, 2011). Ensemble perception has been shown to extend beyond the mean to other statistics such as the variance and range of a set of items (Ariely, 2001; Utochkin and Vostrikov, 2017; Khayat and Hochstein, 2018; Sama et al., 2021). Importantly, these statistics (particularly variance and range), can be useful in aiding the detection of outliers and may also be integral to visual search mechanisms (Ariely, 2001). Critically, while there is an abundance of research investigating the nature of ensemble processing in the perceptual domain, very little research has focused on understanding how and if ensemble processing informs object-directed action.

Vision is the dominant sense used to guide action in everyday life. Reaching out to pick up a goal object is an intuitively trivial action performed routinely in daily life. These intuitions mask a complex process that must consider not only the agent's intention but also the target's 3D geometry, material properties, and spatial relationships with our eyes, body, and limbs. Motion capturing techniques have shown, for decades, that the hand, wrist, and fingers smoothly preconfigure in-flight to suit the spatial and functional features of the target (Jeannerod, 1981, 1984, 1988; Stelmach et al., 1994; Cuijpers et al., 2004; Whitwell et al., 2008). For example, the hand's in-flight aperture (grip aperture) scales to the size of the goal object while the wrist rotates smoothly to suit the orientation of the object as the reach unfolds (e.g., Jeannerod, 1988; Kelso et al., 1994; for review, see Jeannerod, 1999). A number of different lines of evidence strongly suggest that the visual-guidance of actions like reaching out to pick up a goal object, is under the control of visuomotor modules housed in the intraparietal cortical areas of the "dorsal stream" (for review, see Milner and Goodale, 2006; Kravitz et al., 2011). In non-human primates, support for this proposal stems from single- (e.g., Taira et al., 1990; Murata et al., 2000) and multi-unit recordings (e.g., Schaffelhofer and Scherberger, 2016), cortical cooling (e.g., Gallese et al., 1994; Kermadi et al., 1997) and lesion experiments (e.g., Battaglini et al., 2002); while in humans, support comes from neuroimaging (e.g., Culham et al., 2003; Frey et al., 2005), transcranial magnetic stimulation (e.g., Tunik et al., 2005; Rice et al., 2007; Le et al., 2014, 2017), and neuropsychological work (e.g., Goodale et al., 1994; Whitwell et al., 2020).

One of the most counterintuitive findings to come out of the kinematic study of reaching and grasping is that the hand's in-flight grip aperture is relatively refractory to the perceptual distortions of size induced by pictorial illusions. For example, in the Ebbinghaus illusion, two identically sized circles appear larger or smaller when they are surrounded by an annulus of smaller or larger circles, respectively. Aglioti et al. (1995) replaced the 2D inner disks, which are subjected to the illusion, with graspable 3D disks that were just as susceptible to the illusion when viewed face-on. When participants were asked to choose to pick up one or the other disk based on a same/different judgment about their relative size, Aglioti et al. (1995) found that although their choice was based almost exclusively on the illusory size, grip aperture remained tuned to the real size of the disk, resisting the influence of the perceived size of the illusion. This dissociation was later replicated (Haffenden and Goodale, 1998; Marotta et al., 1998; de Grave et al., 2005), and subsequent studies have extended it to other illusions (e.g., Brenner and Smeets, 1996; Servos et al., 2000; Bartelt and Darling, 2002; Ganel et al., 2008; Stöttinger et al., 2012; Whitwell et al., 2016, 2018; Smeets et al., 2020; though see Kopiske et al., 2016; Whitwell and Goodale, 2017; and Smeets and Brenner, 2006 for review). Furthermore, grip aperture is refractory to attentional crowding, which reduces the sensitivity to the size of targets embedded in a cluster of distractor objects (Chen et al., 2015). Thus, ensemble perception reduces its fidelity to individual target features like target size in favor of group statistical analogs, whereas the visuomotor system conserves fidelity to target size. Additional compelling evidence favoring a functional and anatomical distinction between the visual analysis of object geometry for perception and action comes from cases of action blindsight and visual agnosia, in which the patient, due to their compromised visual perception, cannot reliably report the size or shape of the goal object yet, remarkably, they reliably and seamlessly exploit these spatial features to inform the movements of their hand when reaching out to pick up these same objects (Goodale et al., 1991; Perenin and Rossetti, 1996; Jackson, 1999; Karnath et al., 2009; Whitwell et al., 2011, 2020). These studies strongly suggest that the visuomotor system parameterizes the details of goal-directed grasps and filters out sources of information that are typically used to inform ensemble perception.

Since the spatial organization of items in an ensemble display is typically random, these displays lack drastic size-contrast cues and the structured organization of elements seen in typical visual illusions (e.g., the Ebbinghaus illusion). Yet ensemble displays still impart a strong perceptual bias, in that the perception of a feature value of a single item from the set is routinely pulled toward the average value of the set (Brady and Alvarez, 2011; Sama et al., 2019). Does this bias toward the ensemble average influence grasping? Corbett and Song (2014) examined whether adaptation to two ensembles, presented on the left and right sides of the screen, which varied in average size would bias grasping behavior. The participants were cued to grasp one of two test dots which replaced the ensembles after an adaptation period. The non-grasped dot was the average size of all the dots in the adapting display, while the size of the target dot varied in set increments from the non-grasped dot. Participants completed their grasp by touching their fingers to the computer screen, matching the size of the 2D test dot, and then reported whether the test dot they "grasped" was larger or smaller than the non-grasped dot. The authors reported that perceptual judgments were biased as an inverse function of the average size of the adapting ensemble (i.e., a test dot adapted to a small average ensemble size was perceived as being larger than the non-grasped dot and vice versa). Additionally, the authors observed a perceptual bias in early but not late stages of grasping. Importantly, it is possible that grasping 2D targets permits relative visual processing to influence grip aperture. For example, grasps directed at 3D shapes appear to resist both Garner interference and Weber's Law, but "grasps" directed at 2D shapes succumb to Garner interference and abide Weber's Law (Holmes and Heath, 2013; Freud and Ganel, 2015; Ozana and Ganel, 2019). Conversely, in a visual crowding paradigm where participants were asked to make perceptual judgments and "grasps" toward a computer monitor where a 2D tilted bar surrounded by tilted flanker bars was presented, Bulakowski et al. (2009) found that perception integrated information from the surrounding flankers while the action did not. Because the 2D stimuli used in both studies likely did not fully engage the visuomotor system, it remains unknown whether ensemble perception can influence grasping under more ecologically valid circumstances. We have addressed this issue in the current study by using real 3D objects in our ensemble displays.

Importantly, in the studies discussed above, the grasping target consistently had an explicit size or orientation that the visuomotor system could utilize when planning and executing a grasping movement. Since grasping movements are tuned to the veridical dimensions of target objects, the visuomotor system efficiently controls movement by discounting irrelevant information when the properties of the target are explicitly available (Milner and Goodale, 2006). However, in cases where there is more ambiguity in a target object's features, there may be more incentive for the visuomotor system to make use of all available perceptual information, including ensemble statistics. To this end, the present study aims to determine whether ensemble statistics bias grasping when visual information about the target is unconstrained and can afford a number of different grasp postures. Specifically, participants were tasked with grasping a circular 3D cylindrical target placed in the center of an ensemble display consisting of elliptical and circular cylinders. By using a single target of constant size and shape across the experimental session, we hoped to minimize scrutiny of the target and free up spatial attention to engage the ensemble statistics of the display. Although the size of the circular target was explicit and required a constrained grip aperture, the orientation of the grasp posture for a circular target was unconstrained, in that participants could place their fingers at almost any number of points along the circumference of the target to successfully grasp it. This allowed the orientation of the elliptical cylinders to generate perceptual biases that could conceivably bias the orientation of the grasp posture in favor of the ensemble mean orientation (note that this does not imply a conscious illusory percept of the target's orientation, but rather a potential implicit bias of ensemble statistics on grasping behavior). We also varied the sizes of the ellipses in the ensemble, to determine whether the mean size of the ellipses could bias grip aperture. If ensemble processing can strongly influence grasping, then both grip orientation and grip aperture should be biased toward the mean orientation and size of the ensemble, respectively. If ensemble processing can only weakly affect grasping, then only grip orientation, in which the selection of grasp posture is relatively unconstrained, should be biased by ensemble processing. If grasping is not influenced by ensemble statistics, then we should observe no influence of mean orientation and size on grip orientation and grip aperture, respectively.

To isolate any obstacle avoidance effects on the grasping task, we administered a series of control trials in which the target was presented in isolation. If the non-target objects serve as obstacles to the central target, grip aperture would be expected to be smaller in the ensemble grasping task compared with the baseline grasping task (Bonfiglioli and Castiello, 1998; Chen et al., 2015). In a separate task, participants were asked to provide manual estimations of the perceived average size and orientation of the ensemble to ensure that the participants were able to perceive and report differences in ensemble statistical values. To make a manual estimate, participants separated their thumb and index finger to create a gap and oriented them in space so that these reports of size and orientation matched the average size and orientation of the ensemble. To ensure that the participants received the same haptic feedback for their perceptual estimates as they would for the grasping task, they were asked to grasp the target after completing their estimate. Based on the rich literature on the perceptual processing of ensemble statistics (see Whitney and Yamanashi Leib, 2018, for review), we hypothesized that within the perceptual-estimation session: (1) grip aperture (GA) should reflect perceived average ensemble size in the size-estimation task and (2) grip orientation (GO) should reflect perceived average ensemble orientation.

Taken together, the motivation for our study was to examine whether ensemble statistics, which are implicitly extracted and affect perception and memory (e.g., Brady and Alvarez, 2011; Sama et al., 2021), also affect visuomotor programming. Note that this differs from the design of visual-illusion paradigms that are used to investigate potential dissociations between action and perception, in that we are not concerned with whether ensemble statistics affect the perceived properties of the to-be-grasped target, but rather, whether such statistics implicitly bias grasping movements made toward that target. In a broader sense, we are interested in whether the statistics of the environment affect our everyday interactions with objects.

MATERIALS AND METHODS

Participants

Fifteen participants (M_{age} = 25.2, SD_{age} = 4.54 years; 11 males), with normal or corrected-to-normal vision, were recruited from the University of Toronto community. Participants were right-handed as assessed by a modified version of the Edinburgh Handedness Inventory (Oldfield, 1971), and were compensated at a rate of $10 CAD/h for completing two, 1.5-h experimental sessions. Of note, 10 of these participants (M_{age} = 25.2, SD_{age} = 7.64 years; 4 males) took part in an initial version of the study, with the remaining five participants (M_{age} = 24, SD_{age} = 1 year; 4 males) taking part in a second round of data collection that entailed making slight modifications to the experimental procedure (see the "Modifications to the Experimental Procedure" section for more details). All participants gave informed consent prior to the start of the study. All experimental procedures were conducted in accordance with the University of Toronto Ethics Review Board.

Stimuli

Each ensemble was made up of 25 objects that were designed with 3D-modeling software (*Blender*, version 2.79b, Windows. Blender Foundation, Amsterdam, the Netherlands) and printed in plastic using a 3D printer (ProJet® MJP 2500 Series, Objex Unlimited, Toronto, ON, Canada). The target object in the center of the display was shaped like a circular cylinder (diameter = 2.77 cm, height = 2.00 cm, and volume = 12.05 cm^3). We used a single target size and location to encourage conditions of "kinematic consistency," which have been shown to maximize the opportunity for ventral-stream involvement in grasping by minimizing the requirement for *de novo* dorsal-stream driven computations (Haffenden and Goodale, 2002). It was surrounded by 8 and 16 objects, evenly distributed 4.70 cm apart along two concentric rings 6 and 12 cm away from the middle, respectively (see **Figure 1**). Half the surrounding objects had the same size and shape as the target object so that it would not pop out visually. The other objects were elliptical cylinders. Their dimensions varied in three steps above and below a volume of 8.61 cm^3 in the small ensemble size condition and 15.60 cm^3 in the large ensemble size condition (see **Table 1** for details). This resulted in a small average size ensemble display with an average volume of 10.33 cm^3 and a large average size ensemble display with an average volume of 13.72 cm^3. Orientations of the elliptical cylinders were also manipulated in three steps above and below 70° in the clockwise (CW) ensemble orientation condition and 110° in the counter-clockwise (CCW) ensemble orientation condition. This resulted in an average ensemble orientation of 70° in the CW condition and 110° in the CCW condition (circular cylinders did not convey orientation information; see **Table 2**). Each individual value of elliptical size and orientation (six each) was repeated twice within a given ensemble display (yielding 12 elliptical cylinders on each display), and specific size and orientation values were randomly assigned to positions on the inner (four ellipses) and outer (eight ellipses) rings of the ensemble displays. A square peg on the bottom of each cylinder fit into slots on an acrylic disk which ensured that the cylinders were accurately placed within the ensemble display. The entire display subtended approximately 24.5° of visual angle, and the inner ring subtended 9.9°.

Experimental Setup

Participants sat at a table with their right hand resting on an infrared (IR) button box positioned 18 cm from the table edge and 11.5 cm from the midline. Thirty centimeters directly in front of them was a display mount, tilted at a 45° angle, on which ensemble display disks could be interchanged. The target object was a cylinder held by a peg on a pentagonal platform in the center of the mount and was positioned 40 cm from the table edge. Behind the display and out of reach of the participant, a raised IR light acted as a timing flag for stimulus onset in the 3D-motion recording (see **Figure 1A**). Each ensemble disk had a pentagonal cut-out in the center, so it could be fitted on the mount in a specific and consistent orientation (see **Figure 1B**). There were five displays in total, one of which was an empty disk (i.e., no ensemble) that acted as a baseline measure for grasping. The other four varied in average size and orientation, resulting in (1) small/CW, (2) small/CCW, (3) large/CW, and (4) large/CCW ensemble display conditions (see **Figure 1C**). Liquid-crystal shutter goggles (PLATO system, Translucent Technologies Inc., ON, Canada) were worn to control stimulus presentation and were kept opaque while the ensemble displays were being set-up.

3D movement of the hand and fingers was recorded using three Qualisys Track Manager (QTM) camera units (Qualisys AB, Göteborg, Sweden). Surface electromyography (EMG) was recorded from five muscles (one shoulder muscle: anterior deltoid; and four forearm muscles: brachioradialis, common extensor digitorum, first dorsal interosseous, and the flexor digitorum profundus) using disposable surface electrodes (3 M Ag/AgCl, Red DotTM electrodes, 3 M Health Care, MN, United States) and a custom EEG set-up (ANT Neuro, Hengelo, The Netherlands) at a sampling frequency of 2,048 Hz. These target muscles are used in reach-to-grasp movements. Specifically, the anterior deltoid and brachioradialis support reaching and lifting movements, whereas the common extensor digitorum, first dorsal interosseous, and the flexor digitorum profundus contribute mainly to the precision grip (Kapandji, 1980; Maier and Hepp-Reymond, 1995; Bonnefoy et al., 2009). Additionally, the target muscles have been identified to be informative as an indirect measure of grip force (Hoozemans and Van Dieen, 2005; Lashgari et al., 2021). The EMG data were used only in the multivariate analysis. The experimental script was run on a Windows computer using MATLAB (version 2019b, MathWorks Inc., MA, United States). This computer was connected to a system of LabJack U3s (LabJack Corporation, CO, United States) that facilitated communication between the script, PLATO goggles, IR flag, IR button box, EEG system, and QTM cameras. Event flags were sent to the EEG system from the LabJack to synchronize EMG data with trial timing and 3D movement data. The timing lag of events and flags for all the equipment was measured to be <2.5 ± 3.28 ms on average, using an oscilloscope (PicoScope 2204A and software version 6, Pico Technology, England).

Pilot Study

A pilot study was run to equate differences in perceptual sensitivity for object size and orientation features. Specifically, we aimed to ensure that the difference in perceptual sensitivity between two different physical values on the size continuum was equated to the difference in perceptual sensitivity between two different physical values on the orientation continuum. Participants were asked to rank the size or orientation of 16 elliptical cylinders, eight of which only varied in size (small to large), and eight that only varied in orientation (CW to CCW). The order of ranking size and orientation was counterbalanced across participants, and the presentation of the cylinders was pseudorandomized, such that each object

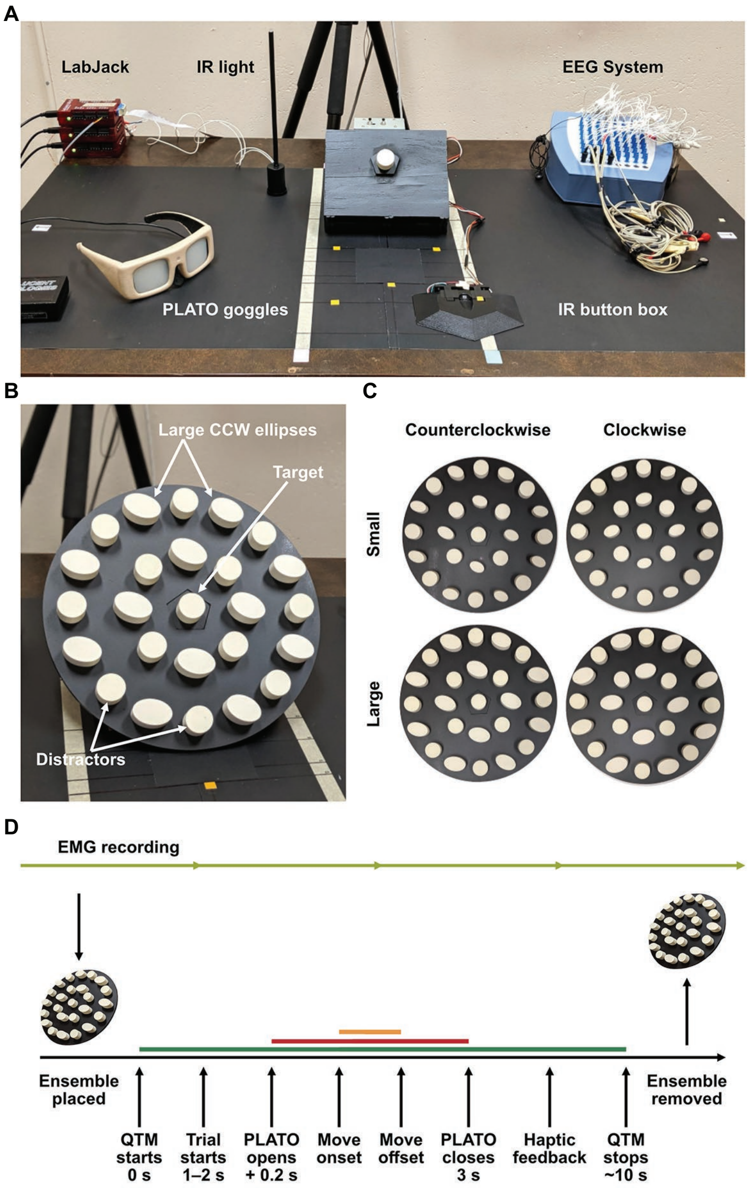

FIGURE 1 | (A) Experimental set-up, **(B)** mounted ensemble display, and **(C)** ensemble display stimuli. The central target object was held in place on a peg in the center of a pentagonal base, which the displays were fitted on to. Cylindrical distractors labeled in **(B)** were interleaved between ellipses to prevent visual pop-out of the target. The four ensemble conditions of small × CW, large × CW, small × CCW, and large × CCW are photographed in panel **(C)**. This standardized the presentation of the displays and ensured that the target position was constant on all trials. **(D)** Experimental procedure for a single trial. After completing their manual estimation on perceptual trials, participants grasped the target object to ensure haptic feedback of the target was present in both grasping and perceptual-estimation sessions. Electromyography (EMG) was recorded continuously throughout the session (light green line). The motion capture recording length is depicted by the dark green line, the stimulus presentation is depicted by the red line, and movement duration by the orange line.

was presented an equal number of times. The vertical axis was denoted as 90°, with any angle falling to the right being referred to as CW and angles greater than 90° or on the left side of the axis referred to as CCW. The smallest size and most CCW orientation were given a score of 1, and the largest size and most CW orientation a score of 8. Participants ranked objects one at a time and each object was ranked four times, with the resulting ranks being used to generate psychometric functions to guide the physical dimensions chosen for our ensemble stimuli. The ratio of the perceived rank to the actual rank of the objects was used to match the perceived difference between the large and small average ellipse size to the perceived difference between CW and CCW average orientation of our stimuli. This pilot procedure ensured that any difference between ensemble size and orientation processing in the main experiment could not be accounted for by differences in perceptual sensitivity across the stimulus features.

TABLE 1 | Size dimensions of cylinders in the ensemble displays.

Object size	Length (cm)	Width (cm)	Depth (cm)	Area (cm^2)	Volume (cm^3)
Circular cylinder	2.77	2.77	2.00	6.03	12.05
Small ellipse 1	1.77	2.66	2.00	3.70	7.40
Small ellipse 2	1.82	2.73	2.00	3.90	7.80
Small ellipse 3	1.87	2.80	2.00	4.10	8.21
Small ellipse 4	1.96	2.93	2.00	4.51	9.01
Small ellipse 5	2.00	3.00	2.00	4.71	9.42
Small ellipse 6	2.04	3.06	2.00	4.90	9.80
Small average size ensemble					10.33
Large ellipse 1	2.47	3.70	2.00	7.16	14.31
Large ellipse 2	2.50	3.74	2.00	7.33	14.67
Large ellipse 3	2.53	3.79	2.00	7.52	15.03
Large ellipse 4	2.59	3.88	2.00	7.87	15.75
Large ellipse 5	2.61	3.92	2.00	8.05	16.10
Large ellipse 6	2.64	3.97	2.00	8.23	16.46
Large average size ensemble					13.72

The dimensions of the elliptical cylinders varied in three steps above and below a volume of 8.61 cm^3 in the small average size condition and 15.60 cm^3 in the large average size condition. Each display held 12 elliptical cylinders, and as such each individual size was repeated twice within a display for its respective size condition.

TABLE 2 | Orientation values of cylinders in the ensemble displays.

Object orientation	Degrees
Circular cylinder	NA
Clockwise ellipse 1	62.5
Clockwise ellipse 2	65
Clockwise ellipse 3	67.5
Clockwise ellipse 4	72.5
Clockwise ellipse 5	75
Clockwise ellipse 6	77.5
Clockwise average orientation ensemble	70
Counter-clockwise ellipse 1	102.5
Counter-clockwise ellipse 2	105
Counter-clockwise ellipse 3	107.5
Counter-clockwise ellipse 4	112.5
Counter-clockwise ellipse 5	115
Counter-clockwise ellipse 6	117.5
Counter-clockwise average orientation ensemble	110

Orientations of the elliptical cylinders were set to three steps above and below 70° in the clockwise average orientation condition and 110° in the counter-clockwise average orientation condition. Each display held 12 elliptical cylinders, and as such each individual orientation was repeated twice within a display for its respective orientation condition.

3D Motion Capture

The movement of the hand and fingers were recorded using eight passive IR markers attached to the inner corner of the nail for the thumb and index finger, the second joint of the index finger, first joint of the thumb, index, and little fingers, and the styloid process of the radius and ulna of the wrist. The main markers used in the univariate analysis were the markers on the distal phalanges of the thumb and index finger (the remaining six markers were used for multivariate analyses). Motion was recorded at a sampling rate of 240 Hz. Cameras were calibrated at the beginning of each session and at times when marker tracking became irregular (i.e., abnormal number of tracked markers displayed by the cameras).

Procedure

The experiment was separated into grasping and perceptual-estimation sessions. In each session, the participant was instructed to perform different tasks; however, the general set-up and sequence of events were kept the same. All participants completed both sessions in 1 day, and session order was counterbalanced across participants. At the beginning of each trial, participants were required to rest their index finger on the IR button-box. This allowed us to precisely measure movement onset. The participant's middle, ring, and little finger were secured using skin-friendly tape to ensure that they only grasped using their index finger and thumb. At the start of each trial, the ensemble disk corresponding to the condition on that trial (i.e., small/CW, small/CCW, large/CW, and large/CCW) would be mounted on the display, after which the experimenter would start the motion capture recording. After a random time interval between 1 and 2 s, the IR flag would turn on (this allowed us to align the trial data with a signal that was visible in the QTM data), and after 200 ms, the PLATO goggles would open. This marked the time of stimulus onset and acted as a go-signal for participants to begin their response. In the grasping session, the participant would pick up the target object (i.e., the central circular cylinder) using their thumb and index finger, place it back on the peg and return their index finger to the starting position. In the perceptual-estimation session, the participant would perform a manual-estimation task (i.e., judgments of either average size or orientation) by adjusting the distance between their thumb and index finger to report the perceived average size of the ensemble display and adjusting the angle between their thumb and index finger to report the perceived average orientation of the ensemble display. For both manual estimation tasks, participants were told to hold their fingers in place until the goggles closed before returning their hand to the starting position. In both sessions, the PLATO goggles remained open for 3 s (see **Figure 1D**). Participants were instructed to remain fixated on the central target object throughout the experiment, and although eye-tracking equipment was not used, fixation was monitored by the experimenter. If the participant made a faulty response, the incorrect display was used, or there were any major disturbances to the motion or EMG recordings (e.g., the cameras were disturbed, or the object dropped), the trial was excluded without replacement (which, including poor data recording, accounted for four trials on average per participant). At the beginning of each session, participants were given 10 practice trials to become accustomed to the task. In the grasping session, this consisted of grasping the central target surrounded by an ensemble display. In the perceptual session, the first half of the practice trials were matched to the estimation task they would encounter first in the experimental session, and the second half of the practice trials matched the other task. The presentation of ensemble displays was pseudorandomized such that each display was presented an equal number of times in the experimental trials and the same display was never shown twice in a row.

Perception – Manual Estimation Task

Participants gave manual perceptual estimations of average size and average orientation in separate blocks of trials. For the average size estimation task, participants were told to adjust the distance between the thumb and index finger of their right hand (keeping a constant orientation) until it matched their perceptual estimation of the average size of the ensemble objects. For the average orientation estimation task, they were told to rotate the imaginary line between their thumb and index finger (keeping the distance between the digits constant) until it matched their perceptual estimation of the average orientation of the ensemble objects. Participants were instructed to use the long axis of the ellipses for their responses in the size and orientation tasks.

Due to occlusion of the infrared-markers by the hand under certain movements, participants were asked to give their size estimation with their thumb and index finger orientated at a roughly constant 45°, and average orientation was always reported by turning the hand while holding the size of their GA constant. When reporting the CCW average ensemble orientation, participants were asked to rotate their hand CCW instead of CW as the latter resulted in the occlusion of the infrared markers. For both tasks, participants held their manual estimation until the goggles closed, after which they returned their hand to the starting position. In order to provide the same haptic feedback encountered in the grasping trials, the goggles then reopened, and the participant performed a typical grasp of the target before returning their hand to the starting position to await the start of the next trial. This haptic feedback was not recorded for the first set of participants, but the methods were modified afterward to include it (see "Modifications to the Experimental Procedure" section for more details). The session consisted of 90 trials, starting with 10 practice trials, followed by 80 experimental trials split into four blocks (two blocks each for the average size and orientation estimation tasks, the order of which was counterbalanced across participants using an ABAB design) of 20 trials each.

Action – Grasping Task

The opening of the goggles served as a "go-signal" for the participants, and they were instructed to reach for the central target object as quickly and accurately as possible, grasp it using a precision grip (between the thumb and index finger of the right hand), and lift it a short distance above the display before placing the object back and returning their hand to the start position. The session consisted of 110 trials, the first 10 being practice trials, followed by 10 baseline trials, 80 grasping trials (split into four blocks of 20 trials each, where each ensemble display was presented five times), and concluded with another 10 baseline trials. In the baseline trials, the central target object was presented alone on an empty display (i.e., with no surrounding ensemble). This allowed us to investigate the influence of obstacle avoidance on grasping targets embedded within an ensemble display and thus the baseline trials served as a control condition.

Modifications to the Experimental Procedure

After collecting data for 10 participants, we made two modifications to the experimental procedure based on methodological and theoretical considerations. First, we adjusted how the participants placed their fingers on the starting position at the beginning of each trial. For the first 10 participants, the hand starting position was a relaxed open palm with their right index finger in the IR button box. By using this starting position, the thumb and index finger were widely separated at the beginning of each trial, and as such maximum grip aperture (MGA) was flagged as occurring at the start of movement onset as the hand lifted from the table, instead of at roughly 75% of movement duration, as is typically reported with grasping tasks (Jeannerod, 1984; Hu and Goodale, 2000). Because of this, for the first 10 participants, we visually assessed the timepoint where MGA was found on a trial-by-trial basis, and where MGA occurred at movement onset, we manually adjusted the time interval to calculate MGA from 50 to 100% movement duration, to coincide with the standard procedure in the field. To avoid this unnecessary step for the final round of data collection, for the last five participants, we adjusted the starting position, so the thumb was touching the tip of the index finger as it rested on the button box. Second, we recorded and analyzed the haptic feedback component of the perceptual-estimation trials. That is, after participants made their manual estimation of either average size or orientation, they returned their thumb and index finger to the starting position, and then initiated a grasping movement to the central target, identical to the procedure used in the grasping trials. This allowed us to investigate whether making a prior perceptual estimation of either average size or orientation affected subsequent grasping movements to the target embedded within the ensemble display (in subsequent sections we refer to these distinctions as "perception," "grasping," and "haptic feedback"). We compared the data collected before and after these modifications and found that the data were very similar across both collection rounds except for GO during grasping (see "Data Collection Round – Original Experimental Procedure vs. Modified Experimental Procedure" section of the results for more details).

Data Preprocessing

QTM Data Preprocessing

After data collection, the individual markers in the motion capture recordings were automatically labeled using a customized model in the Qualisys Track Manager software (version 1.8, Qualisys AB, Göteborg, Sweden). Each trial was then visually inspected and mislabeled markers were manually corrected. Missing coordinate data that spanned less than 20 frames (4.80 ms) were automatically gap-filled using non-uniform rational B-spline interpolation (Piegl and Tiller, 1987). Larger gaps were manually filled if they were near the start or end of the recording (before the go-signal or after the participant had returned their hand to the starting position).

Otherwise, trials with large gaps were excluded. In a small number of trials, the recorded data were poor (e.g., 70+ recorded markers, instead of the expected nine). In these cases, it was not feasible to confidently individuate the markers and the trials were flagged for exclusion (including issues during data capture, this accounted for four trials on average per participant).

The pre-processed marker positions were then exported into MATLAB where velocity, peak velocity, onset and offset velocity, acceleration, stimulus onset time, movement onset and offset time, movement duration, reaction time, grip aperture, and grip orientation were defined. To reduce recording artifacts, the positional and velocity data were smoothed using low-pass Butterworth filters for position (n = 2, cut-off frequency = 8 Hz) and velocity (n = 2, cut-off frequency = 12 Hz), in the forward and backward direction to remove phase shift. The IR flag marker was used in conjunction with the timestamps collected in the trial data in the MATLAB experimental script to ensure that the timing of the MATLAB and QTM computer was aligned. Movement onset was defined as the time point when the index finger was lifted from the IR button box, movement offset was defined as when the velocity dropped below 10% of the peak velocity. Movement duration was defined as the time between movement onset and offset, and reaction time was defined as the time between stimulus onset and movement onset.

EMG Preprocessing

Asa (version 4.1, ANT Neuro, Hengelo, The Netherlands) was used to export the EMG files which were analyzed in MATLAB using Letswave6.[1] The data were high pass filtered (Butterworth, n = 4, low cut-off frequency = 2 Hz) to remove artifacts and linear detrending and removal of DC offset were also applied to the data. Full-wave rectification of the signal was followed by smoothing with a low-pass Butterworth filter (n = 4, high cut-off frequency = 5 Hz) to construct the linear envelope. The signal was then down sampled to 240 Hz using the nearest neighbor interpolation method to match the sampling rate of the QTM data. The EMG signal was then aligned to movement onset and segmented from the session's maximum reaction time to the maximum movement duration with a 200 ms buffer on either end.

Data Exclusion and Cleaning

In addition to trials flagged for exclusion during data collection and preprocessing, trials were also excluded based on reaction time (<250 ms), percentage of total recording frames where the IR marker was tracked successfully (<95%), and the presence of outliers (beyond 1.5 times the interquartile range) for grip aperture or orientation. Based on these criteria, 16% of trials were excluded for the perception trials, 19% were excluded for the haptic feedback trials (recorded after modifications to the experimental procedure), and 11% were excluded for the grasping trials. This left a total of 1,007 trials for the perceptual data, 1,329 trials for the grasping data, and 324 trials for the haptic feedback data for the final analysis. Additionally, due to technical failure, the EMG data for one participant's perception session could not be extracted.

DATA ANALYSIS

Univariate Analyses

Dependent Variables

Grip aperture was defined as the distance, in millimeters, between the thumb and index markers in 3D space during grasping or manual estimation. Grip orientation was defined as the angle between the horizontal axis of the ensemble display and the projection of the vector connecting the thumb and index fingers onto the display surface.

The dependent variables for the grasping and haptic feedback tasks were MGA and GO at the time of MGA, whereas the dependent variables for the perceptual manual estimation tasks were GA and GO at movement offset averaged over 16.7 ms (four frames). In the size-discrimination task, the relevant dependent measure was GA as this was scaled according to the participant's estimate of average ensemble size. Likewise, GO was the relevant dependent measure in the orientation-discrimination task.

Perception – Manual Estimation Task

Multilevel models were used to model GA as a function of average ensemble size (small vs. large), average ensemble orientation (CW vs. CCW), the interaction between size and orientation, and the round of data collection (original experimental procedure vs. modified experimental procedure), for the size- and orientation-discrimination tasks separately. The intraclass correlation (ICC) for the models suggested that grip aperture was mildly clustered within participants (Size discrimination task: $ICC = 0.38$, $N = 515$, $\alpha = 0.05$, $p < 0.00001$; Orientation discrimination task: $ICC = 0.56$, $N = 492$, $\alpha = 0.05$, $p < 0.00001$), suggesting that it was appropriate to account for the interdependence of trial observations by including a random intercept for participant in our analysis. Grip orientation was modeled similarly, and the ICC for the models suggested that GO was significantly clustered within participants for the size-discrimination task ($ICC = 0.720$, $N = 515$, $\alpha = 0.05$, $p < 0.00001$) but not for the orientation-discrimination task: $ICC < 0.00001$, $N = 429$, $\alpha = 0.05$, $p > 0.05$). Therefore, the random intercept for participant was not strictly necessary in the orientation-discrimination task model.

To account for the nesting of trials within participants, all models included a random intercept for participant. Models were estimated with an unstructured covariance matrix using the lmer function from the lme4 package (version 1.1-23; Bates et al., 2015) in R version 3.6.2 (R Core Team, 2019). The lmerTest package (version 3.0-1; Kuznetsova et al., 2017) was used to report results of statistical tests including degrees of freedom which were estimated using Satterthwaite's approximation. Effect sizes are reported as partial R^2 values (Edwards et al., 2008).

Action – Grasping Task

For the grasping trials, MGA and GO were modeled separately as a function of average ensemble size, orientation, their interaction, and the round of data collection. Both grip aperture ($ICC = 0.75$, $N = 1{,}081$, $\alpha = 05$, $p < 0.00001$) and grip

---

[1] https://www.letswave.org/

orientation (*ICC* = 0.67, *N* = 1,081, α = 0.05, $p < 0.00001$) were moderately clustered within participants.

Grasping vs. Baseline vs. Haptic Feedback Tasks

To examine the influence of obstacle avoidance and prior perceptual processing on subsequent grasping movements, MGA and GO were modeled separately as a function of the type of grasping task (grasping vs. baseline vs. haptic feedback). The main grasping task was specified as the reference level, and so the baseline task was compared with the main grasping task to examine the effects of obstacle avoidance, while the haptic feedback task was compared to the main grasping task to examine effects of perceptual estimation on grasping. The ICC for both models suggested that both maximum grip aperture (*ICC* = 0.68, *N* = 1,653, α = 0.05, $p < 0.00001$) and grip orientation (*ICC* = 0.66, *N* = 1,653, α = 0.05, $p < 0.00001$) were moderately clustered within participants.

Variability of Grasping Movements

As grasps were directed to a single target that had a constant shape and size, it was possible that the grasping movement became stereotyped with repetition over the experimental session. In order to examine whether this occurred, we conducted a *post-hoc* analysis of the SD of MGA and GO across the grasping session (calculated for each participant; split into one bin of 10 practice trials, one bin of 10 initial baseline trials, four bins of 20 grasping trials each, and one bin of 10 final baseline trials). SD of MGA and GO were modeled separately as a function of trial bin, with the first bin (practice trials) as the reference level. The ICC for both models suggested that SD of MGA (*ICC* = 0.36, *N* = 1,446, α = 0.05, $p < 0.00001$) and GO (*ICC* = 0.56, *N* = 1,446, α = 0.05, $p < 0.00001$) were clustered within participants. All models included a random intercept for participant, and the dependent variable was modeled as a function of bin. Since the data for MGA and GO had slightly non-normally distributed residuals, we re-ran the analysis on square root transformed data. The results for GO did not differ from the original, and, while the transformed vs. non-transformed results were slightly different for MGA, the overall result was the same. That is, there was no decreasing trend of variability in grasping movements over time compared with the practice trials. Thus, we report the results using the non-transformed data for both GO and MGA, but the transformed results for both can be found in the **Supplementary Materials**.

Multivariate Analyses

The QTM and EMG data were combined and used to train the support vector machine (SVM) models in the multivariate analysis. Specifically, this included the 3D coordinate data for all eight QTM markers, calculated velocity and acceleration, grip aperture, grip orientation, and the EMG channels from the five muscles (see **Figure 2**). SVM classification (LibSVM ver. 3.24, Chang and Lin, 2011) was used to determine whether average ensemble size (small vs. large) and orientation (CW vs. CCW) could be decoded from the kinematic and EMG data. SVM classification was performed across the timepoints between stimulus onset to movement offset (+200 ms on either end). Leave-one-out cross-validation was used to assess the performance of the classifier. Five classification permutations were performed for each participant. In each permutation, trials were randomized within their category and averaged in pairs. The averaged accuracy values for each participant were then calculated and combined. One-tailed one-sample *t*-tests, corrected for false discovery rate, were used to test if accuracy values at each time-point were significantly greater than chance.

RESULTS

Univariate Results

Perception – Manual Estimation Task

In the size-discrimination task, there was a significant main effect of size (*b* = 11.60, *SE* = 0.53, *t*(497.52) = 21.76, $p < 0.0001$, $R^2 = 0.49$) on GA. Grip aperture was the relevant dependent measure in the size-discrimination task, since changes in this measure were meant to scale with participants' estimates of perceived average size. As expected, we observed that GA was significantly larger for the large average size ensemble displays (*M* = 63.8, *SE* = 1.79, 95% *CI* = [60.0, 67.7]) compared with the small average size displays (*M* = 52.2, *SE* = 1.8, 95% *CI* = [48.4, 56.1]). The main effect of orientation (*b* = −0.42, *SE* = 0.53, *t*(497.08) = −0.79, *p* = 0.431, $R^2 < 0.005$; M_{CW} = 58.2, *SE* = 1.79, 95% *CI* = [54.4, 62.1]; M_{CCW} = 57.8, *SE* = 1.80, 95% *CI* = [54.0, 61.7]; see **Figure 3A**) and the interaction between size and orientation were not significant (*b* = 0.53, *SE* = 1.07, *t*(496.95) = 0.50, *p* = 0.619, $R^2 < 0.00001$). There was a significant main effect of size (*b* = −3.02, *SE* = 0.58, *t*(496.94) = −5.24, $p < 0.0001$, $R^2 = 0.05$), and orientation (*b* = 2.39, *SE* = 0.58, *t*(496.74) = 4.15, $p < 0.001$, $R^2 = 0.03$), on GO in the size-discrimination task. The results indicated that GO was larger in the small average size display (*M* = 46.3, *SE* = 3.04, 95% *CI* = [39.7, 52.8]) than in the large average size display (*M* = 43.2, *SE* = 3.03, 95% *CI* = [36.7, 49.8], and it was also larger in the CCW average orientation display (*M* = 45.9, *SE* = 3.04, 95% *CI* = [39.4, 52.5]) compared with the CW orientation display (*M* = 43.6, *SE* = 3.03, 95% *CI* = [37.0, 50.1]; see **Figure 3B**). The interaction between size and orientation was not significant (*b* = 0.59, *SE* = 1.15, *t*(496.68) = 0.51, *p* = 0.609, $R^2 < 0.005$).

In the orientation-discrimination task, there was a significant main effect of size (*b* = 5.43, *SE* = 0.42, *t*(474.22) = 12.86, $p < 0.0001$, $R^2 = 0.26$) on GA. Specifically, GA was significantly larger in the large average size display (*M* = 62.2, *SE* = 1.69, 95% *CI* = [58.6, 65.8]) compared with the small average size display (*M* = 56.8, *SE* = 1.69, 95% *CI* = [53.1, 60.4]). The main effect of orientation (*b* = −0.73, *SE* = 0.42, *t*(474.24) = −1.73, *p* = 0.085, $R^2 = 0.01$; M_{CW} = 59.9, *SE* = 1.69, 95% *CI* = [56.2, 63.5]; M_{CCW} = 59.1, *SE* = 1.69, 95% *CI* = [55.5, 62.8]; see **Figure 4A**) and the interaction between size and orientation were not significant (*b* = 0.01, *SE* = 0.84, *t*(474.02) = 0.08, *p* = 0.941, $R^2 < 0.00001$). There was a significant main effect of orientation (*b* = 114.58, *SE* = 2.03, *t*(478.38) = 56.35, $p < 0.0001$, $R^2 = 0.87$), but not size (*b* = 2.72,

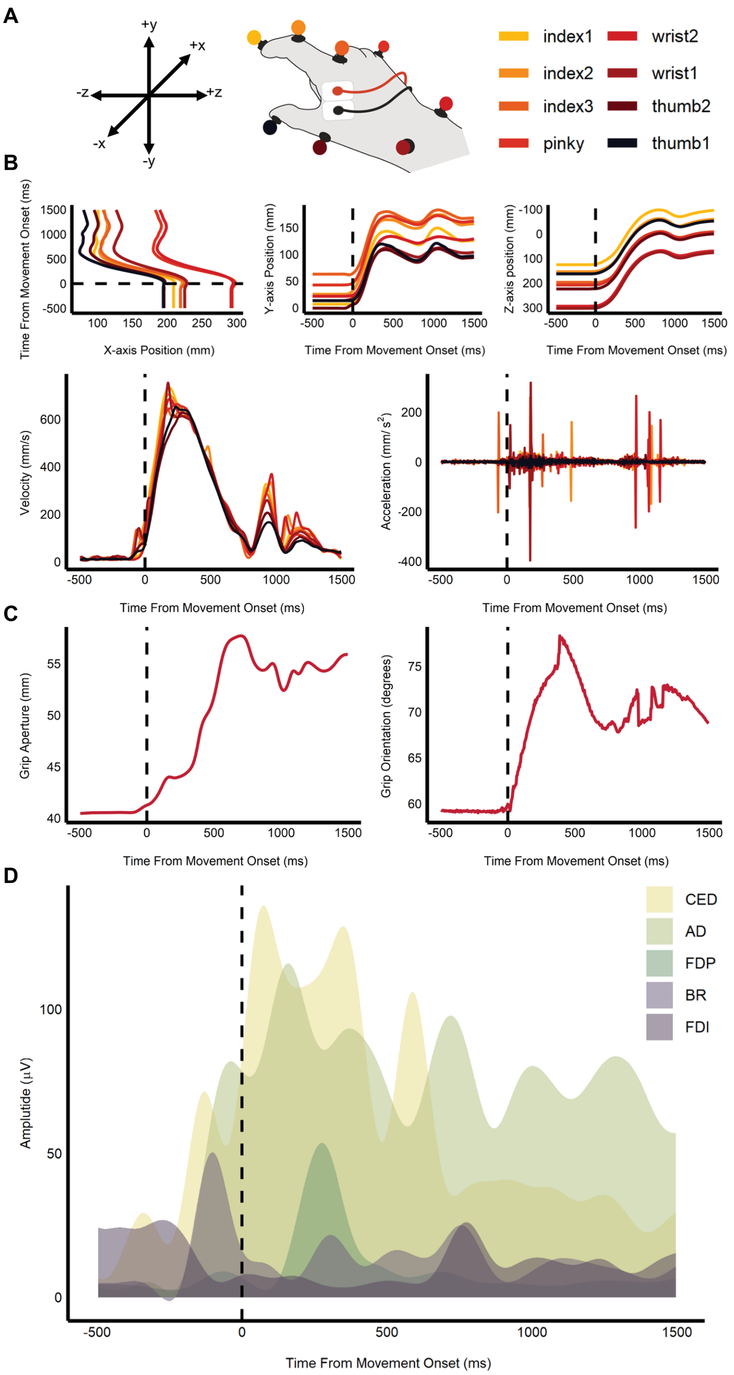

FIGURE 2 | Sample of kinematic and EMG measures used in the multivariate analysis. Plot shows **(A)** the coordinate map of the *x*, *y*, and *z*-axes and an illustration of the markers' position on the hand; **(B)** change in marker position, velocity, and acceleration over time; **(C)** change in grip aperture and orientation over time; and **(D)** plot of EMG amplitudes in the five recorded muscles: anterior deltoid (AD), brachioradialis (BR), common extensor digitorum (CED), first dorsal interosseous (FDI), and the flexor digitorum profundus (FDP) for one trial. The dashed line represents movement onset.

SE = 2.03, *t*(477.82) = 1.34, *p* = 0.181, $R^2 < 0.005$) on GO in the orientation-discrimination task. The interaction between size and orientation was significant (*b* = 13.48, *SE* = 4.05, *t*(475.51) = 3.33, $p < 0.001$, $R^2 = 0.02$). Grip orientation was the relevant dependent measure in the orientation-discrimination task, since changes in this measure were meant to scale with participants' estimates of perceived average orientation. As expected, GO was significantly larger in the CCW average orientation display (*M* = 147.4, *SE* = 2.22, 95% *CI* = [142.7, 152.0]) than in the CW average orientation display (*M* = 32.78,

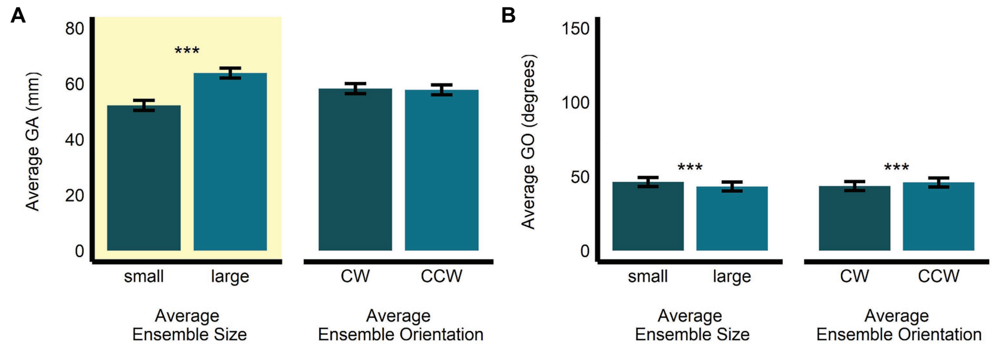

FIGURE 3 | Univariate results of the perceptual average size-discrimination task. Estimated marginal means of average **(A)** grip aperture and **(B)** grip orientation are given for the small and large average size ensemble displays, and for the CW and CCW average orientation ensemble displays. ***$p < 0.0001$; error bars depict SEM; GA, grip aperture; GO, grip orientation; CW, clockwise; CCW, counter-clockwise. Grip aperture was the grasp parameter most relevant to the size-discrimination task and is highlighted in yellow.

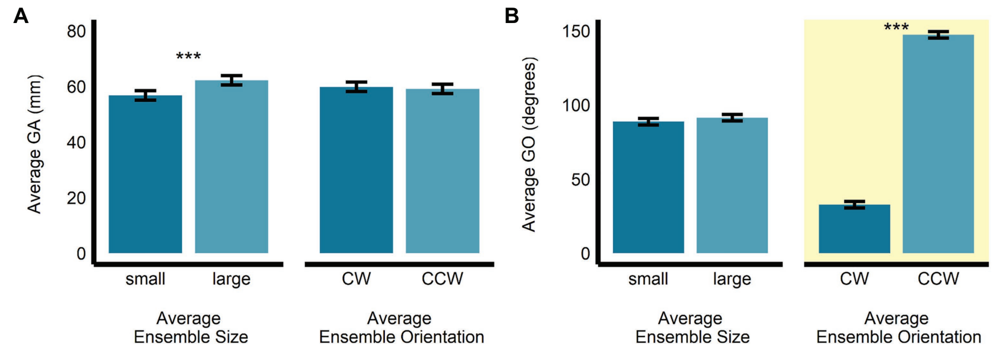

FIGURE 4 | Univariate results of the perceptual average orientation-discrimination task. Estimated marginal means of average **(A)** grip aperture and **(B)** grip orientation are given for the small and large average size ensemble displays, and for the CW and CCW average orientation ensemble displays. ***$p < 0.0001$; error bars depict SEM; GA, grip aperture; GO, grip orientation; CW, clockwise; CCW, counter-clockwise. Grip orientation was the grasp parameter most relevant to the orientation-discrimination task and is highlighted in yellow.

$SE = 2.18$, 95% $CI = [28.23, 37.33]$). GO did not significantly differ between the small ($M = 88.7$, $SE = 2.2$, 95% $CI = [84.1, 93.3]$) and large ($M = 91.4$, $SE = 2.2$, 95% $CI = [86.8, 96.0]$) average size displays (see **Figure 4B**).

Further examination of the significant interaction between size and orientation revealed that GO was significantly larger for the large compared with the small ensembles for the CCW average orientation displays ($b = -9.46$, $SE = 2.94$, $t(476) = -3.22$, $p < 0.005$), but not for the CW average orientation displays ($b = 4.02$, $SE = 2.79$, $t(478) = 1.44$, $p = 0.15$, $R^2 < 0.005$; see **Figure 5A**). In contrast, the significant difference in GO between CW and CCW ensemble displays was apparent for both the small ($b = -1.08$, $SE = 0.88$, $t(477) = -37.43$, $p < 0.0001$) and large ($b = -121$, $SE = 2.86$, $t(477) = -42.46$, $p < 0.0001$) average size ensemble displays (see **Figure 5B**).

Action – Grasping Task

Maximum grip aperture was not significantly affected by average ensemble size ($b = 0.02$, $SE = 0.16$, $t(1063.01) = 0.148$, $p = 0.88$, $R^2 < 0.001$; $M_{\text{Large}} = 62.5$, $SE = 1.2$, 95% $CI = [59.9, 65.1]$; $M_{\text{Small}} = 62.5$, $SE = 1.2$, 95% $CI = [59.9, 65.1]$), orientation ($b = -0.29$, $SE = 0.16$, $t(1063.02) = -1.86$, $p = 0.064$, $R^2 < 0.005$; $M_{\text{CCW}} = 62.4$, $SE = 1.2$, 95% $CI = [59.8, 65.0]$; $M_{\text{CW}} = 62.7$, $SE = 1.2$, 95% $CI = [60.1, 65.3]$), or their interaction ($b = -0.03$, $SE = 0.31$, $t(1{,}063) = -0.09$, $p = 0.93$, $R^2 < 0.001$; see **Figure 6A**).

Similarly, GO was not significantly affected by average ensemble size ($b = 0.50$, $SE = 0.38$, $t(1{,}063) = 1.34$, $p = 0.18$, $R^2 < 0.005$; $M_{\text{Large}} = 63.5$, $SE = 1.36$, 95% $CI = [59.5, 67.5]$; $M_{\text{Small}} = 63.0$, $SE = 1.86$, 95% $CI = [59.0, 67.0]$), orientation ($b = 0.07$, $SE = 0.38$, $t(1{,}063) = 0.20$, $p = 0.84$, $R^2 < 0.001$; $M_{\text{CCW}} = 63.3$, $SE = 1.86$, 95% $CI = [59.3, 67.3]$; $M_{\text{CW}} = 63.2$, $SE = 1.86$, 95% $CI = [59.2, 67.2]$; $b = 0.07$, $SE = 0.38$, $t(1{,}063) = 0.20$, $p = 0.84$, $R^2 < 0.001$), or their interaction ($b = 0.51$, $SE = 0.75$, $t(1{,}063) = 0.68$, $p = 0.50$, $R^2 < 0.001$; see **Figure 6B**).

Data Collection Round – Original Experimental Procedure vs. Modified Experimental Procedure

The effect of round of data collection (original procedure vs. modified procedure; see "Modifications to the Experimental

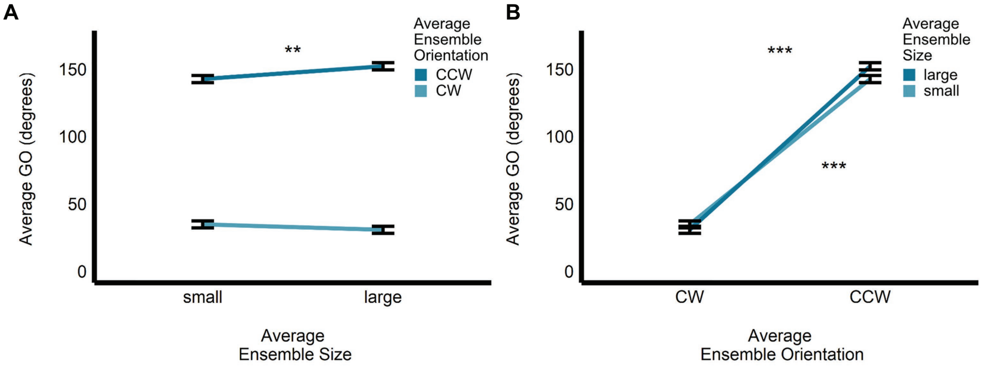

FIGURE 5 | Univariate results of the size-by-orientation interaction for GO in the perceptual orientation-discrimination task. Differences in the estimated marginal means of GO are plotted for **(A)** small vs. large average size, for CW and CCW ensemble displays, and **(B)** CW vs. CCW average orientation, for small and large ensemble displays. ***p* < 0.005, ****p* < 0.0001; error bars depict SEM; GO, grip orientation; CW, clockwise; CCW, counter-clockwise.

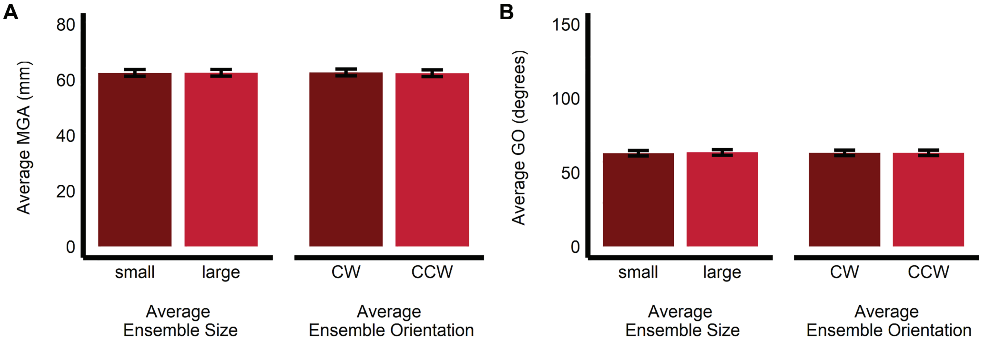

FIGURE 6 | Univariate results of the grasping task. Estimated marginal means of average **(A)** maximum grip aperture and **(B)** grip orientation are given for the small and large average size ensemble displays, and for the CW and CCW average orientation ensemble displays. Error bars depict SEM; MGA, maximum grip aperture; GO, grip orientation; CW, clockwise; CCW, counter-clockwise.

Procedure" for more details) was not significant for both GA and GO in the perceptual manual-estimation task (size-discrimination task: $b_{GA} = -0.91$, $SE = 3.55$, $t(12.98) = -0.26$, $p = 0.81$, $R^2 < 0.01$, $b_{GO} = 2.4$, $SE = 6.05$, $t(12.71) = 0.40$, $p = 0.698$, $R^2 = 0.01$; orientation-discrimination task: $b_{GA} = -1.13$, $SE = 3.55$, $t(12.92) = -0.34$, $p = 0.74$, $R^2 = 0.01$, $b_{GO} = -1.26$, $SE = 3.91$, $t(12.76) = -0.31$, $p = 0.76$, $R^2 = 0.01$).

For the grasping trials, the effect of round of data collection was not significant for MGA ($b = -2.66$, $SE = 2.40$, $t(13.0) = -1.11$, $p = 0.29$, $R^2 = 0.09$), but there was a significant effect on GO ($b = 12.42$, $SE = 3.70$, $t(12.99) = 3.36$, $p < 0.05$, $R^2 = 0.46$). Together, this demonstrates that, by and large, the modifications we made to our experimental procedure did not appreciably affect the main results of our univariate analyses.

The Effect of Obstacle Avoidance and Perceptual Processing on Grasping Movements

As we stated above, to examine the influence of obstacle avoidance and prior perceptual processing on subsequent grasping movements, we compared the data in the main grasping trials with those in the baseline grasping (i.e., grasping the central target in the absence of a surrounding ensemble) and haptic feedback (i.e., conducting a grasping movement immediately after making a discrimination of average size or orientation in the perceptual manual-estimation task) trials, respectively. We found that there was a significant main effect of task on MGA ($F(2, 1638.12) = 164.84$, $p < 0.0001$, $R^2 = 0.17$) and GO ($F(2, 1688.70) = 6.95$, $p < 0.001$, $R^2 = 0.01$).

Specifically, the baseline task ($M = 66.5$, $SE = 1.16$, 95% $CI = [64.0, 69.0]$) had significantly larger values of MGA compared with both the main grasping task ($M = 63.0$, $SE = 1.15$, 95% $CI = [60.5, 65.4]$; $b = 3.52$, $SE = 0.20$, $t(1,636) = 17.85$, $p < 0.0001$) and haptic feedback task ($M = 63.0$, $SE = 1.16$, 95% $CI = [60.5, 65.5]$; $b = 3.49$, $SE = 0.26$, $t(1,638) = 13.55$, $p < 0.0001$). MGA in the grasping and haptic feedback tasks did not significantly differ ($b = -0.03$, $SE = 0.21$, $t(1,640) = -0.15$, $p = 0.987$; see **Figure 7A**). Similarly, grip orientation was significantly smaller (more CW) in the baseline task ($M = 59.6$, $SE = 2.26$, 95% $CI = [54.7, 64.4]$) compared with both the grasping ($M = 61.2$, $SE = 2.23$, 95% $CI = [56.4, 66.0]$; $b = -1.62$, $SE = 0.44$, $t(1,636) = -3.72$, $p < 0.001$) and haptic feedback ($M = 61.0$, $SE = 2.26$, 95% $CI = [56.1, 65.8]$; $b = -1.41$,

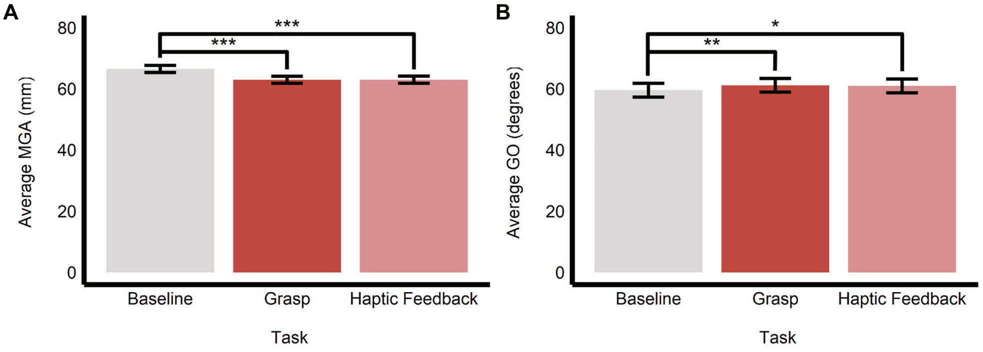

FIGURE 7 | Effects of obstacle avoidance and prior perceptual processing on grasping movements. Estimated marginal means of **(A)** maximum grip aperture and **(B)** grip orientation are plotted for the three different kinds of grasping tasks employed in this study. Comparing the baseline and grasp tasks reveals the effects of obstacle avoidance, whereas comparing the grasp and haptic feedback tasks reveals the effects of prior perceptual processing on subsequent grasping movements. $^{*}p < 0.05$, $^{**}p < 0.005$, $^{***}p < 0.0001$; error bars depict SEM; MGA, maximum grip aperture; GO, grip orientation.

$SE = 0.5$, $t(1{,}639) = -2.48$, $p < 0.05$) tasks. Like the results with MGA above, GO did not significantly differ between the grasping and haptic feedback tasks ($b = 0.21$, $SE = 0.46$, $t(1{,}641) = 0.46$, $p = 0.891$; see **Figure 7B**).

Variability of Grasping Movements

Because grasping movements might have become stereotyped with repetition, thereby obscuring any influence of the ensembles, we tested whether variability declined over time, by comparing variability in each grasping bin to that observed in the practice bin. However, we observed no such trend (in fact, the data trended in the opposite direction, with some bins showing significantly greater variability compared with the practice trials). There was an overall effect of bin on the SD of MGA ($F(6, 1425.32) = 29.89$, $p < 0.0001$, $R^2 = 0.11$) and GO ($F(6, 1425.15) = 13.82$, $p < 0.0001$, $R^2 = 0.06$). The SD of MGA was smaller in the practice trials ($M = 2.30$, $SE = 0.12$, 95% $CI = [2.04, 2.56]$) compared to the baseline trials ($M_{\text{Initial baseline}} = 2.44$, $SE = 0.12$, 95% $CI = [2.18, 2.70]$; $b = 0.14$, $SE = 0.07$, $t(1{,}425) = 1.99$, $p = 0.047$; $M_{\text{Final baseline}} = 3.05$, $SE = 0.12$, 95% $CI = [2.79, 3.31]$; $b = 0.76$, $SE = 0.07$, $t(1{,}425) = 10.49$, $p < 0.0001$) and the 1st and 4th quartile of the grasping trials ($M_{\text{Grasp bin1}} = 2.43$, $SE = 0.12$, 95% $CI = [2.18, 2.68]$; $b = 0.13$, $SE = 0.06$, $t(1{,}426) = 2.15$, $p = 0.032$; $M_{\text{Grasp bin 4}} = 2.59$, $SE = 0.12$, 95% $CI = [2.34, 2.84]$; $b = 0.30$, $SE = 0.06$, $t(1{,}425) = 4.77$, $p < 0.0001$; see **Figure 8A**). The SD of GO was smaller in the practice trials ($M = 4.06$, $SE = 0.51$, 95% $CI = [2.97, 5.14]$) compared with all other baseline and grasping bins (all ts > 5.05, all ps < 0.0001; see **Figure 8B**).

Multivariate Results

When trained on the perceptual data, the classification accuracy between the small and large ensemble size begins to increase after movement onset, becoming significantly greater than chance level (50%) after 112.50 ms (approximately 5.34% of movement duration) and remains significantly greater than chance throughout the rest of the movement duration (see **Figure 9A**). This change is not seen when the classifier is trained and tested on the grasping data as the classification accuracy remains at chance level throughout movement duration (see **Figure 10A**). Classification accuracy of the haptic feedback trials did not differ significantly from chance, except for one timepoint (accounting for 4.16 ms) occurring at 40.04% movement duration.

Similarly, when trained on the perceptual data, classification of ensemble orientation (i.e., CW vs. CCW) becomes significantly greater than chance level 25 ms before movement onset (−1.19% of movement duration) and remains significantly greater than chance throughout movement duration (see **Figure 9B**). In contrast, when the classifier is trained on the grasping data, classification accuracy does not significantly differ from chance throughout the movement duration (see **Figure 10B**). Classification accuracy of the haptic feedback trials did not significantly differ from chance at any timepoint.

DISCUSSION

In this study, we investigated whether ensemble statistics can bias grasping behavior. We did this by asking participants to reach out to grasp a target circular cylinder that was surrounded by a background ensemble of circular and elliptical cylinders that varied systematically in their orientation and size. Notably, unlike ellipses, circular targets afford multiple uniquely comfortable or efficient grasp postures, meaning that participants would be free to orient their grip however they saw fit (in other words, the circular target did not constrain a specific grasp posture with respect to grip orientation). We reasoned that this uncertainty may render the visuomotor system more susceptible to the influence of ensemble perceptual processing. Furthermore, it is also conceivable that the visuomotor system might be biased by the mean size of the ensemble, even though a smooth and successful grasp requires that grip aperture remain tuned to the real size of the target.

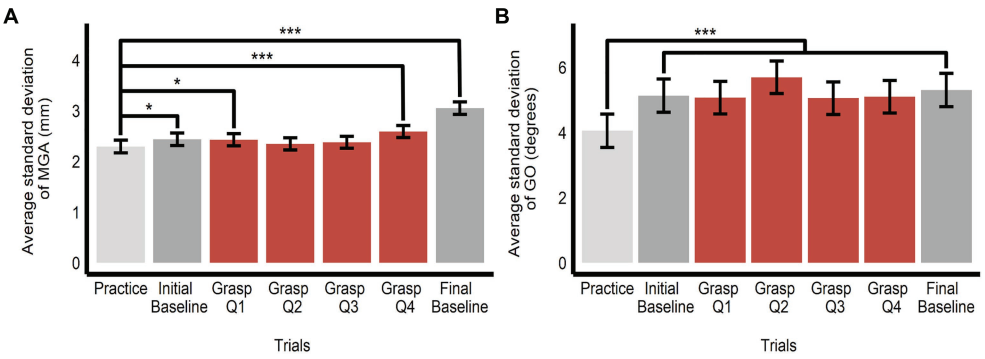

FIGURE 8 | Variability of grasping movements. Estimated marginal means of average SD of **(A)** maximum grip aperture and **(B)** grip orientation across the grasping trials (split into one bin of 10 practice trials, one bin of 10 initial baseline trials, four bins of 20 grasping trials each (Q1–Q4), and one bin of 10 final baseline trials). Comparisons are made between practice trials and all other bins. **p* < 0.05, ****p* < 0.0001; error bars depict SEM; MGA, maximum grip aperture; GO, grip orientation.

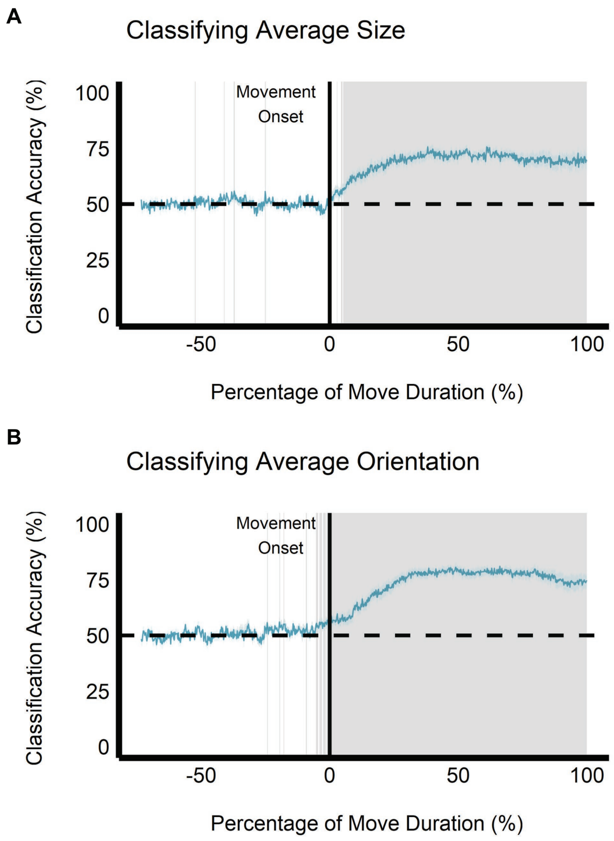

FIGURE 9 | Multivariate results of the perceptual manual-estimation task. Support vector machine (SVM) classification accuracy is plotted for discriminations of **(A)** average ensemble size (small vs. large) and **(B)** average ensemble orientation (CW vs. CCW) across the duration of movement. Negative percentage values of movement duration show baseline accuracy values beginning at stimulus onset. The gray shaded area represents timepoints where SVM classification accuracy is significantly different than chance level after correcting for false discovery rate. Gray shaded rectangles = $p < 0.05$; Light blue region = depicts SEM.

Using traditional univariate techniques and more powerful SVM multivariate statistical models, we found that both grip orientation and maximum grip aperture were not influenced by ensemble perception. This was true even on trials where participants provided a manual estimate of average size or orientation before grasping the target (haptic feedback trials). Importantly, the visuomotor system's insensitivity to ensemble statistics cannot be due to a failure of our setup to induce standard ensemble perceptual effects, because, in a separate block of trials, both ensemble-mean size and orientation significantly biased perceptual estimates of the average size and orientation of the ensemble. Additionally, haptic feedback from the target cannot be responsible for rectifying the perceptual effects, in a general sense, because we observed perceptual sensitivity to average size and orientation despite providing the participants an opportunity to grasp the target after each estimate.

Perceptual Estimations

The univariate results revealed that, as predicted, perceptual estimates of average size and orientation were biased toward the average ensemble size and orientation, respectively, of the ensemble displays. Specifically, in the size-matching task, GA was wider when the average ensemble size was large (and smaller when the average ensemble size was small). In the orientation-matching task, GO was more CW when the average ensemble orientation was CW (and more CCW when the average ensemble orientation was CCW).

In testament to the strength of the bias induced by ensemble perception, we observed effects of the *non-relevant* ensemble property on the estimates. Thus, in addition to the bias of ensemble size on the size estimates, participants demonstrated bias in the *orientation of their estimates* toward the mean orientation of the ensemble when reporting average size. Furthermore, in addition to the bias of ensemble orientation on orientation estimates, participants demonstrated bias in the *size of their estimates* toward the mean size of the ensemble when reporting average orientation. Remarkably, these effects

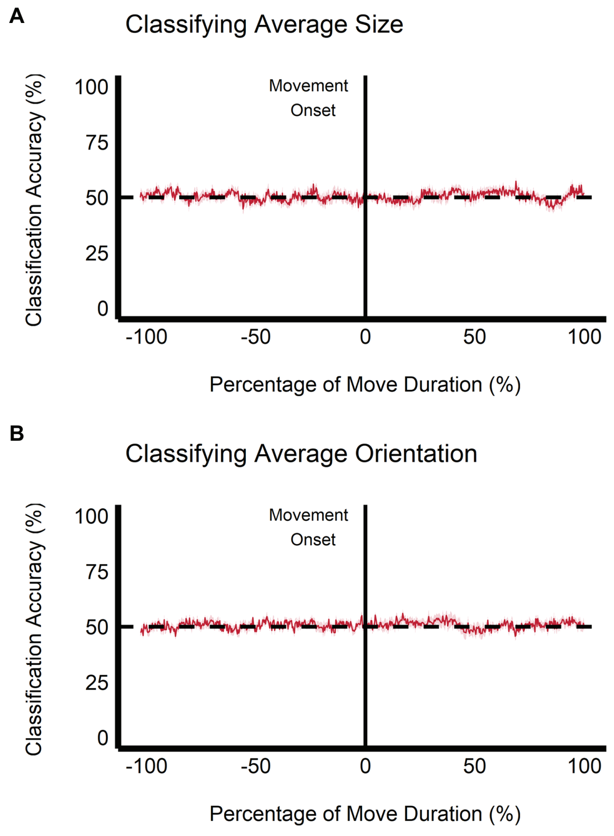

FIGURE 10 | Multivariate results of the grasping task. SVM classification accuracy is plotted for discriminations of **(A)** average ensemble size (small vs. large) and **(B)** average ensemble orientation (CW vs. CCW) across the duration of movement. Negative percentage values of movement duration show baseline accuracy values beginning at stimulus onset. Light red region = depicts SEM.

occurred despite our instruction to the participants to focus only on the task-relevant property of the target (size or orientation) and reinforce the view that ensemble perception is a holistic, rather than analytical, process that emerges out of entrenched structures that are largely refractory to knowledge, much like the phenomenology of pictorial illusions (see "Grasping" section below for a discussion of how our paradigm differs from those using visual illusions to investigate perceptual effects on grasping). Indeed, parallel summary representations for visual features outside the focus of attention have been demonstrated previously (Alvarez and Oliva, 2008, 2009; Emmanouil and Treisman, 2008; Attarha and Moore, 2015; Yörük and Boduroglu, 2020), and the implicit processing of one summary feature can bias the explicit processing of another (Sama et al., 2021).

We also observed that GO was more CCW in the small ensemble size than the large ensemble size in the size-discrimination task. This was unexpected as the bias toward the CW and CCW ensemble orientations would be averaged across size (i.e., the small average size ensembles included both the small × CW and small × CCW displays) and should result in similar values for GO across ensemble size. In fact, that is what we observed in the orientation-estimation task where no significant difference in GO between the small and large average ensemble size was observed. Upon further examination of the pairwise comparisons, we found that GO was larger for the large size than the small average ensemble size for the CCW but not the CW displays. This result was unexpected given that GO should be largely independent of ensemble size. More research might be required to better understand the effect observed.

Additionally, we observed that classification accuracy achieved above chance levels when classifying perceptual estimations of average size and orientation. These results suggest that ensemble size and orientation can be decoded from the kinematic and EMG data of the perceptual trials, and together with the results of the univariate analysis, demonstrate that participants were quite sensitive to perceptual differences of ensemble statistical values in our displays.

Grasping

In contrast to the perceptual estimates, the univariate analysis of grasping did not detect any bias of ensemble size and orientation on maximum grip aperture and grip orientation, respectively. The failure of ensemble perception to influence grip aperture is consistent with studies which report that this measure resists the perceptual bias induced by pictorial illusions on targets embedded in them (Brenner and Smeets, 1996; Haffenden and Goodale, 1998; Jackson and Shaw, 2000; Servos et al., 2000; Danckert et al., 2002; Chen et al., 2015; Knol et al., 2017). Note, however, an important distinction between our paradigm and those used when studying the effects of visual illusions on grasping. In the latter, it is important to demonstrate that the illusion affects the perceived properties of the to-be-grasped target, to put any effect (or lack thereof) of the illusion on grasping into context. In our paradigm, we were not concerned with whether ensemble statistics have a direct effect on the perception of the circular target, which might then bias the grasps, but rather, whether such statistics, which are implicitly extracted and inform perceptual judgment, estimation, and memory (e.g., Brady and Alvarez, 2011; Sama et al., 2021), can inform the parameterization of the details of reach-to-grasp actions, particularly when the grasp conditions, a same-sized target disk with multiple grip posture affordances, ostensibly favor a computationally efficient resolution using ensemble summary statistics. In this sense, our purpose is not to investigate dissociations between perception and action *per se*, but to test whether implicitly extracted perceptual information of the surrounding scene biases how we interact with objects within that scene.

Although our univariate analyses allowed for a direct comparison of the most relevant grasp variables, it is limited by data averaging and by its nature is unable to reveal complex relationships between multiple variables. To circumvent this issue, and to provide complementary evidence for our univariate results, we examined grasping behavior (and perceptual estimations) using a more powerful multivariate analysis, which included both the kinematic and EMG data. This analysis still failed to detect any influence of mean ensemble size and orientation on multiple visuomotor measures (i.e., MGA, GO, velocity, acceleration, and the EMG data). These findings are in line with that of Bulakowski et al. (2009) who found that information from the surround was incorporated in the perception of, but not actions directed toward, an oriented target bar in a visual crowding paradigm. The multivariate techniques were applied across the time course of the reach, and we did not detect any change in classification accuracy. Thus, our time-course analysis does not support a distinction between early and late stage visuomotor processing as predicted with the planning and control model of visuomotor function (Glover and Dixon, 2002; Glover, 2004). Taken together, these results strongly indicate that ensemble perception does not bias grasping movements.

Features and Limitations of the Design

An important aspect of ensemble perception, ensemble summary statistics, and the representations that underlie them, is that they are generated independently of the requirement to respond. Thus, the simultaneous presentation format was an important feature of our design, in which ensemble representations could be generated using all items of the ensemble before the participant responds. This feature of our design differentiates our study from a recent study by Hamidi et al. (2021), who similarly sought to test ensemble summary statistics on perception and action. In Hamidi et al.'s design, on each trial, participants were presented with only a single target object and, depending on the condition, either estimated its size or reached to grasp it. Given this serial presentation format and the inter-trial-intervals that are necessarily involved, this meant that the time required to generate an ensemble representation was on the scale of minutes, rather than the more typical scale of seconds or fractions of a second used here and elsewhere. Notably, previous experiments designed to manipulate ensemble statistical summary generation in the temporal domain have relied on rapid serial visual presentation, in which participants view all of the items of the ensemble within a few seconds (Chong and Treisman, 2003; Leib et al., 2014; Ying et al., 2020). This difference in time scales suggests the recruitment of different memory systems. Moreover, it is not clear how the requirement to respond to each one of the items interacts with the processes under investigation. Specifically, it is not clear whether Hamidi et al. (2021) manipulated an ensemble representation, as we conceive it, or if they manipulated learned stimulus-response mappings. The latter can be conceptualized, for example, as a shifted prior probability governing the relationship between visible target size and response output. One way to disentangle these two ideas would have been to test for after-effects. Updates to underlying stimulus-response priors, for example, should persist for several trials after the prior-shifting influence has been withdrawn, whereas the influence of an ensemble statistical summary should behave more transiently. In short, it is not clear whether Hamidi et al.'s operational use of the term "ensemble" is comparable to ours.

Another feature of our design is the use of real 3D objects and "real-time" visual conditions, because we were interested in testing ensemble statistical influence on dorsal-stream driven grasps. As we pointed out in the introduction, real-time 3D visual and haptic feedback are foundational conditions for typical dorsal-stream driven goal-directed action. Furthermore, our choice of using a single sized-target was designed to encourage ventral-stream engagement, thus maximizing our chances of observing an effect of perceptual ensemble representations on grasping behavior. Given all of these considerations, our results uniquely demonstrate the insensitivity of grasping movements to ensemble statistics using a more powerful multivariate analytical technique, incorporating multidimensional kinematic and EMG data.

A possible limitation of our study is that only one target object was used. Although this was an important feature of our design, geared to promote ventral-stream influence on grasping, it could also have contributed to grasping movements becoming highly stereotyped with repetition. To test for this, we conducted a *post-hoc* analysis to investigate whether the SD of MGA or GO changed significantly throughout the grasping session. If grasping behavior was becoming more practiced, there should be a reduction in variability over time. However, our results did not show a monotonic decline across the grasping session, demonstrating that grasping behavior did not become increasingly stereotyped from the initial practice trials onward. The visual illusion and grasping literature have also examined whether illusory effects on grasping persist with repeated grasping movements. On the one hand, some suggest that the effects of visual illusions on grasping gradually decrease as grasps are repeated (Cesanek et al., 2016; Whitwell et al., 2016). On the other hand, some suggest that the illusory effects remain constant throughout the experiment (Franz et al., 2001; Kopiske et al., 2016). Kopiske et al. (2017) investigated this discrepancy in the framework of motor adaptation. One of their secondary considerations was whether there was an effect of having multiple target sizes, as the studies which showed a decrease in the illusion effect used fewer objects than the studies which showed a constant illusion effect. They found a decreasing illusion effect with repeated trials, which could be explained by an error-correction model of sensorimotor adaptation, but importantly, found no effect of presenting single vs. multiple target sizes. This finding, taken together with our results that grasping movements did not become highly stereotyped over time, suggests that using a single target size did not hinder our ability to observe an effect of ensemble perception on grasping should it exist.

A second possible limitation of our study stems from the fact that after collecting data from 10 participants, we modified the experimental procedure by correcting the starting position of the right index finger and thumb from separated in the original procedure to touching in the modified procedure and recorded the haptic feedback portion of the manual estimation trials for further analysis (see "Modifications to the Experimental Procedure" section in the Materials and Methods section for more details). Notably, these changes were specific to the grasping task, as they did not influence the perceptual results. Nevertheless, we showed that maximum grip aperture for the grasping task did not differ between the original and modified experimental procedures whatsoever. We did, however, find a subtle *overall* CCW shift in grip orientation. We attributed this overall shift in grip orientation to the change in starting posture with the modified experimental procedure, where the index finger and thumb were pinched together. Importantly, this change did not interact with any of the unique conditions, indicating that it was independent of the any of the effects of our experimental manipulations and can thus be reasonably considered moot.

The Effects of Obstacle Avoidance and Perceptual Processing on Grasping Movements

To examine the influence of obstacle avoidance on our grasping data, we compared the baseline grasping trials (i.e., grasping the central target presented without a surrounding ensemble) to the main grasping and haptic feedback trials. We observed that MGA was larger in the baseline grasping task compared to when the target was embedded in the ensemble display (i.e., for both the main and haptic feedback grasping trials). These findings are in-line with what one would predict if obstacle avoidance mechanisms were operating on grip aperture (e.g., Saling et al., 1998; de Grave et al., 2005; Chen et al., 2015). Additionally, we observed that grip orientation was more CW in the baseline grasping task relative to the main grasping and haptic feedback grasping tasks, which may have been induced by the configuration of flanking objects (de Grave et al., 2005). Although the surrounding ensemble objects appear to induce general obstacle avoidance effects, there were no effects of variations in average size or orientation on GO in the main grasping task. Thus, it seems reasonable to conclude that the influence of the ensemble on MGA and GO, relative to no ensemble whatsoever, was general and independent of the mean ensemble size and orientation. Furthermore, obstacle avoidance is a natural component of prehension and while it is mainly controlled by dorsal-stream mechanisms, it is not completely isolated from ventral-stream processing (McIntosh et al., 2004; Schindler et al., 2004; Rice et al., 2006, 2008; Hesse et al., 2012), making it a prime target to further explore the interdependence of the two streams.

Haptic Feedback From 2D vs. 3D Objects

In an ensemble adaptation paradigm by Corbett and Song (2014), perceptual biases were observed during the early but not late stages of grasping. In our study, we did not observe any influence of perceptual processing on grasping movements. One reason for this discrepancy is likely explained by the absence of haptic feedback from a 3D target in Corbett and Song (2014). Haptic feedback is an important aspect of grasping and when absent can shift visuomotor behavior to being governed more by ventral-stream mechanisms such as in pantomimed grasping (e.g., Bingham et al., 2007; Schenk, 2012; Fukui and Inui, 2013; Whitwell et al., 2014, 2015). Corbett and Song acknowledged this issue and asked participants to touch their fingers to the monitor to receive some visual and haptic feedback when "grasping"; however, the haptic feedback was not veridical owing to the 2D stimulus. As discussed in the Introduction section, tactile feedback from a 2D object may not be enough to restrict the visuomotor operations that specify the kinematic parameters of the grasp to those that are typical of natural grasping (Holmes and Heath, 2013; Freud and Ganel, 2015; Ozana and Ganel, 2019). We used 3D objects in our study (as did Hamidi et al., 2021), providing veridical haptic feedback, and grasping was observed to be refractory to perceptual biases.

Future Directions

Although we observed no effects of mean ensemble size and orientation on grasping, it is possible that the present study may not have sufficiently induced a need for the visuomotor system to utilize ensemble size or orientation as the task could have been completed by simply focusing on the target object's size. Although extraction of multiple ensemble characteristics within a single ensemble seems to occur automatically and in parallel (Chong and Treisman, 2005; Attarha and Moore, 2015; Yörük and Boduroglu, 2020), attention to a specific feature may be necessary to optimize ensemble processing within that dimension (Emmanouil and Treisman, 2008). It is plausible that no ensemble effect was observed in the grasping task because the visual system discounted ensemble size and orientation altogether as they were not directly relevant to the task. If the task was manipulated such that ensemble perception would markedly benefit performance, there may be an observable effect of ensemble statistics on visuomotor control. Such manipulations could include the use of a speeded object grasping task (e.g., where matching hand posture to the ensemble average would allow for the fastest adoption of the necessary grasp position), or the use of higher-level ensemble displays (e.g., biasing grasp behavior using real-world tools that are often handled in specific orientations). Furthermore, as we used a limited number of ensemble configurations and a constant target size, a future study should use a wider range of stimuli both in terms of the ensemble display and target objects.

Another interesting follow up experiment would explore 2D ensemble backgrounds and a 3D target, to help reduce any obstacle-avoidance effects. Finally, utilizing an ensemble display within a more conventional visual illusion paradigm where ensemble statistics directly affect the perception of the to-be-grasped target will help to put the present series of results into context.

CONCLUSION

Understanding if and how the perceptual and action systems interact would deepen our understanding of both ensemble statistical processing and visuomotor control, as well as the relation between the ventral perception stream and dorsal action stream (Milner and Goodale, 2006). Practical applications of a system that uses ensemble-like processing could be in computer vision where a balance between perceptual constancy and outlier detection could guide algorithms which are robust to failure yet sensitive to unexpected conditions (i.e., those employed in self-driving vehicles). Given the benefits of ensemble perception (e.g., the ability to circumvent the capacity limitation in visual attention and visual working memory; Cohen et al., 2016), future research employing more complex paradigms will have to determine whether this mechanism could allow the visuomotor system to change focus or ignore irrelevant factors by perceiving the gist of our surroundings. As for the results of the present grasping paradigm, the physical constraints of interacting with our environment dictate that only visual information immediately relevant to motor behavior is considered by the visuomotor system.

DATA AVAILABILITY STATEMENT

The raw data supporting the conclusions of this article will be made available by the authors, without undue reservation.

ETHICS STATEMENT

The studies involving human participants were reviewed and approved by University of Toronto Social Sciences, Humanities, and Education Research Ethics Board. The participants provided their written informed consent to participate in this study.

AUTHOR CONTRIBUTIONS

RW, JC, MN, and AFa contributed to the conception and design of the study. JC, MN, LG, and AFr contributed to the set-up of the experimental materials and advised the data collection and statistical analysis process. AFa generated the experimental materials, performed the data collection and statistical analysis, and wrote the first draft of the manuscript. All authors contributed to manuscript revision, read, and approved the submitted version.

FUNDING

This work was funded by an NSERC Discovery Grant to JC (grant #435647) and MN (RGPIN-2020-06018).

ACKNOWLEDGMENTS

We would like to thank Sahar Popal, Brian Lau, Tegwende Seedu, Cash Singson II, Jane Lui, Karanbir Bhatti, Michelle Au, Josiah Baldassini, Andrea De Bartolo, Meryl Rae Villacastin, and Christina Pereira for their assistance.

SUPPLEMENTARY MATERIAL

The Supplementary Material for this article can be found online at: https://www.frontiersin.org/articles/10.3389/fpsyg.2021.597691/full#supplementary-material

REFERENCES

Aglioti, S., DeSouza, J. F., and Goodale, M. A. (1995). Size-contrast illusions deceive the eye but not the hand. *Curr. Biol.* 5, 679–685. doi: 10.1016/S0960-9822(95)00133-3

Alvarez, G. A. (2011). Representing multiple objects as an ensemble enhances visual cognition. *Trends Cogn. Sci.* 15, 122–131. doi: 10.1016/j.tics.2011.01.003

Alvarez, G. A., and Oliva, A. (2008). The representation of simple ensemble visual features outside the focus of attention. *Psychol. Sci.* 19, 392–398. doi: 10.1111/j.1467-9280.2008.02098.x

Alvarez, G. A., and Oliva, A. (2009). Spatial ensemble statistics are efficient codes that can be represented with reduced attention. *Proc. Natl. Acad. Sci. U. S. A.* 106, 7345–7350. doi: 10.1073/pnas.0808981106

Ariely, D. (2001). Seeing sets: representation by statistical properties. *Psychol. Sci.* 12, 157–162. doi: 10.1111/1467-9280.00327

Attarha, M., and Moore, C. M. (2015). The perceptual processing capacity of summary statistics between and within feature dimensions. *J. Vis.* 15:9. doi: 10.1167/15.4.9

Bartelt, R., and Darling, W. G. (2002). Opposite effects on perception and action induced by the Ponzo illusion. *Exp. Brain Res.* 146, 433–440. doi: 10.1007/s00221-002-1198-2

Bates, D., Mächler, M., Bolker, B., and Walker, S. (2015). Fitting linear mixed-effects models using lme4. *J. Stat. Softw.* 67, 1–48. doi: 10.18637/jss.v067.i01

Battaglini, P. P., Muzur, A., Galletti, C., Skrap, M., Brovelli, A., and Fattori, P. (2002). Effects of lesions to area V6A in monkeys. *Exp. Brain Res.* 144, 419–422. doi: 10.1007/s00221-002-1099-4

Bingham, G., Coats, R., and Mon-Williams, M. (2007). Natural prehension in trials without haptic feedback but only when calibration is allowed. *Neuropsychologia* 45, 288–294. doi: 10.1016/j.neuropsychologia.2006.07.011

Bonfiglioli, C., and Castiello, U. (1998). Dissociation of covert and overt spatial attention during prehension movements: selective interference effects. *Percept. Psychophys.* 60, 1426–1440. doi: 10.3758/BF03208003

Bonnefoy, A., Louis, N., and Gorce, P. (2009). Muscle activation during a reach-to-grasp movement in sitting position: influence of the distance. *J. Electromyogr. Kinesiol.* 19, 269–275. doi: 10.1016/j.jelekin.2008.04.010

Brady, T. F., and Alvarez, G. A. (2011). Hierarchical encoding in visual working memory: ensemble statistics bias memory for individual items. *Psychol. Sci.* 22, 384–392. doi: 10.1177/0956797610397956

Brenner, E., and Smeets, J. B. (1996). Size illusion influ4ences how we lift but not how we grasp an object. *Exp. Brain Res.* 111, 473–476. doi: 10.1007/BF00228737

Bulakowski, P. F., Post, R. B., and Whitney, D. (2009). Visuomotor crowding: the resolution of grasping in cluttered scenes. *Front. Behav. Neurosci.* 3:49. doi: 10.3389/neuro.08.049.2009

Cesanek, E., Campagnoli, C., and Domini, F. (2016). One-shot correction of sensory prediction errors produces illusion-resistant grasping without multiple object representations. *J. Vis.* 16:20. doi: 10.1167/16.12.20

Chang, C. -C., and Lin, C. -J. (2011). LIBSVM: a library for support vector machines. ACM transactions on intelligent systems and technology. Available at: http://www.csie.ntu.edu.tw/~cjlin/libsvm

Chen, J., Sperandio, I., and Goodale, M. A. (2015). Differences in the effects of crowding on size perception and grip scaling in densely cluttered 3-D scenes. *Psychol. Sci.* 26, 58–69. doi: 10.1177/0956797614556776

Chen, Z., Zhuang, R., Wang, X., Ren, Y., and Abrams, R. A. (2020). Ensemble perception without attention depends upon attentional control settings. *Atten. Percept. Psychophysiol.* doi: 10.3758/s13414-020-02067-2 [Epub ahead of print]

Chong, S. C., and Treisman, A. (2003). Representation of statistical properties. *Vis. Res.* 43, 393–404. doi: 10.1016/S0042-6989(02)00596-5

Chong, S. C., and Treisman, A. (2005). Attentional spread in the statistical processing of visual displays. *Percept. Psychophys.* 67, 1–13. doi: 10.3758/BF03195009

Cohen, M. A., Dennett, D. C., and Kanwisher, N. (2016). What is the bandwidth of perceptual experience? *Trends Cogn. Sci.* 20, 324–335. doi: 10.1016/j.tics.2016.03.006

Corbett, J. E., and Song, J. H. (2014). Statistical extraction affects visually guided action. *Vis. Cogn.* 22, 881–895. doi: 10.1080/13506285.2014.927044

Cuijpers, R. H., Smeets, J. B. J., and Brenner, E. (2004). On the relation between object shape and grasping kinematics. *J. Neurophysiol.* 91, 2598–2606. doi: 10.1152/jn.00644.2003

Culham, J. C., Danckert, J. L., DeSouza, J. F., Gati, J. S., Menon, R. S., and Goodale, M. A. (2003). Visually guided grasping produces fMRI activation in dorsal but not ventral stream brain areas. *Exp. Brain Res.* 153, 180–189. doi: 10.1007/s00221-003-1591-5

Dakin, S. C., and Watt, R. J. (1997). The computation of orientation statistics from visual texture. *Vis. Res.* 37, 3181–3192. doi: 10.1016/S0042-6989(97)00133-8

Danckert, J. A., Sharif, N., Haffenden, A. M., Schiff, K. C., and Goodale, M. A. (2002). A temporal analysis of grasping in the Ebbinghaus illusion: planning versus online control. *Exp. Brain Res.* 144, 275–280. doi: 10.1007/s00221-002-1073-1

de Grave, D. D., Biegstraaten, M., Smeets, J. B., and Brenner, E. (2005). Effects of the Ebbinghaus figure on grasping are not only due to misjudged size. *Exp. Brain Res.* 163, 58–64. doi: 10.1007/s00221-004-2138-0

Edwards, L. J., Muller, K. E., Wolfinger, R. D., Qaqish, B. F., and Schabenberger, O. (2008). An R2 statistic for fixed effects in the linear mixed model. *Stat. Med.* 27, 6137–6157. doi: 10.1002/sim.3429

Emmanouil, T. A., and Treisman, A. (2008). Dividing attention across feature dimensions in statistical processing of perceptual groups. *Percept. Psychophys.* 70, 946–954. doi: 10.3758/PP.70.6.946

Franz, V. H., Fahle, M., Bülthoff, H. H., and Gegenfurtner, K. R. (2001). Effects of visual illusions on grasping. *J. Exp. Psychol. Hum. Percept. Perform.* 27, 1124–1144. doi: 10.1037/0096-1523.27.5.1124

Freud, E., and Ganel, T. (2015). Visual control of action directed toward two-dimensional objects relies on holistic processing of object shape. *Psychon. Bull. Rev.* 22, 1377–1382. doi: 10.3758/s13423-015-0803-x

Frey, S. H., Vinton, D., Norlund, R., and Grafton, S. T. (2005). Cortical topography of human anterior intraparietal cortex active during visually guided grasping. *Cogn. Brain Res.* 23, 397–405. doi: 10.1016/j.cogbrainres.2004.11.010

Fukui, T., and Inui, T. (2013). How vision affects kinematic properties of pantomimed prehension movements. *Front. Psychol.* 4:44. doi: 10.3389/fpsyg.2013.00044

Gallese, V., Murata, A., Kaseda, M., Niki, N., and Sakata, H. (1994). Deficit of hand preshaping after muscimol injection in monkey parietal cortex. *Neuroreport* 5, 1525–1529. doi: 10.1097/00001756-199407000-00029

Ganel, T., Tanzer, M., and Goodale, M. A. (2008). A double dissociation between action and perception in the context of visual illusions: opposite effects of real and illusory size. *Psychol. Sci.* 19, 221–225. doi: 10.1111/j.1467-9280.2008.02071.x

Glover, S. (2004). Separate visual representations in the planning and control of action. *Behav. Brain Sci.* 27, 3–24. doi: 10.1017/s0140525x04000020

Glover, S., and Dixon, P. (2002). Dynamic effects of the Ebbinghaus illusion in grasping: support for a planning/control model of action. *Percept. Psychophys.* 64, 266–278. doi: 10.3758/BF03195791

Goodale, M. A., Meenan, J. P., Bülthoff, H. H., Nicolle, D. A., Murphy, K. J., and Racicot, C. I. (1994). Separate neural pathways for the visual analysis of object shape in perception and prehension. *Curr. Biol.* 4, 604–610. doi: 10.1016/S0960-9822(00)00132-9

Goodale, M. A., Milner, A. D., Jakobson, L. S., and Carey, D. P. (1991). A neurological dissociation between perceiving objects and grasping them. *Nature* 349, 154–156. doi: 10.1038/349154a0

Haffenden, A. M., and Goodale, M. A. (1998). The effect of pictorial illusion on prehension and perception. *J. Cogn. Neurosci.* 10, 122–136. doi: 10.1162/089892998563824

Haffenden, A. M., and Goodale, M. A. (2002). Learned perceptual associations influence visuomotor programming under limited conditions: kinematic consistency. *Exp. Brain Res.* 147, 485–493. doi: 10.1007/s00221-002-1250-2

Hamidi, M., Giuffre, L., and Heath, M. (2021). A summary statistical representation influences perceptions but not visually or memory-guided grasping. *Hum. Mov. Sci.* 75:102739. doi: 10.1016/j.humov.2020.102739

Hesse, C., Lane, A. R., Aimola, L., and Schenk, T. (2012). Pathways involved in human conscious vision contribute to obstacle-avoidance behaviour. *Eur. J. Neurosci.* 36, 2383–2390. doi: 10.1111/j.1460-9568.2012.08131.x

Holmes, S. A., and Heath, M. (2013). Goal-directed grasping: the dimensional properties of an object influence the nature of the visual information mediating aperture shaping. *Brain Cogn.* 82, 18–24. doi: 10.1016/j.bandc.2013.02.005

Hoozemans, M. J., and Van Dieen, J. H. (2005). Prediction of handgrip forces using surface EMG of forearm muscles. *J. Electromyogr. Kinesiol.* 15, 358–366. doi: 10.1016/j.jelekin.2004.09.001

Hu, Y., and Goodale, M. A. (2000). Grasping after a delay shifts size-scaling from absolute to relative metrics. *J. Cogn. Neurosci.* 12, 856–868. doi: 10.1162/089892900562462

Jackson, S. R. (1999). Pathological perceptual completion in hemianopia extends to the control of reach-to-grasp movements. *Neuroreport* 10, 2461–2466. doi: 10.1097/00001756-199908200-00005

Jackson, S. R., and Shaw, A. (2000). The Ponzo illusion affects grip-force but not grip-aperture scaling during prehension movements. *J. Exp. Psychol. Hum. Percept. Perform.* 26:418. doi: 10.1037//0096-1523.26.1.418

Jeannerod, M. (1981). "Intersegmental coordination during reaching at natural visual objects" in *Attention and performance*. *Vol. 9*. eds. J. Long and A. Baddeley (Hillsdale, NKJ: Erlbaum), 153–168.

Jeannerod, M. (1984). The timing of natural prehension movements. *J. Mot. Behav.* 16, 235–254. doi: 10.1080/00222895.1984.10735319

Jeannerod, M. (1988). *The neural and behavioural organization of goal-directed movements*. Oxford, UK: Clarendon.

Jeannerod, M. (1999). Visuomotor channels: their integration in goal-directed prehension. *Hum. Mov. Sci.* 18, 201–218. doi: 10.1016/S0167-9457(99)00008-1

Kapandji, I. A. (1980). *Physiologie articulaire, tome 1, Membre supérieur*. Paris, France: Maloine.

Karnath, H. O., Ruter, J., Mandler, A., and Himmelbach, M. (2009). The anatomy of object recognition – visual form agnosia caused by medial occipitotemporal stroke. *J. Neurosci.* 29, 5854–5862. doi: 10.1523/JNEUROSCI.5192-08.2009

Kelso, J. A. S., Buchanan, J. J., and Murata, T. (1994). Multifunctionality and switching in the coordination dynamics of reaching and grasping. *Hum. Mov. Sci.* 13, 63–94. doi: 10.1016/0167-9457(94)90029-9

Kermadi, I., Liu, Y., Tempini, A., and Rouiller, E. M. (1997). Effects of reversible inactivation of the supplementary motor area (SMA) on unimanual grasp and bimanual pull and grasp performance in monkeys. *Somatosens. Mot. Res.* 14, 268–280. doi: 10.1080/08990229770980

Khayat, N., and Hochstein, S. (2018). Perceiving set mean and range: automaticity and precision. *J. Vis.* 18:23. doi: 10.1167/18.9.23

Knol, H., Huys, R., Sarrazin, J. C., Spiegler, A., and Jirsa, V. K. (2017). Ebbinghaus figures that deceive the eye do not necessarily deceive the hand. *Sci. Rep.* 7, 1–17. doi: 10.1038/s41598-017-02925-4

Kopiske, K. K., Bruno, N., Hesse, C., Schenk, T., and Franz, V. H. (2016). The functional subdivision of the visual brain: is there a real illusion effect on action? A multi-lab replication study. *Cortex* 79, 130–152. doi: 10.1016/j.cortex.2016.03.020

Kopiske, K. K., Cesanek, E., Campagnoli, C., and Domini, F. (2017). Adaptation effects in grasping the Müller-Lyer illusion. *Vis. Res.* 136, 21–31. doi: 10.1016/j.visres.2017.05.004

Kravitz, D. J., Saleem, K. S., Baker, C. I., and Mishkin, M. (2011). A new neural framework for visuospatial processing. *Nat. Rev. Neurosci.* 12, 217–230. doi: 10.1038/nrn3008

Kuznetsova, A., Brockhoff, P. B., and Christensen, R. H. B. (2017). lmerTest Package: tests in linear mixed effects models. *J. Stat. Softw.* 82, 1–26. doi: 10.18637/jss.v082.i13

Lashgari, E., Pouya, A., and Maoz, U. (2021). Decoding object weight from electromyography during human grasping. BioRxiv [Preprint]. doi: 10.1101/2021.03.26.437230

Le, A., Vesia, M., Yan, X., Niemeier, M., and Crawford, J. D. (2014). The right anterior intraparietal sulcus is critical for bimanual grasping: a TMS study. *Cereb. Cortex* 24, 2591–2603. doi: 10.1093/cercor/bht115

Le, A., Vesia, M., Yan, X., Niemeier, M., and Crawford, J. D. (2017). Parietal area BA7 integrates motor programs for reaching, grasping, and bimanual coordination. *J. Neurophysiol.* 117, 624–636. doi: 10.1152/jn.00299.2016

Leib, A. Y., Fischer, J., Liu, Y., Qiu, S., Robertson, L., and Whitney, D. (2014). Ensemble crowd perception: a viewpoint-invariant mechanism to represent average crowd identity. *J. Vis.* 14:26. doi: 10.1167/14.8.26

Maier, M. A., and Hepp-Reymond, M. C. (1995). EMG activation patterns during force production in precision grip. *Exp. Brain Res.* 103, 108–122. doi: 10.1007/BF00241969

Marotta, J. J., DeSouza, J. F. X., Haffenden, A. M., and Goodale, M. A. (1998). Does a monocularly presented size-contrast illusion influence grip aperture? *Neuropsychologia* 36, 491–497. doi: 10.1016/S0028-3932(97)00154-1

McIntosh, R. D., McClements, K. I., Dijkerman, H. C., Birchall, D., and Milner, A. D. (2004). Preserved obstacle avoidance during reaching in patients with left visual neglect. *Neuropsychologia* 42, 1107–1117. doi: 10.1016/j.neuropsychologia.2003.11.023

Milner, A. D., and Goodale, M. A. (2006). *The visual brain in action*, Oxford psychology series, No. 27, vol. 27. Oxford: OUP.

Murata, A., Gallese, V., Luppino, G., Kaseda, M., and Sakata, H. (2000). Selectivity for the shape, size, and orientation of objects for grasping in neurons of monkey parietal area AIP. *J. Neurophysiol.* 83, 2580–2601. doi: 10.1152/jn.2000.83.5.2580

Oldfield, R. C. (1971). The assessment and analysis of handedness: the Edinburgh inventory. *Neuropsychologia* 9, 97–113. doi: 10.1016/0028-3932(71)90067-4

Ozana, A., and Ganel, T. (2019). Weber's law in 2D and 3D grasping. *Psychol. Res.* 83, 977–988. doi: 10.1007/s00426-017-0913-3

Parkes, L., Lund, J., Angelucci, A., Solomon, J. A., and Morgan, M. (2001). Compulsory averaging of crowded orientation signals in human vision. *Nat. Neurosci.* 4:739. doi: 10.1038/89532

Perenin, M. T., and Rossetti, Y. (1996). Grasping without form discrimination in a hemianopic field. *Neuroreport* 7, 793–797. doi: 10.1097/00001756-199602290-00027

Piegl, L., and Tiller, W. (1987). Curve and surface constructions using rational B-splines. *Comput. Aided Des.* 19, 485–498. doi: 10.1016/0010-4485(87)90234-X

R Core Team (2019). R: A Language and Environment for Statistical Computing. Vienna, Austria: R Foundation for Statistical Computing. Available at: https://www.R-project.org/

Rice, N. J., Edwards, M. G., Schindler, I., Punt, T. D., McIntosh, R. D., Humphreys, G. W., et al. (2008). Delay abolishes the obstacle avoidance deficit in unilateral optic ataxia. *Neuropsychologia* 46, 1549–1557. doi: 10.1016/j.neuropsychologia.2008.01.012

Rice, N. J., McIntosh, R. D., Schindler, I., Mon-Williams, M., Demonet, J. F., and Milner, A. D. (2006). Intact automatic avoidance of obstacles in patients with visual form agnosia. *Exp. Brain Res.* 174, 176–188. doi: 10.1007/s00221-006-0435-5

Rice, N. J., Tunik, E., Cross, E. S., and Grafton, S. T. (2007). Online grasp control is mediated by the contralateral hemisphere. *Brain Res.* 1175, 76–84. doi: 10.1016/j.brainres.2007.08.009

Saling, M., Alberts, J., Stelmach, G. E., and Bloedel, J. R. (1998). Reach-to-grasp movements during obstacle avoidance. *Exp. Brain Res.* 118, 251–258. doi: 10.1007/s002210050279

Sama, M. A., Nestor, A., and Cant, J. S. (2019). Independence of viewpoint and identity in face ensemble processing. *J. Vis.* 19, 1–17. doi: 10.1167/19.5.2

Sama, M. A., Srikanthan, D., Nestor, A., and Cant, J. S. (2021). Global and local interference effects in ensemble encoding are best explained by interactions between summary representations of the mean and range. *Atten. Percept. Psychophysiol.* doi: 10.3758/s13414-020-02224-7 [Epud ahead of print]

Schaffelhofer, S., and Scherberger, H. (2016). Object vision to hand action in macaque parietal, premotor, and motor cortices. *eLife* 5:e15278. doi: 10.7554/eLife.15278

Schenk, T. (2012). No dissociation between perception and action in patient DF when haptic feedback is withdrawn. *J. Neurosci.* 32, 2013–2017. doi: 10.1523/JNEUROSCI.3413-11.2012

Schindler, I., Rice, N. J., McIntosh, R. D., Rossetti, Y., Vighetto, A., and Milner, A. D. (2004). Automatic avoidance of obstacles is a dorsal stream function: evidence from optic ataxia. *Nat. Neurosci.* 7, 779–784. doi: 10.1038/nn1273

Servos, P., Carnahan, H., and Fedwick, J. (2000). The visuomotor system resists the horizontal-vertical illusion. *J. Mot. Behav.* 32, 400–404. doi: 10.1080/00222890009601389

Smeets, J. B., and Brenner, E. (2006). 10 years of illusions. *J. Exp. Psychol. Hum. Percept. Perform.* 32:1501. doi: 10.1037/0096-1523.32.6.1501

Smeets, J. B. J., Kleijn, E., van der Meijden, M., and Brenner, E. (2020). Why some size illusions affect grip aperture. *Exp. Brain Res.* 238, 969–979. doi: 10.1007/s00221-020-05775-1

Stelmach, G. E., Castiello, U., and Jeannerod, M. (1994). Orienting the finger opposition space during prehension movements. *J. Mot. Behav.* 26, 178–186. doi: 10.1080/00222895.1994.9941672

Stöttinger, E., Pfusterschmied, J., Wagner, H., Danckert, J., Anderson, B., and Perner, J. (2012). Getting a grip on illusions: replicating Stöttinger et al. [Exp Brain Res (2010) 202: 79–88] results with 3-D objects. *Exp. Brain Res.* 216, 155–157. doi: 10.1007/s00221-011-2912-8

Taira, M., Mine, S., Georgopoulos, A. P., Murata, A., and Sakata, H. (1990). Parietal cortex neurons of the monkey related to the visual guidance of hand movement. *Exp. Brain Res.* 83, 29–36. doi: 10.1007/BF00232190

Tunik, E., Frey, S. T., and Grafton, S. H. (2005). Virtual lesions of the anterior intraparietal area disrupt goal-dependent on-line adjustments of grasp. *Nat. Neurosci.* 8, 505–511. doi: 10.1038/nn1430

Utochkin, I. S., and Vostrikov, K. O. (2017). The numerosity and mean size of multiple objects are perceived independently and in parallel. *PLoS One* 12:e0185452. doi: 10.1371/journal.pone.0185452

Whitney, D., and Yamanashi Leib, A. (2018). Ensemble perception. *Annu. Rev. Psychol.* 69, 12.1–12.25. doi: 10.1146/annurev-psych-010416-044232

Whitwell, R. L., Buckingham, G., Enns, J. T., Chouinard, P. A., and Goodale, M. A. (2016). Rapid decrement in the effects of the Ponzo display dissociates action and perception. *Psychon. Bull. Rev.* 23, 1157–1163. doi: 10.3758/s13423-015-0975-4

Whitwell, R. L., Ganel, T., Byrne, C. M., and Goodale, M. A. (2015). Real-time vision, tactile cues, and visual form agnosia: removing haptic feedback from a "natural" grasping task induces pantomime-like grasps. *Front. Hum. Neurosci.* 9:216. doi: 10.3389/fnhum.2015.00216

Whitwell, R. L., and Goodale, M. A. (2017). Real and illusory issues in the illusion debate (why two things are sometimes better than one): commentary on Kopiske et al. (2016). *Cortex* 88, 205–209. doi: 10.1016/j.cortex.2016.06.019

Whitwell, R. L., Goodale, M. A., Merritt, K. E., and Enns, J. T. (2018). The Sander parallelogram illusion dissociates action and perception despite control for the litany of past confounds. *Cortex* 98, 163–176. doi: 10.1016/j.cortex.2017.09.013

Whitwell, R. L., Lambert, L., and Goodale, M. A. (2008). Grasping future events: explicit knowledge of the availability of visual feedback fails to reliably influence prehension. *Exp. Brain Res.* 188, 603–611. doi: 10.1007/s00221-008-1395-8

Whitwell, R. L., Milner, A. D., Cavina-Pratesi, C., Byrne, C. M., and Goodale, M. A. (2014). DF's visual brain in action: the role of tactile cues. *Neuropsychologia* 55, 41–50. doi: 10.1016/j.neuropsychologia.2013.11.019

Whitwell, R. L., Sperandio, I., Buckingham, G., Chouinard, P. A., and Goodale, M. A. (2020). Grip constancy but not perceptual size constancy survives lesions of early visual cortex. *Curr. Biol.* 30, 3680.e5–3686.e5. doi: 10.1016/j.cub.2020.07.026

Whitwell, R. L., Striemer, C. L., Nicolle, D. A., and Goodale, M. A. (2011). Grasping the non-conscious: preserved grip scaling to unseen objects for immediate but not delayed grasping following a unilateral lesion to primary visual cortex. *Vis. Res.* 51, 908–924. doi: 10.1016/j.visres.2011.02.005

Ying, H., Burns, E., Choo, A., and Xu, H. (2020). Temporal and spatial ensemble statistics are formed by distinct mechanisms. *Cognition* 195:104128. doi: 10.1016/j.cognition.2019.104128

Yörük, H., and Boduroglu, A. (2020). Feature-specificity in visual statistical summary processing. *Atten. Percept. Psychophysiol.* 82, 852–864. doi: 10.3758/s13414-019-01942-x

Conflict of Interest: The authors declare that the research was conducted in the absence of any commercial or financial relationships that could be construed as a potential conflict of interest.

frontiers in Neuroscience

ORIGINAL RESEARCH
published: 19 July 2021
doi: 10.3389/fnins.2021.679910

Visually and Tactually Guided Grasps Lead to Different Neuronal Activity in Non-human Primates

Daniela Buchwald[1,2]* and *Hansjörg Scherberger*[1,2]*

[1] Neurobiology Laboratory, Deutsches Primatenzentrum GmbH, Göttingen, Germany, [2] Faculty of Biology and Psychology, University of Goettingen, Göttingen, Germany

Movements are defining characteristics of all behaviors. Animals walk around, move their eyes to explore the world or touch structures to learn more about them. So far we only have some basic understanding of how the brain generates movements, especially when we want to understand how different areas of the brain interact with each other. In this study we investigated the influence of sensory object information on grasp planning in four different brain areas involved in vision, touch, movement planning, and movement generation in the parietal, somatosensory, premotor and motor cortex. We trained one monkey to grasp objects that he either saw or touched beforehand while continuously recording neural spiking activity with chronically implanted floating multi-electrode arrays. The animal was instructed to sit in the dark and either look at a shortly illuminated object or reach out and explore the object with his hand in the dark before lifting it up. In a first analysis we confirmed that the animal not only memorizes the object in both tasks, but also applies an object-specific grip type, independent of the sensory modality. In the neuronal population, we found a significant difference in the number of tuned units for sensory modalities during grasp planning that persisted into grasp execution. These differences were sufficient to enable a classifier to decode the object and sensory modality in a single trial exclusively from neural population activity. These results give valuable insights in how different brain areas contribute to the preparation of grasp movement and how different sensory streams can lead to distinct neural activity while still resulting in the same action execution.

Keywords: grasping, object interaction, non-human primate, multi-sensory, electrophysiology

Edited by:
Marco Santello,
Arizona State University, United States

Reviewed by:
Thomas G. Brochier,
UMR7289 Institut de Neurosciences de la Timone (INT), France
Marc H. Schieber,
University of Rochester, United States

****Correspondence:***
Daniela Buchwald
dagbuchwald@gmail.com
Hansjörg Scherberger
hscherb@gwdg.de

Specialty section:
This article was submitted to Perception Science, a section of the journal Frontiers in Neuroscience

Received: *12 March 2021*
Accepted: *18 June 2021*
Published: *19 July 2021*

Citation:
Buchwald D and Scherberger H (2021) Visually and Tactually Guided Grasps Lead to Different Neuronal Activity in Non-human Primates. Front. Neurosci. 15:679910. doi: 10.3389/fnins.2021.679910

1. INTRODUCTION

Sensory-motor transformation flexibly links sensory information from several sensory modalities to meaningful action activations. Our different senses constantly pick up information about our environment, which needs to be processed, interpreted, and ultimately results in various actions (Gibson, 1958; Schlegel et al., 2009; Schaffelhofer and Scherberger, 2016). One of the most important senses for many animals is vision, but other senses like touch or proprioception are equally relevant, in particular for object manipulation (Land and Fernald, 1992; Grigg, 1994; Goodman and Bensmaia, 2018). Van Essen estimated 2003 that in humans about 27% of cortex is dedicated to process predominantly visual input, while only 7% are dedicated to predominantly somatosensory and motor processes (Van Essen, 2003).

Since grasping movements are so abundant in primates, they make a good example to investigate how the primate brain generates movements and how different senses can influence these movements (Raos et al., 2004; Stone and Gonzalez, 2014; Iturrate et al., 2016; Camponogara and Volcic, 2019). Each grasping movement is a joint effort of many different brain areas. For example if an object is seen, visual information is processed through visual areas like the primary visual cortex V1 or the anterior intraparietal area AIP, where it might serve as a basis to select future actions (Snowden et al., 1991; Murata et al., 2000; Lehmann and Scherberger, 2015; Schaffelhofer and Scherberger, 2016; Self et al., 2019). AIP is connected to its own specific areas (e.g., secondary somatosensory cortex, premotor cortex) and therefore plays an important role for processing visual and tactile information for the planning and execution of grasping movements (Binkofski et al., 1999; Luppino et al., 1999; Borra et al., 2007). Furthermore, past studies have shown that AIP responds to visual properties of objects that are about to be grasped. For example, Baumann et al. (2009) demonstrated that neurons in AIP encode object orientations as well as grip types during a delayed grasping task with a visually presented target. It is therefore an important area for the processing of object interactions (Taira et al., 1990; Sakata et al., 1995; Borra et al., 2007; Lehmann and Scherberger, 2013; Schaffelhofer, 2014; Schaffelhofer and Scherberger, 2016).

Not all objects are perceived purely visually. In fact, primates often touch new objects with their hands to gather additional, tactile object properties, and they are very efficient in doing so (Klatzky et al., 1993; Englerova et al., 2019). This tactile information is passing through multiple brain areas, including the primary somatosensory cortex, where object features and structures are processed (Warren et al., 1986; Johansson, 1991; Delhaye et al., 2018; Umeda et al., 2019; Liu et al., 2021). Such information can then be used to generate more targeted actions, and absence of haptic feedback can severely impair the control of hand movements (Miall et al., 2019; Okorokova et al., 2020). However, somatosensory cortex is not only processing tactile feedback but also proprioception, therefore providing also important feedback about the position and kinematics of the arm and hand during grasping (Grigg, 1994; Filimon et al., 2009; Delhaye et al., 2018; Chowdhury et al., 2020; Lutz and Bensmaia, 2021). For example, seeing a food item might trigger a grasping action, whereas seeing a predator might instead lead to a fleeing response. To coordinate the involved muscles of the body, the brain first needs to set an action goal and from there a movement plan, before the goal-directed movement can be executed. Two areas involved in these processes are the premotor and motor cortex, where movements are first planned and then executed (Fritsch and Hitzig, 1870; Churchland et al., 2006; Fluet et al., 2010; Arbuckle et al., 2020). The hand area in the premotor cortex, area F5, is directly and bi-directionally connected to AIP, and both areas are part of the fronto-parietal grasping network (Luppino et al., 1999; Rizzolatti and Luppino, 2001; Borra et al., 2007). Information from various senses serves not only as a basis for movement selection, but also provides important feedback to adjust ongoing movements and therefore suggests the involvement of various sensory brain areas for motor control (Saunders and Knill, 2004; Christensen et al., 2007; Oya et al., 2020).

In this study we investigated how the brain generates grasping movements based exclusively on visual or tactile object information. In order to do so, we not only tapped into the fronto-parietal grasping network of premotor area F5, AIP and M1, but also added parallel recordings from S1 in order to obtain a fuller picture of how different sensory modalities influence the sensory and motor side of grasp planning and execution.

2. MATERIALS AND METHODS

2.1. Animals

Animal housing and all experiments were performed in accordance with European and German law and in agreement with the "Guidelines for the Care and Use of Mammals in Neuroscience and Behavioural Research" (National Research Council, 2003), as well as the NC3Rs "Guidelines for non-human primate accommodation, care and use" (National Centre for the Replacement, Refinement and Reduction of Animals in Research, 2017). Authorization for conducting this experiment was granted by the Animal Welfare Division of the Office for Consumer Protection and Food Safety of the State of Lower Saxony, Germany (permit no. 14/1442 and 19/3132).

For this project we trained one purpose-bred, male rhesus monkey (*Macaca mulatta*) in a delayed grasping task. He was born in 2011 at the German Primate Center (Deutsches Primatenzentrum GmbH, Göttingen, Germany) and housed together with another monkey in a setting that additionally allowed visual interaction with other groups of monkeys. On training days, intake of fluids through water bottles and rewards (such as juice or fruits) was monitored, since fluids served as the main reward for the animal. The animal was conditioned using positive reinforcement training, in which correct actions always resulted in a reward for the animal. Access to food was never restricted.

2.2. Implantation and Neuronal Signal Acquisition

In order to observe brain activity while the monkey explores and lifts up objects, a titanium head post was implanted on the skull in a sterile procedure and eight floating microelectrode arrays (FMA, Microprobes for Life Sciences, Gaithersburg, MD, USA, see Musallam et al., 2007) were implanted in cortex several months later in a second procedure. Each array consisted of 36 electrodes, where 32 were used to record brain activity and 4 served either as ground or reference electrodes. The length of the electrodes varied from 1.5 to 7.1 mm. For further details on the implantation methods, see (Michaels et al., 2015; Buchwald, 2020).

Since the goal of this study was to investigate visual and tactile object recognition, grasp planning, and finally grasp execution, four brain areas were chosen for FMA implantation: anterior intraparietal cortex (AIP), primary somatosensory cortex (S1, area 3b), primary motor cortex (M1), and premotor cortex (area F5). To sample from a larger number of channels from each area, each cortical area was implanted with two arrays.

After the animal fully recovered (about 10–14 days post-op), the implants were connected to two 128-channel neural signal processors (Cerebus systems, Blackrock Microsystems Inc., Salt Lake City, UT, USA) that were synchronized according to manufacturer instructions, which allowed for data acquisition from all 256 electrodes in parallel. Data was recorded with a sampling rate of 30 kHz and 16 bit resolution, and all neural data was stored on a hard drive together with behavioral data for offline analysis (see Analysis methods, below). Behavioral data was recorded using various sensors on the setup, as described in the following section.

2.3. Experimental Setup

During animal training and recording sessions, the monkey was comfortably seated in a custom made primate chair that was adjusted to the monkey's size. His head was fixed using the implanted titanium head post to ensure that the cables of the recording system were not moving during recording, and a reward system for fluid rewards was positioned in front of the animal's mouth.

2.3.1. Turntable Setup

To explore how objects are grasped, a variety of different objects was needed and we therefore employed a turntable setup, similar to those described in previous studies (Schaffelhofer, 2014; Schaffelhofer et al., 2015; Schaffelhofer and Scherberger, 2016). In this setup, a round object plate that fits six objects is operated by a motor. This way each object can be moved to the front in random order without human interaction. Objects were designed to have similar size and equal weight (120 g, including object and connected counter-weight below the plate) to keep the lifting effort similar between objects. Objects were 3D printed in plastic (PA 2200; Electro Optical Systems GmbH, Munich, Germany) by Shapeways Inc. (New York, USA). Objects are displayed in **Figure 1**. In order to allow only one object to be visible and reachable during each trial, several walls out of black plastic were mounted in the setup, see **Figure 2** for illustration.

To instruct the animal to reach out and touch or grasp the object, a red LED was projected onto the object, using a half-transparent mirror. This avoided any unwanted illumination of the object, since the light source was far away from the object and only appeared to be located on top of the object by superposition from the mirror. To keep track of the behavior of the monkey, different sensors were used: a light barrier detected when the object was lifted, and a handrest button detected when the animal's hand was resting on it. Data from these sensors were recorded with a real-time data acquisition system (National Instruments Corp., Austin, TX, USA) and stored to disk together with the neural data. A more detailed description of the setup used in this study can be found in Buchwald et al. (2021).

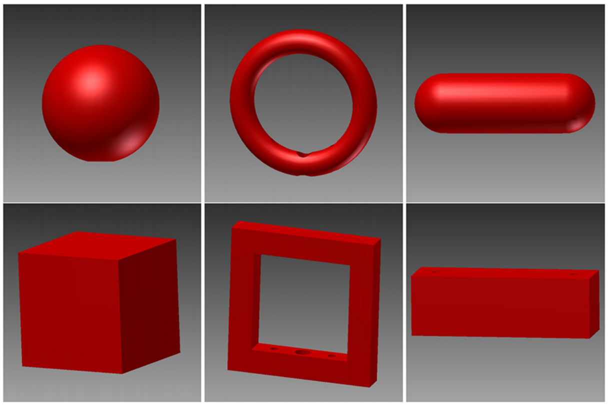

FIGURE 1 | Illustration of the six objects used in this study. Six objects were designed to encourage different grasps and to contain distinct visible and tactile features. Top: sphere, ring, and rounded bar. Bottom: cube, edged version of the ring, and box.

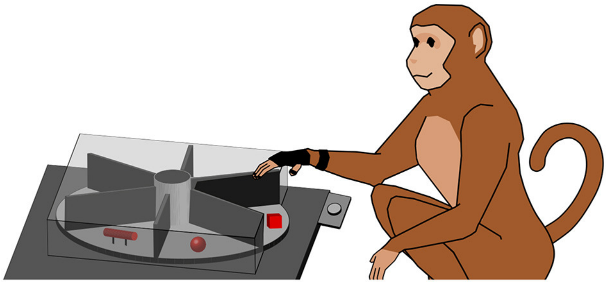

FIGURE 2 | Turntable setup. The monkey working on the turntable (simplified). The turntable consists of a plate (light gray) that features six different objects (red). The object in front of the animal has to be lifted, while the other ones are out of view (illustrated by a cover). For hand tracking, the animal wears a (black) data glove. A handrest button (light gray) is located between animal and turntable.

2.3.2. Magnetic Data Glove

Hand movements of the animal were tracked with a custom-built, magnetic data glove (see Schaffelhofer and Scherberger, 2012). This approach was extremely robust against occlusions, since no line of sight was required for hand tracking, in contrast to many visual tracking methods; the animal's hand simply had to be positioned within the magnetic field to get reliable data. The glove itself consisted of seven sensors on the finger nails of the monkey, and the dorsum and the wrist of the hand. To secure the sensor position on the finger nails, appropriate super glue and Leucotape were used, paying attention that the finger tips of the animal were not covered by the tape to allow free finger tip sensation (see **Figure 3**). The remaining two sensors were sewed to a custom made glove that was adjusted to the animal's hand. The magnetic field generator (Wave, Northern Digital Inc., Waterloo, Canada) was placed below the object plate. The sampling rate of the data glove was 70–100 Hz (depending on computer load). Hand kinematics were stored on a separate computer and synchronized with the neural data by sending a synchronization signal to the neural signal processor that was stored along with the neural data.

2.4. Behavioral Paradigm

To instruct grasping movements with various sensory object information, the monkey was trained in a delayed-grasping task.

FIGURE 3 | Magnetic data glove. Individual sensor coils (white boxes) are fixed to the finger nails using super glue and Leucotape, taking care not to cover the finger tips. Additional two sensors on the dorsum of the hand and the wrist are sawn onto a custom made glove that the animal was trained to wear. Purple: gloved hand of the experimenter.

He was instructed to first either look at an object or to explore it with his hand in the dark before quickly grasping and lifting it up. This way the monkey only had either visual or tactile information to base his grasping action on.

The monkey was placed in a dark setup so that no other objects could distract the monkey. For an illustration of the task paradigm see **Figure 4**. At the start of each trial the motor would rotate the turntable and bring a random object to the front.

The task consisted of five epochs: First 500 ms of baseline epoch where recorded, where the animal had to sit still in the dark. Then the cue epoch followed. During visual trials the object was illuminated for 700 ms, so that the monkey could see the object. He was not allowed to touch it at this point. During tactile trials the opposite was true: A red LED instructed the animal to reach out in the dark and touch the object. To ensure that he indeed interacted with the object, he had to briefly lift it up. This assured that the whole hand of the monkey had contact with the object. Usually he explored it shortly, until he recognized the correct grip type to apply to this object. He was given 3,000 ms to reach out, explore and lift, and return his hand to the handrest position. Afterward the memory period followed, where the monkey had to memorize the object in the dark while keeping his hand placed on the handrest position. The duration of the memory period varied between 1,000 and 1,500 ms (chosen at random) to ensure that he could not predict the following go cue, in which the red LED turned off to instruct the animal to grasp the object in the dark. The movement epoch was kept short (870 ms) to ensure that the animal could not use this time epoch to further explore the object, but had to be ready to quickly select an appropriate grip type and lift up the object (for 700 ms) before returning to the handrest button in order to receive a fluid reward [small amount of his favorite juice (grape or pear)].

2.5. Data Analysis

2.5.1. Movement and Reaction Time Analysis

The first important question was to check whether the animal was using the object information in this task, or whether he was simply able to guess a correct grip type, even when he could not know the object. For this, we compared the (pooled) reaction and movement times of all ten sessions in the various task conditions and modalities. Incorrect trials (such as failure to lift the object or trying to grasp during the memory period) were excluded from further analysis. Reaction time was defined as the time between the occurrence of the Go cue and the movement start. Movement time started when the animal lifted his hand from the handrest button and ended when the object was lifted completely. Results were plotted as a histogram and the mean reaction and movement times were calculated.

2.5.2. Hand Kinematic Analysis

The second essential question was whether the animal would use the same grip type between visual and tactile trials. For this, the animal was equipped with the magnetic data glove that recorded the positions of seven sensors with up to 100 Hz. The position of these sensors could then be used to calculate the angles between each joint of the monkey's hand, as described in Schaffelhofer and Scherberger (2012). This data was then aligned with the behavioral task events to find where each trial started, ended and when the object interaction occurred. To check whether grip types between different modalities were similar, a linear discriminant analysis (LDA) was used and verified with leave-one-out analysis. This analysis searched for common features across trials that can be used to classify the data. Results were plotted in a confusion matrix. The goal was to test whether a classifier could differentiate between visual and tactile trials on the basis of hand kinematics, or gets confused between them. Since the number of trials per object varied between 14 and 18, a correction was done before each training step, so that the classifier used the same number of trials for each condition for training, avoiding an over-representation of some conditions. In addition to the classification approach, we also calculated the Euclidean distance between the grasp kinematics and displayed the clusters in a dendrogram.

2.5.3. Neural Data Analysis

Neural data was recorded during ten session from four brain areas: AIP, F5, M1, and S1. During recordings, continuous data (30 kS/s) was collected and stored on a hard drive. Channels containing only noise signals were marked and later removed from further analyses. For spike detection, data was filtered with a median filter (window length: 3.33 ms), the resulting signal subtracted from the raw signal, and a 4th order non-causal Butterworth filter (5,000 Hz) applied to low-pass filter the data (Butterworth, 1930). Then, a principal component analysis (PCA) artefact cancellation procedure was performed, as described in Musial et al. (2002). This step was done to exclude common noise that occurred across channels, therefore only PCA dimensions with a coefficient larger than 0.36 (with respect to normalized data) were kept. For spike sorting, a modified version of Wave_Clus was used (based on Kraskov et al., 2004; Chaure

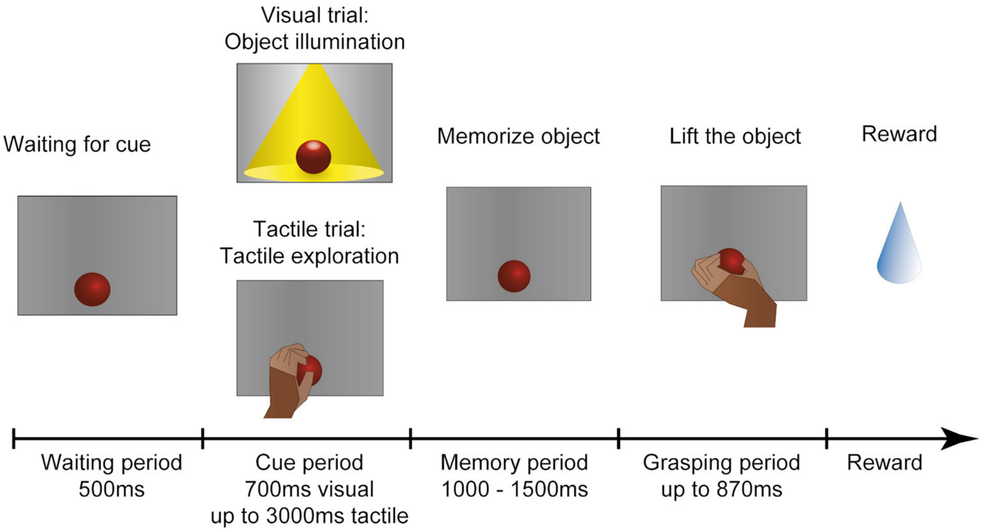

FIGURE 4 | Task paradigm. After an object has arrived in front of the animal, he has to wait in the dark with the hand in a resting position. In the following cue period the animal could then identify the object either visually or tactually. In the visual task, the object is illuminated for 700 ms. In the tactile task (indicated to the animal by a red LED that turns off), the monkey remains in the dark and instead has to reach out, touch and briefly lift the object (maximal duration: 3,000 ms). The animal is then required to return his hand to the resting position and memorize the object for 1,000–1,500 ms before the red cue LED turns off and he is instructed to lift the object within 870 ms. All successful trials are rewarded with a fluid reward. First published in Buchwald et al. (2021).

TABLE 1 | Number of units with a firing rate higher than 1 Hz per area and recording day.

Recording day	#units F5	#units AIP	#units M1	#units S1
18.05.2018	36	5	88	60
01.08.2018	26	7	62	50
02.08.2018	27	6	54	46
07.08.2018	25	14	60	53
09.08.2018	24	14	55	52
04.06.2019	22	5	61	49
16.10.2019	22	7	69	61
24.10.2019	22	12	65	45
15.11.2019	28	9	67	43
22.11.2019	26	6	67	41

et al., 2018). Furthermore, units with a firing rate below 1 Hz were excluded from all analyses. The number of remaining units for each recording session and area is provided in **Table 1**.

2.5.3.1. Population Analysis

The spike sorted data was then further analyzed with a sliding window analysis of variance (ANOVA; window size: 100 ms) that investigated differences between the mean of groups of data points, here the number of spikes between the different conditions (objects) and modalities (visual and tactile trials). Afterwards a correction for multiple comparisons was applied (Bonferroni correction). The percentage of tuned units (y-axis) was then plotted over time (x-axis).

2.5.3.2. Classification

To further quantify whether or not observed significant differences might be big enough for the brain to differentiate between the origin of sensory data (or simply between sensory modalities) a classifier was trained on the neural data. Again, LDA served as a basis for this step and the classifier was then validated using leave-one-out cross-validation. Here, a correction for the number of trials was implemented to ensure that no condition is over-represented by randomly selecting an equal number of trials for all conditions and modalities. Results are then plotted as a confusion matrix for three different time epochs: Early memory, late memory (first and last 500 ms of the memory period, respectively) and grasp epoch.

3. RESULTS AND DISCUSSION

3.1. Movement and Reaction Time Analysis

Using the above methods, we first tried to evaluate whether the animal would use the sensory information he collected during the cue period. The assumption is that grasping a known object will result in less hesitation, i.e., shorter reaction time, and faster movement times, especially when the animal is extremely familiar with the objects (Gibson, 1958; Eimas, 1967; Dhawan et al., 2019). Results can be found in **Figures 5**, **6**. During tactile exploration (**Figures 5A**, **6A**), a very broad distribution of longer reaction and movement times can be observed, with a mean of 323 and 757 ms, respectively. In **Figures 5B,C**, **6B,C**, reaction and movement times are displayed during visual and tactile grasp period, respectively. In contrast, during movement execution, we found a very similar distribution of reaction time, with an identical mean of 259 ms, and likewise of movement time, with

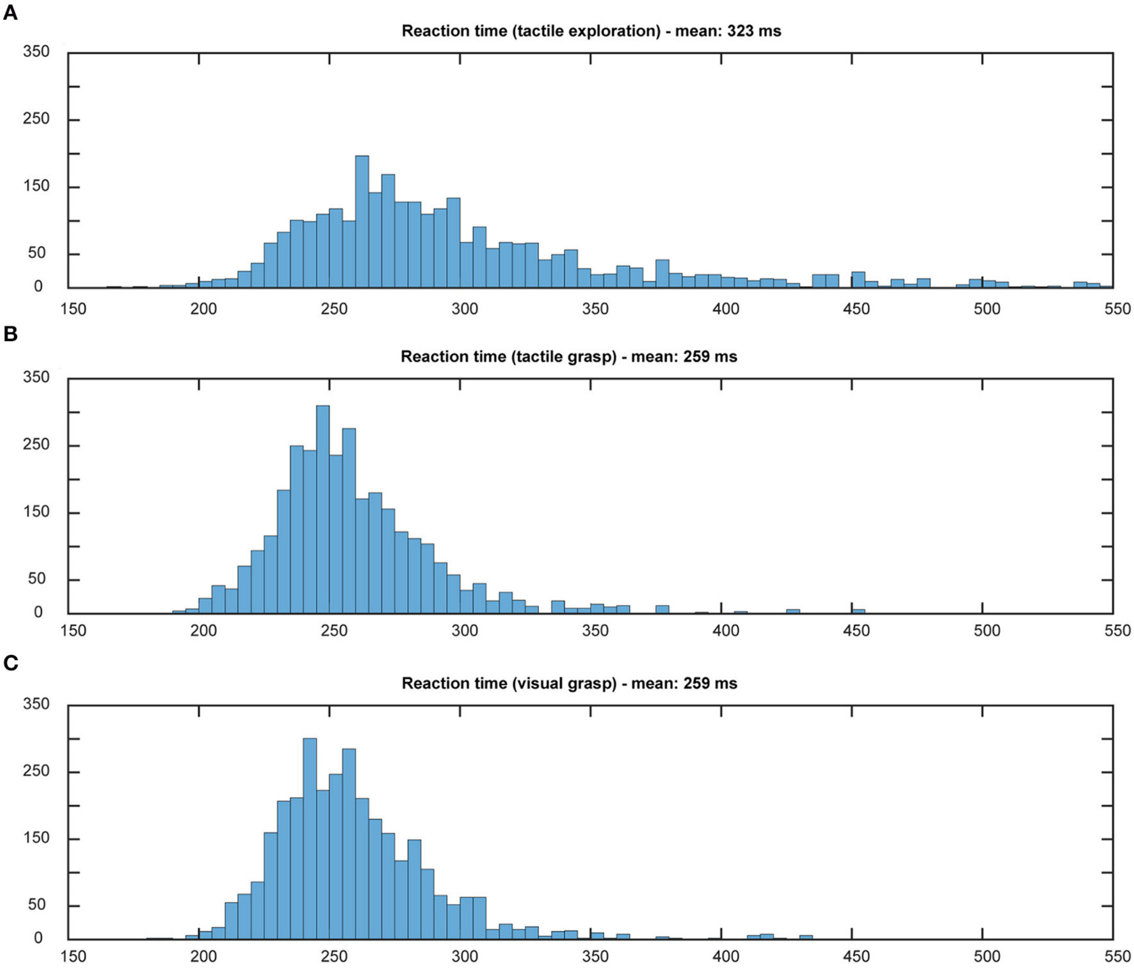

FIGURE 5 | Distribution of reaction times. Histograms illustrate the distribution of reaction time in both tasks, all 10 sessions pooled. Bin width: 5 ms, cut off at 550 ms. During tactile exploration **(A)** the object was unknown and on average a longer reaction time could be observed. When looking at grasp movement execution in the tactile **(B)** and visual grasp **(C)** both distributions appear identical and with the same mean, indicating less hesitation due to knowledge about the object and therefore appropriate grasp to lift it.

a mean of 308 and 310 ms for visually and tactually guided grasps, respectively. This indicates that the animal is aware of the object identity in both tasks. While this is somewhat obvious for visual trials, where the monkey saw the object and one can therefore assume that he goes the easier route of remembering the object and recalling the appropriate grip type that proved best in the past, this is also likely the case for tactile trials after tactile exploration. Touching the object and quickly lifting it up was sufficient to inform the monkey about the object identity, in line with results from human participants (Klatzky and Lederman, 1992). From observation and kinematic data we can also confirm that the monkey had to correct his hand shape in many trials during tactile exploration, since he usually approached quickly with a more uniform hand shape and only on touch found the correct grip (see example video in the **Supplementary Materials**). Not knowing the object therefore results in a longer movement time, further indicating that the shorter movement time during tactile grasp period stems from knowledge about the object information.

3.2. Hand Kinematic Analysis

An important check of behavior was to see whether or not the monkey grasps objects always with the same grip type. While monkeys generally optimize their grasping strategy to act as quickly as possible, it is not a priori clear how the animal weights different strategies. On the one hand, humans only need to make contact with a few key features of objects to correctly group them (Klatzky and Lederman, 1992). However, the animal might simply go with its first point of contact, which might lead to a more awkward but still successful lift as it depends on where the animal first hit the objects and managed to get a firm grasp. Here it probably helps that the monkey was trained for over a year before the first data was collected, and became very good at quickly distinguishing

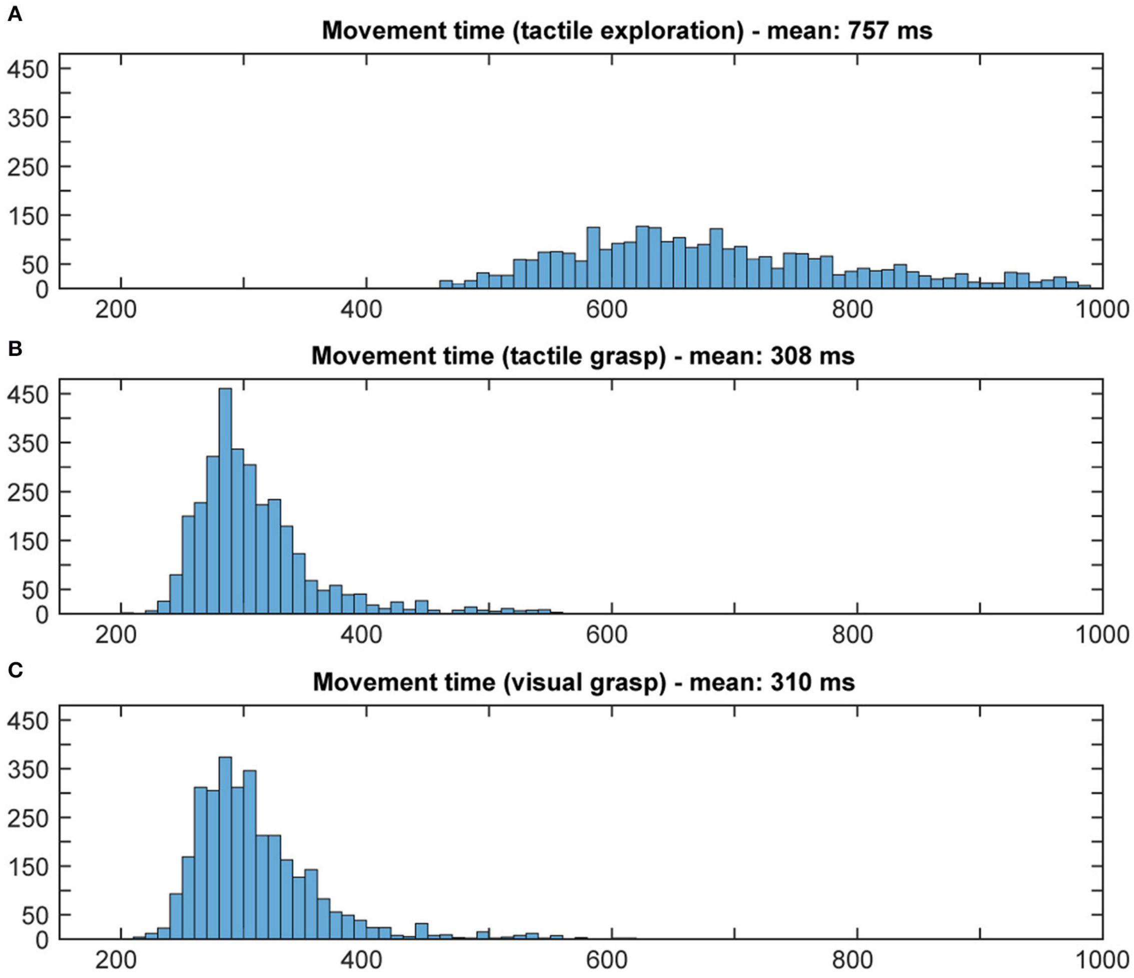

FIGURE 6 | Distribution of movement times. Histograms illustrate the distribution of movement time in both tasks, all 10 sessions pooled. Bin width: 10 ms, cut off at 1,000 ms. During tactile exploration **(A)** the object was unknown, leading to multiple and varying grasp attempts and on average a much longer movement time. When looking at grasp movement execution in the tactile **(B)** and visual grasp **(C)** both distributions look similar, indicating that the animal was able to execute an appropriate grasp of the object based on the object information gathered from the cue period.

the six objects, similar to what was found in other animals (Gibson, 1958; Eimas, 1967; Dhawan et al., 2019).

To test whether or not the monkeys uses the first or second strategy, we monitored the animal's hand kinematics via video, which revealed that the monkey has developed a dedicated grasp for each object that was applied independently of the sensory modality in a particular trial. Even during the tactile exploration phase, he quickly made contact with the object and after realizing which of the six objects he handled, adjusted his hand to his preferred grip type for that object (see video in **Supplementary Materials**). To quantify these observations, data from the magnetic kinematic glove was used to train an LDA classifier in the different modalities of this task and to evaluate the data using leave-one-out cross-validation (see **Figure 7**, top). To do so, we took the average joint angles between 450 and 550 ms after the animal successfully lifted the object. This ensured that the animal had already settled in a stable grasp position for each object and would no longer make grasp adjustments, but also would not yet loosen his grasp and return to the handrest button; this was allowed only after 750 ms after he had lifted the object. During this period, almost no confusion occurred between different objects, as became apparent by the three diagonals in the confusion matrix (**Figure 7**). For example, the condition "cube, visible" was only confused with "cube, tactile," indicating that while the animal chose different grasps for all six objects, the sensory modality did hardly affect the chosen grip. This was somewhat remarkable, since the objects were initially designed in pairs, where each pair (cube/sphere, bar/blockbar, ring/blockring) was supposed to be grasped by the same grip type. While it was hard to recognize any grip differences between these object pairs by visual inspection, the kinematics analysis revealed that the animal did grasp each of the six objects at least slightly differently. One likely explanation is that while the objects were similar in size (with the diameter

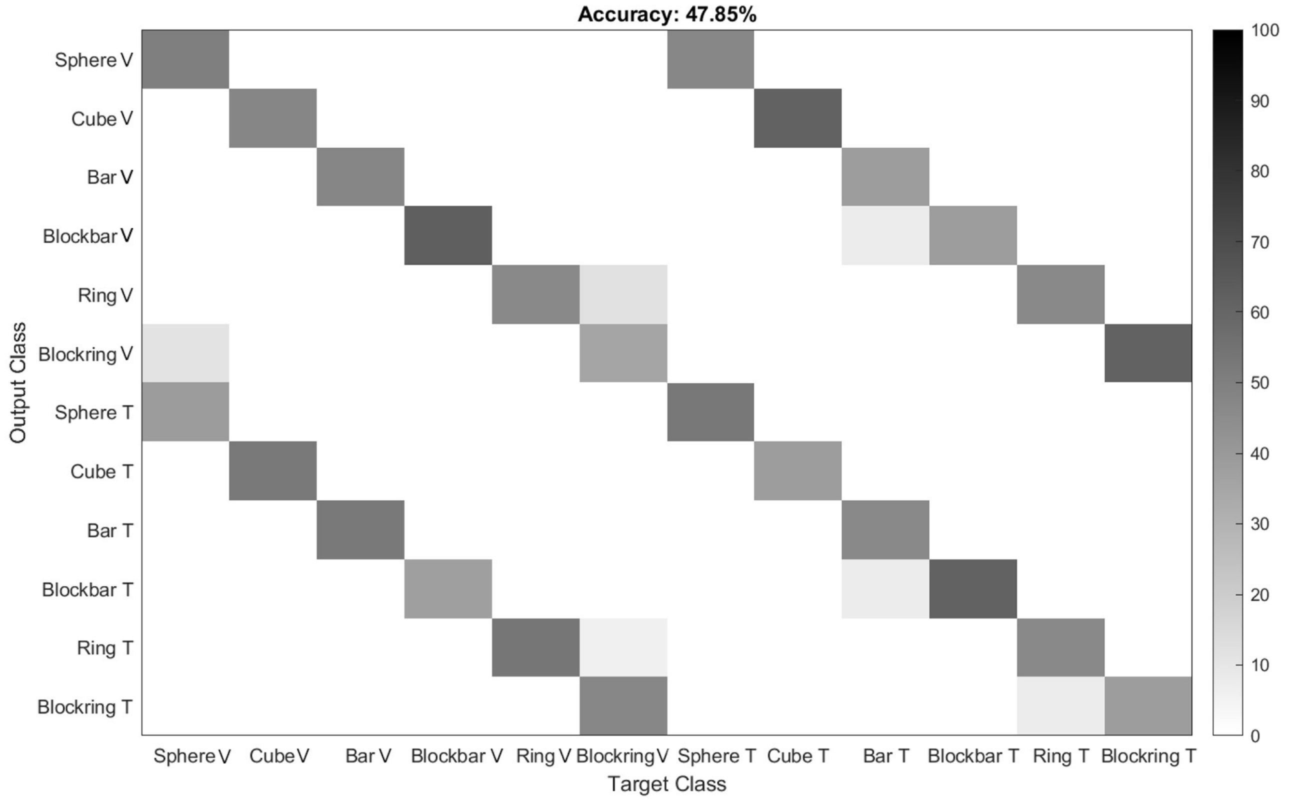

FIGURE 7 | Classification of grip types from one example session. To evaluate whether the animal grasps the same object with the same grip during the visual and tactile task, an LDA classifier was trained on the kinematic data. Results indicate that the classifier indeed can not distinguish between visually and tactually guided grasps, with performance being close to chance level. Gray levels indicate classification performance in percent.

of all object pairs being identical), handling of round and edged objects was different, possibly to avoid object edges or simply because flat surfaces required slightly different finger positions or pressure distributions than round ones. The overall accuracy of the classifier was close to chance level (about 48%), hinting that while the object was easy to classify, the sensory modality had only a minor impact on the hand shape of the monkey. If the classifier was trained only on objects, independent of sensory modality, accuracy was about 93%. In contrast, if only the sensory modality was known to the classifier, it fell to chance level (52%), supporting the idea that while objects can be separated nicely (due to very distinct grasp movements), the sensory modality can not be decoded from the hand kinematics alone. This matched the observation that objects are grasped the same between sensory modalities and this was also a strong indicator that the differences in neural activity, as described below, are not driven by differences in grip types, but indicate differential neural processing due to different sensory input. Furthermore we clustered the joint angles by calculating the Euclidean distance between all grasps to see how much the grasp kinematics differed between sensory modalities (see **Figure 8**). We always found very low Euclidean distances for trials of different sensory modality (visual vs. tactual) and interaction with the same object.

3.3. Neural Population Analysis

Neural data was recorded in parallel from 256 electrodes, four cortical areas, and across ten recording sessions. A sliding two-way ANOVA (factor sensory modality, two levels, and factor objects, six levels) was applied to test for significant differences between objects and sensory modalities in various epochs of the task. **Figure 9** shows the fraction of neurons with significant selectivity for the six objects, separately for visual trials (**Figure 9A**) and tactile trials (**Figure 9B**). The overall result was similar for both trials, with the largest peaks of selectivity occurring when the object was interacted with, either when looking at it (mainly in F5 and AIP) or when it was tactually explored and lifted up. Furthermore, F5 showed sustained preparatory activity during the visual and tactile task, while this was much rarer in the other three areas. Only before movement start, the percentage of object-modulated neurons increased once again, with a peak during object interaction.

Figure 10 shows the percentage of significantly selective units for sensory modality over time. High rates of selectivity were expected during the cue epoch, since the monkey performs two different actions (looking at an illuminated object while sitting still, vs. touching an object in the dark). In line with this setting, a high number of significantly tuned units was also observed at the start of the memory period, which is the time point when the light

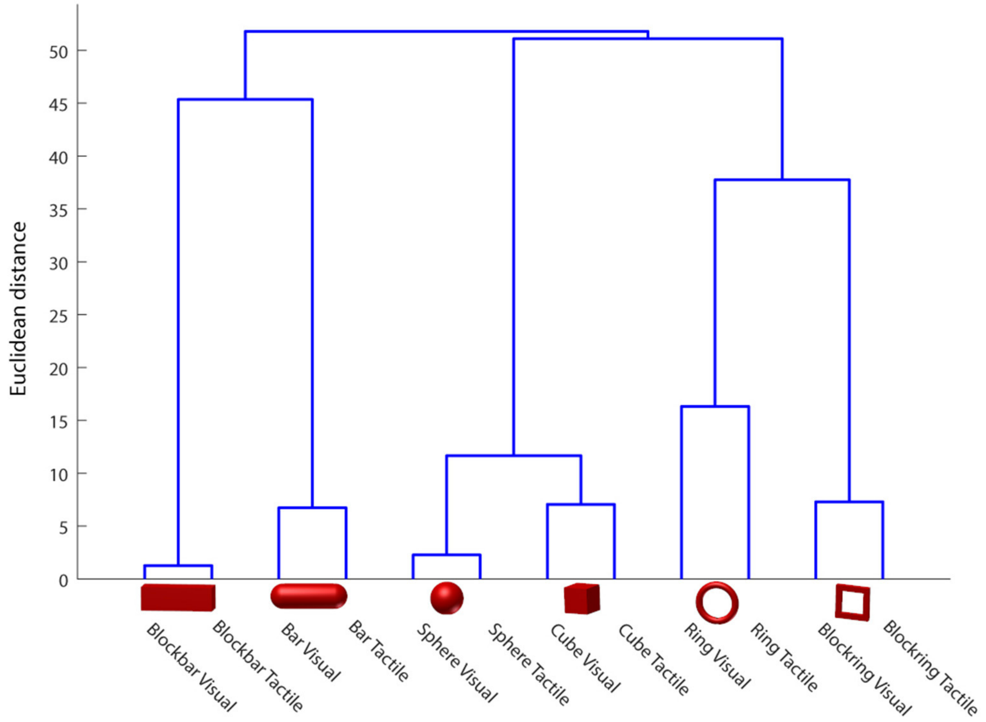

FIGURE 8 | Hand shape difference based on Euclidean distance in the joint angle space. Euclidean distance between classes was calculated and plotted as a dendrogram, indicating high similarity between visually and tactually guided grasps to the same object. Data of one example session.

turns off or when the monkey returned to the handrest button after tactile exploration. Since he just stopped moving, a high number of significantly tuned units was expected. Interestingly, though, while this effect declined over time, it was still present in all four cortical areas shortly after movement start. While the effect was not as huge as during the early memory epoch, a number of units continued to show significant tuning even after movement start. Only about 250 ms after the movement started, the percentage of tuned units became insignificant for AIP and S1, whereas for M1 and F5, this downward trend took about 500 ms. This came as a surprise because as was established before, the movement the monkey executed during visual and tactile trials did not differ, at least not to an extent that a different hand shape could be observed or a classifier was able to decode the sensory condition from the hand shape. Therefore, even though the same movement was prepared in visual and tactile trials, a significant tuning differences was observed in the population analysis, which, however, might be based on a small pool of neurons.

3.4. Classification of Neural Data

While the differences found by the neural population analysis may seem small, we wanted to evaluate whether they are strong enough for a classifier to recognize the sensory modality. For this, the neural data of each session was used to train an LDA classifier, validated with leave-one-out cross validation (see **Figure 11**). The resulting confusion matrix could show two distinct patterns: First, whenever the actual condition and prediction match, a diagonal should form in the middle of the confusion matrix. Secondly, since we first listed all visually and then all tactually perceived object conditions, a partition into four quadrants would indicate a separation between both sensory modalities, independent of objects. Chance level for classifying these 12 classes is 8.33% (six objects times two sensory modalities).

In AIP, which is known to react to the visual properties of objects about to be grasped, the overall performance of the classifier was low, even though above chance (17, 18, and 22% for Early, Late Memory and Grasping epoch, respectively). When only the sensory modality was decoded, a higher accuracy was reached during Early Memory (76%), likely due to a lasting influence of the visual activity during the visual task. This fell to 64% during Late Memory and 58% during Grasp. Similarly, due to the overall low performance of AIP neurons, decoding of object information from AIP was hard. During early memory, an accuracy of 22% was observed (chance level: 16.66; classification of six objects). Accuracy remained poor during late memory (27%) and only got better in the Grasping Epoch (36%) when tactile object interactions occurred. The overall low performance of object classification could be due to the low number of recorded units in AIP (5–14 units per session, see **Table 1**). It is also possible that the few recorded units were not object-selective, which would explain the mismatch of this study with the previous literature, e.g., see (Schaffelhofer and Scherberger, 2016). Still, one can see a stronger performance in decoding sensory modality in the early memory period, which once again might be a result

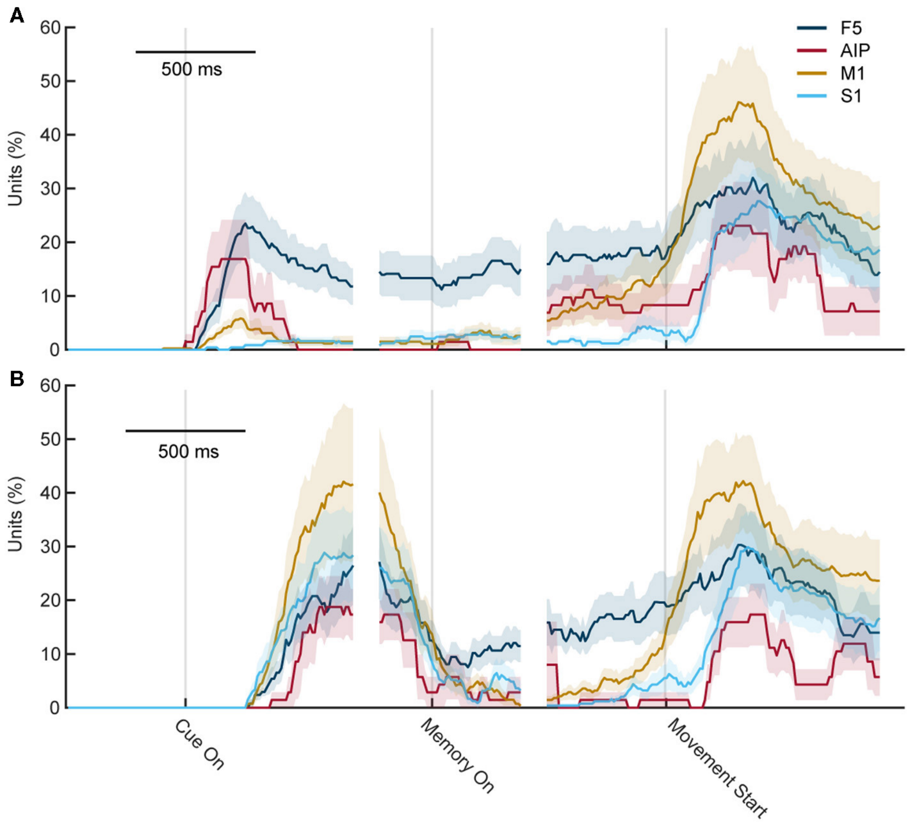

FIGURE 9 | Percentage of object-selective units throughout both tasks. Percentage of units with significant selectivity for objects (ANOVA, factor objects) in the cortical areas F5, M1, AIP, and S1 for each time point during the task. **(A)** During visual trials, differences first rise when the object is seen and some remaining selectivity can be seen in F5. Shortly before grasping, object selectivity rises again and reaches a peak after movement start. **(B)** During tactile trials, the first rise is slightly delayed as the first 250 ms contains the reach movement of the exploration phase. F5 also shows some selectivity during movement planning and the main peaks occur during movement execution.

of the two different tasks the monkey solved ahead of this period (seeing an object vs. touching an object in the dark). During late memory and grasping, classification of sensory modalities was harder and the main diagonal, indicating correct decoding, became spurious.

A stronger performance was observed in the premotor area F5 (20–36 units per session), where even during early memory a good decoding above chance level was found (51%), with a strong focus on determining not only the correct object (again 51% if only objects were classified), but also the correct sensory modality under which an object was perceived (92% when only sensory modality is decoded).

Areas M1 and S1 (54–80 and 41–61 units per session, respectively) also showed a similar pattern: During early memory, when the cue period still had a strong influence on the brain state (such as remaining motor activity only slowly receding) the sensory modality could be predicted well (the plots are separated into the four blocks where the visual and tactile objects are listed, 32% for M1, 23% for S1). For M1, when only objects were decoded the classifier reached an accuracy of 30% while sensory modality could be classified with 99% accuracy. Similarly, in S1 an accuracy of 21% for objects and 97% for sensory modality were found. This was followed by a good prediction of the object, but worse predictions of the sensory modality during late memory and grasping. This effect was stronger for M1, where the classification of objects reached 76% during late memory and 91% during grasping, when motor cortex was involved in leading the monkey's hand movements. For the sensory modality, accuracy fell from 78% in late memory to 64% during grasping, possibly because, at this point, movement execution (grasping according to object shape) became more important than the sensory origin of the object shape information. Similar findings could be seen in S1, although weaker. For object decoding, accuracy rose from 21% and 37% during early and late memory to 78%, possibly due to the direct influence of tactile perception on the brain area. On the other hand, classification accuracy of the sensory modality fell from 97% and 63 to 56%, close to chance level, similarly highlighting the fact that, while sensory modality still influences the brain activity during early memory, it becomes less important as the task progresses toward movement execution.

Overall these results indicate that activity in all four cortical areas can be used to predict the sensory modality under which an object was perceived at all three time points: best

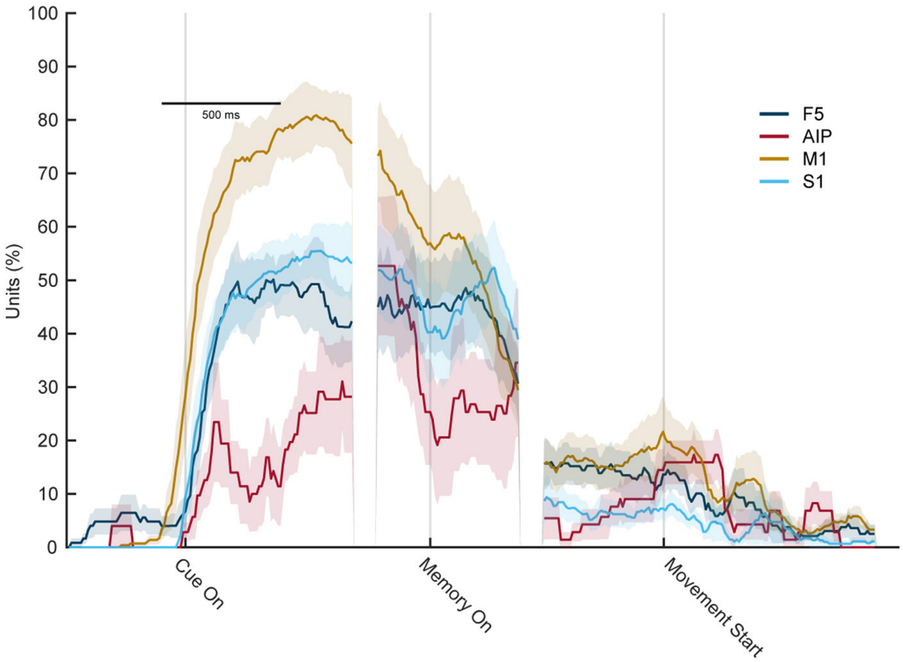

FIGURE 10 | Percentage of sensory modality-selective units throughout the task. Percentage of units with significant selectivity for the sensory modality (ANOVA, factor sensory condition) in each area F5, M1, AIP, and S1 for each time point during the task. Early in the memory epoch, all four cortial areas show significant selectivity. However, this strongly decreases during the late memory and movement execution period, indicating a substantially reduced capacity of individual units to distinguish the sensory modality (vision vs. touch) at the time of movement execution.

during early memory and late memory and with a performance close to chance level during grasping, whereas the additional classification of objects emerged particularly during late memory and grasp. These findings may not appear very surprising during early memory, however, it could have been expected that the different sensory modalities might completely disappear once they become irrelevant to the animal: shortly before the go cue appears, the monkey is most likely just focused on getting the grip type right, to earn his reward as quickly as possible, without unnecessary delays. At a cognitive level, it should therefore be irrelevant for the animal, how he learned about the object identity. Furthermore, the resulting movement is the same, whether the grip type was selected based on visual or tacile object information. This suggests that the same movement was either planned differently by the involved brain areas or these brain areas nevertheless maintain information about the underlying sensory modality, even after it has become irrelevant to the animal in the particular task.

4. CONCLUSION

In this study, we trained one rhesus monkey to grasp objects that he either saw or touched beforehand with the goal to determine whether or not the different sensory information would influence cortical grasp planning. We first could demonstrate that the animal used the same grip type for the same object, independent of the sensory modality of a trial. This was an interesting insight into the strategy used by the animal. Instead of going for an approach of not trying to recognize the identity of an object by thoroughly exploring it with his hand, which might require less effort, he not only explored the object sufficiently, but also maintained this information in order to perform an optimal grip type. For this, it is probably relevant that the animal was very familiar with the objects and obtained a high task performance (over 90% correct trials) throughout all sessions (Kaeser et al., 2014). Due to his familiarity with the objects, the monkey did not actually have to touch the whole object in front of him to recognize the object identity. Instead, it is likely that once his hand encountered one of the unique features of the objects (round vs. edge shape, thickness or others), he could recognize the object already. This was also confirmed by an analysis of the movement times. In analogy to visual trials, where the animals visually explored and recognized each object, a comparison to the same epoch in tactile trials showed that the animal had a similar movement time for both modalities (Camponogara and Volcic, 2021). However, during tactile exploration, his movements were slower, due to the need to frequently correct his handshape.

After having confirmed that any differences should not be a result of the monkey simply executing different movements in both tasks, we looked at the population activity of the four brain areas: AIP, F5, S1, and M1. Here, we found a small but significant difference during the movement planning. While the majority of recorded units did not actually show a significantly difference in their activity, it is interesting that a small subset either still encoded the sensory modality or any associated information,

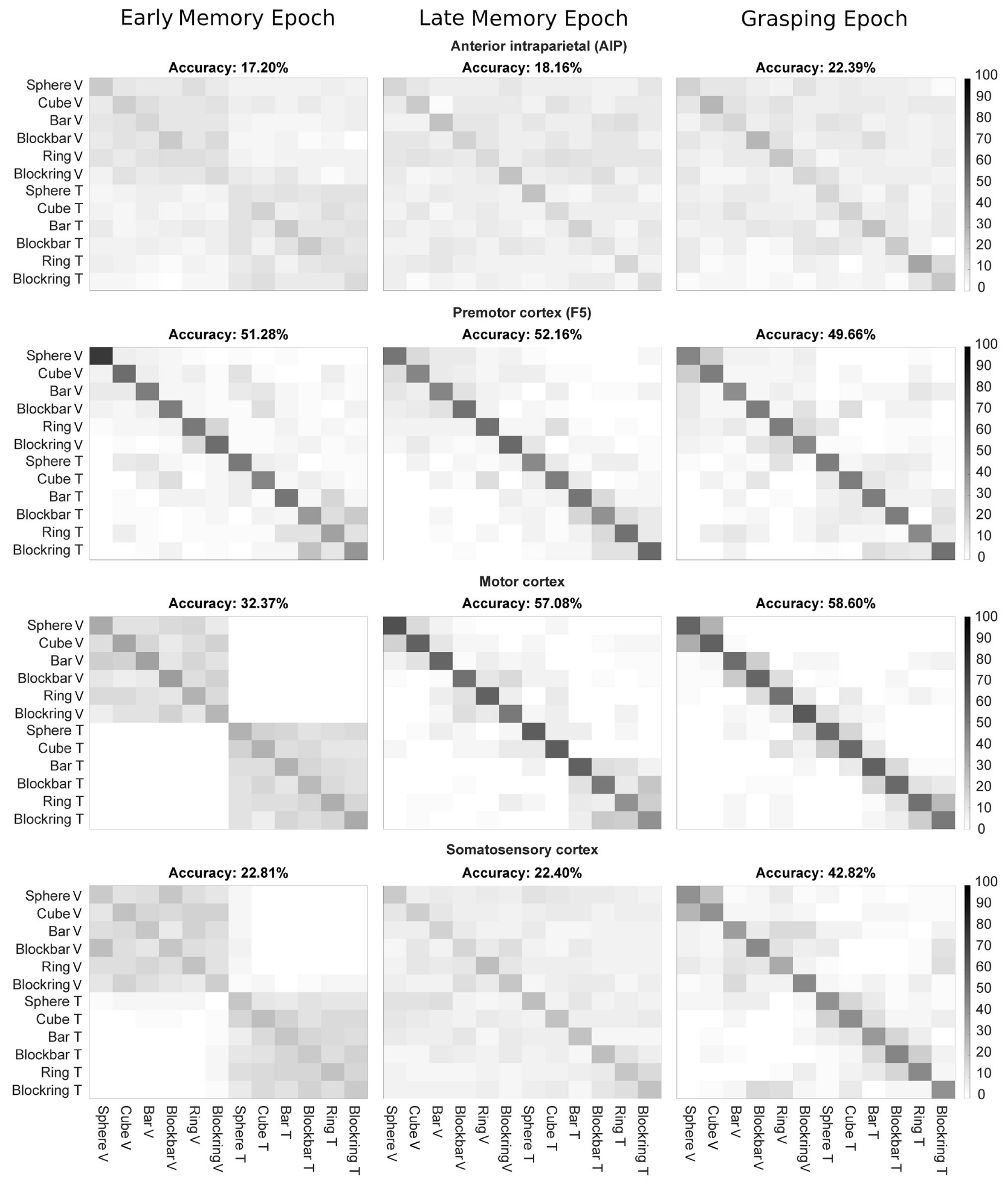

FIGURE 11 | LDA decoding accuracy per epoch, averaged over five recordings. Confusion matrices showing decoding accuracy of 500 ms for three epochs (early memory, late memory, and grasping) for F5, M1, and S1. Decoded epochs are early memory, late memory, and grasping. Axis labels indicate the object in visual (V) and tactile (T) trials. X-axis: instructed task condition, y-axis: decoded task condition.

even though this should be irrelevant after the object was recognized and the grip type determined.

These finding have interesting implications for the classification of brain activity. Whereas the classifier should be able to predict the intended grip type independent of the sensory modality, completely ignoring this information could introduce noise, since the variance of neural activity rises. For practical applications, like the decoding of intended hand movements for neural prosthetics, one might therefore have to pay attention to the sensory modalities from which object information was acquired, since they might influence how the brain acts before and even after the start of the movement, even though the particular sensory modality might be irrelevant for the actual movement.

DATA AVAILABILITY STATEMENT

The original contributions presented in the study are included in the article/**Supplementary Material**, further inquiries can be directed to the corresponding author/s.

ETHICS STATEMENT

The animal study was reviewed and approved by the Animal Welfare Division of the Office for Consumer Protection and Food Safety of the State of Lower Saxony, Germany (permit no. 14/1442 and 19/3132).

AUTHOR CONTRIBUTIONS

DB and HS conceived and designed the experiments. DB performed the experiments. DB analyzed the results. DB and HS wrote the article. All authors provided comments and approved the manuscript.

FUNDING

This work was supported by Deutsche Forschungsgemeinschaft (German Research Foundation; SFB 889, Project C9).

ACKNOWLEDGMENTS

We thank Natalie Bobb, Sabine Borchert, Matthias Dörge, and Benjamin Dann for technical assistance.

SUPPLEMENTARY MATERIAL

The Supplementary Material for this article can be found online at: https://www.frontiersin.org/articles/10.3389/fnins.2021.679910/full#supplementary-material

REFERENCES

Arbuckle, S. A., Weiler, J., Kirk, E. A., Rice, C. L., Schieber, M., Pruszynski, J. A., et al. (2020). Structure of population activity in primary motor cortex for single finger flexion and extension. *J. Neurosci*. 40, 9210–9223. doi: 10.1523/JNEUROSCI.0999-20.2020

Baumann, M. A., Fluet, M.-C., and Scherberger, H. (2009). Context-specific grasp movement representation in the macaque anterior intraparietal area. *J. Neurosci*. 29, 6436–6448. doi: 10.1523/JNEUROSCI.5479-08.2009

Binkofski, F., Buccino, G., Posse, S., Seitz, R. J., Rizzolatti, G., and Freund, H.-J. (1999). A fronto-parietal circuit for object manipulation in man: evidence from an fMRI-study. *Eur. J. Neurosci*. 11, 3276–3286. doi: 10.1046/j.1460-9568.1999.00753.x

Borra, E., Belmalih, A., Calzavara, R., Gerbella, M., Murata, A., Rozzi, S., et al. (2007). Cortical connections of the macaque anterior intraparietal (AIP) area. *Cereb. Cortex* 18, 1094–1111. doi: 10.1093/cercor/bhm146

Buchwald, D. (2020). *Monkey see, monkey touch, monkey do: influence of visual and tactile input on the fronto-parietal grasping network* (Ph.D. thesis). Georg-August-Universität Göttingen, Göttingen, Germany.

Buchwald, D., Schaffelhofer, S., Dörge, M., Dann, B., and Scherberger, H. (2021). A turntable setup for testing visual and tactile grasping movements in non-human primates. *Front. Behav. Neurosci*. 15:96. doi: 10.3389/fnbeh.2021.648483

Butterworth, S. (1930). On the theory of filter amplifiers. *Wireless Eng*. 7, 536–541.

Camponogara, I., and Volcic, R. (2019). Grasping movements toward seen and handheld objects. *Sci. Rep*. 9:3665. doi: 10.1038/s41598-018-38277-w

Camponogara, I., and Volcic, R. (2021). A brief glimpse at a haptic target is sufficient for multisensory integration in reaching movements. *Vision Res*. 185, 50–57. doi: 10.1101/2020.10.04.325712

Chaure, F. J., Rey, H. G., and Quian Quiroga, R. (2018). A novel and fully automatic spike-sorting implementation with variable number of features. *J. Neurophysiol*. 120, 1859–1871. doi: 10.1152/jn.00339.2018

Chowdhury, R. H., Glaser, J. I., and Miller, L. E. (2020). Area 2 of primary somatosensory cortex encodes kinematics of the whole arm. *eLife* 9:e48198. doi: 10.7554/eLife.48198

Christensen, M. S., Lundbye-Jensen, J., Geertsen, S. S., Petersen, T. H., Paulson, O. B., and Nielsen, J. B. (2007). Premotor cortex modulates somatosensory cortex during voluntary movements without proprioceptive feedback. *Nat. Neurosci*. 10, 417–419. doi: 10.1038/nn1873

Churchland, M. M., Byron, M. Y., Ryu, S. I., Santhanam, G., and Shenoy, K. V. (2006). Neural variability in premotor cortex provides a signature of motor preparation. *J. Neurosci*. 26, 3697–3712. doi: 10.1523/JNEUROSCI.3762-05.2006

Delhaye, B. P., Long, K. H., and Bensmaia, S. J. (2018). Neural basis of touch and proprioception in primate cortex. *Comprehens. Physiol*. 8, 1575–1602. doi: 10.1002/cphy.c170033

Dhawan, S. S., Tait, D. S., and Brown, V. J. (2019). More rapid reversal learning following overtraining in the rat is evidence that behavioural and cognitive flexibility are dissociable. *Behav. Brain Res*. 363, 45–52. doi: 10.1016/j.bbr.2019.01.055

Eimas, P. D. (1967). Overtraining and reversal discrimination learning in rats. *Psychol. Rec*. 17, 239–248. doi: 10.1007/BF03393710

Englerova, K., Klement, D., Frynta, D., Rokyta, R., and Nekovarova, T. (2019). Reactions to novel objects in monkeys: what does it mean to be neophobic? *Primates* 60, 347–353. doi: 10.1007/s10329-019-00731-2

Filimon, F., Nelson, J. D., Huang, R.-S., and Sereno, M. I. (2009). Multiple parietal reach regions in humans: cortical representations for visual and proprioceptive feedback during on-line reaching. *J. Neurosci*. 29, 2961–2971. doi: 10.1523/JNEUROSCI.3211-08.2009

Fluet, M.-C., Baumann, M. A., and Scherberger, H. (2010). Context-specific grasp movement representation in macaque ventral premotor cortex. *J. Neurosci*. 30, 15175–15184. doi: 10.1523/JNEUROSCI.3343-10.2010

Fritsch, G., and Hitzig, E. (1870). Ueber die elektrische Erregbarkeit des Grosshirns. *Arch. Anat. Physiol. Wiss. Med*. 37, 300–332.

Gibson, J. J. (1958). Visually controlled locomotion and visual orientation in animals. *Brit. J. Psychol.* 49, 182–194. doi: 10.1111/j.2044-8295.1958.tb00656.x

Goodman, J. M., and Bensmaia, S. J. (2018). The neural basis of haptic perception. *Stevens Handb. Exp. Psychol. Cogn. Neurosci.* 2, 1–39. doi: 10.1002/9781119170174.epcn205

Grigg, P. (1994). Peripheral neural mechanisms in proprioception. *J. Sport Rehabil.* 3, 2–17. doi: 10.1123/jsr.3.1.2

Iturrate, I., Leeb, R., Chavarriaga, R., and Millán, J. D. R. (2016). "Decoding of two hand grasping types from EEG," in *Proceedings of the 6th International Brain-Computer Interface Meeting* (Graz).

Johansson, R. S. (1991). How is grasping modified by somatosensory input. *Motor Control Concepts Issues* 14:331.

Kaeser, M., Chatagny, P., Gindrat, A.-D., Savidan, J., Badoud, S., Fregosi, M., et al. (2014). Variability of manual dexterity performance in non-human primates (*Macaca fascicularis*). *Int. J. Comp. Psychol.* 27:2. doi: 10.46867/ijcp.2014.27.02.04

Klatzky, R. L., and Lederman, S. J. (1992). Stages of manual exploration in haptic object identification. *Percept. Psychophys.* 52, 661–670. doi: 10.3758/BF03211702

Klatzky, R. L., Loomis, J. M., Lederman, S. J., Wake, H., and Fujita, N. (1993). Haptic identification of objects and their depictions. *Percept. Psychophys.* 54, 170–178. doi: 10.3758/BF03211752

Kraskov, A., Stögbauer, H., and Grassberger, P. (2004). Estimating mutual information. *Phys. Rev. E* 69:066138. doi: 10.1103/PhysRevE.69.066138

Land, M. F., and Fernald, R. D. (1992). The evolution of eyes. *Annu. Rev. Neurosci.* 15, 1–29. doi: 10.1146/annurev.ne.15.030192.000245

Lehmann, S. J., and Scherberger, H. (2013). Reach and gaze representations in macaque parietal and premotor grasp areas. *J. Neurosci.* 33, 7038–7049. doi: 10.1523/JNEUROSCI.5568-12.2013

Lehmann, S. J., and Scherberger, H. (2015). Spatial representations in local field potential activity of primate anterior intraparietal cortex (AIP). *PLoS ONE* 10:e0142679. doi: 10.1371/journal.pone.0142679

Liu, M., Batista, A., Bensmaia, S., and Weber, D. J. (2021). Information about contact force and surface texture is mixed in the firing rates of cutaneous afferent neurons. *J. Neurophysiol.* 125, 496–508. doi: 10.1152/jn.00725.2019

Luppino, G., Murata, A., Govoni, P., and Matelli, M. (1999). Largely segregated parietofrontal connections linking rostral intraparietal cortex (areas AIP and VIP) and the ventral premotor cortex (areas F5 and F4). *Exp. Brain Res.* 128, 181–187. doi: 10.1007/s002210050833

Lutz, O. J., and Bensmaia, S. J. (2021). Proprioceptive representations of the hand in somatosensory cortex. *Curr. Opin. Physiol.* 21, 9–16. doi: 10.1016/j.cophys.2021.04.002

Miall, R. C., Rosenthal, O., Ørstavik, K., Cole, J. D., and Sarlegna, F. R. (2019). Loss of haptic feedback impairs control of hand posture: a study in chronically deafferented individuals when grasping and lifting objects. *Exp. Brain Res.* 237, 2167–2184. doi: 10.1007/s00221-019-05583-2

Michaels, J. A., Dann, B., Intveld, R. W., and Scherberger, H. (2015). Predicting reaction time from the neural state space of the premotor and parietal grasping network. *J. Neurosci.* 35, 11415–11432. doi: 10.1523/JNEUROSCI.1714-15.2015

Murata, A., Gallese, V., Luppino, G., Kaseda, M., and Sakata, H. (2000). Selectivity for the shape, size, and orientation of objects for grasping in neurons of monkey parietal area AIP. *J. Neurophysiol.* 83, 2580–2601. doi: 10.1152/jn.2000.83.5.2580

Musallam, S., Bak, M. J., Troyk, P. R., and Andersen, R. A. (2007). A floating metal microelectrode array for chronic implantation. *J. Neurosci. Methods* 160, 122–127. doi: 10.1016/j.jneumeth.2006.09.005

Musial, P., Baker, S., Gerstein, G., King, E., and Keating, J. (2002). Signal-to-noise ratio improvement in multiple electrode recording. *J. Neurosci. Methods* 115, 29–43. doi: 10.1016/S0165-0270(01)00516-7

National Centre for the Replacement Refinement and Reduction of Animals in Research (2017). *NC3Rs Guidelines: Non-human Primate Accommodation, Care and Use*. National Centre for the Replacement Refinement and Reduction of Animals in Research.

National Research Council (2003). *Guidelines for the Care and Use of Mammals in Neuroscience and Behavioral Research*. National Academies Press.

Okorokova, E. V., Goodman, J. M., Hatsopoulos, N. G., and Bensmaia, S. J. (2020). Decoding hand kinematics from population responses in sensorimotor cortex during grasping. *J. Neural Eng.* 17:046035. doi: 10.1088/1741-2552/ab95ea

Oya, T., Takei, T., and Seki, K. (2020). Distinct sensorimotor feedback loops for dynamic and static control of primate precision grip. *Commun. Biol.* 3, 1–13. doi: 10.1038/s42003-020-0861-0

Raos, V., Umiltá, M.-A., Gallese, V., and Fogassi, L. (2004). Functional properties of grasping-related neurons in the dorsal premotor area F2 of the macaque monkey. *J. Neurophysiol.* 92, 1990–2002. doi: 10.1152/jn.00154.2004

Rizzolatti, G., and Luppino, G. (2001). The cortical motor system. *Neuron* 31, 889–901. doi: 10.1016/S0896-6273(01)00423-8

Sakata, H., Taira, M., Murata, A., and Mine, S. (1995). Neural mechanisms of visual guidance of hand action in the parietal cortex of the monkey. *Cereb. Cortex* 5, 429–438. doi: 10.1093/cercor/5.5.429

Saunders, J. A., and Knill, D. C. (2004). Visual feedback control of hand movements. *J. Neurosci.* 24, 3223–3234. doi: 10.1523/JNEUROSCI.4319-03.2004

Schaffelhofer, S. (2014). *From vision to action: hand representations in macaque grasping areas AIP, F5, and M1* (Ph.D. thesis). Georg-August-Universität Göttingen, Göttingen, Germany.

Schaffelhofer, S., Agudelo-Toro, A., and Scherberger, H. (2015). Decoding a wide range of hand configurations from macaque motor, premotor, and parietal cortices. *J. Neurosci.* 35, 1068–1081. doi: 10.1523/JNEUROSCI.3594-14.2015

Schaffelhofer, S., and Scherberger, H. (2012). A new method of accurate hand-and arm-tracking for small primates. *J. Neural Eng.* 9:026025. doi: 10.1088/1741-2560/9/2/026025

Schaffelhofer, S., and Scherberger, H. (2016). Object vision to hand action in macaque parietal, premotor, and motor cortices. *eLife* 5:e15278. doi: 10.7554/eLife.15278

Schlegel, P., Steinfartz, S., and Bulog, B. (2009). Non-visual sensory physiology and magnetic orientation in the blind cave salamander, proteus anguinus (and some other cave-dwelling urodele species). Review and new results on light-sensitivity and non-visual orientation in subterranean urodeles (amphibia). *Anim. Biol.* 59, 351–384. doi: 10.1163/157075609X454971

Self, M. W., Jeurissen, D., van Ham, A. F., van Vugt, B., Poort, J., and Roelfsema, P. R. (2019). The segmentation of proto-objects in the monkey primary visual cortex. *Curr. Biol.* 29, 1019–1029. doi: 10.1016/j.cub.2019.02.016

Snowden, R. J., Treue, S., Erickson, R. G., and Andersen, R. A. (1991). The response of area MT and V1 neurons to transparent motion. *J. Neurosci.* 11, 2768–2785. doi: 10.1523/JNEUROSCI.11-09-02768.1991

Stone, K. D., and Gonzalez, C. L. (2014). Grasping without sight: insights from the congenitally blind. *PLoS ONE* 9:e110175. doi: 10.1371/journal.pone.0110175

Taira, M., Mine, S., Georgopoulos, A., Murata, A., and Sakata, H. (1990). Parietal cortex neurons of the monkey related to the visual guidance of hand movement. *Exp. Brain Res.* 83, 29–36. doi: 10.1007/BF00232190

Umeda, T., Koizumi, M., Katakai, Y., Saito, R., and Seki, K. (2019). Decoding of muscle activity from the sensorimotor cortex in freely behaving monkeys. *Neuroimage* 197, 512–526. doi: 10.1016/j.neuroimage.2019.04.045

Van Essen, D. C. (2003). Organization of visual areas in macaque and human cerebral cortex. *Vis. Neurosci.* 1, 507–521.

Warren, S., Hamalainen, H. A., and Gardner, E. P. (1986). Objective classification of motion-and direction-sensitive neurons in primary somatosensory cortex of awake monkeys. *J. Neurophysiol.* 56, 598–622. doi: 10.1152/jn.1986.56.3.598

Conflict of Interest: The authors declare that the research was conducted in the absence of any commercial or financial relationships that could be construed as a potential conflict of interest.

Advantages of publishing in Frontiers

OPEN ACCESS
Articles are free to read
for greatest visibility
and readership

FAST PUBLICATION
Around 90 days
from submission
to decision

HIGH QUALITY PEER-REVIEW
Rigorous, collaborative,
and constructive
peer-review

TRANSPARENT PEER-REVIEW
Editors and reviewers
acknowledged by name
on published articles

Frontiers
Avenue du Tribunal-Fédéral 34
1005 Lausanne | Switzerland

Visit us: www.frontiersin.org
Contact us: frontiersin.org/about/contact

REPRODUCIBILITY OF RESEARCH
Support open data
and methods to enhance
research reproducibility

DIGITAL PUBLISHING
Articles designed
for optimal readership
across devices

FOLLOW US
@frontiersin

IMPACT METRICS
Advanced article metrics
track visibility across
digital media

EXTENSIVE PROMOTION
Marketing
and promotion
of impactful research

LOOP RESEARCH NETWORK
Our network
increases your
article's readership